Aalborg Universitet

AALBORG UNIVERSITY
DENMARK

Removal of pesticides from groundwater through use of advanced oxidation processes and membrane filtration

Madsen, Henrik Tækker

Publication date:
2014

Document Version
Publisher's PDF, also known as Version of record

Link to publication from Aalborg University

Citation for published version (APA):
Madsen, H. T. (2014). Removal of pesticides from groundwater through use of advanced oxidation processes and membrane filtration. Department of Chemistry and Bioscience, Aalborg University.

General rights
Copyright and moral rights for the publications made accessible in the public portal are retained by the authors and/or other copyright owners and it is a condition of accessing publications that users recognise and abide by the legal requirements associated with these rights.

? Users may download and print one copy of any publication from the public portal for the purpose of private study or research.
? You may not further distribute the material or use it for any profit-making activity or commercial gain
? You may freely distribute the URL identifying the publication in the public portal ?

Take down policy
If you believe that this document breaches copyright please contact us at vbn@aub.aau.dk providing details, and we will remove access to the work immediately and investigate your claim.

Downloaded from vbn.aau.dk on: April 29, 2017

REMOVAL OF PESTICIDES FROM GROUNDWATER THROUGH USE OF ADVANCED OXIDATION PROCESSES AND MEMBRANE FILTRATION

HENRIK TÆKKER MADSEN

DEPARTMENT OF CHEMISTRY, BIOTECHNOLOGY AND ENVIRONMENTAL ENGINEERING
AALBORG UNIVERSITY ESBJERG · NIELS BOHRS VEJ 8 · DK-6700 ESBJERG

REMOVAL OF PESTICIDES FROM GROUNDWATER THROUGH USE OF ADVANCED OXIDATION PROCESSES AND MEMBRANE FILTRATION

Ph.D. Thesis

By

Henrik Tækker Madsen

Section of Chemical Engineering

Department of Biotechnology, Chemistry and Environmental Engineering

Aalborg University

Campus Esbjerg, Niels Bohrs Vej 8, DK-6700, Esbjerg, Denmark

Thesis submitted to the Doctoral School of Engineering and Science, Aalborg University, Denmark, for the degree of Doctor of Philosophy

September 2014

Removal of pesticides from groundwater through use of advanced oxidation processes and membrane filtration
Ph.D. thesis, September 2014
Henrik Tækker Madsen

All rights reserved. No part of this work may be published by print, photocopy or any other means without permission from the publisher.

Address: Department of Chemistry and Bioscience
Section of Chemical Engineering
Aalborg University
Niels Bohrs Vej 8
DK-6700 Esbjerg

Phone: +45 9040 9940
Fax: +45 9940 7710

Homepage: www.esbjerg.aau.dk
E-mail: campus@esbjerg.aau.dk

Printed by: UniPrint, Aalborg University

ISBN: 978-87-93100-57-2

Abstract

Use of pesticides has utterly changed our society and has probably helped save millions from starvation, but it also presents a problem since pesticides may lead to cancer and other serious illnesses. Pollution of slow generating drinking water resources such as groundwater aquifers is especially problematic since it may create a long lasting exposure of the population to pesticides. Current standard drinking water treatment processes, aeration and sand filtration, have been shown to be incapable of removing the pesticides, and there is a need for new and better techniques. This thesis has studied the use of the two state of the art water treatment technologies, membrane filtration and electrochemical oxidation.

Filtration with NF/RO membranes had previously been found to be an effective method for removal of pesticides, but we found that in groundwater the most significant part of the pollution consisted not of pesticides, but of pesticide transformation products. Therefore, the applicability of commercial NF/RO membranes to treat groundwater polluted with transformation products was investigated. It was also investigated whether the existing drinking water treatment systems could be used as non-chemical pre-treatment methods for a subsequent NF/RO membrane filtration. To improve the pesticide rejection of existing membranes, the addition of functionalised particles to the membranes was studied. Both the use of adsorbents and water transporting aquaporin proteins were investigated. To completely remove pesticides, the electrochemical oxidation of the key groundwater pollutant BAM was investigated. Special focus was given to the study of degradation pathways, which were determined in the presence of both inert and electroactive electrolytes. Next to these experiments, methods for identifying and quantifying degradation pathways were developed. Finally, the combination of NF/RO membrane filtration and electrochemical oxidation was studied to search for synergies.

In the pre-treatment experiments, a ceramic UF membrane was found to give the lowest fouling index, but sand filtration gave a comparable fouling index and performed better on some of the selected fouling parameters, and could as such be an effective pre-treatment method for groundwater. For the removal of pesticides and pesticide transformation products, it was shown that NF membranes might be incapable of removing transformation products even though they obtain high rejections for pesticides. It was also shown that the rejection could be predicted from the spatial geometry of the pollutants. Adding adsorbents to the membranes could increase the apparent rejection. However, only limited adsorption of small polar transformation products was obtained with the chosen adsorbents, and the adsorbents were found to influence both the structural integrity and the rejection properties of the membrane. By using aquaporins in the active layer of the membrane, it was shown that a high flux of water could be obtained while maintaining a high rejection (> 97%) of even the smallest of the tested transformation products, DEIA. BAM was efficiently degraded by both BDD and Pt anodes, but with the BDD anode giving the highest rate of removal and fewest degradation intermediates. The type of electrolyte was found to be the most important factor determining the degradation pathway, and using an electroactive chloride solution

led to a more complex and completely different set of degradation intermediates compared to the inert sulphate solution. Finally, it was shown that by combining electrochemical oxidation with a RO membrane, in a scheme in which the electrochemical cell was used to treat the RO concentrate, the energy consumption of the total treatment could be reduced with 94.7%.

The overall conclusion from this thesis is that the combination of membranes and electrochemical oxidation is an effective way of treating pesticide polluted groundwater. The exact costs of the treatment compared to alternatives such as activated carbon have not been evaluated, but the flexibility of the membrane/electrochemical oxidation scheme offers possibilities for drinking water production such as “designed water” that cannot be obtained with the alternatives.

Synopsis

Brug af pesticider har ændret vores samfund fuldstændigt, og har formentlig hjulpet til med at redde millioner fra sultedøden, men det udgør også et problem, da pesticider kan føre til kræft og andre alvorlige sygdomme. Forurening af langsomt dannede drikkevandsressourcer, som grundvand, er specielt problematisk, da det kan udsætte befolkningen for en langvarig eksponering af pesticider. Det er blevet vist, at nuværende standardmetoder til drikkevandsbehandling, beluftning og sandfiltrering, ikke er i stand til at fjerne pesticiderne, og derfor er der behov for nye og bedre teknikker. Denne afhandling har studereret brugen af to "state of the art" vandbehandlingsteknologier, membranfiltrering og elektrokemisk oxidation.

Filtrering med NF/RO membraner var tidligere blevet fundet til at være en effektiv metode til at fjerne pesticider, men vi fandt, at den største del af forureningen i grundvand ikke udgøres af pesticider, men af omdannelsesprodukter fra pesticider. Derfor blev anvendeligheden af kommercielle NF/RO membraner til at behandle grundvand forurenet med omdannelsesprodukter undersøgt. Det blev også undersøgt om de eksisterende drikkevandsbehandlingssystemer kunne bruges som ikke-kemiske forbehandlingsmetoder til en efterfølgende NF/RO filtrering. For at forbedre pesticidtilbageholdelsen af eksisterende membraner blev tilførslen af funktionelle partikler til membranerne studeret. Både brugen af adsorbenter og vandtransporterende aquaporin proteiner blev undersøgt. For fuldstændigt at fjerne pesticider undersøgtes den elektrokemiske oxidation af det vigtige grundvandsforurenende stof, BAM. Særlig fokus blev givet til studiet af nedbrydningsveje, som blev bestemt i både inerte og elektroaktive elektrolytter. Sideløbende med disse eksperimenter blev der udviklet metoder til identifikation og kvantificering af nedbrydningsveje. Endeligt blev kombinationen af NF/RO membranfiltrering og elektrokemisk oxidation studeret med henblik på at søge efter synergier.

I forbehandlingsforsøgene blev en keramisk UF membran fundet til at give det laveste foulingindeks, men sandfiltrering gav et sammenligneligt foulingindeks og præsterede bedre på nogle af de udvalgte foulingparametre, og kunne derfor være en effektiv metode til forbehandling af grundvand. For fjernelsen af pesticider og omdannelsesprodukter blev det vist, at NF membraner kan være ude af stand til at fjerne omdannelsesprodukter selvom membranerne har høje tilbageholdelser af pesticider. Det blev ligeledes vist, at tilbageholdelsen kunne forudsiges ud fra stoffernes rumlige geometri. Ved at tilføre adsorberende partikler til membranerne kunne den tilsyneladende tilbageholdelse øges. Imidlertid kunne der kun opnås en begrænset adsorption af små polære omdannelsesprodukter med de valgte adsorbenter, og adsorbenterne blev fundet til at påvirke membranens strukturelle stabilitet og tilbageholdelsesevne. Ved at bruge aquaporiner i membranens aktive lag blev det vist, at en høj vandflux kunne opnås samtidig med, at en høj tilbageholdelse (> 97%) af selv det mindste af de testede omdannelsesprodukter, DEIA, blev bevaret. BAM blev effektivt nedbrudt med både BDD og Pt anoder, men den højeste nedbrydningshastighed og de færreste mellemprodukter blev opnået med BDD anoden. Typen af elektrolyt blev fundet til at være den mest afgørende faktor for bestemmelse af nedbrydningsvejen,

og brugen af en elektroaktiv kloridopløsning førte til en mere kompleks og fuldstændig anderledes blanding af mellemprodukter sammenlignet med den inerte sulfatopløsning. Endelig blev det vist, at ved at kombinere den elektrokemiske oxidation med en RO membran, i en opsætning, hvor den elektrokemiske celle blev anvendt til at behandle koncentratstrømmen fra RO membranen, kunne energiforbruget af den samlede behandling reduceres med 94,7%.

Den overordnede konklusion fra denne afhandling er, at kombinationen af membraner og elektrokemisk oxidation er en effektiv måde at behandle pesticidforurenet grundvand på. De præcise udgifter til behandlingen sammenlignet med alternativer, såsom aktiveret kul, blev ikke evalueret, men fleksibiliteten af membran/elektrokemi-systemet giver muligheder i drikkevandsproduktionen som for eksempel ”designet vand”, der ikke kan opnås med alternativerne.

Preface

This thesis is submitted in partial fulfilment of the requirements for the Ph.D. degree at the Department of Biotechnology, Chemistry and Environmental Engineering, Aalborg University, Denmark. The Ph.D. project was carried out under supervision of Professor Erik G. Søgaard from the Section of Chemical Engineering at Aalborg University Esbjerg, and is concerned with the use of membrane filtration and electrochemical oxidation for removal of pesticides from groundwater used for drinking.

For me, doing a Ph.D. was never part of an elaborate master plan. Instead, it was in many ways something that more or less happened as I went along the way. From an early age I have been interested in environmental sciences, and looking back it was the original motivation for me to become a chemical engineer. As one teacher once told me: *"There are two types of chemical engineers: Those who pollute and those who clean up"*. I like to believe I belong to the second group. Later I discovered that I still loved asking and trying to answer questions, which is essentially what research is all about. When my supervisor, Erik G. Søgaard, provided me with the opportunity of going into environmental research, it was therefore natural for me to continue my career in this direction. We chose to work on pesticide pollution of drinking water, which I was quite happy with, since it allowed me to do research on a topic of both personal interest and national concern.

The thesis is structured as a collection of papers with an introduction, followed by chapters covering the state of the art of the applied techniques, the used methodologies and finally condensed chapters presenting the papers. The whole thesis is concluded with the conclusion and my perspectives on future research topics within this field and possible applications of membranes and electrochemical oxidation in micropollutant abatement. At the end of the thesis, two appendixes describing how to apply models to membrane filtration is found.

The introduction is somewhat longer than what is traditionally seen in Ph.D. theses. This is done to make room for the contextual framework from which the research has its origin. In this chapter it is investigated why we use pesticides at all, and by using Denmark as a concrete example, it is evaluated how big the pesticide problem is, how pesticide pollution of groundwater is different from surface water and how the current drinking water treatment techniques affect the pesticides. It is my personal opinion that in order to make research relevant and interesting, the background and reason for conducting the research needs to be presented thoroughly. Especially for research within the field of engineering, which in many ways could be called applied science. Readers who wish to skip this background may begin at section 1.5.

Since I have been involved with both membrane filtration and electrochemical oxidation as techniques for removal of pesticides, state of the art has been split in two chapters (chapters 2 and 3), one focusing on membranes and the other on electrochemical oxidation. The chapters describe

the general background theory of the techniques as well as the state of the art knowledge in the application of the techniques for pesticide removal.

Chapter 4 covers the methodologies and is aimed at being a reference chapter where descriptions of the setups and specific methods used in the experiments can be found when necessary.

Chapters 5 to 10 represent the condensed papers. Each chapter is concerned with a specific topic and some chapters therefore draw upon multiple papers. Chapter 5 is concerned with methods for determining pathways in chemical reactions and represents the analytical work that was done in the initial phase of the Ph.D. Part of this work is a continuation of my master thesis on hydrogen sulphide scavenging with triazines, and is as such not directly related to the topic of the Ph.D. The principles and methods for determining reaction pathways are however the same, which is the reason for bringing it into the Ph.D. thesis. The remaining paper chapters are directly related to the topic of the Ph.D., with chapter 6 being concerned with methods for a non-chemical pre-treatment of the groundwater prior to NF/RO membrane filtration, chapter 7 and 8 being concerned with NF/RO membrane filtration of pesticide polluted water, chapter 9 with electrochemical oxidation of pesticides and chapter 10 with the combination of membranes and electrochemical oxidation.

It has been three exciting years doing the Ph.D., and it is my modest hope that in this thesis I can pass just a fraction of the excitement onto you as a reader.

Henrik Tækker Madsen

2014

Acknowledgments

Although a Ph.D. study officially is a one-person endeavour that is just an illusion. Behind the scenes are many other people without whom this thesis would have been very different, and they all deserve to be credited.

First and foremost I would like to thank my supervisor Erik G. Søgaard. He gave me the opportunity of doing the Ph.D., and it is safe to say that had it not been for him, I would probably not even have started out on a Ph.D. study. He was the one who almost dragged me into the Ph.D., which I am very grateful for. As a supervisor he has given me much freedom to decide what I wanted to do in my Ph.D., and he has always been supportive in times of trouble such as when receiving a particularly harsh review of one of my papers. Finally, he has been a fantastic travel companion, and I have many fond memories, like having to rush through Leuven in Belgium to catch the airport train because we lost time in a small coffee house.

Jens Muff also deserves special thanks. During my Ph.D., I have been lucky to share an office with him, and he has in many ways acted as my day-to-day supervisor, assisting both on practical and scientific matters. He has co-authored three of the papers in this thesis, but his hand has been on more or less all of the papers.

During the uncountable hours I have spent in the laboratory, I have enjoyed working next to and together with Dorte Spangsmark and Linda Madsen. They have always been helpful with the analytical work and are truly the wizards of the laboratories.

I also wish to send thanks to my other colleagues at the university. Especially Rudi Nielsen, Morten Simonsen, Krzysztof Kowalski and lastly Heidi Thomsen who worked magic with all the administrative paper work.

During my studies I was fortunate to spend six months at the research group of Professor Bart Van der Bruggen in Leuven, Belgium. He and all the people in his research group made me feel welcome and made my stay there both a personal and a scientific success. For that I will always be grateful.

As part of my work in both research and teaching I was often in need of water from local waterworks or tours around the facilities. In this Palle Rühe from Forsyningen Esbjerg, was always helpful for which I would like to offer my gratitude.

Finally, but not least, warm thanks goes out to my friends and family, who have had to endure listening to talks about my research on pesticide removal for the last three years. They were always patient and provided helpful advice and sometimes much needed refuge from the studies.

List of supporting papers

I. Madsen, H. T. and Søgaard, E. G. (2012). *Case study of treatment of waste water for 17α-ethinylestradiol and microorganisms with UV and photocatalysis in an on-going process of introducing AOP techniques in the Danish water sector.* Water Practice & Technology, **7**.

II. Madsen, H. T. and Søgaard, E. G. (2012). *Use of ESI-MS to determine reaction pathway for hydrogen sulphide scavenging with 1,3,5-tri-(2-hydroxyethyl)-hexahydro-s-triazine*. European Journal of Mass Spectrometry, **18**, 377-383.

III. Madsen, H. T. and Søgaard, E. G. (2014). *Fouling Formation During Hydrogen Sulfide Scavenging With 1,3,5-tri-(hydroxyethyl)-hexahydro-s-triazine*. Petroleum Science and Technology, **32**, 2230-2238.

IV. Madsen, H. T., Jensen, C. V. and Søgaard, E. G. (2014). *Triazine based H_2S scavenging: Development of a conceptual model for understanding of fouling formation*. Petroleum Science Technology, **32**, 2803-2806.

V. Kowalski, K. P, Madsen, H. T. and Søgaard E. G. (2014). *Comparison of sand and membrane filtration as non-chemical pre-treatment strategies for pesticide removal with nanofiltration/low pressure reverse osmosis membranes*. Water Science & Technology: Water Supply, **14**, 532-539.

VI. Madsen, H. T. and Søgaard, E. G. (2014). *Applicability and modelling of nanofiltration and reverse osmosis for remediation of groundwater polluted with pesticides and pesticide transformation products*. Separation and Purification Technology, **125**, 111-119.

VII. Madsen, H. T., Bajraktari, N., Hélix-Nielsen, C., Van der Bruggen, B. and Søgaard, E. G. (2015). *Use of biomimetic forward osmosis membrane for trace organics removal*. Journal of Membrane Science, **476**, 469-474.

VIII. Madsen, H. T., Ammi-said, A., Van der Bruggen, B. and Søgaard, E. G. (2015). *Addition of adsorbents to nanofiltration membrane to obtain complete pesticide removal*. Water Air & Soil Pollution, **226**:160.

IX. Madsen, H. T., Søgaard, E. G. and Muff, J. (2014). *Study of degradation intermediates formed during electrochemical oxidation of pesticide residue 2,6-dichlorobenzamide (BAM) at boron doped diamond (BDD) and platinum-iridium anodes*. Chemosphere, **109**, 84-91.

X. Madsen, H. T., Søgaard, E. G. and Muff, J. (2015). *Study of degradation intermediates formed during electrochemical oxidation of pesticide residue 2,6-dichlorobenzamide (BAM) in chloride medium at boron doped diamond (BDD) and platinum anodes*. Chemosphere, **120**, 756-763.

XI. Madsen, H. T., Søgaard, E. G. and Muff, J. (2015). *Reduction in energy consumption of electrochemical pesticide degradation through combination with membrane filtration*. Chemical Engineering Journal, **276**, 358-364.

Table of contents

Abstract iii

Synopsis v

Preface vii

Acknowledgments ix

List of supporting papers xi

Abbreviations xvii

Chapter 1 Introduction 1

1.1 Pesticide pollution in Denmark 2

1.2 Limitation of the pesticide surveillance 7

1.3 Consequences of the pesticide pollution 9

1.4 Groundwater treatment and drinking water production in Denmark 9

1.5 Strategies for pesticide removal 11

1.6 Research objectives 14

Chapter 2 Membrane filtration for removal of pesticides 15

2.1 Principles of membrane filtration 15

2.2 Removal of pesticides with membranes 17

2.3 Transport model for pesticides through membranes 20

2.4 Emerging technologies in membrane science – nanoparticles 23

Chapter 3 Electrochemical oxidation for degradation of pesticides 25

3.1 Principles of electrochemical oxidation 25

3.2 Electrochemical oxidation of pesticides and degradation pathways 29

3.3 Electrochemical oxidation of membrane concentrates 34

Chapter 4 Methodology 35

4.1 Characterisation of pesticides, membranes and groundwater 35

4.2 Analytical methods for quantitative pesticide analysis 39

4.3 Experimental setups 42

Chapter 5 Methods for detection and identification of reaction products 49

5.1 Use of ESI-MS to determine reaction pathway for H_2S scavenging pesticides 49

5.2 Use of HPLC/UV/ESI-MS to determine degradation pathway for EO of BAM 57

5.3 Evaluation of detection and identification protocols 59

Chapter 6 Non-chemical pre-treatment strategies for NF/RO membranes 61

6.1 Background 61
6.2 Results 62
6.3 Evaluation 63
Chapter 7 Applicability of NF/LPRO/RO membranes for pesticide removal 65
7.1 Background 65
7.2 Results 66
7.3 Evaluation 68
Chapter 8 Advanced membrane filtration for pesticide removal 69
8.1 Background 69
8.2 Results 70
8.3 Evaluation 72
Chapter 9 Degradation of BAM with electrochemical oxidation 73
9.1 Background 73
9.2 Results 74
9.3 Evaluation 77
Chapter 10 Combined use of electrochemical oxidation and membrane filtration 79
10.1 Background 79
10.2 Results 80
10.3 Evaluation 82
Conclusion 83
Future perspectives 85
Areas of further research 85
Areas of applications for membranes and AOPs in micropollutant abatement 86
Bibliography 89
Appendix A1 Modelling steric rejection of non-spherical molecules 101
Appendix A2 Log-normal model for rejection of molecules 103

Paper I: Case study of treatment of waste water for 17α-ethinylestradiol and microorganisms with UV and photocatalysis in an on-going process of introducing AOP techniques in the Danish water sector.

Paper II: Use of ESI-MS to determine reaction pathway for hydrogen sulphide scavenging with 1,3,5-tri-(2-hydroxyethyl)-hexahydro-s-triazine.

Paper III: Fouling Formation During Hydrogen Sulfide Scavenging With 1,3,5-tri-(hydroxyethyl)-hexahydro-s-triazine.

Paper IV: Triazine based H_2S scavenging: Development of a conceptual model for understanding of fouling formation.

Paper V: Comparison of sand and membrane filtration as non-chemical pre-treatment strategies for pesticide removal with nanofiltration/low pressure reverse osmosis membranes.

Paper VI: Applicability and modelling of nanofiltration and reverse osmosis for remediation of groundwater polluted with pesticides and pesticide transformation products.

Paper VII: Use of biomimetic forward osmosis membrane for trace organics removal.

Paper VIII: Addition of adsorbents to nanofiltration membrane to obtain complete pesticide removal.

Paper IX: Study of degradation intermediates formed during electrochemical oxidation of pesticide residue 2,6-dichlorobenzamide (BAM) at boron doped diamond (BDD) and platinum-iridium anodes.

Paper X: Study of degradation intermediates formed during electrochemical oxidation of pesticide residue 2,6-dichlorobenzamide (BAM) in chloride medium at boron doped diamond (BDD) and platinum anodes.

Paper XI: Reduction in energy consumption of electrochemical pesticide degradation through combination with membrane filtration.

Abbreviations

AC	Activated carbon
AOP	Advanced oxidation process
AqP	Aquaporin
BAM	2,6-dichlorobenzamide
BDD	Boron doped diamond
CFU	Colony forming unit
COD	Chemical oxygen demand
DEIA	Desethyl-desisopropyl-atrazine
DFT	Density functional theory
DI	Degradation intermediates
EE2	17α-ethinylestradiol
EOTR	Electrochemical oxygen transfer process
ESI-MS	Electrospray ionisation mass spectrometry
FO	Forward osmosis
GCE	General current efficiency
HET	1,3,5-tris(2-hydroxyethyl)-hexahydro-s-triazine
HF	Hartree Fock
HPT	1,3,5-tris(2-hydroxypropyl)-hexahydro-s-triazine
HTI	Hydration Technology Innovations
ICE	Instantaneous current efficiency
LPRO	Low pressure reverse osmosis
MCE	Mineralisation current efficiency
MF	Microfiltration
MWCO	Molecular weight cut-off
MWd	Molecular width
NF	Nanofiltration
PES	Polyethersulfone
PIP	Piperazine
PTP	Pesticide transformation product
RO	Reverse osmosis
SPE	Solid phase extraction
STO	Slater type orbital
TFC	Thin film composite
TMC	Trimesoylchloride
TOC	Total organic carbon
UF	Ultrafiltration
ULPRO	Ultra low pressure reverse osmosis
UMFI	Unified membrane fouling index

Chapter 1 Introduction

This thesis is concerned with remediation of groundwater polluted with pesticides. Pesticide pollution is a hot topic, which can easily be seen by skimming through both scientific publications and news media stories. Part of this is due to the controversial dual nature of pesticides, which at the same time are a problem and a necessity for our society to exist in its current form. One thing is certain; the use of pesticides has utterly changed our society.

The history of pesticide use is almost as old as human agriculture, and one of the earliest written reports on the use of pesticides can be found in Homer's Iliad, where he refers to the use of sulphur as a mean for pest control [1]. It was not however until two events occurring close to each other in the middle of the 20th century that the modern era of pesticide use was initiated. In 1939 and throughout World War II a major breakthrough in the pesticide field was made; the synthesis of DDT (dichlorodiphenyltrichloroethane, or more properly 1,1,1-trichloro-2,2-bis(4-chlorophenyl)ethane). DDT was discovered by Swiss chemist Paul Müller and was quickly used worldwide to combat malaria and other pests, and thus became the first of the modern pesticides [2]. Around the same time, in 1944 in Mexico, American agronomist Norman Borlaug was selected to be part of a project about boosting grain yields, launched by the Rockefeller foundation and the Mexican government. The purpose was to increase the Mexican wheat production, with Mexico at that time being a wheat importing country, and the project resulted in the development of high yielding and disease resistant wheat strains, which turned Mexico into a net exporter of wheat. This was the beginning of what became known as the "Green Revolution". After the success in Mexico, the use of high yielding varieties of crops such as wheat, maize and rice spread to the rest of the World, and as a result Norman Borlaug is often credited for having saved a billion people from starvation. A fact that led him to receive the Nobel Peace Prize in 1970. A side effect of the Green Revolution was the introduction of new farming practices and introduction of new species into already established ecosystems. This made the new crop varieties increasingly vulnerable to pests, and necessitated the use of more efficient pest control, which fuelled the development of new pesticides. Originally, pesticides were as such a very important tool to improve the health and nutritional situation for people everywhere, and they continue to be so today.

As the use of pesticides increased, awareness of the environmental impact of these compounds began to emerge, but it was not until 1962 with the publication of Silent Spring by Rachel Carson that the environmental effect of the use of pesticides was made a concern. Since then toxicological and epidemiological studies have shown pesticides to lead to cancer, genetic malfunctions, neuro-development disorders and damages to the immune system even at very low concentrations (pg/L to ng/L) [3–5], all of which have resulted in a growing public concern of the use of pesticides. To minimize the environmental and health related effects of the pesticides, monitoring programs and legislation have been put up, but even though much has happened to improve the use of pesticides,

they continue to be controversial and the pollution is widespread. In their fifth global environment outlook, the United Nations Environment Programme (UNEP) states that more than 90% of water and fish samples from aquatic environments are contaminated by pesticides [6], and a recent Danish study found that 99% of the children participating in the study had pesticide residues in their urine [7] with similar result found in an American study [8]. One of the key areas is the pollution of drinking water resources, especially groundwater. The retention time for groundwater is variable, but will most often be much longer than the retention times of rivers, lakes and reservoirs that are the typical surface water bodies used for drinking water. With retention times that can be several thousand years, pollution of groundwater aquifers can be potentially devastating for the water supply since the pollution may be long lasting. In Denmark, almost the entire drinking water production is based on groundwater, and the degree of pesticide pollution of the nation's drinking water resources has been closely monitored since the end of the eighties. This makes the Danish case suitable to get an overview of the current pesticide pollution of groundwater with respect to both amount, spread, and type of pesticides.

1.1 Pesticide pollution in Denmark

The monitoring of pesticides in Denmark is carried out by GEUS (the national geological investigations for Denmark and Greenland) in the GRUMO program and by the waterworks in their own quality control. The data is presented in a yearly report by GEUS where the latest report covers the development in the pesticide pollution of the groundwater from 1989-2012, both years included [9]. The GRUMO program has been regularly updated with analyses for an increasing number of compounds from the original 8 to now 31 pesticides and transformation products. These are listed in table 1.

From the pesticides in the monitoring program it is clear that herbicides are the main source of groundwater pesticide pollution. The reason for this may be that the pesticides that are most likely to end up in the groundwater are those that are applied on the ground near aquifers. In Denmark, these areas are mostly used for agriculture or by the municipalities, and here herbicides constitutes the main part of the applied pesticides (81.5% in 2010) [10]. With five out of ten, the pesticides mainly belong to the triazine family (thiadiazine being a derivative of triazine). Interestingly it can be seen that two thirds of the compounds in the monitoring program are not actual pesticides, but pesticide transformation products (PTPs). These are compounds that are formed via microbial metabolism or physico-chemical processes during the percolation of the pesticides from the surface to the groundwater aquifers.

Table 1 Pesticides and transformation products analysed for in the Danish groundwater monitoring program GRUMO [9]. The waterworks do not analyse for TCA, picolinafen, 2-hydroxyterbutylazine, 2-hydroxy-desethyl-terbutylazine, CyPM, CL153815, PPU and desamino-PPU, but do instead analyse for desethyl-terbutylazine, hydroxyatrazine, hydroxysimazine, MCPA, 2,4-D, diuron, ethylenethiourea and desamino-metribuzin.

Pesticide	Systematic name	Class
Atrazine	6-chloro-N^2-ethyl-N^4-isopropyl-1,3,5-triazine-2,4-diamine	Herbicide
Bentazon	3-isopropyl-1H-2,1,3-benzothiadiazin-4(3H)-one	Herbicide
Dichlorprop	(RS)-2-(2,4-dichlorophenoxy)-propionic acid	Herbicide
Dichlobenil	2,6-dichloro-benzonitrile	Herbicide
Mechlorprop	(RS)-2-(4-dichloro-o-tolyoxy)-propionic acid	Herbicide
Glyphosate	N-(phosphonomethyl)-glycine	Herbicide
Hexazinone	3-cyclohexyl-6-dimethylamino-1-methyl-1,3,5-triazine-2,4-(1H,3H)-dione	Herbicide
Metribuzin	4-amino-6-tertbutyl-4,5-dihydro-3-methylthio-1,2,4-triazine-5-one	Herbicide
Simazine	6-chloro-N^2,N^4-diethyl-1,3,5-triazine-2,4-diamine	Herbicide
TCA	Trichloroacetic acid	Herbicide
Picolinafen	4′-fluoro-6-(α,α,α-trifluoro-*m*-tolyloxy)pyridine-2-carboxanilide	Herbicide
Transformation product		**Mother compound**
AMPA	2-amino-3-(5-methyl-3-oxo-1,2-oxazol-4-yl)-propanoic acid	Glyphosate
BAM	2,6-dichlorobenzamide	Dichlobenil
2,6-dichlorobenzoic acid	-	Dichlobenil
4-CPP	2-(4-chlorophenoxy)-propionic acid	Phenoxy acids
2,6-DCPP	2-(2,6-dichlorophenoxy)-propionic acid	Phenoxy acids
Desamino diketo metribuzin	6-*tert*-butyl-2,3,4,5-tetrahydro-1,2,4-triazine-3,5-dione	Metribuzin
Diketo metribuzin	4-amino-6-*tert*-butyl-2,3,4,5-tetrahydro-1,2,4-triazine-3,5-dione	Metribuzin
Desethyl atrazine (DEA)	6-chloro –N^4-isopropyl-1,3,5-triazine-2,4-diamine	Atrazine a.o.t.*
Desisopropyl atrazine (DIA)	6-chloro-N^2-ethyl-1,3,5-triazine-2,4-diamine	Atrazine a.o.t.
Desethyl desisopropyl atrazine (DEIA)	6-chloro-1,3,5-triazine-2,4-diamine	Atrazine a.o.t.
Desethyl hydroxy atrazine (DEHA)	4-amino-6-(propan-2-ylamino)-1,3,5-triazine-2-ol	Atrazine a.o.t.
Desisopropyl hydroxy atrazine (DIHA)	4-amino-6-(ethylamino)-1,3,5-triazine-2-ol	Atrazine a.o.t.
Desethyl desisopropyl hydroxy atrazine (DEIHA)	4,6-diamino-1,3,5-triazine-2-ol	Atrazine a.o.t.
4-nitrophenol	-	Parathion
2-hydroxyterbutylazine	4-(*tert*-butylamino)-6-(ethylamino)-1,3,5-triazin-2-ol	Terbutylazine
2-hydroxy-desethyl-terbutylazine	4-amino-6-(*tert*-butylamino)-1,3,5-triazin-2-ol	Terbutylazine
CyPM	(2E)-2-(2-((6-(2-cyanophenoxy)pyrimidin-4-yl)oxy)phenyl)-3-methoxy-2-enoic acid	Azoxystrobin
CL153815	6-(4-(triflouromethyl)phenoxy)pyridine-2-carboxylic acid	Picolinafen
PPU	1-(4,6-dimethoxypyrimidin-2-yl)-1-(3-(ethylsulfonyl)pyridine-2-yl)urea	Rimsulfuron
Desamino-PPU	N-(3-(ethylsulforyl)pyridine-2-yl)-4,6-dimethoxypyrimidin-2-amine	Rimsulfuron

*a.o.t. = and other triazines

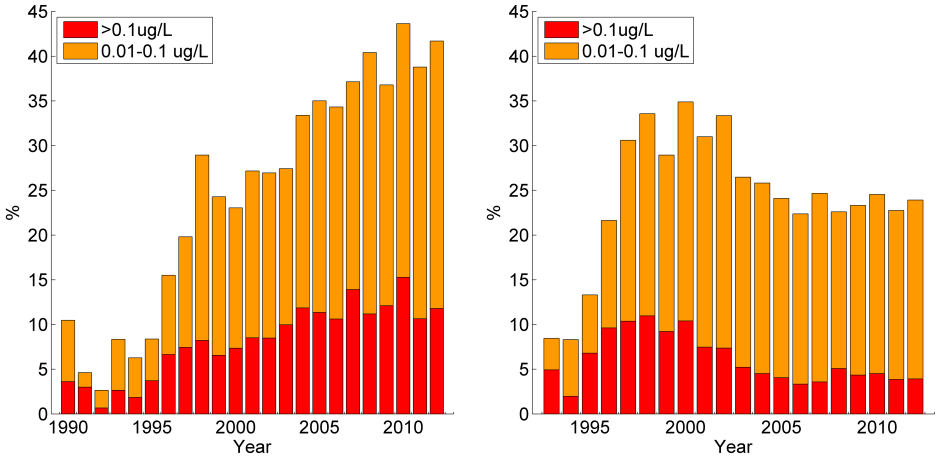

Figure 1 Development of the Danish pesticide pollution over time. The diagram to the left shows the development for the groundwater assessed in the GRUMO program and the diagram to the right shows the drinking water wells assessed by the waterworks [9]. The y-axis shows the percentage of the wells in the programme that has been found to be contaminated.

The groundwater monitoring in the GRUMO program is used to evaluate the relative pollution of the Danish groundwater, whereas the analyses made by the waterworks are used to evaluate the degree of pesticides that the consumers are exposed to.

In figure 1, the results of both monitoring programs are shown. For the groundwater a general increasing trend is seen, which might seem to indicate a growing pesticide pollution. However, the periods in which the main increases are seen (1990 - 1998, and 2004) are due to an increasing number of pesticides being analysed for. Furthermore, the fact that only younger groundwater has been analysed since 2003 may also explain part of the increase. As such the increase in number of polluted wells is probably not due to a higher degree of contamination, but instead changes in the monitoring program [11]. The latest results from 2012 show that 41.7% of the groundwater was contaminated with pesticides and that 11.8% of the wells exceeded the 0.1 µg/L threshold limit. The cumulative result for the period 1990-2012, shows that 51.7% of the groundwater intakes have been contaminated with pesticides during this period (above 0.1 µg/L in 37.7% of the cases) [9].

For the drinking water wells an increasing trend in the number of polluted wells is also seen during the nineties, but again this is probably due to the fact that the monitoring program became more extensive during that period. From around year 2000 the percentage of contaminated drinking water wells has been decreasing to a level around 23-25%, with 4-5% of the wells exceeding the concentration 0.1 µg/L [9]. The fact that the percentage of contaminated wells are lower compared to the groundwater, and the relative stable value from 2007 to 2012, is a result of waterworks closing wells as these become contaminated [9]. Even though the amount of drinking water wells exceeding the pesticide limit is relatively low, the total percentage of affected drinking water wells is substantial, and it may be concluded from the monitoring program that a significant percentage of

the Danish population[i] possibly will be exposed to a background concentration of pesticides through the drinking water supply if no counter-measures are taken.

Another important conclusion from the two bar plots in figure 1 is that the pesticide pollution is stable. Increases and decreases happen because new compounds are being analysed for or wells being taken out of order. The concentration of pesticides in the groundwater does not seem to decrease significantly, and data for specific pesticides only show a very slight decrease over the years [9]. This is even though many of the pesticides have been banned since the middle of the nineties, and the pesticide pollution may therefore be expected to be present for many years to come.

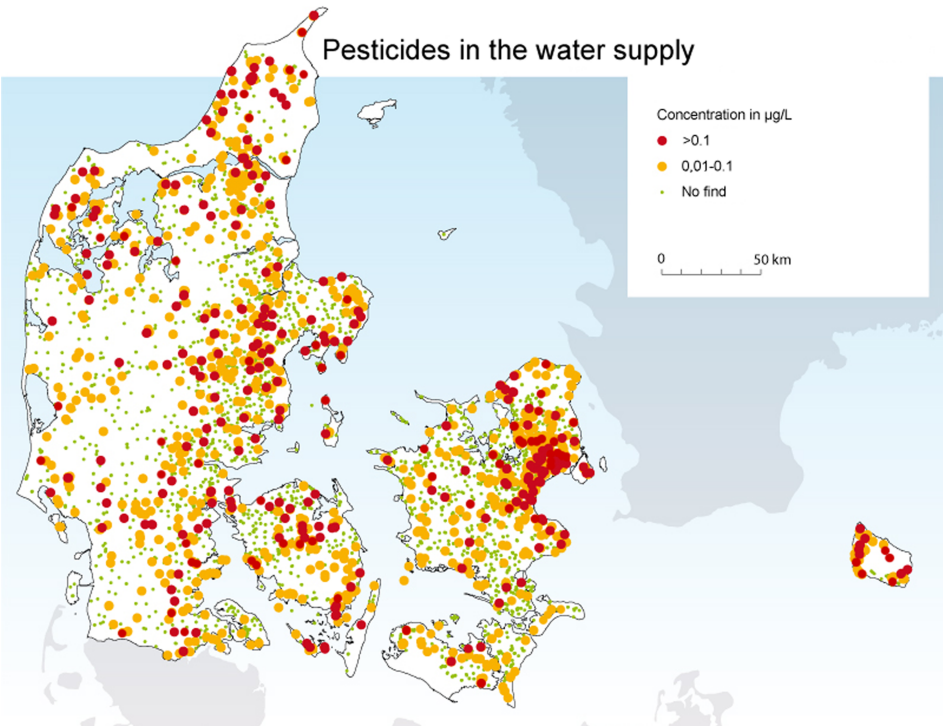

Figure 2 Map of waterworks wells (1993-2004) and drinking water wells (1993-2010) where pesticides have been found [12]. The map does not include the wells of small private waterworks or single farms.

[i] Depending on in which population centers the contaminated wells are situated.

Figure 2 shows how the contaminated drinking water wells are distributed geographically in Denmark. Interestingly, the highest amount of wells with a pesticide concentration above 0.1 µg/L is found around heavily populated areas, especially around Copenhagen and the eastern part of Jutland. Traditionally, pesticide pollution is thought to be connected to agriculture, in which case the contamination should be heaviest in the rural areas. One of the reasons for this picture is the high amount of drinking water wells around the cities relative to rural areas, but it also points to the fact that earlier practices by both property owners, industry and municipalities have had a significant effect on the groundwater. Another reason is that many Danish cities are located near the coast, where the groundwater aquifers are unconfined and placed close to the surface. These aquifers are as such more vulnerable to pesticides percolating down from the surface. The geology of the Danish subsurface is also part of the explanation for the spread of the pesticide pollution. Eastward from eastern Jutland, the geology is characterized by loamy soils, while westward the underground consists of sandy soils [11]. In places with sandy soils drinking water is collected from deeper aquifers since the shallower aquifers often have too high concentrations of nitrate. Analyses show that in these shallower aquifers the pesticide pollution is more significant [9]. Finally, the western part of Denmark on average gets more rain (around 350-400 mm), compared to the eastern part (around 150-250 mm) [11]. This means that the degree of dilution will be lower in the eastern part of Denmark, and lower amounts of rain may also give rise to different flow patterns for the rain water, affecting how the pesticides are transported [13].

To evaluate which of the pesticides that are the biggest contributors to the groundwater and drinking water contamination, the top five of the pesticides found in the monitoring programs are shown in table 2.

The main pesticide problem is caused by the dichlobenil transformation product BAM. Another big contributor is atrazine and its transformation products. Atrazine itself is also found, but in lower amounts compared to its transformation products. The most important of these seems to be DEIA.

Table 2 Top five of the pesticides found in the monitoring programs for 2012 [9].

Groundwater			Drinking water		
Name	Finds (%)	>0.1µg/L (%)	Name	Finds (%)	>0.1µg/L (%)
BAM	16.9	5.8	BAM	17.7	2.9
DEIA	13.7	2.6	DEIA	2.4	0.1
DIA	10.7	0.7	Bentazon	2.2	0.3
DEIHA	6.4	0.6	Mechlorprop	1.6	0.1
Diketo-metribuzin	5.8	0.4	Hexazinon	1.2	0.1

1.2 Limitation of the pesticide surveillance

The evaluation of the pesticide contamination of the Danish groundwater is mainly based on the analysis of the pesticides and transformation products presented in table 1. However, these pesticides only represent 26.7% of the total sale of pesticides in the period 1988 to 2012, and 30.8% of the total sale of herbicides, fungicides, insecticides and growth regulators. Of the pesticides included in the groundwater monitoring program, glyphosate is by far the most used, and if it is excluded, the remaining pesticides account for only 8.5% and 9.8% respectively. This is because many of the pesticides currently in the groundwater monitoring program were banned or regulated already in the 1990s. Atrazine was made illegal in 1994 along with hexazinon and dichlobenil in 1996, metribuzin and simazine in 2004, terbuthylazine in 2009 and rimsulfuron in 2010, while for TCA there has been no sale after 1988. Several of the remaining pesticides in the monitoring program underwent regulation and restrictions were put on their use. From the groundwater monitoring program these were bentazon in 1995, and dichlorprop and mechlorprop in 1997 [11]. This leaves glyphosate, picolinafen and azoxystrobin as the only approved and unregulated pesticides included in the monitoring program. A large part of the pesticides currently in use is therefore not included in the monitoring programs.

The number of pesticides and transformation products in the GRUMO program has over the years varied significantly. From originally 9, to around 50 between 1990 and 2004, 34 substances between 2005 and 2008, 21 in 2010 and currently 31 [11,14]. The reason that some pesticides are not included in the current monitoring is therefore because they have not previously been found to infiltrate the groundwater. To determine which of the pesticides that could infiltrate the groundwater, the Danish parliament asked GEUS, the Department of Agroecology (DJF, Aarhus University), and the Department of Bioscience (NERI, Aarhus University), to initiate a surveillance program for the leaching potential of pesticides: The Leaching Assessment Programme (PLAP) [15]. Of the 42 pesticides investigated in this program, 21 pesticides and transformation products were found to have resulted in pronounced leaching with average concentrations above 0.1 µg/L in the sucking cups and drains one meter below terrain. These were: Azoxystrobin, CyPM, bentazon, CL153815, primicarb-desmethyl-formamido, propyzamide, tebuconazole, glyphosate, AMPA, PPU, bifenox acid, ethofumesate, TFMP, metamitron, desamino-metamitron, metribuzin-desamino-diketo, metribuzin-diketo, terbutylazine, desethyl-terbutylazine, 2-hydroxydesethyl-terbuthylazine and 2-hydroxyterbutylazine. 17 other pesticides have also been found to be leaching, but in average concentrations below 0.1 µg/L. The leaching assessment shows that a wide range of pesticides and their transformation products have leaching potential and that the degree of leaching may be highly dependent on the geology [13].

Another example of leaching of pesticides not included in the current pesticide monitoring program is the LOOP program. Up until 2007 pesticide monitoring was a combined result of the GRUMO program and the LOOP program. Today it is only in the GRUMO program that pesticides are measured. The LOOP program was focused on investigating the effect of the application of fertilizers and pesticides in agriculture on the upper groundwater. Although the number of analyses in the LOOP program is small compared to the GRUMO program, the results from LOOP are interesting because they show that it is possible for other pesticides than the ones included in the

GRUMO program to infiltrate the groundwater aquifers, see table 3. Especially interesting are metamitron and MCPA. Both pesticides are sold in more than 100,000 kg/year and are not included in GRUMO. Metamitron and MCPA were formerly included in the groundwater monitoring program, but were from 1993 to 2003 only found in 0.2 and 1.2% of the wells [16]. However, the same could be said about a pesticide such as atrazine, although as shown its transformation products are some of the most widely found groundwater pollutants. Therefore it is possible that after having infiltrated the upper groundwater, pesticides such as metamitron and MCPA are converted to transformation products that are not analysed for.

Overall, the results from PLAP and LOOP show that it is likely that the groundwater monitoring program does not give the complete overview of the pesticides and transformation products in the Danish groundwater, and that the total pesticide load may be larger in reality.

Table 3 Results from the pesticide monitoring in the LOOP program [17].

	Number of analysed sites	Sites with findings (%)	Sites with ≥ 0.1 µg/L (%)
4-Nitrophenol	57	45.6	3.5
DEIA	53	30.2	9.4
AMPA	68	23.5	8.8
DIA	99	22.2	8.1
Glyphosate	68	22.1	11.8
Bentazon	108	20.4	1.9
TCA	49	18.4	2
DEA	105	15.2	1.9
Desethylterbutylazin	61	13.1	3.3
Metamitron	100	11	0
Mechlorprop	137	10.2	0
Hydroxy atrazine	82	9.8	0
4-CPP	53	9.4	1.9
BAM	93	8.6	1.1
Isoproturon	108	8.3	2.8
MCPA	137	8	0
Metribuzin	67	7.5	0
Dichlorprop	137	6.6	0
Atrazine	137	6.6	1.5
Maleinhydrazid	40	5	0

1.3 Consequences of the pesticide pollution

A direct consequence of the pesticide contamination of a drinking water well is often that the well is closed. From 1999 to 2009 3,386 wells have been closed (out of service), and of these wells 1,279 were found to contain pesticides, with 602 exceeding 0.1 µg/L [11]. It is difficult to assess how many wells have been closed directly due to pesticide contamination, because many other factors can contribute to the closing of a well. However, it seems very plausible that wells with pesticide concentrations exceeding 0.1 µg/L have been closed because of pesticides, and this number therefore represents the lowest number of wells that can have been closed because of pesticides. The highest possible number of wells closed because of pesticides is the case in which all wells with pesticide finds have been closed as a consequence of this. From these considerations it is estimated that between 60-130 wells have been closed on a yearly average from 1999 to 2009 [11]. Establishing a new well costs around 880,000 and 1,420,000 DKK (118,000 and 190,000 €) depending on whether the well can be established at the same extraction site and assuming that the old well can undergo standard closing [18]

In places where a new well can be established easily or the output of existing unpolluted wells can be increased, the closing of one well may not be a serious problem. However, when whole areas are found to be polluted, the consequences can be immense. One example is the local area of the university; Esbjerg. Here drinking water was originally extracted directly from beneath the city, but as more and more aquifers were found to be polluted, many of the original wells were closed. To obtain enough water, the city had to look far beyond its own borders and today more than two thirds of the city's water is produced from wells 35-45 km away from the city. Furthermore, the water supply company pays the farmers who own the land above the aquifers not to use pesticides on their fields. Another example is found in Copenhagen. As can be seen from figure 2, the groundwater under and around Copenhagen is heavily polluted with pesticides, but because the renewable water resources in eastern Denmark are smaller compared to western Denmark, it has not been possible in all cases to apply the same solution as in the case of Esbjerg. Therefore, active carbon filters with subsequent UV treatment have been installed as a final barrier at two waterworks, Hvidovre (pesticides) and Frederiksberg (chlorinated solvents) [12].

1.4 Groundwater treatment and drinking water production in Denmark

Because Danish drinking water production is based on groundwater, the treatment process is simple compared to standard drinking water production in other countries where surface water is used, and it is also called "simple treatment".

In general, water is pumped from the well to the waterworks where it is aerated to vent out gasses such as methane and hydrogen sulphide. The aeration also saturates the water with oxygen (around 10 mg/L), which is used to oxidise iron, manganese and ammonium. Because of the relative redox potential of oxygen compared to these three species, only iron is actually oxidized in this process, and only partly. The main part of the oxidation occurs in the sand filters. Here bacteria oxidize ammonium to nitrate, while the iron and manganese are oxidized efficiently by the autocatalytic environment that occurs as ferrihydrite coats the sand grains. In some case, the removal of iron and manganese may be further enhanced through biological processes. After this, the legal drinking

water requirements are met [12]. An overview of the process and the changing water composition can be seen in figure 3.

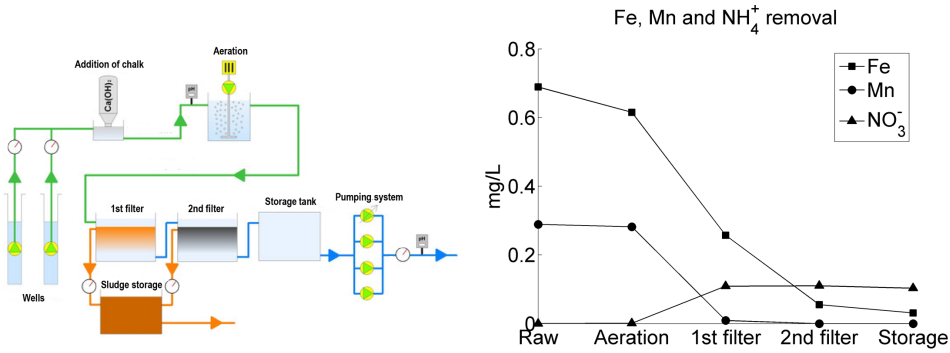

Figure 3 General process diagram for Danish waterworks (left). The addition of chalk is not part of the standard simple treatment. To the right, an example of concentrations of iron, manganese and ammonium through the different steps in the process is shown [12].

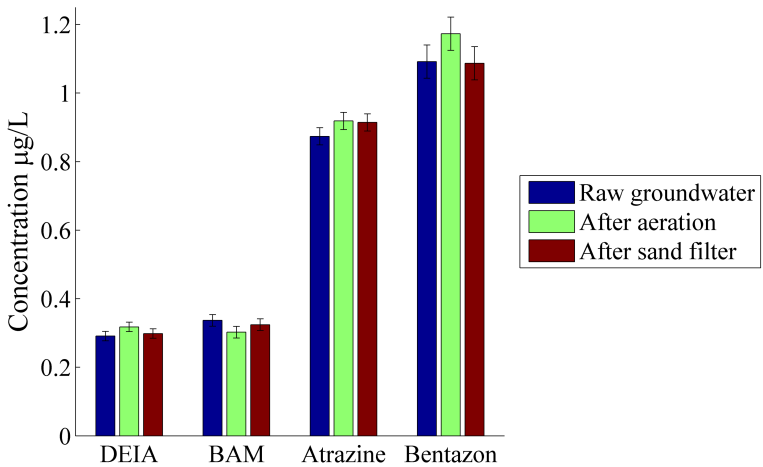

Figure 4 Effect of current drinking water treatment on key pesticides/PTPs. The figure shows the concentration of two pesticides and two PTPs in raw groundwater and after the water has been through first aeration and then sand filtration. In general the concentration is found to be the same during all process steps, and the variations in the specific values are within the expected analytical uncertainty.

The problem with pesticides is that they are not affected by these treatment processes. This was shown by Søgaard et al., who measured the concentration of seven pesticides before and after aeration and sand filtration and found that only for one of the pesticides, mechlorprop, did the concentration decrease [19]. The decrease was ascribed to the partly hydrophilic nature of this pesticide. We found similar results for a different aeration and sand filtration setup where the concentration of four pesticides: BAM, bentazon, atrazine and DEIA was measured [20], figure 4.

To remove pesticides it is therefore necessary to introduce additional unit operations.

1.5 Strategies for pesticide removal

If a Danish waterworks has to apply more advanced water treatment techniques than the simple water treatment, it requires a special permit. The acquisition of such a permit depends on technical, economic, environmental and health effects of the technique in question. The latter is evaluated in a statement from the National Board of Health, represented by the medical health inspectors [12]. For techniques to be allowed in the Danish drinking water sector, they must therefore remove the pesticide while changing the water composition as little as possible. Based on this, it seems reasonable to expect a solution that does not include addition of chemicals to the water to be more likely to win acceptance.

The current technology that is used for pesticide removal is granular active carbon filters followed by UV disinfection, but active carbon filtration suffers from a number of drawbacks, mainly related to saturation of the filters, bacterial growth, low affinity for small polar compounds, foot print size and price [21]. One possible alternative is advanced oxidation processes (AOPs). AOPs comprise a set of techniques for generating highly reactive hydroxyl radicals ($E^0 = 2.80$ V, [22]) that have proven to be very effective at degrading a wide range of organic micropollutants [23–26]. In table 4 an overview of the most common AOPs are given. There exists others such as gamma radiation/electron beam [27,28], sub- and supercritical water oxidation [29], microwave assisted oxidation [30] and combinations of the techniques listed in table 4, but for the moment these are of less practical interest.

Table 4 Overview of AOP techniques with and without addition of chemicals. Based on overviews found in [25,26].

With chemical addition	Without chemical addition
UV/H_2O_2 and or O_3	Photocatalysis
Fenton and photo-Fenton	Electrochemical oxidation
Ultrasound/H_2O_2 and/or O_3	
Alkaline ozonation	
O_3/H_2O_2 with or without catalyst	

Although effective for removal of micropollutants, AOPs suffer from a high energy usage, which was demonstrated in the initial work of this thesis. Here the photocatalytic degradation of the endocrine disruptor 17α-ethinylestradiol (EE2), a compound that is very similar in molecular structure to pesticides, was investigated [31]. The work was used to evaluate the effect of a UV system at a wastewater treatment plant. The UV system had been installed to disinfect the wastewater as a final polishing step, and we were interested in investigating its effect on organic micropollutants and whether it could be improved by employing photocatalytic surfaces. Using the photocatalytic surfaces increased the rate of removal increased with 66% compared to the photolysis reaction, but even with this improvement it was estimated that at a standard flow rate and with the UV system operating at maximum capacity, the system would only be able to reduce the concentration of EE2 with 1.29%. To obtain a complete removal, the UV system therefore had to be significantly larger, and already at its current size it was a major energy consumer at the wastewater treatment plant.

Another issue with the use of AOPs is the formation of by-products [23,32–34]. In theory, the high redox potential of the hydroxyl radical leads to complete mineralisation of the pollutant, but since the mineralisation is not a one-step process, oxidation intermediates will be formed during the reaction. These degradation intermediates (DIs) can potentially carry a higher toxicity than the original micropollutant and therefore needs to be controlled.

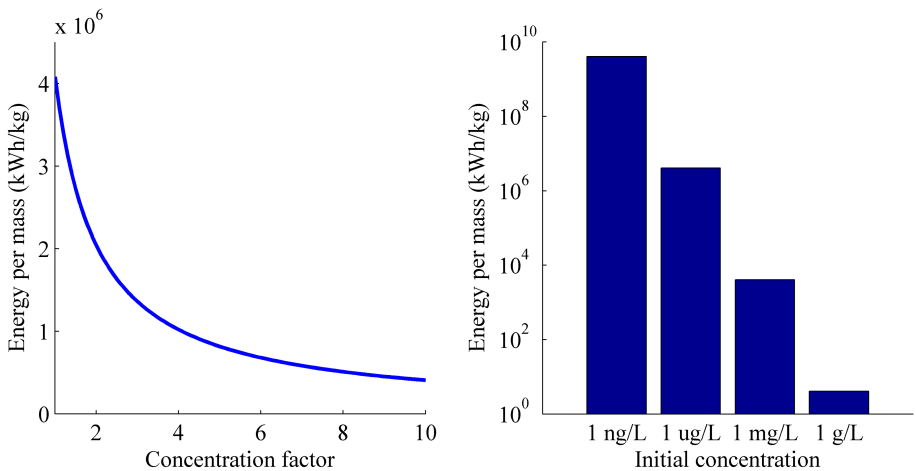

Figure 5 Theoretical effect of concentration on energy consumption of 99% EE2 degradation. To the left is shown the effect of the concentration factor with a starting concentration of 1 µg/L, and to the right the effect of initial concentration is shown. The concentration factor can be used to evaluate the effect of applying membrane filtration to environmental relevant concentrations (µg/L), while the initial concentration illustrates the difference between energy consumptions of typical laboratory investigations (mg/L – g/L) and environmental concentrations (ng/L – µg/L).

In total these results point to the need for a separation of the pesticides from the main body of the water prior to degradation with AOPs. This will result in a smaller volume of water in need of treatment, and the higher concentration may potentially further benefit the cost of the degradation because of the first order kinetics of AOP degradation of low concentration pollutants, where rate of reaction is proportional to pollutant concentration. A higher rate of reaction would lead to shorter reaction times and thereby lower energy consumption per mass of pollutant. Returning to the photocatalytic degradation of EE2, the theoretical energy consumption per kilogram EE2 can be calculated from the kinetic data and plotted as a function of the concentration factor, see figure 5. In the calculations a starting concentration of 1 µg/L is assumed, and it can be seen that an eightfold reduction in energy can be obtained by increasing the concentration with a factor of ten. This is of course based on the assumption that reaction conditions are the same and that the concentration is sufficiently low to allow for first order kinetics. At higher concentrations, a surface driven AOP will experience saturation at the surface and the kinetics becomes zero order and independent of pollutant concentration.

One way of increasing the concentration is by membrane filtration as suggested by Miralles-Cuevas et al. [35]. They used a nanofiltration membrane to concentrate five different pharmaceuticals prior to degradation with a photo-Fenton process, and found that H_2O_2 was used more efficiently when filtration had been used to concentrate the pharmaceuticals. They also found that the increase of the inorganic content reduced the kinetic constant, highlighting the importance of optimizing the use of membranes. Another advantage of combining AOPs with membranes is that the pesticides are removed from the main water stream before degradation occurs. This ensures that possible DIs do not end up in the main part of the water, and can be more easily handled. One AOP that could benefit particularly from a membrane pre-concentration is electrochemical oxidation. Membrane filtration would lead to an increase in ionic strength, which would give a lower ohmic resistance of the solution and hereby possibly a more cost effective degradation.

Though the use of membranes together with AOPs is new, membranes for pesticide removal have been extensively studied in literature [21,36–39], and there are even reports from water treatment plants where membranes have been employed to remove pesticides [40–42]. Based on these experiences, there is no doubt that membranes are capable of removing pesticides, but several obstacles remain. Generally the focus has been on nanofiltration membranes with a pore size close to 1 nm, which gives them a molecular cut-off (MWCO) around 200 Da. This has been sufficient for many of the pesticides investigated in literature, but the tendency has been to focus on the pesticides that are actually applied during pest control. As can be seen in table 1 and table 2 the majority of pollutants found in the groundwater are not pesticides, but transformation products. Many of these have molecular masses below 200 Da, which may affect the efficiency of the way they are rejected by the membranes. Furthermore, even when good rejections are obtained, there are always a small percentage of the pesticides that are transported through the membranes, and current membrane technology is therefore incapable of ensuring a complete removal of pesticides. This may be important if the pesticides exert effect down to ng/L and pg/L levels. Also, membranes tend to foul over time, and a pre-treatment may be necessary to avoid significant loss of performance.

1.6 Research objectives

Based on the information presented so far the overall objective of this thesis is

To study how pesticides and pesticide transformation products in groundwater can be removed by using systems of membrane filtration and electrochemical oxidation without introducing additional chemicals to the drinking water.

To fulfil this objective, the following specific tasks are addressed:

- Develop analytical HPLC ESI-MS and HPLC UV methods for qualitative and quantitative determination of pesticides and the intermediates formed during reaction.
- Explore the possibility of using the existing aeration and sand filtration process as a pre-treatment method without use of chemicals to reduce fouling and scaling on the membranes.
- Investigate the applicability of commercial membranes for removing pesticides and pesticides transformation products from polluted groundwater.
- Study the use of more advanced membrane techniques to increase the membranes applicability for treatment of pesticide polluted waters.
- Investigate the efficiency of electrochemical oxidation for degradation of key pesticides/PTPs and determination of the type and amount of degradation intermediates.
- Study the effect of coupling membrane filtration with electrochemical oxidation on the degradation of key pesticides/PTPs.

Chapter 2 Membrane filtration for removal of pesticides

Because of the short comings of activated carbon filters there have been an increasing interest in the use of membranes for removal of pesticides, and as a result, there is already a relatively thorough understanding of the principles of membrane filtration for pesticide removal.

2.1 Principles of membrane filtration

The general principle of membrane filtration is the use of a semi-permeable barrier to separate the components of a solution by using one or more gradients as the driving force. One way of categorising membrane filtration is as such the driving gradient as seen in table 5.

Table 5 Overview of membrane processes categorised based on driving force.

Pressure driven		Non-pressure driven	
Membrane process	Driving force	Membrane process	Driving force
Microfiltration (MF)	Pressure	Dialysis	Concentration
Ultrafiltration (UF)	Pressure	Electrodialysis	Electrical potential
Nanofiltration (NF)	Pressure	Pervaporation	Pressure
Reverse osmosis (RO)	Pressure	Forward osmosis	Osmosis
		Membrane distillation	Vapour pressure

For removal of pesticides the main focus has been on pressure driven membranes, which are also the most widely used type of membranes in industry. The pressure driven membranes are primarily divided based on their pore size and/or the type of particles that they are used to filtrate away. In figure 6 an overview of the different areas in which the four types of pressure driven membranes are typical used is illustrated, where moving from right to left the pore size of the membranes changes from around 10 µm for MF membranes to practically non-porous for the tightest RO membranes [43]. Since many pesticides are close to the size of glucose it can be seen from figure 6 that for removal of pesticides, the membranes of main interest are RO and NF membranes. Nanofiltration membranes are typically viewed as being between RO and UF, but there is no clear cut of where the specific range is. Another typical feature of NF membranes is that their surface is more charged compared to RO and UF membranes, which also affects the performance of these membranes. There is another category of membranes in between RO and NF membranes that have not been shown in the figure 6. These are called low pressure reverse osmosis (LPRO) or ultralow pressure reverse osmosis (ULPRO) membranes. As the name suggests these are reverse osmosis membranes that operate at lower pressures compared to standard RO membranes. Together with NF membranes these have had the highest focus in the investigations since they are more economical to use compared to RO membranes used for desalination [21,39].

The two most important design parameters of NF/RO membranes are rejection and recovery. Rejection is the measure of how well a given compound is retained by the membrane, and is calculated from the feed (C_F), concentrate (C_C) and permeate (C_P) concentrations as shown in equation 1.

$$\text{Rejection} = 1 - \frac{C_P}{\frac{1}{2}(C_F + C_C)} \tag{1}$$

Where rejection determines the applicability of a given membrane to remove pesticides from water, recovery determines how much of the feed water is recovered as permeate. It is defined as the ratio of the feed (F_F) and permeate (F_P) flow.

$$\text{Recovery} = \frac{F_P}{F_F} \tag{2}$$

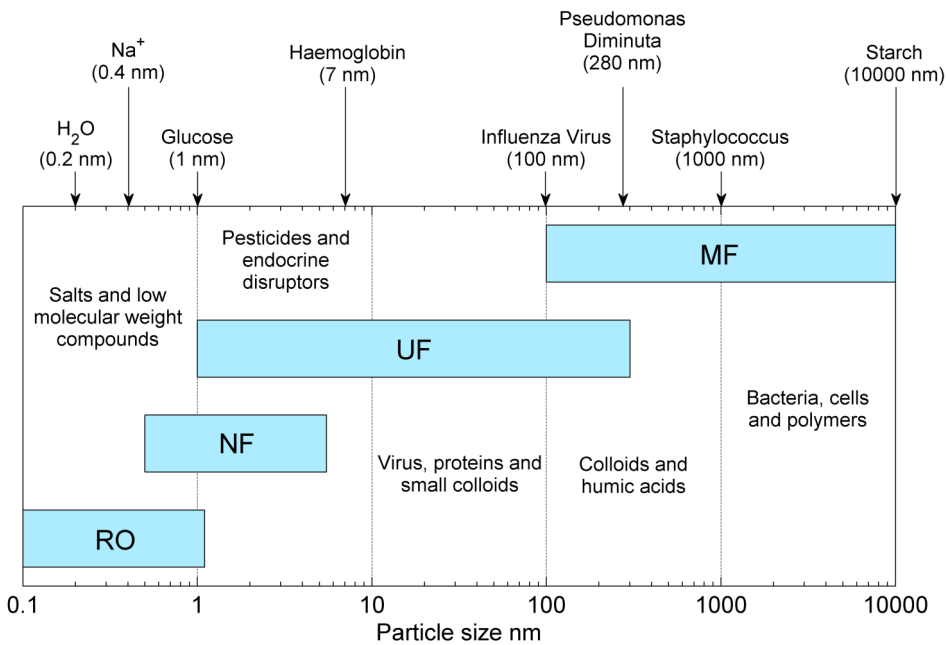

Figure 6 Range of applicability for MF, UF, NF and RO membranes. The horizontal bars shows the range of particles sizes within which each of the four membranes types are most typically used, and compares the size of the particles to the size of well-known examples.

From an economical perspective and also with respect to removal of pesticides, it is desirable to have as high a recovery as possible because this will decrease the loss of water as concentrate and increase the concentration of pesticides in the concentrate. But as recovery increases, the concentration of solutes increases and this may lead to problems with fouling and scaling of the membranes. Fouling refers to deposition of organics, colloidal particles and microorganisms (biofouling) on the membrane, while scaling refers to the precipitation of inorganic salts for which the ion product exceeds the solubility constant. Therefore, the composition of the feed water will often be the limiting factor for the recovery.

2.2 Removal of pesticides with membranes

Because the NF/RO membranes used for pesticide removal operate in the transition area between porous and non-porous membranes, several factors influence the rejection of pesticides. The following properties of membranes and pesticides have been found to affect the rejection [21,44–46]:

1. Size of pesticide and pore radius of membrane
2. Charge of membrane and pesticide
3. Dipole moment of pesticide
4. Relative hydrophobicity of membrane and pesticide

In general, the size of the pesticides relative to the pore radius of the membrane is the most important factor determining rejection of pesticides. This has been shown in studies in which the molecular weight cut-off (MWCO) of membranes has been correlated to the rejection of pesticides with varying molecular weight [46–48]. MWCO is defined as the molecular weight at which 90% rejection is obtained, and because of the readily availability of the molecular weight, this has been a popular size parameter for pesticides. However, studies have also shown that deviations from the molecular weight/MWCO correlation exists [49,50], showing that the model is not perfect. This is because the use of molecular weight fails to take into account the spatial geometry of the pesticides, which is important when the length and width of the pesticides are very different. It has been shown that for uncharged alcohols that do not interact with the membrane, the rejection can be described by considering each molecule as a freely rotating parallelepiped [44], and this may offer an improved approach to describing the steric rejection by NF/RO membranes. However, whether the model applies to pesticides has not been investigated, and it is possible that other interactions between pesticides and membranes may affect the applicability of the model.

Most NF membranes have a negative surface charge at neutral pH due to the existence of carboxylic groups in the active layer. The presence of charge bearing groups in the molecular structure of a pesticide may therefore highly influence the expected rejection, with negatively charged pesticides experiencing a higher rejection than expected based on steric considerations [51]. Most pesticides are uncharged at neutral pH, but many contain carboxylic and/or amine groups that may become charged. Furthermore, the charge of the membrane may also affect the rejection of uncharged pesticides via their dipole moment. In a study by Van der Bruggen et al., a comparison between pesticides and saccharides showed that a high dipole moment could lead to a reduced rejection

because the individual pesticide oriented itself along the axis of its dipole moment, which lowered the cross sectional area of the part of the pesticide facing the membrane [50].

The relative hydrophobicity of the pesticide and membrane may also influence the rejection, since it determines the degree of adsorption of pesticide to the membrane that can be expected. In a study of aromatic and non-phenylic pesticides, a clear correlation was identified between the $\log K_{ow}$ of the pesticides and the degree of adsorption [52,53]. The rejection was not correlated with $\log K_{ow}$, but this may be ascribed to the further complexity of the rejection process. If diffusion of pesticides through the membrane polymer matrix is important for the overall rejection, adsorption becomes very important since it is the first step in the transport process. If the rejection is mainly driven by pore flow, then the influence of adsorption on the rejection value decreases.

Not only interaction between membrane and pesticide determines the rejection. Rejection of pesticides are usually found to be higher in real waters compared to the synthetic laboratory solutions in demineralised or distilled water, which further complicates the mechanism of rejection [46]. The following parameters of the feed solution have all been found to affect pesticide rejection [46,54–56].

1. Ionic content and pH
2. Presence of organic foulants in the water
3. Presence of other pesticides/micropollutants in the water

The higher ionic content of real waters compared to demineralised and distilled water is one of the most important reasons for the observed increase in rejection. In studies of tangential streaming potential of membranes in solutions with varying ionic content, it has been shown that the zeta potential becomes increasingly negative with increasing ionic content and that this increase in negative charge can be explained with anion adsorption [57,58]. Anions adsorption will tend to dominate over cation adsorption because the hydrated radius is smaller for anions, and they are therefore better able to rid themselves of their sphere of hydration. The ions may adsorb in the pores or on the membrane surface where they partially block the pore entrance and hereby lower the effective pore radius. Another effect that has been suggested is that the increase in ionic strength will reduce the electrical double layer as it is known to occur for suspended particles. The contraction of the electrical double layer will lead to a reduced repulsion of the pore walls, and the pores may contract and result in a smaller pore radius [59].

The effect of organic foulants in the water is also important for the rejection, but more complex since they may both lead to increased or decreased rejection depending on how they interact with the pesticide and the membrane. Low molecular weight fractions of humic compounds have been found to increase the rejection of triazine pesticides, because they enter into complexation with the pesticides and hereby increase the apparent size of the pesticides. However, in the same study a lower rejection was also observed for one of the triazine/humic compound combinations, illustrating the complex interplay [54]. An enhancement of this effect can be observed when divalent cations such as calcium are present. These ions may also enter into the complexation and hereby increase the rejection. In the study, increased rejection were observed at very low calcium

concentrations (4 mg/L), and this effect may as such be important for groundwater pollution where high amounts of both calcium and organics can be found [54].

Not only humic compounds, but also other pesticides or micropollutants may affect the rejection. It has been found that the rejection of individual pesticides is different in solutions containing multiple pesticides compared to solutions of only single pesticides [56]. Furthermore, the effect may also depend on the type of membrane. For loose NF membranes, i.e. relatively large pore radius, it was found that the rejection increased, while for tight NF membranes, i.e. relatively small pore radius, it decreased. The decrease has been explained by competitive adsorption of the pesticides, where the occupation of an adsorption site by one pesticide leads to less adsorption and therefore higher flux of another pesticide through the membrane. For the loose NF membrane it was speculated that the largest pesticide could adsorb in the pores and hereby block the transport of the smaller pesticides [56].

Finally, organics may also foul the membrane and hereby change the surface chemistry, which can impact the rejection. If the pesticides are readily dissolved in the fouling layer, the effect of the fouling layer may be to increase the concentration of pesticides in the close proximity of the membrane, and this may lead to a decrease in rejection due to selected transport of the pesticide through the fouling material. If on the other hand the fouling layer acts as an additional barrier for the pesticides to cross, the rejection may increase [55].

In general, the use of membranes is found to be an effective method for rejection of pesticides. In an recent overview by Plakas and Karabelas, the results from several studies where collected and arranged after type of membrane and pesticide used in the studies [60]. Although many of the same pesticides have been used in the studies, the overall finding is that for most of the investigated pesticides rejections > 90% can be obtained by choosing the best membrane. However, for some small pesticides like diuron, it has been difficult to obtain rejection values > 90%. In the case of diuron this is ascribed to its elongated molecular structure, which gives it a small cross sectional area when facing the membrane with shortest side, see figure 7.

This highlights the importance of being able to predict rejection not only from molecular weight, but also from length and width of the pesticides.

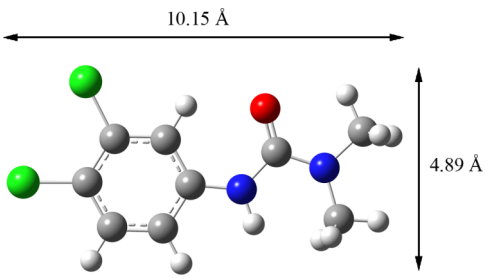

Figure 7 Spatial geometry of the pesticide diuron.

2.3 Transport model for pesticides through membranes

For filtration of uncharged species, there are generally two types of models that can be applied to describe rejection: Diffusive and steric (pore flow) models.

The model used to describe diffusive transport is called the Solution Diffusion Model [43]. In this model the membrane is considered non-porous and rejection occurs via competitive diffusive transport of water and solute/pesticide across the membrane. Diffusion of the solute is due to the existence of a concentration gradient across the membrane and can be described by equation 3.

$$J_S = \frac{P_S}{l} \cdot \Delta C \quad , \quad P_S = D_S K_S \tag{3}$$

Here l is the thickness of the active layer of the membrane and P_S is the permeability constant, which is the product of the diffusion coefficient, D_S, and the sorption coefficient, K_S. The sorption coefficient is the ratio of the activity of the solute in the solvent phase and in the membrane, which means that different permeabilities can be measured for different solvents. In this work, the solvent has exclusively been water, and the permeability is therefore a good approximation of the diffusion coefficient. With knowledge of the permeability of a given solute, the water flux can be used to model the rejection. The Solution Diffusion model has especially been successfully used to describe desalination processes, but as can be seen from equation 3, it is limited by the need to know diffusion and sorption coefficient that will be unique for each pesticide and membrane. Application of the solution diffusion model is therefore not straightforward in the case of pesticide filtration, and it may also be argued whether it is the correct model to use. With use of scanning electron microscopy (SEM) and atomic force microscopy (AFM), pores have been directly observed in NF/RO membranes[ii] and it may as such be more appropriate to use a pore flow model.

As already mentioned a steric pore flow model has been proposed and validated for uncharged and hydrophilic alcohols by Kiso et al. [44,61]. This model has been the most used model in the investigation of the rejection of pesticides in the thesis, and will therefore be discussed in more detail.

For a steric model the basic property is the ratio of solute radius to pore radius, λ.

$$\lambda = \frac{r_s}{r_p} \tag{4}$$

When the radius of the solute is larger than the pore radius, the solute will be completely rejected by the membrane. When the solute radius is smaller than the pore radius, the solute may enter the pore and this is described with a steric partitioning coefficient, Φ. For spherical solutes, Φ is calculated directly from λ [44,61–63].

[ii] It should however be mentioned that when the membranes are investigated with SEM and AFM, they have been dried and coated with a thin conductive layer of metal (gold, platinum, etc.) The membranes are as such not observed in their true fully hydrated environment, and the porous vs dense debate continues.

$$\Phi = (1-\lambda)^2 \tag{5}$$

However, if we want to take into account that the solute is not spherical, a different approach is necessary. As previously mentioned Kiso et al. considered the molecules to be freely rotating parallelepiped in which length was determined as the longest axis through the molecular structure, and the width as the average side length of the rectangle enclosing the molecule perpendicular to the length axis. This average width was then called molecular width, MWd. Drawings and a detailed description can be found in the paper by Kiso et al. [61]. With the length and MWd it is possible to calculate the cross sectional area of the solute, and the steric partitioning factor then becomes the ratio between the cross sectional areas of solute and pore. Because the cross sectional area of a non-spherical solute changes with rotation, the steric partitioning coefficient must be calculated at angles from 0 to $\pi/2$, and Kiso et al used a sinus function to describe this rotation.

When inside the pore, the permeation is dependent on both convective and diffusive transport described by the convective and diffusive hindrance factors (K_c and K_d), which are defined as

$$K_c = \frac{v}{v_w} \quad , \quad K_d = \frac{D_p}{D_\infty} \tag{6}$$

Here v is the solute velocity in the pore and v_w is the solute velocity in the solvent. Similarly D_p is the solute diffusion coefficient in the pore and D_∞ is the bulk diffusivity. The values of velocity and diffusivity need not be determined because the hindrance factors can be calculated from empirical coefficients. The enhanced drag coefficient (K^{-1}) is used to calculate K_d and the lag coefficient (G) is used to calculate K_c. These two empirical coefficients can be calculated from the λ-value of the solute.

$$K^{-1}(\lambda) = a + b\lambda + c\lambda^2 + d\lambda^3 \tag{7}$$

$$G(\lambda) = e + f\lambda + g\lambda^2 + h\lambda^3 \tag{8}$$

Where the values of the constants have been reported in literature [62,64,65] .

For $0 < \lambda \leq 0.8$

$$a = 1.0, b = -2.30,\ c = 1.154 \text{ and } d = 0.224$$

$$e = 1.0, f = 0.054,\ g = -0.988 \text{ and } h = 0.441$$

And for $0.8 < \lambda \leq 1.0$

$$a = -0.105,\ b = 0.318,\ c = -0.213 \text{ and } d = 0$$

$$e = -6.830, f = 19.348,\ g = -12.518 \text{ and } h = 0$$

It has later been shown that it is possible to use the first set of constants to describe the entire range from $0 < \lambda \leq 1.0$ with satisfactory results [61].

In case of NF/RO filtration of pesticides, the pores of the membranes can be expected to be relatively long and narrow compared to the pesticides, and the lag coefficient should therefore be multiplied with (2-Φ) for correction. Otherwise the hindrance factors are equal to the lag and drag coefficients.

$$K_c = (2-\Phi)G(\lambda) \tag{9}$$

$$K_d = K^{-1}(\lambda) \tag{10}$$

However, as seen, it is necessary to use λ in the calculations, which necessitates the knowledge of a solute radius. The common approach is to use a correlation of the size parameters for the solutes and their Stokes radius. In the work by Kiso et al., a correlation between MWd and the Stokes radius is used [61].

$$r_s \cdot 10^{-9} = 1.42\left(MWd \cdot 10^{-9}\right) - 0.142 \cdot 10^{-9} \tag{11}$$

With knowledge of the hindrance factors, it is possible to show that the transport equation for a solute across a porous membrane by diffusive and convective flux can be described with equation 12.

$$J_S = -K_d D_\infty \frac{dC}{dx} + K_c C \frac{J_W}{A_k} \tag{12}$$

Which can be rewritten to an expression for rejection[iii].

$$R = 1 - \frac{K_c \Phi}{1-(1-K_c\Phi)\exp(-Pe)} \tag{13}$$

If the pore radius of a membrane is known, equation 13 can be used to calculate rejection values of solutes based on their geometrical parameters. If the pore radius is unknown, the rejection can be measured for a number of solutes with known geometries, and used to calculate the pore radius. This is done by calculating the rejection for the known compounds over a range of pore radii, finding the squared difference between measured and calculated values and then minimising the sum of squares.

Although the model has been found to give good results, it is also limited by some of the approximations underlying it. From the previous discussion, it can be seen that the model assumes no interactions between the solute and the membrane (which may be questioned as was discussed in section 2.2) and that only pore transport is occurring. From a fundamental point of view, the most critical assumption is however that the model assumes a uniform pore size, contrary to what is

[iii] See [149] for derivation.

observed for real porous membranes, which are found to have a distribution of pore sizes. One steric pore flow model that acknowledges this pore size distribution is the log-normal model, where the pore size distribution is assumed to follow the log-normal distribution. In this model, the rejection is a function of two factors: the average pore radius, $\bar{r}$, and the standard deviation of the distribution of pore radii, S_p [66].

$$R(r) = \int_0^r \frac{1}{S_p\sqrt{2\pi}} \frac{1}{r} \exp\left(-\frac{\left(\ln(r) - \ln(\bar{r})\right)^2}{2S_p^2} \right) dr \tag{14}$$

The model may be solved with software with build in solvers for these kinds of distributions or by calculating the rejection, for a combinatorial set of average pore radii and standard deviations, and then determine the set that gives the lowest squared difference with the measured rejections. Even though this model takes the existence of a pore size distribution into account, it may be considered even simpler since it does not take any hydrodynamic lag in the pores into account. Other models exist, both variations of the models already described in this text and models that have not been covered. For a more thorough evaluation of these the reader is referred to literature. A good place to start may be the paper of Van der Bruggen et al. [66] that offers a comparison of a set of different steric models. In appendix A1 and A2, examples of Matlab files for solving the models covered here may be found.

To end the discussion on membranes, some of the emerging technologies that may improve the pesticide removal with membranes are highlighted.

2.4 Emerging technologies in membrane science – nanoparticles

One of the areas of membrane science that has received much attention recently is the implementation of nanoparticles. Especially inorganic metal/metal oxide nanoparticles have been used and a range of different metals has been investigated. Some of the most studied materials are: silver, iron, zirconium, aluminium, magnesium, titanium and silica, but also more exotic particles such as carbon nanotubes have been investigated [67]. The nanoparticles contribute to the functionality of the membrane in different ways, and an overview of some of these can be seen in table 6. The main effect of the addition of nanoparticles to the membrane structure is to increase the hydrophilicity and in this way increase water flux and lowering fouling. This can be done because of the hydrophilic nature of metal oxides and the fact that most foulants are hydrophobic.

With respect to pesticide removal, the most interesting aspect of doping with nanoparticles is the effect on rejection properties. Increased rejection of pesticides could be obtained if doping with nanoparticles increased the water flux without increasing the flux of pesticides to the same extend or if the nanoparticles could result in a narrower pore size distribution. However, no clear effect of nanoparticles on rejection has been found.

Table 6 Overview of the use of nanoparticles in membranes. From Kim and Van der Bruggen [68].

Type	Size (nm)	Functionality
Titanium dioxide	20-30	Chemical resistance High water permeability Photocatalysis
Iron oxide	4-6	Sorbent Catalysis
Silver	1-70	Biofouling prevention
Alumoxane	10-21	High water permeability Narrow size pore distribution
Ferroxane	100	Resistant to acid, corrosive media and oxidant
Carbon nanotube	1-9	Unique structure Sorbent Electrical and thermal conductivity

In an overview of Taurozzi et al. [69], rejection values were reported to both increase, decrease and stay unaffected. None of the experiments involved pesticides. An interesting case was reported by Balta et al. [70] who used ZnO in a UF membrane, and were able to increase the rejection of methylene blue significantly from around 60% to > 90%. Part of this increase was explained as an improved electrostatic repulsion of the cationic dye by the ZnO particles, but the MWCO was also found to change from around 430 to 340 Da and may as such also have contributed to the increased rejection. Still, a MWCO of 340 Da is too high to make the membrane applicable for pesticide removal, where a MWCO between 100 and 200 Da is necessary. To obtain a MWCO in this range, it is often necessary to use a thin film composite (TFC) membrane. In a study by Rajaeian et al. functionalised TiO_2 nanoparticles were added to the polyamide layer of a TFC membrane, and here it was found that by adding small amounts of particles (0.005 wt.%), the rejection of NaCl could be increased from around 50% to 54% [71]. In total it seems that the addition of nanoparticles can be used to increase rejection, but the effect is not expected to be substantial. However, one approach that could be promising is to use the nanoparticles as adsorbents of pesticides, as suggested by Ng et al. who stressed the ability of silica nanoparticles to trap molecular sized impurities [67].

Another very interesting area of membrane research is the use of aquaporin proteins as a kind of organic nanoparticle. Aquaporins are pore-forming proteins that are found in living cells where they enable a selective transport of water across the membrane, and by incorporating them into industrial membranes, a high water flux biomimetic membrane can be produced. The idea was first brought up in 2006 by Bowen [72], but has since then been reported in several membrane papers [73–79]. So far the research has been focused on how to incorporate the protein channels in the membrane structure without destroying their biological activity and on their use in desalination. The applicability of aquaporin membranes on the removal of pesticides has therefore not been investigated, but due to the high selectivity of the aquaporins, the prospects are very interesting.

Chapter 3 Electrochemical oxidation for degradation of pesticides

As with membrane filtration, electrochemical oxidation for degradation of organic pollutants is a relatively new technology that has mainly been developed over the past twenty years, primarily beginning with the work of Comninellis in the early nineties [80]. Since then much research into electrode materials and fundamentals of the degradation process has been made together with investigations of the applicability of the technology to treat an immense amount of otherwise recalcitrant compounds. Especially on wastewater much work has been done, as shown in the several reviews on the use electrochemical oxidation in this area [26,80–82]. Several reviews that are focused on more general water treatment and the mechanisms of electrochemical oxidation also exists [83–85]. On the other hand, research on degradation of pesticides with electrochemical oxidation is scarce compared to the use of other AOPs [25] and some of the most commonly investigated pesticides are the organophosphates, which with respect to Danish groundwater pollution is a limited problem, except for a few extreme cases related to dumps of chemical waste [86].

The main advantage of electrochemical oxidation in relation to many of the other AOPs, is that no chemicals are used and the only reactant that is added to the system is the electron [23]. The general principle of electrochemical oxidation of organics, is the generation of hydroxyl radicals through oxidation of water, reaction scheme 15, which will mineralise present organic pollutants, R, reaction scheme 16, [81].

$$H_2O \rightarrow \bullet OH_{ads} + H^+ + e^- \tag{15}$$

$$\bullet OH_{ads} + R \rightarrow mCO_2 + nH_2O + xH^+ + ye^- \tag{16}$$

In reality, the process is more complicated and will depend both on electrode material and water composition.

3.1 Principles of electrochemical oxidation

The process described in reaction schemes 15 and 16 is a generalisation of the part of the electrochemical oxidation process that is called the electrochemical oxygen transfer process (EOTR). In this process, the pollutant is degraded by quasi adsorbed oxygen species on or in the vicinity of the anode, but depending on the anode material this can occur both via physisorbed hydroxyl radicals ($MO_x(\bullet OH)$) or via chemisorbed active oxygen (MO_{x+1}) as shown in figure 8.

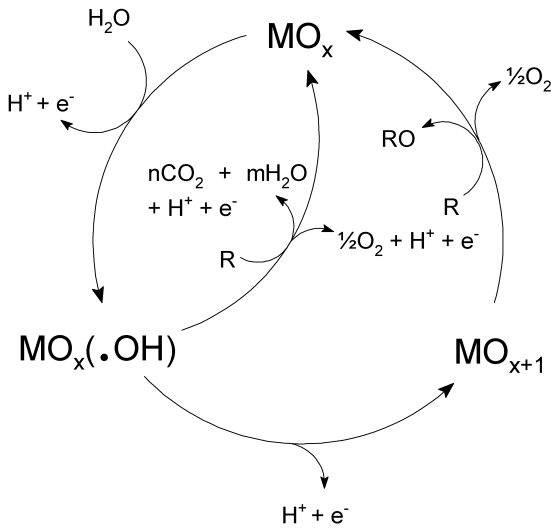

Figure 8 Schematic illustration of the EOTR process. Reprinted from Comninellis, C. (1994) *Electrochimica Acta*, 39,11-12, p. 1857-1862 [87] with permission from Elsevier

Whether the degradation occurs via physisorbed hydroxyl radicals or chemisorbed active oxygen depends on the anode material. If there is a higher oxidation state available for the anode material above the potential for oxygen evolution (1.23 V vs. SHE), then the adsorbed hydroxyl radical may form an oxide with the metallic anode material (MO). Anodes that tend to form these oxides are called active, while anodes that do not interact with the hydroxyl radicals are called non-active [80]. Active anodes are generally more specific with respect to the compounds they oxidize and may therefore not lead to complete mineralisation. Also, the stronger the interaction between the hydroxyl radical and the anode surface is, the higher is the electrochemical activity towards oxygen evolution [23]. Oxygen evolution is a competitive side reaction to the oxidation reaction and results in a loss of efficiency, and to obtain the most efficient oxidation process non-active anodes with a high O_2 overpotential[iv] should be preferred. In a review of Comninellis et al. an overview of different anode materials is given, see table 7 [23]. In general the boron doped diamond (BDD) anode is accepted as the most efficient anode with respect to both limiting oxygen evolution and the ability to mineralise pollutants and applications of this anode material has been reported in numerous studies, as is evident from table 8.

[iv] The overpotential for a reaction is the difference in potential between the thermodynamic (theoretical) reduction potential and the potential at which the reaction is experimentally observed to occur at a given electrode material.

Table 7 Comparison of anode materials according to oxygen overpotential and oxidation power. Active anodes are found in the top and non-active in the bottom of the table. Prepared after Comninellis et al., (2008) *J. Chem. Tech. Biotech.*, 83, p. 769-776 [23].

Electrode	Oxidation potential / V	Overpotential of O_2 evolution (V)	Adsorption enthalpy of M-OH	Oxidation power of the anode
RuO_2-TiO_2	1.4-1.7	0.18	Chemisorption of OH radical	
IrO_2-Ta_2O_5	1.5-1.8	0.25		
Ti/Pt	1.7-1.9	0.3		
Ti/PbO_2	1.8-2.0	0.5		
Ti/SnO_2-Sb_2O_5	1.9-2.2	0.7		
p-Si/BDD	2.2-2.6	1.3	Physisorption of OH radical	

The oxidation at the anode is not limited to organic pollutants, and other redox active species may also undergo oxidation depending on their formation potential. Formation of other oxidising species can play an important role in the electrochemical oxidation of pollutants since these oxidising species are not bound to the anode surface and may be transported to the bulk solution where they can mediate oxidation of organics. This type of electrochemical oxidation is called indirect oxidation and the most widely studied indirect oxidation agent is the chloride ion [22,80].

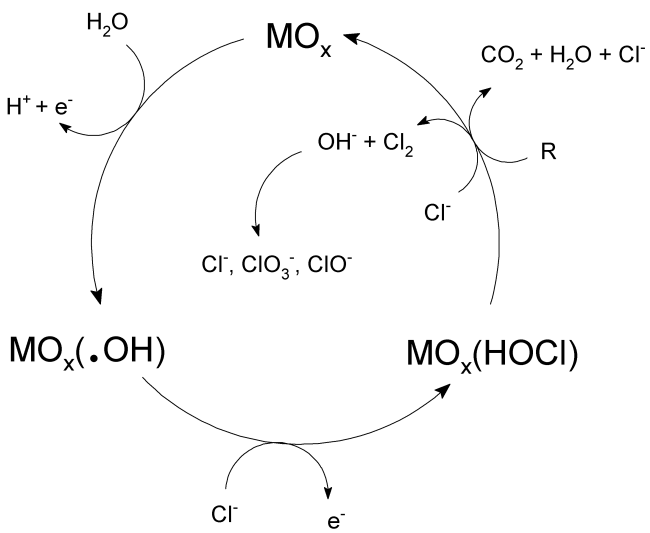

Figure 9 Schematic representation of the chloride mediated indirect oxidation process at non-active anodes. Reprinted from Bonfatti, et al. (2000) *J. Electrochem. Soc.*, 147, 2, p. 592-596 [88] with permission from the Electrochemical Society.

The indirect oxidation may be illustrated with a scheme similar to the one presented for the EOTR process, see figure 9. The first step of the process is the oxidation of the chloride ion at the surface of the anode to form adsorbed oxychloro species. These may then react with the organic pollutant, in which case surface oxidation takes place, or with another chloride ion to form chlorine, which may further react to form hypochlorous acid or hypochlorite depending on the solution pH. These chloro-species are then free to move into the bulk and act as oxidising agents. Since both ClO^- /HClO and Cl_2 may act as the oxidising agent, the collective term "active chlorine" is often used.

The presence of chloride in the solution may in this way enhance the degradation process of the pollutant, but the disadvantage is that chlorinated organic DIs are likely to be formed, and these may carry a higher toxicity than their parent compound [22].

To evaluate the efficiency of the electrochemical oxidation, the current efficiency is often applied. Current efficiency is a measure of the charge used to oxidise organic compounds relative to the total charge used in the process, and can as such be used to estimate the influence of side reactions. In practise there are several ways of determining the current efficiency, but three that are often used are: Instantaneous Current Efficiency (ICE), General Current Efficiency (GCE) and Mineralisation Current Efficiency (MCE).

ICE and GCE can both calculated from COD, with the following formulas [22].

$$ICE = \frac{(COD_t - COD_{t+\Delta t})V}{\frac{8I_{app}\Delta t}{F}} \tag{17}$$

$$GCE = \frac{(COD_0 - COD_t)V}{\frac{8I_{app}\Delta t}{F}} \tag{18}$$

Where I is the current intensity (A), V the solution volume (L) and F is Faraday's constant (96,485 C mol^{-1}). Multiplying the applied current with time gives the applied charge and dividing this with Faraday's constant converts it into a number of electrons. To convert this to an oxygen consumption, the number of moles of electrons is multiplied with a factor of 8, which is the equivalent grams of oxygen per moles of electrons spent in the standard oxygen reduction. It can be seen that ICE represents the current efficiency for the incremental removal of COD, whereas GCE is an average value for the current efficiency going from the starting COD to the COD at time t.

MCE is based on TOC and compared to ICE it is directed at the mineralization of organics instead of the total oxygen demand. It is calculated as the ratio of experienced TOC removal to the theoretical TOC removal [89,90].

$$MCE = \frac{\Delta TOC_{\exp}}{\Delta TOC_{theory}} \cdot 100 \quad , \quad \Delta TOC_{theory} = \frac{I_{app} \cdot M_C \cdot \Delta t}{F \cdot V \cdot ne} \tag{19}$$

Here M_C is the molecular mass of carbon and ne is the average number of electrons per carbon atom transferred in the mineralisation of the compounds of interest.

Although measures of current efficiency are practical methods for determining the efficiency, and hereby to a certain extend the costs, of an electrochemical treatment, it should be mentioned that current efficiencies based on COD and TOC may be of limited use when it comes to micropollutants such as pesticides. In natural (un-spiked) waters, the concentration of micropollutants will be well below the detection limit for COD and TOC, and it may be more practical to calculate the current efficiency directly from the concentration of the micropollutant.

3.2 Electrochemical oxidation of pesticides and degradation pathways

In the beginning of this chapter, it was stated that the amount of work on pesticide degradation with electrochemical oxidation was scarce, which of course is a statement that should be considered relative to other AOPs such as the much more studied photocatalysis process. In table 8 a general overview of the research on pesticide degradation with electrochemical oxidation is provided, where the studies are compared based on the type of anode, pesticide and solution/electrolyte used in the experiments. In these studies, the effects of a range of parameters have been investigated. These include:

1. Electrode material
2. Type of supporting electrolyte
3. Current intensity/density
4. Initial pH of the solution
5. Starting concentration of pesticide

Probably the most important parameter has been found to be the electrode/anode material. As seen in table 8, BDD has been the preferred anode material and in the studies where this electrode material has been compared to metal oxides, BDD has in all cases been found to be superior concerning rate of reaction and mineralisation efficiency [103,107,116]. In all the studies with BDD presented in table 8 complete mineralisation has been obtained, whereas the mixed metal anodes often cannot obtain appreciable degradation of either the pesticides or degradation intermediates. In a comparative study of atrazine degradation with BDD and $Ti/Ru_{0.3}Ti_{0.7}O_2$, the oxide anode only resulted in partial degradation of atrazine while the degradation intermediate cyanuric acid was not affected [116]. In another study, the use of a PbO_2 anode resulted in the formation of formaldehyde showing an incomplete mineralisation of the pesticide methamiphodos. The use of SnO_2 resulted in less formaldehyde, and with a BDD anode no formaldehyde was seen [101]. Efficient degradation of pesticides can be obtained with metal oxide anodes, especially in the presence of chloride ions [86,98] and other halogens [115] which may form strong oxidants via the indirect oxidation mechanism. In the study referred to previously, the performance in atrazine removal of the $Ti/Ru_{0.3}Ti_{0.7}O_2$ anode became comparable to that of the BDD anode when 0.1 M NaCl was used as supporting electrolyte, and cyanuric acid could be degraded as well [116]. However, even in the presence of chloride, stable intermediates can be formed when using metal oxide anodes [86,115], which may limit the use of these anodes.

As seen with chloride, the supporting electrolyte can have a huge impact on the efficiency of the electrochemical oxidation process. Of the electrolytes investigated for pesticide degradation, chloride has in all cases but one been found to be superior. Only for the degradation of o-nitrophenol with BDD was the use of Na_2SO_4 found to be better than NaCl [117]. This was explained with the formation of persulphate, but the hypothesis may be questioned given the fact that the effect has not been observed in any of the other studies using sulphate based electrolytes. In general, NaCl is found to be the best supporting electrolyte for increasing rate of removal due to the formation of active chlorine. Concentration of the electrolyte is also important, and an optimum value may exist as shown by Bouya et al. who found a 2% NaCl solution to be optimal [112]. The decrease at higher concentrations of NaCl was hypothesised to be due to potentiostatic buffering by the chlorine evolution reaction. However, below the optimum value increasing the NaCl concentration will increase the rate of removal as shown by Malpass et al. who found an almost linear dependency of the TOC removal with NaCl concentration for the degradation of atrazine with a $Ti/Ru_{0.3}Ti_{0.7}O_2$ anode [98].

The investigation of current density, or in cases where electrode area has not been reported, current intensity, has been part of most of the studies in table 8. In general the rate of reaction increases with increasing current density [32,109,111,112,117,119], but increasing the current density too much may also have detrimental effects on the effectiveness of the electrochemical oxidation. In some of the studies increasing current density has resulted in lower rates of reaction as a function of applied electrical energy [98,103,110], which has been attributed to increased consumption of electrical energy by side reactions. Therefore, there may exist an optimum current density as shown by Malpass et al. [98]. Several optimum current densities have been reported ranging from around 20 to 80 mA cm^{-2} [98,101,107,112,116,117], but the specific value will depend on both the pesticide of interest as well as the setup used to investigate the degradation. This is due to the existence of a limiting current density, i_{lim}, for processes under mass transport control [85].

$$i_{\mathrm{lim}} = n \cdot F \cdot k_m \cdot C_{org} \tag{20}$$

Here n is the number of electrons involved in the mineralisation, F is the Faraday constant, k_m the collective mass transfer coefficient for the system and C_{org} the concentration of the organic pollutant. The mass transfer coefficient is the effective result of the flow regime in the cell and the diffusion coefficient of the pesticide. The type of pesticide can as such influence the limiting current density through the specific number of electrons required for the mineralisation, through its concentration and through its diffusion coefficient, while the setup can affect the limiting current density through the flow regime within the cell.

Table 8 Overview of studies on electrochemical oxidation of pesticides. The aim of the overview is to be a complete list, but given the many synonyms used for electrochemical oxidation processes in paper titles as well as the relatively loose classification for pesticides, some studies may have been overlooked. The table should however still be useful for creating an overview of the research in this area.

Anode	Pesticide	Solution specifications	Reference
Ti/Pt	Methylparathion	1, 2 and 3% (w/v) NaCl	[91]
BDD	4-CPA, MCPA, 2,4-D, 2,4,5-T	0.05 M Na_2SO_4; pH 3	[89]
BDD	Diuron, dichloroaniline	0.05 M phosphate buffer, 0.05 M H_2SO_4	[92]
Ti/Pt	Methylparathion	20 g/L NaCl	[93]
BDD	Amitrole	0.05 M Na_2SO_4	[94]
BDD	Atrazine, cyanuric acid, desethyldesisopropyl-atrazine	0.05 M sulphate buffer, 0.1 M phosphate buffer, 0.1 M NaOH, 0.05 M $HClO_4$, 0.05 M H_2SO_4	[95]
Ti/Pt	Demeton-S-methyl, metamidophos, fenthion, diazinon	4% (w/v) NaCl	[96]
BDD	MCPA, CPMP, MCPP	1 M $HClO_4$	[32]
BDD	Mecoprop (MCPP)	0.05, 0.10 and 0.5 M Na_2SO_4	[97]
Ti/$Ru_{0.3}Ti_{0.7}O_2$	Atrazine	0.1 M NaCl, NaOH, $NaNO_3$, $NaClO_4$, H_2SO_4, Na_2SO_4	[98]
Ti/$Ru_{0.3}Sn_{0.7}O_2$, Ti/$Ir_{0.3}Ti_{0.7}O_2$, Ti/$Ru_{0.3}Ti_{0.7}O_2$	Carbaryl	0.1 M NaCl, 0.033 M H_2SO_4	[99]
BDD	Methidathion	2, 3 and 4% NaCl	[100]
Pb/PbO_2, Ti/SnO_2, Si/BDD	Methamidophos	5% Na_2SO_4	[101]
BDD	Propham	0.05 M Na_2SO_4, 0.1 M $NaNO_3$, 0.1 M NaCl, 0.1 M $LiClO_4$, 0.05 M K_2SO_4; pH 3, 6, 9 and 11	[102]
BDD, Ti/PbO_2	Mecoprop (MCPP)	0.1 M $HClO_4$	[103]
Ti/Pt_{90}-Ir_{10}	Parathion, malathion, other organophosphates	Drainage water	[86]
BDD	Chlortoluron carbofuran bentazone	50 mM Na_2SO_4, pH 3	[104]
BDD	Atrazine	0.05 M Na_2SO_4 pH 2-7	[105]
BDD	Acetamiprid	Phosphate buffer, pH 7	[106]
BDD, Nb/PbO_2	Chlorpyrifos	H_2SO_4, pH 2	[107]
BDD, SnO_2	Bupirimate	2, 3 and 4% NaCl	[108]
BDD	Atrazine, cyanuric acid	0.1 M Na_2SO_4, pH 6.7	[109]
BDD, Pt	2-nitrophenol	0.05 M Na_2SO_4 pH 3	[110]
Ti/SnO_2	Pretilachlor	0.1 M Na_2SO_4 , pH 7.2	[111]
SnO_2	Cypermethrin	2% NaCl, NaOH, Na_2CO_3, H_2SO_4, Na_2SO_4	[112]
BDD	Endosulfan, deltamethrin	NaCl	[113]
BDD	Buprofezin	1g/L NaCl, Na_2CO_3, Na_2SO_4	[114]
Glassy carbon	Diazinon	0.1 M NaCl, KBr, KI	[115]
BDD, Ti/$Ru_{0.3}Ti_{0.7}O_2$	Atrazine, cyanuric acid	0.1 M NaCl, Na_2SO_4	[116]
BDD	o-nitrophenol	0.05 M Na_2SO_4 pH 3	[117]
Pt, BDD	Diuron	0.05M Na_2SO_4 pH 3	[118]

As seen from table 8, many experiments have been conducted at low pH values around 2-3. Many of the studies have also found that the rate of reaction is increased by lowering the pH [91,108,114,117], which may be explained by the increased oxidation potential of the hydroxyl radicals at lower pH, and it may justify the choice of a low pH. However, cases of optimal conditions at neutral pH have also been reported. In a study of the degradation of triazines with a BDD anode, Polcaro et al. found the rate of removal to be higher at neutral pH values compared to both acidic and basic values [95]. Speciation of the cyanuric acid to a less stable isomer was invoked as the explanation in this case, and it shows that the optimum pH is both a function of the oxidative potential of the hydroxyl radicals and the specific pesticide.

In investigations of the effect of the pesticide concentration, it has been found that higher initial concentrations leads to faster and more efficient treatments [103,107,110]. For all studies, the kinetics have been found to be pseudo first order, with the concentration of hydroxyl radicals being sufficiently larger or stable compared to the pesticide concentration. From traditional first order kinetic theory, increased pesticide concentration would not be expected to increase the rate constant, and the explanation for the increased rate of removal with concentration is therefore an increased mass transfer of pesticide from bulk to surface. The positive effect of increased pesticide concentration on the rate of removal is an important fact to keep in mind, especially for the combination with membranes where the purpose is to concentrate the pesticides prior to degradation. As an example, in one study the concentration was increased with a factor of four, but the time required for complete mineralization only increased with a factor of two [103]. Furthermore, as concentration increased, the current efficiency also increased, making the process even more economical.

Overall the studies on pesticide degradation with electrochemical oxidation show that the process is generally very effective, especially if performed with a BDD anode and with chloride as the supporting electrolyte. However, as with membranes, the studies have focused much on the pesticides as they are actually applied and not on the transformation products that are found in especially groundwater. Although the electrochemical oxidation must be expected to also be effective for the degradation of these compounds, it is necessary to investigate the exact degradation kinetics and degradation pathways to be able to evaluate the specific applicability of electrochemical treatment for a given pesticide/PTP. Furthermore, many studies are carried out a very low pH values. As discussed, the process is more efficient here, but not many natural waters can be found with pH values this low. In general there is a need to investigate the effectiveness of the degradation of pesticides in real water matrixes. As have been shown for the supporting electrolytes, different ionic environments may significantly impact the degradation and also the presence of other organic compounds may influence the effectiveness of the pesticide degradation. Oxidation of other organic compounds will be in competition with pesticide oxidation, and pesticides may adsorb to organics and particles and be shielded by these against oxidation.

3.2.1 Degradation pathways for pesticides with electrochemical oxidation

During a study of the degradation of chlorinated phenoxy acid pesticides by Boye et al., it was noted that the time it took for the pesticide concentration to be reduced below the detection limit was closely related to the time for complete mineralization [32]. The conclusion from this observation was that the amount of degradation intermediates was small. With an unselective nature such as that of the hydroxyl radical, degradation intermediates and pesticide molecules are also roughly expected to be degraded equally well, and at the end of an experiment the TOC and pesticide curves should therefore follow each other closely, assuming that the diffusion coefficients of the mother compound and the DIs are similar. However, between start and end of the experiment degradation intermediates may still be produced and exist in significant amounts. Due to the potential risk associated with degradation intermediates, control of these and general knowledge of the degradation pathway is important.

Of the studies on the electro-oxidative degradation pathways of pesticides, the most notable contributions have been made by the group of Brillas [32,103,105] and most knowledge has been gathered for phenoxy acid, triazine pesticides and organophosphates. Complete or partly mapped degradation pathways have been made for the following pesticides: Diuron, dichloroaniline, atrazine, cyanuric acid, DEIA, MCPA, CPMP, MCPP, malthion methamidophos, methyl-parathion, o-nitrophenol, parathion, pretilachlor and propham [32,86,92,93,95,97,101–103,105,111,117]. There is still some way to go before all pesticides have been investigated, but from these initial studies some general reaction principles for electrochemical oxidation of pesticides can be inferred.

Many pesticides contain one or more aromatic rings to which functional groups are bonded. From the investigations, it seems that the first point of attack tends to be electronegative centres such as ether bonds, nitro-groups, amine groups and chlorine atoms. These groups can be substituted by a hydroxy group or undergo a bond cleavage. As an example, for atrazine the first step is the loss of the ethyl group and then the isopropyl group resulting in two primary amines that are subsequently substituted with hydroxy groups [105]. Similar results have been found for DEIA [95]. The overall result is loss of side groups and formation of aromatic rings with hydroxy groups. In all cases three hydroxy groups seems to be the maximum number that are added to the aromatic ring before ring cleavage occurs. The result is a mixture of saturated and unsaturated dicarboxylic acids that are further degraded to oxalic acid, which is finally oxidised to CO_2.

All of these studies except one have focused on the EOTR mechanism, and it is as such the reaction between the pesticides and hydroxyl radicals/active oxygen that has been studied. However, in real waters the presence of the chloride ion is ubiquitous, and it may be expected that indirect oxidation mediated by chlorine species will occur. These may lead to formation of chlorinated DIs that may be especially troublesome. An improved understanding of the pathway for the indirect oxidation is therefore required.

3.3 Electrochemical oxidation of membrane concentrates

There is only very limited research on treatment of pesticides in membrane concentrates. Radjenovic et al. investigated the use of a $Ti/Ru_{0.7}Ir_{0.3}O_2$ anode for degradation of a range of trace organic contaminants in RO concentrate, and found most of them to be completely removed at current densities of 250 A m^{-2} [120]. In another study by Pérez et al., the use of a BDD anode to remove pharmaceuticals from RO treated wastewater was investigated [121]. For current densities between 20 and 100 mA cm^{-2}, they found rate constants in the range of $2 \cdot 10^{-2}$ min^{-1} to $8.6 \cdot 10^{-2}$ min^{-1}, which are not very different from the rate constants often found for pesticides in synthetic waters. Except for these selected studies, the main focus of papers on application of electrochemical treatment of membrane concentrates has been on the overall removal of organics measured as COD [122–127]. In general organics have been removed effectively, but one of the main obstacles has been the formation of chlorinated organics. Much of the research has been on wastewater effluents where the organic content can be relatively high, and this may have worsened the halogenation problem. Still, because organics and chloride ions can be expected to be present in most membrane concentrates, chlorination of organics should not be overlooked.

Chapter 4 Methodology

In this chapter the different experimental setups and the methods of analysis that have been applied during the Ph.D. will be covered. The experimental work has been carried out at Aalborg University Esbjerg, Denmark, and partly at KU Leuven, Belgium, where synthesis of membranes and tests of biomimetic membranes were made. All experimental setups will be presented, but of the analytical methods only the pesticide/PTP analysis will be presented; this was the main method used during the Ph.D. study, and it was specifically developed for this work. Furthermore, the pesticides/PTPs used in this study and the method used for determination of their spatial geometries are presented.

4.1 Characterisation of pesticides, membranes and groundwater

4.1.1 Pesticides and PTPs

In this thesis, two pesticides and two pesticide transformation products were chosen for the experiments: Atrazine, bentazon, BAM and DEIA. As seen previously BAM and DEIA are the main polluting compounds in the Danish groundwater. Furthermore, they are PTPs and have not been studied in the context of membrane filtration and AOPs before. Of the pesticides still in use, bentazon was the pesticide most often found in Danish groundwater at the onset of the Ph.D. study, and was therefore included in the study. Although atrazine has long been banned in Denmark, and is only found in a small amount of the groundwater samples, it was included as a reference compound. In an overview of membrane filtration of pesticides presented by Karabelas and Plakas, atrazine accounted for 23.9% of the total sum of pesticides used in the experiments [60]. Because of its widespread use in scientific work, atrazine was used to link this study to former studies.

In table 9 an overview of the data for the four compounds are given. Numbers of this kind are often presented in membrane filtration studies, but for many of these compounds, the amount of data is scarce and values often originate from isolated studies that have not been reconfirmed, which may lead to contradictory values. Based on the log $K_{o/w}$ values for bentazon and BAM, bentazon would be expected to have the highest aqueous solubility, but the reported solubilities give BAM the highest aqueous solubility. The pKa values are also often reported for protonated species, without that being properly indicated. The applicability of these data may as such be questioned. The geometrical parameters have been determined with use of a quantum mechanical method as described in the next subsection.

Table 9 Physical and chemical properties of pesticides used in the Ph.D. study.

	Atrazine	Bentazon	BAM	DEIA
Chemical structure	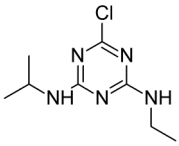	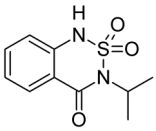	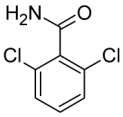	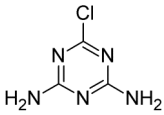
Formula	$C_8H_{14}ClN_5$	$C_{10}H_{12}N_2O_3S$	$C_7H_5Cl_2NO$	$C_3H_4ClN_5$
Molecular weight (Da)	215.69	240.28	190.028	145.55
Length (Å)	13.76	11.98	9.200	8.595
Width (Å)	6.267	7.493	5.784	3.950
Height (Å)	8.752	8.378	9.042	8.060
MWd (Å)	3.689	3.961	3.616	2.821
Log K_{ow}	2.68[54]	-0.46[128]	0.77[129]	-0.1[130]
Aqueous solubility (mg/L) 20 °C	33[128]	570[128]	2730 [131]	66[130]
pKa	1.7[56]	3.3[128]	13-14[132]	-

Modelling of pesticide molecular geometry

To determine the length and width parameters of pesticides the program Gaussian was used. With Gaussian a number of different models can be used to perform calculations on the molecular structure and properties of molecules, and each model differ with respect to precision and computational time. For large molecules mechanistic models can be used. These models consider the atoms in the molecules as charged spheres connected with springs, and due to the simplicity of this approach, time of calculation is low. In the original development of their steric model, Kiso et al. used such a model (MM2) to determine the stable conformation of the alcohols [44]. For higher precision a semi-empirical calculation method can be used. In these models empirical data is used to simplify the quantum mechanical calculations used by ab initio methods, and this allows for calculations on molecular structures of higher precision compared to molecular mechanics, while still being relatively fast. In their latest description of the steric model, Kiso et al. used a semi-empirical method [61]. However, semi-empirical methods are only as good as the empirical data available, and better results can be obtained by using ab initio methods such as Hartree Fock (HF) or Density Functional Theory (DFT).

In this work the DFT model B3LYP was used with a split valence basis set, 6-31++G(d). The use of a split valence basis set means that a higher accuracy can be made for the valence orbitals. These will be represented by a linear combination of Slater type orbitals (STO) whereas the inner core orbitals are only represented by a single STO. The reason for only applying one STO to the inner core orbitals is that a higher flexibility is required for the valence orbitals since these are the most important for chemical properties. By using a linear combination of STOs the electron cloud can be made to both contract and expand if necessary, and in this way the variability of orbitals in different environments can be accounted for. There will for example be a difference for p-orbitals

participating in “tight” σ-bonds compared to “loose” π-bonds. In the 6-31 basis set, six gaussian functions are used to approximate the inner core STO, while the valence orbitals are split into two STOs where three gaussian functions are used for the first and one for the second. “d” indicates that polarisation of atoms heavier than hydrogen are allowed in the basis set. In molecules the electrons on the atoms will affect each other and cause polarisation in the electronic distribution. Gaussian accounts for this by mixing orbitals. s-orbitals will as such be mixed with a little of the p-orbitals, and p-orbitals will be mixed with of some the d-orbitals. Finally, “++” indicates that diffuse functions are added to both heavy atoms and hydrogen atoms. Diffuse functions account for the case in which some electrons are more loosely associated with specific atoms, like for instance anions. In total the result of allowing for both polarisation and the use of diffuse functions, is to increase the accuracy of the model.

As an approximation of the spatial reach of the molecules, the Van der Waals radius was used, and this was taken to be equal to the isovalue density surface of the electrostatic potential at an electron density of 0.002 $e^-/Å^3$ [133].

The same procedure as described by Kiso et al. was used to determine length, width and height of the parallelepiped enclosing the molecule [61].

1. Determine length axis through the molecule.
2. Find side lengths of rectangle enclosing the molecule perpendicular to the length axis.
3. Use side lengths to calculate MWd. According to Kiso et al., this is done by taking the square root to the area of the rectangle found at the previous step.

In figure 10 atrazine has been used as an example to show how length, width and height are defined in this procedure.

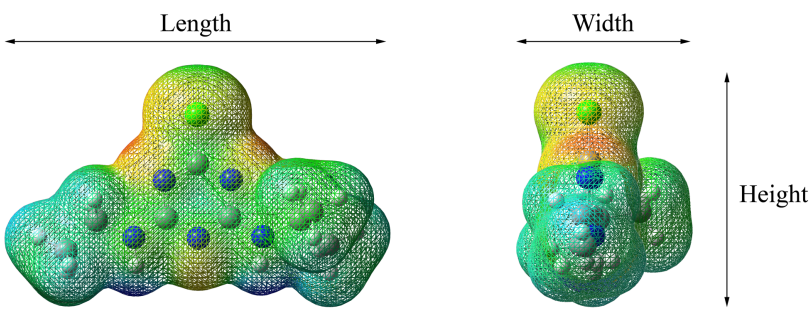

Figure 10 Measurement of spatial geometry. The figure is an example of how to measure length, width and height of a pesticide, in this case atrazine. The mesh surrounding the atoms is the isovalue surface of the electrostatic potential at an electron density of 0.002 $e^-/Å^3$.

4.1.2 Characterisation of groundwater used in experiments

In this study, groundwater from two waterworks was used in the experiments. The two waterworks were Astrup and Hvidovre waterworks, and they represent the extremes of hardness and ionic strength that can be encountered in Denmark. Being situated in the western part of Denmark, Astrup waterworks draws its groundwater from sandy soils with only little chalk and the groundwater is therefore very soft. Hvidovre is found in the eastern part of Denmark, in the Copenhagen area, where the subsurface is rich in chalk and the groundwater is hard.

At both waterworks, the groundwater was extracted after the sand filter. Iron and manganese had therefore been removed. In figure 11 and table 10 the location of the waterworks and the composition of the groundwaters are shown.

4.1.3 Characterisation of commercial membranes

Five commercial membranes were used in the Ph.D.:

- NF membranes (Alfa Laval, Nakskov, Denmark)
  - NF99
  - NF99HF
- LPRO/RO membranes (FILMTEC, The Dow Chemical Company)
  - NF90
  - XLE
  - BW30

To characterise the membranes, contact angle, zeta potential, rejection values for ionic compounds and pure water flux were determined. The results are summarised in table 11.

Figure 11 Location of the two waterworks, Astrup and Hvidovre

Table 10 Compositions of groundwaters used in experiments

Parameter		Astrup	Hvidovre
Ca^{2+}	[mg/L]	37	180
Mg^{2+}	[mg/L]	5.5	29
Na^{+}	[mg/L]	16	63
K^{+}	[mg/L]	1.7	6.3
Cl^{-}	[mg/L]	38	150
SO_4^{2-}	[mg/L]	59	140
HCO_3^{-}	[mg/L]	83	409
pH		7.6	7.2
C_{total}	[mM]	4.9	21
TOC	[mg/L]	< 1	< 1
UV_{254}	[cm^{-1}]	0.005	0.030

Table 11 Characteristics of the five commercial membranes used in the Ph.D.. Rejection data were found by filtrating groundwater from Hvidovre waterworks using the same protocol as for the pesticide filtration. Pure water flux was determined by using demineralised water at 10 bar. Contact angle was determined using distilled water. Zeta potential was determined for a 10 mM KCl solution, pH 5.

	NF99HF	NF99	NF90	XLE	BW30
Ca^{2+} (%)	69.0	74.0	98.5	97.2	98.5
Mg^{2+} (%)	71.2	84.0	96.5	95.8	96.1
Na^{+} (%)	53.0	45.9	91.1	91.8	93.7
K^{+} (%)	52.1	44.1	90.2	90.2	90.9
SO_4^{2-} (%)	88.8	94.3	97.7	97.0	97.5
Cl^{-} (%)	41.3	40.5	94.4	94.2	95.2
HCO_3^{-} (%)	63.5	69.4	95.1	93.3	95.9
Pure water flux (L h^{-1} m^{-2})	60.4	44.3	36.9	38.3	19.9
Contact angle (°)	< 20	24 ± 2	96 ± 3	112 ± 2	66 ± 4
Zeta potential (mV)	-19.4	14.2	-10.5	-19.4	-20

From the relative rejection of monovalent and divalent ions it can be seen that the NF99HF and NF99 membranes are true NF membranes, whereas NF90, XLE and BW30 are better characterised as RO membranes. The flux of NF90 and XLE are however much higher compared to BW30, and are close to the flux of the NF membranes. These are therefore LPRO membranes. The contact angle measurements show that the NF membranes are hydrophilic, whereas the LPRO/RO membranes are hydrophobic.

4.2 Analytical methods for quantitative pesticide analysis

When analysing for pesticides, state of the art is the use of chromatography coupled with mass spectrometry. Earlier, the use of gas chromatography dominated, but because many of the pesticides and their transformation products require a cumbersome derivatisation before they can be analysed due to thermal instability and/or polarity, use of liquid chromatography has in recent years become more widespread. The challenge is then to couple the HPLC that operates under high pressure and large solvent flow, with the mass spectrometer that operates near vacuum and with only very little solvent flow. To overcome this problem a number of techniques have been developed, with two of the most common being electrospray ionization (ESI) and atmospheric pressure chemical ionization (APCI). They both function according to the same principles of creating charged ions, which can then be transported into the mass spectrometer for further analysis. It is also possible to use HPLC/UV systems, which offers highly stable, but less sensitive methods of analysis.

4.2.1 HPLC methods with ESI-MS and UV

Two individual methods were developed for the quantitative analysis of pesticide samples: HPLC/ESI-MS and HPLC/UV. The ESI-MS method was used as the preferred method because its sensitivity was found to be higher, and because the interference of background noise and overlapping analyte peaks could be overcome with use of ion fragmentation. The HPLC/UV method was used when fast analysis of synthetic samples of relatively high concentration (> 0.1

mg/L) was needed. Both methods were developed for single pesticide analysis. This allowed for faster analysis compared to the use of a multi-pesticide method.

For HPLC/ESI-MS analysis, a 1260 Infinity and 1100 series LC/MSD Trap system from Agilent Technology has been used. The HPLC was equipped with a ZORBAX Eclipse Plus C18, 3.5 µm, column, and a UV detector that could be used alongside the ESI-MS. It was also possible to disconnect the ESI-MS from the HPLC and inject the samples directly on the ESI-MS without prior chromatographic separation. This was used for fast qualitative analyses and for calibrating the ESI-MS.

In table 12 the conditions for the HPLC/ESI-MS method are shown. The voltages represent the standard settings for the ESI-MS. An automated optimisation of these was attempted with the MS software, but this lead to unstable signals. To obtain stable signals, the standard settings were used for all pesticides, but it may be possible to increase the sensitivity of the method by carefully optimising the voltage set. However, for this work, the sensitivity obtained with the standard settings was sufficient. The nebulising conditions were chosen to accommodate the high HPLC flow rate. Lower dry gas flows and temperatures have been found to lead to insufficient nebulisation and built up of material in the nebulisation chamber. As eluent, a mixture of methanol (mobile phase A) and demineralised water buffered with 5 mM CH_3COONH_4 (mobile phase B) was used. This is commonly used in HPLC/MS analysis of pesticides [132,134,135]. Often the pH in the water phase is lowered to increase protonation and hereby sensitivity. In this work the pH was 3, except for analysis of DEIA which may undergo hydrolysis at low pH values [136].

Table 12 Optimised conditions for HPLC/ESI-MS method

ESI-MS conditions[a]				HPLC conditions	
Capillar (V)	± 3500	Lens 2 (V)	± 60.0	Eluent MeOH/H_2O (%)	70/30 (pH 3[b])
Capillar exit (V)	± 102	Octopole RF	110	Internal standard	Atrazine-d5
Skimmer (V)	± 40.0	Trap drive (%)	40	Flow rate (µL/min)	400
Octopole 1 (V)	± 12.0	Nebuliser pressure (psi)	40	Injection amount (µL)	5
Octopole 2 (V)	± 1.70	Dry gas flow (L/min)	9		
Lens 1 (V)	± 5.00	Dry gas temperature (°C)	350		

[a)] Positive values for atrazine, BAM and DEIA. Negative for bentazon.
[b)] For DEIA a pH of 6.5 was used.

Table 13 Optimised conditions for HPLC/UV method. ACN = acetonitrile

Pesticide specific conditions			General conditions	
Pesticide	Eluent ACN/H_2O (%)	Wavelength (nm)		
DEIA	30/70	210	Flow rate (µL/min)	400
BAM	50/50	210	Injection amount (µL)	100
Atrazine	70/30	220		

Most HPLC/UV analysis took place at KU Leuven, Leuven, Belgium, where a slightly different setup was used. Here a 1200 Infinity HPLC/UV system with a diode array detector from Agilent Technology and equipped with a ZORBAX Eclipse XDB-C18, 5.0 µm, column was used. The conditions of the method are shown in table 13.

For both methods, the instruments were calibrated from 0.1 to 1 mg/L, with calibration standards of 0.1, 0.2, 0.5, 0.8 and 1.0 mg/L.

4.2.2 Solid phase extraction

To be able to analyse in the concentration range around 1 µg/L, which is the concentration range in which pesticides are normally found in groundwater, it is necessary to concentrate the samples by performing a solid phase extraction (SPE) prior to analysis.

For the SPE Telos ENV 200 mg/6 ml columns were used. Methanol, acetone, ethyl acetate, acetone/ethyl acetate 75/25 and acetone/ethyl acetate 25/75 were investigated as possible eluation liquids. These were investigated by evaluating their ability to dissolve the pesticides. Acetone was found to be the best eluent, since it was the only solvent able to dissolve all pesticides in sufficiently high concentrations. The SPE procedure used was:

- Conditioning of the column with 6 mL MeOH
- Equilibration of column with 6 mL demineralised water
- Application of sample volume to column
- Eluation of interferences with 6 mL demineralised water
- Drying of column, 20 minutes under vacuum
- Eluation of analytes with 10 mL acetone
- Evaporation of acetone (70 °C, N_2 flow)
- Dissolution in 0.5 mL acetonitrile with or without 0.1 mg/L internal standard (atrazine-d5)

To evaluate the method, 10 mL of standard solution of 0.1 mg/L was concentrated a factor ten with the method and compared to a 1 mg/L standard solution. From the results in table 14 it can be seen that for especially atrazine and BAM complete recovery could not be expected. This meant that when SPE was applied, the calibration standards also underwent SPE.

Table 14 Recoveries of the four pesticides with the SPE procedure

	Atrazine	BAM	Bentazon	DEIA
1 mg/L sample (mg/L)	1.01	1.00	0.98	1.00
SPE sample (mg/L)	0.76	0.53	0.97	0.93
Recovery (%)	75	53	99	93

4.3 Experimental setups

4.3.1 Sand filtration and MF/UF setup

The experiments with sand filtration and ceramic MF/UF membranes were carried out with small pilot plants (~100 L).

The sand filtration pilot plant was installed next to a groundwater well and can be seen as the upper part of the setup in figure 12. It consisted of an aeration tower from MicroDrop Aqua and a pressurised sand filter (1m^3 of quartz sand 0.2-1 mm). In the aeration tower, the raw groundwater was sprayed out over a stack of open walled plastic tubes to generate a large contact area between air and water. Experiments were run in both continuous and batch recirculation mode. Continuous mode was used to test the ability of the filter to pre-treat the groundwater before NF/RO filtration, and batch recirculation mode was used to test the effect of the filter on pesticides. Batch recirculation mode was done to avoid release of the pesticides to the environment and to lower the amount of wastewater. Furthermore, it made it possible to investigate the effect of multiple runs through the filtration system, hereby creating an extreme scenario for the pesticide removal. The hypothesis was that if the pesticides were not removed after multiple sand filtration runs, they would not be removed in standard continuous flow mode. In the batch recirculation experiments, 120 L raw groundwater was collected and spiked with pesticides at a concentration around 2 µg/L. The concentration was chosen since it is close to the values that can be expected to be found in real groundwaters. Furthermore, higher concentrations could alter the load of organics, which could affect especially the microorganisms in the sand filter. Also, if any adsorption were to take place, this effect might be drowned in experiments with higher concentrations.

Experiments with MF/UF membranes were performed by collecting 100 L of aerated water and transporting it back to the laboratory. Here four ceramic silicon carbide membranes from LiqTech with reported pore sizes of 3, 1, 0.1 and 0.04 µm were tested. The 3 and 1 µm membranes had a surface area of 0.09 m^2 and 31 flow channels, while the 0.1 and the 0.04 µm membranes had a surface area of 0.05 m^2 and 19 flow channels. Experiments were run in cross flow mode at transmembrane pressures between 200 and 300 mbar. As with the sand filter, the effect of the filtration on pesticides were investigated by spiking the water with pesticides in concentrations of 2 µg/L for the same reasons as previously stated, and 1 L samples were extracted from feed, retentate and permeate. In between runs the membranes were cleaned with a 3 bar back flush.

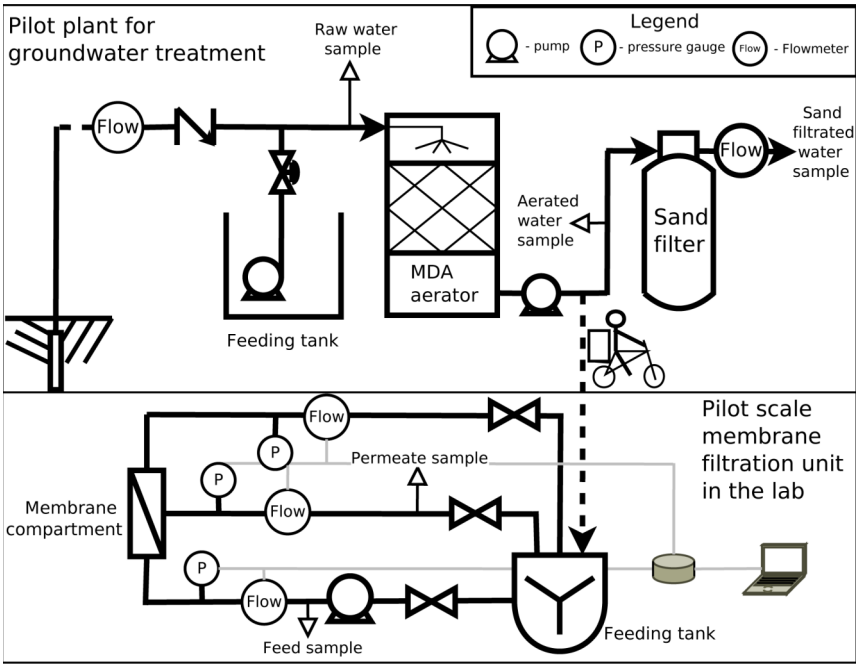

Figure 12 Pilot plants used in investigations of sand filtration and MF/UF membranes. The upper part of the figure shows the setup with the sand filtration, while the bottom part shows the MF/UF membrane setup. The dotted line illustrates the transport of aerated water from the sand filtration plant to the membrane filtration plant.

4.3.2 NF/RO Cross flow filtration setup

Experiments with commercial NF/LPRO/RO membranes were carried out with a DDS Lab-Unit M20 (Alfa Laval, Nakskov, Denmark), which is schematically shown in figure 13. The unit was equipped with a plate and frame module, which made it possible to operate it simultaneously with several membranes or to increase the total membrane area. Two pressure gauges were mounted on the setup. One at the inlet measuring feed pressure and a second at the outlet measuring retentate pressure. The permeate pressure was equal to the pressure of the surroundings. For temperature control, the unit had a heat exchanger mounted at the inlet to the membrane housing. In this work, the unit was modified to also allow for the use of 2.5 inch spiral membranes. The spiral membranes were used in the work described in paper XI, where a larger membrane area was required.

In the experiments with the plate and frame module two membrane sheets, each with an area of 29.5 cm^2, would be clamped onto a support plate and inserted in the module. The membranes would then be compressed with a hydraulic system and washed with distilled water for 30 minutes. After washing, the distilled water was drained away and replaced with 4 L pesticide solution of 1 mg/L, which was left to recirculate for one hour. One hour was chosen to allow for compaction of the

membrane and to ensure that pesticide adsorption to membranes and equipment would not influence the results. In an initial investigation, the concentration in feed and permeate was found to be stable after 10 minutes of recirculation, but one hour was chosen to allow room for variations. Experiments were run at 25 °C, with a transmembrane pressure of 10 bar and a flow rate of 10 L/min. The high flow rate was part of the design of the membrane system to lower concentration polarisation. To measure rejection, triplicate samples were collected over a 10 minute period. Feed samples were sampled directly to HPLC vials, while 20 mL of permeate were collected for solid phase extraction.

When using spiral membranes a transmembrane pressure of 5 bar was used, otherwise the setup and the conditions were identical to the plate and frame mode.

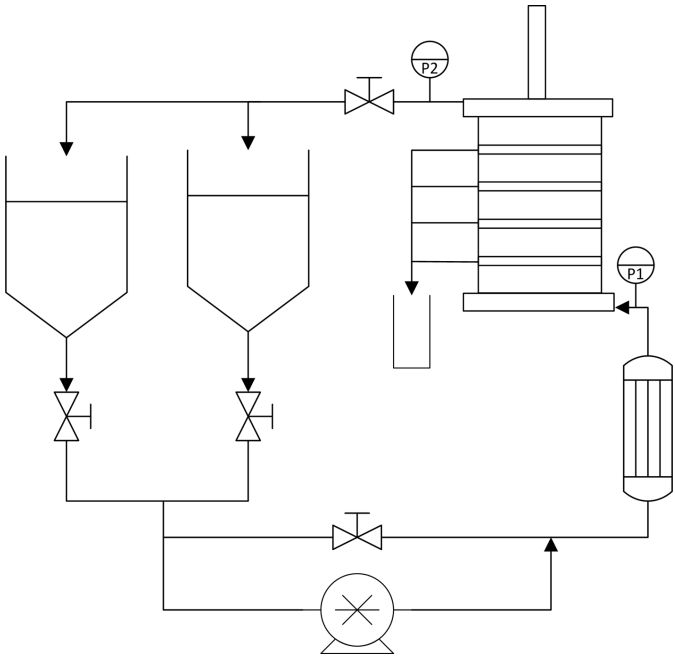

Figure 13 Sketch of the filtration setup used in experiments with commercial NF/RO membranes. The upper right hand corner of the figure represents the membrane stack, and shows how several permeate samples can be extracted simultaneously. Retentate flows out of the top stream line and the transmembrane pressure is controlled with the valve placed on this line. Below the membrane stack the heat exchanger is found. The valve placed in parallel to the pump is used to ensure a gradual increase in pressure during the upstart and shutdown phases. When spiral membranes were used, the tubing to the membrane stack were disconnected and connected to the spiral membrane housing. Here only one permeate outlet was available, but otherwise the system was identical to the one presented in the figure.

4.3.3 Dead end filtration setup

Experiments with dead end filtration were carried out using a Sterlitech HP4750 cell equipped with magnetic stirrer suspended above the membrane surface. The setup is shown in figure 14, and it was especially used to measure adsorption of pesticides/PTPs to membranes.

In filtration/adsorption experiments, a 200 mL 1 mg/L solution was transferred to the cell and filtrated at a transmembrane pressure of 10 bar. Pressure was created with nitrogen gas. Permeate was collected to determine the filtrated volume and concentration. In each experiment 100 mL of permeate was collected to obtain a recovery of 50%, and rejection and adsorption was determined by measuring concentrations and volumes of permeate, concentrate and feed.

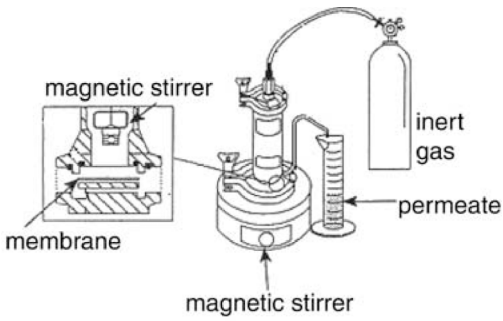

Figure 14 Dead end filtration setup.

4.3.4 Membrane synthesis

NF membranes were made according to the method described by Zhang et al. [137]. The membranes were thin film composites and the synthesis was therefore a two-step process with an initial synthesis of a UF PES support membrane on top of which a thin layer of polyamide (piperazine) was deposited.

Chemicals

PES beads (Radel-100, Solvay Speciality Polymers Germany GmbH, Düsseldorf, Germany), N-methyl-2-pyrrolidone (NMP; 99.5%, Sigma Aldrich), non-woven fabric (FO2471, Viledon, Weinheim, Germany), piperazine (PIP; 99%, Across Organics, Geel, Belgium), trimesoylchloride (TMC; 98%, Across Organics, Geel, Belgium), n-hexane and distilled water.

Synthesis of support membrane

The supper membrane was produced via a phase inversion process where a PES polymer solution was transformed from a liquid to a solid state. The transformation was induced by immersion precipitation where the polymer solution was immersed in a non-solvent (distilled water in this case) in which the polymer was no longer soluble leading to precipitation.

1. 12.5 g of PES beads were dissolved in 41 mL of NMP to obtain a 23 wt/wt% solution. The solution was very viscous and stirring over night was preferred to ensure complete dissolution.
2. Before use, the beaker with the solution was placed under vacuum to remove air bubbles, which may otherwise lead to imperfections in the membrane.
3. A 30 x 50 cm piece of non-woven support was taped on a glass plate and wetted with NMP. NMP was applied to the fabric to avoid polymer solution entering the pores. Excess NMP was removed by gently drying the fabric with a piece of paper. This was found to be an important step, as an insufficient drying resulted in a reduced adhesion of the polymer solution to the fabric, which could ruin the casting process.
4. The wetted fabric was placed on a casting machine in a glove box where the humidity could be controlled. This was set to 40%. Polymer solution was poured in the casting knife and a layer with a thickness of 250 µm was cast.
5. The cast film was lowered into 2 L distilled water (non-solvent), which induced the phase inversion process. To ensure sufficient time of reaction, the membrane was left in the water bath for 15 minutes.
6. After formation of the membrane, it was thoroughly washed with distilled water to remove leftover solvent, and left for storage in a distilled water bath.

Thin film membrane

The thin film was prepared through an interfacial polymerisation reaction. Here two monomers were lead to react on the surface of the membrane to form a dense film. First an aqueous solution of one monomer (amine, PIP) was applied to the membrane and then a non-aqueous solution was added with the second monomer (acid chloride, TMC). At the interface of the two phases the monomers reacted to form a thin polymeric film. The polymerisation reaction is shown in figure 16.

1. The PES support membrane was placed between two support frames to ensure a flat and stable surface throughout the synthesis.
2. 10 mL 4 wt/vol% aqueous PIP solution was poured on the membrane, spread out onto the membrane and left for 30 seconds. After this, the excess PIP solution was drained to a waste container and additional excess PIP left on the membrane was removed with compressed air until no excess solution was visible.
3. 10 mL 0.5 wt/vol% TMC in hexane solution was poured on the membrane, spread out and left to react for 30 seconds. After reaction, excess TMC solution was drained to a waste container, and the membrane was washed with 20 mL hexane to remove unreacted monomers.
4. To finish the reaction, the membrane was heated at 60 °C in a vacuum oven for 8 minutes. This final step completed the interfacial reaction, and led to cross-linking of the PIP monomer.
5. Finally, the membrane was washed with distilled water and cut into pieces with a desired size.

The whole process is illustrated in pictures in figure 15.

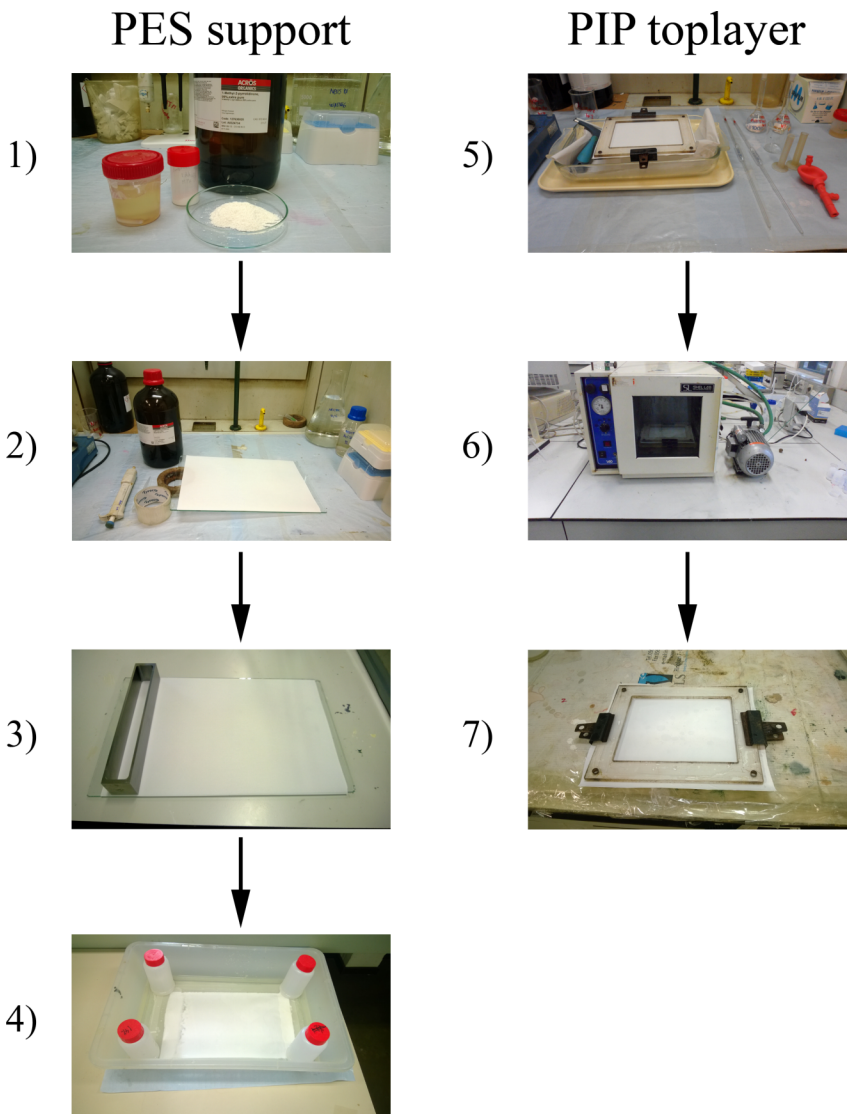

Figure 15 TFC membrane synthesis in pictures. 1) Preparation of PES solution. The PES polymer is mixed with NMP solvent and possibly functional particles. 2) Preparation of PES membrane non-woven support. 3) Casting of membrane (casting machine is not shown since it was placed inside a glove box). 4) Immersion precipitation of PES membrane. 5) Making of piperazine top layer. 6) Cross linking in vacuum oven. 7) The final TFC PIP membrane.

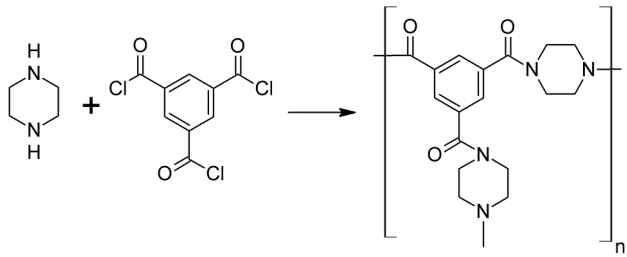

Figure 16 The polymerisation reaction used in this synthesis. Because of the use of excess PIP and the three functional groups on TMC cross-linking is allowed.

4.3.5 Electrochemical oxidation

The general setup used for electrochemical oxidation is shown in figure 17. In the experiments volumes of 1 or 3 L solution of pesticides in concentrations between 10 and 100 mg/L in distilled water were used. To ensure complete dissolution, solutions were left under stirring overnight. Before an experiment was initiated the pesticide solution was recirculated through the system to ensure homogenisation and avoid influence of adsorption to the equipment. Three commercial electrochemical cells were used:

1. A tubular cell with mixed metal anode (Ti/Pt_{90}-Ir_{10}) and AISI 316 cathode from Watersafe S.A. Greece.
2. A DiaCell type 100 with BDD anode and cathode from Adamant Technologies S.A. Switzerland.
3. A Micro Flow Cell with interchangeable Ti and BDD anodes and an AISI 316 cathode from Electrocell, Denmark.

Details about the different cells and the experimental conditions can be found in papers IX, X and XI.

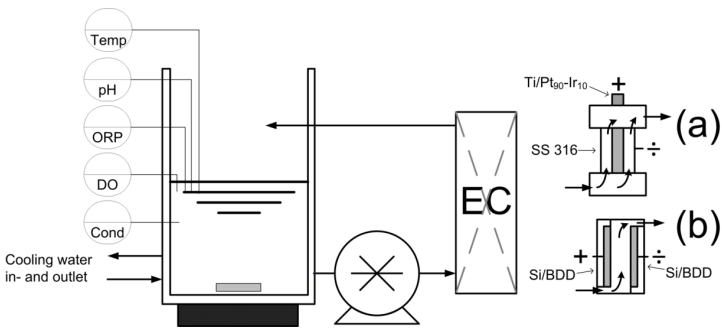

Figure 17 Setup for electrochemical oxidation experiments with use of two cells. (a) TI/Pt_{90}-Ir_{10} and (b) BDD. The setups that used the Micro Flow cell from Electrocell were similar with only a different electrochemical cell and a separate cooler.

Chapter 5 Methods for detection and identification of reaction products

This chapter covers studies that describe how compounds formed during reactions in aqueous solutions can be detected and identified, and is especially minded for the application on degradation intermediates formed during AOP degradation of pesticides. In general there is very little information on how to systematically identify reaction products when techniques such as GC/MS are not applicable, and the purpose of this chapter is to give examples of how this can be done. Far too often scientific papers state that they used a given analytical instrument to identify reaction products, while failing to describe exactly how this was done. For more researchers to be able to make these important studies and to make judgement on the proposed reaction pathways of others, information about the methods behind the detection and identification needs to be presented.

As a result, the structure of this chapter will deviate a bit from the other paper chapters. First of all, it will be split in two parts: One presenting results from papers II, III and IV, which focused on the use of direct injection on ESI-MS to investigate reactions with highly concentrated pesticide solutions, and a second part presenting results from papers IX and X, which focused on the use of HPLC/UV/ESI-MS to follow formation of degradation intermediates during electrochemical oxidation of dilute pesticide solutions. Secondly, the results sections are split into subsections describing first how the peaks may be detected and then how they may be identified.

5.1 Use of ESI-MS to determine reaction pathway for H_2S scavenging pesticides

Direct injection on ESI-MS was applied in a study of the reaction between hydrogen sulphide and two triazine pesticides. This particular project was not part of the work on pesticide pollution of groundwater, but was carried out alongside with the main Ph.D. project. Two triazines were investigated: 1,3,5-tris(2-hydroxyethyl)-hexahydro-s-triazine (HET) and 1,3,5-tris(2-hydroxypropyl)-hexahydro-s-triazine (HPT). These are very similar to triazine pesticides/PTPs such as atrazine and DEIA, and both the triazines and their reaction products are classified as biocides. The described method is therefore readily applicable as a general method for use with pesticides of which biocides are a subcategory.

The main purpose of the study was to elucidate the connection between the offshore use of triazine based H_2S scavengers and the onshore fouling at a refinery.

Specifically the study addressed three questions:

1. How did the reaction system for the scavenging process look like and which products were formed?
2. How could the observed fouling at the refinery be explained from the scavenging reaction?
3. How could the postulated model for the reaction system be verified?

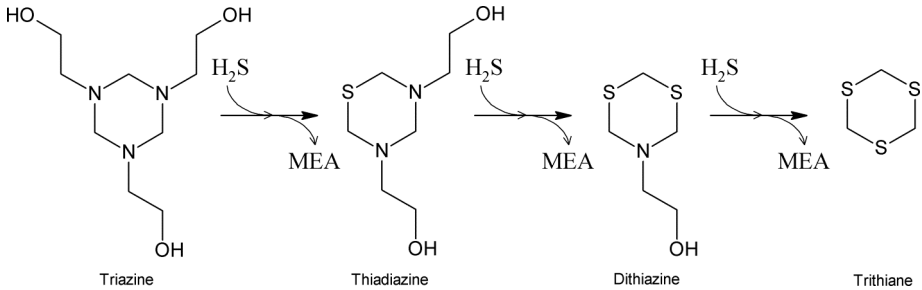

Figure 18 Established reaction system for 1,3,5-tris(2-hydroxyethyl)-hexahydro-s-triazine and hydrogen sulphide. The reaction system includes the final step from dithiazine to trithiane, although this is not typically encountered in experiments.

5.1.1 Background

In the production of oil and gas, a key operation is the removal of hydrogen sulphide. One of the most popular methods for this process is to use triazine based scavengers, especially HET. Still, even though the oil should be free of scavenging reaction products, there had been indications that this was not the case. During refining of the oil, severe incidents of fouling had been observed and the fouling had subsequently been found to consist of mainly carbon and sulphur in an equimolar ratio. Since the final theoretical reaction product of the scavenging reaction is the compound s-trithiane, see figure 18, which has a molecular composition similar to that of the fouling, the presence of triazine reaction products had been suspected to be the cause of fouling.

However, previous studies had found the reaction to terminate with the formation of the dithiazine compound, which would give a very different type of fouling [138,139]. Another study had suggested that the fouling was a polymer based on dithiazine molecules linked by carbon-sulphur chains [140], but the origin of the carbon-sulphur chains was unknown. Therefore, we studied the reaction to investigate which compounds were formed and whether any of these could explain the observed fouling. For this we used direct ESI-MS.

5.1.2 Detection of reaction products

Since electrospray is a gentle way to ionize molecules, the molecules are not fragmented and the ESI-MS spectra display the composition of the solution. That is, each peak represents a species actually present in the solution. This is important because samples do not need to undergo chromatographic separation prior to analysis, but can be injected directly into the MS, and because knowledge of the charge process allows one to deduce the molar mass of the compounds from the mass to charge ratios of the peaks. Protonation is the most common charge process to occur, but depending on the ionic environment of the solution, molecule-cation complexes can also give rise to peaks with strong intensity. Of these the sodiated peaks are the most commonly seen. With this in mind, peaks can be correlated to molecules for which the molar mass is known. An example of how ESI-MS can be used to search for compounds with known nominal mass can be seen in figure 19. Using this procedure, the presence of triazine, the thiadiazine and the dithiazine was observed, and the general reaction pathway with no s-trithiane observed was thus confirmed. However, three other peaks appeared during the reaction at m/z values of: 74, 86 and 120 m/z.

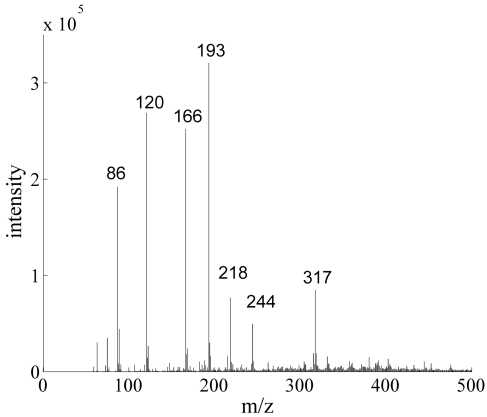

Table 15 m/z values for triazine and reaction products

HET triazine compounds	m/z value for protonated peak
Triazine	220
Thiadiazine	193
Dithiazine	166
Trithiane	139

Figure 19 ESI mass spectrum of spent scavenger. When a triazine solution has reacted with gas containing H_2S it is called spent scavenger, and by using ESI-MS, the qualitative composition of the solution can be determined. By comparison with the table to the right, the peaks originating from the scavenging process can be identified. In this case, the spectrum was recorded for a sample collected from an offshore platform, and some of the remaining peaks are from compounds not related to the scavenging process. This could be confirmed by comparison with laboratory experiments in which only the pure scavenger and H_2S was used.

5.1.3 Identification of unknown reaction products

To identify the three unknown peaks, tandem mass spectrometry and a combinatorial algorithm were applied. With tandem mass spectrometry, the peaks were isolated and then fragmented, and this gave clues to the origin of the peaks. Thiadiazine was found to fragment to the 120 m/z peak and the 74 m/z peak, while the dithiazine fragmented to the 86 m/z peak. Upon further isolation of the 120 m/z peak, it was found to fragment to the 86 m/z peak as well. All this was in accordance with the observed changes in peak intensity. As can be seen in figure 20 all three peaks appeared simultaneous with the thiadiazine, but where the peaks at 74 and 120 m/z disappeared with the thiadiazine, the peak at 86 m/z stayed in the spectrum so that only it and the dithiazine peak were present at the end.

With their origin established, a combinatorial algorithm was used to find sets of elements that would give the desired molar mass. By creating two matrixes, A and B, representing the number of a given element in a combination and the nominal mass of the elements respectively, a vector, C, of total molar masses for each combination was calculated.

$$A = [C \quad H \quad O \quad N \quad S]$$

$$A = \begin{bmatrix} & & \vdots & & \\ 5 & 7 & 1 & 0 & 1 \\ 5 & 7 & 1 & 0 & 2 \\ 5 & 7 & 1 & 0 & 3 \\ 5 & 7 & 1 & 1 & 1 \\ & & \vdots & & \end{bmatrix} \qquad B = \begin{bmatrix} M_C \\ M_H \\ M_O \\ M_N \\ M_S \end{bmatrix} \qquad C = A \cdot B \tag{21}$$

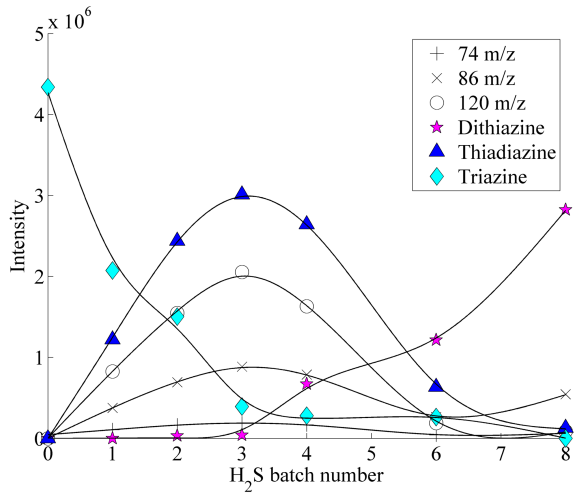

Figure 20 Plot of intensities of peaks observed during reaction between HET and H_2S

After this the composite matrix D was constructed from A and C.

$$D = [A \quad C] \tag{22}$$

With matrix D all possible elemental combinations that gave the nominal mass that had been detected with the MS could be isolated. Many of these did not have any real chemical meaning, especially because of hydrogen's ability to only form one bond. Therefore, to remove combinations with excess and too little hydrogen two selection rules were invoked.

1. $n(H) \leq 3 \cdot n(C) + 1 \cdot n(O) + 2 \cdot n(N) + 1 \cdot n(S)$
2. $n(H) \geq 2 \cdot n(C)$

Rule one was based on the typical number of hydrogen atoms that maximum can be bonded to terminal carbon, oxygen, nitrogen and sulphur atoms. In reality, the molecular structure will contain fewer hydrogen atoms simply because not all carbon, oxygen, nitrogen and sulphur atoms will be terminal, but it is also important not to exclude possible solutions. Therefore a few false positives were accepted. Rule number two represented the minimum number of hydrogen atoms that for these compounds could be expected to be contained in the molecular structure. If the carbon atoms were tertiary, took part in double bonds, or had other functional groups such as oxo groups, the number could be less. However, terminal carbon atoms would count in the opposite direction and because of the structure of the starting molecules, the presence of tertiary carbon atoms was not expected. The second rule can be removed if no good results can be obtained, but in this case it was found to work well.

To illustrate the effectiveness of the algorithm, the number of possible results for each of the peak masses can be seen in table 16, where it is seen that especially for the two small compounds only a limited number of combinations are possible. It may also be interesting to note that fewer combinations give the nominal mass of the triazine compound compared to the dithiazine and thiadiazine, but this is a result of the maximum number of atoms used in the calculations. A higher starting number of carbon, hydrogen, oxygen, nitrogen and sulphur atoms would have yielded more combinations at higher nominal masses. It would however not affect the results for lower nominal masses because the number of atoms here is already sufficient to give practically all possible combinations. It was also interesting to note that none of the combinations for the 74 and 86 m/z peak contained sulphur. Sulphur atoms therefore had to be retained in the structure of the 120 m/z compound and the compound left from the dithiazine decomposition. Finally it was noticed that the difference between the 120 m/z peak and the 86 m/z peak was equal to the mass of a hydrogen sulphide molecule.

Table 16 Results from the combinatorial algorithm, given in number of possible combinations. In the calculations the number of C, H, O and N atoms in the structure of triazine plus three S atoms has been used to create the total number of combinations (N_{Total}).

	74 m/z	86 m/z	120 m/z	Dithiazine	Thiadiazine	Triazine
N_{Total}	14080	14080	14080	14080	14080	14080
Correct nominal mass	35	45	75	94	81	59
Rule 1	17	17	47	72	78	58
Rule 2	8	4	23	32	38	22

With the possible combinations of elements in the structure and knowledge of the origin of the peaks determined, the final step was to put it together and establish the reaction pathway. Since the composition of the solution had been found to be stable over time, and only change after reaction with hydrogen sulphide, the same mechanism of reaction as in the scavenging reaction was hypothesised to be occurring. The reaction mechanisms for the reaction from triazine to thiadiazine and further to dithiazine is known to occur via protonation of the nitrogen atoms, which leads to a ring opening after an S_N2 reaction with the hydrosulphide ion. Based on this it was hypothesised that both nitrogen and sulphur atoms could be protonated, and that instead of reaction with the hydrosulphide ion, the protonation might lead to a reconfiguration in the molecular structure. The result of this approach can be seen in figure 21.

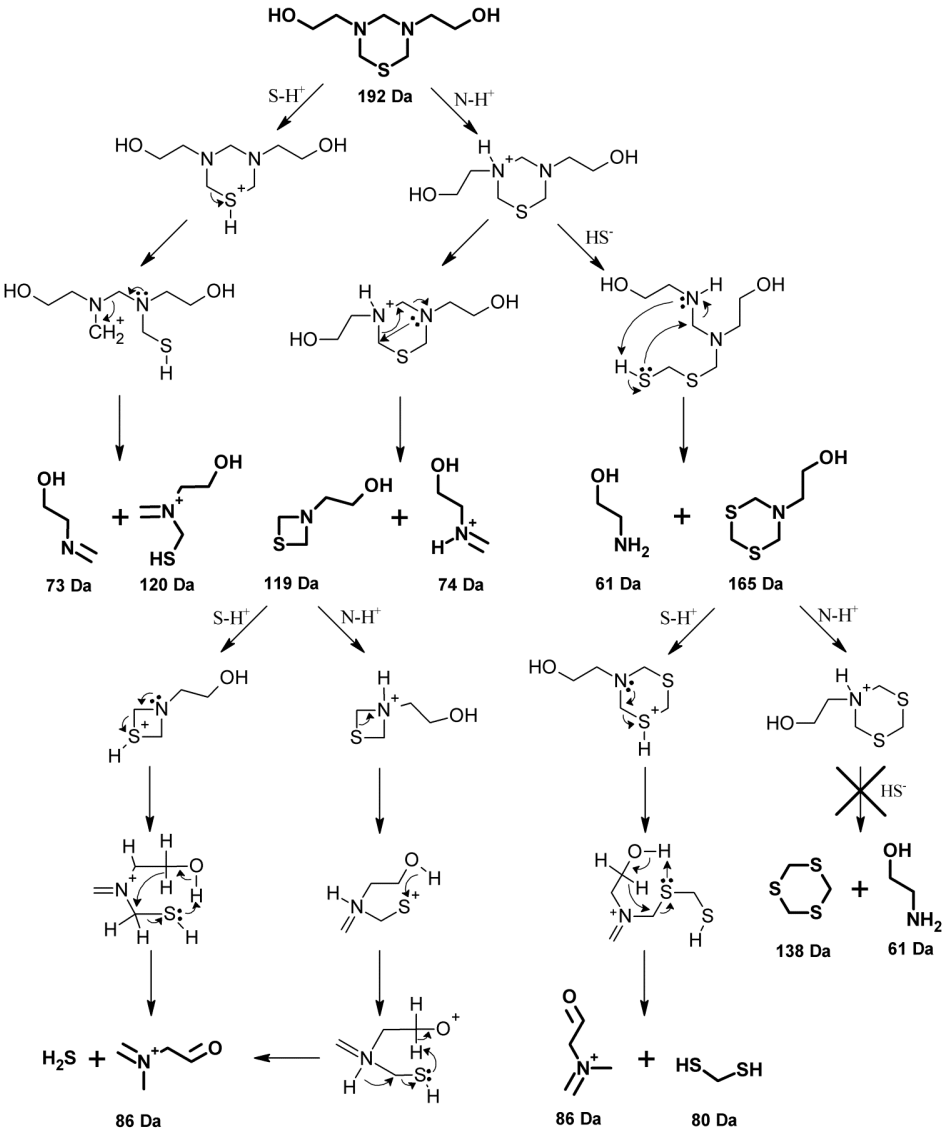

Figure 21 Formation of by-products. The figure shows the mapped reaction pathway leading to the formation of the by-products observed in the reaction between HET and H_2S, and is based on the results of the tandem mass spectrometry and combinatorial algorithm.

5.1.4 Verification and evaluation of identification method

To verify the identification results obtained with ESI-MS, the model was used to predict the products formed in the reaction between the propyl based triazine, HPT, and hydrogen sulphide. Further, it was investigated whether the model could explain the structure of the observed fouling. For the reaction between HPT and hydrogen sulphide, the reaction system shown in figure 22 was predicted. When compared to the actual findings in figure 23, it is clear that the model was able to predict the behaviour of this triazine, which supported the validity of the model and thereby also the method of identification with ESI-MS.

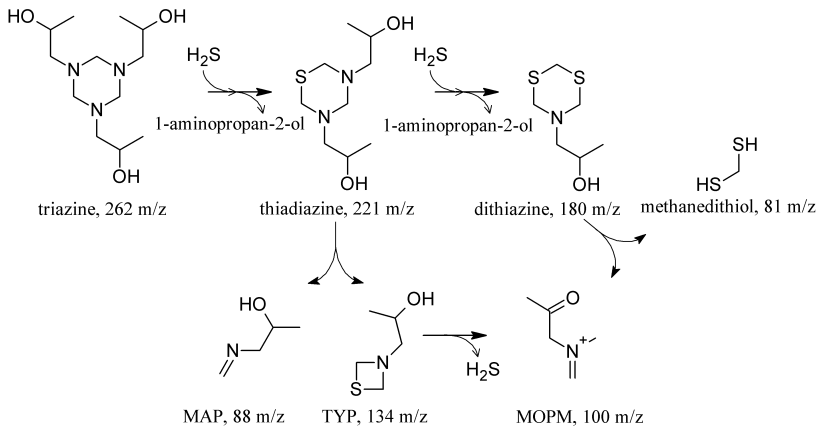

Figure 22 Predicted reaction system for scavenging of H_2S and HPT. The acronyms for the reaction products are based on the systematic name of the compounds, which can be found in paper IV.

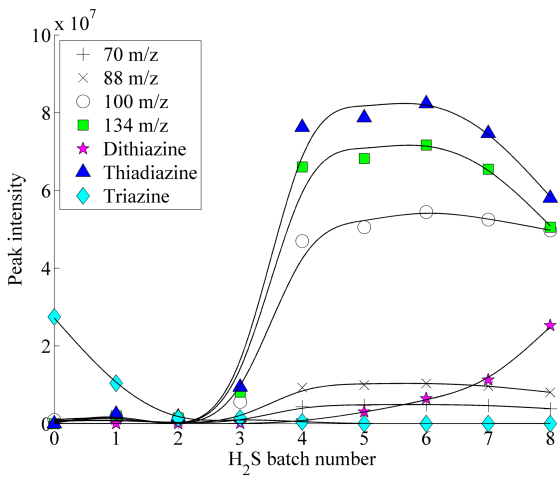

Figure 23 Development in peak intensity of compounds formed in the reaction between HPT and H_2S.

With respect to the structure of the fouling, it had been found to be a dithiazine polymer with linking carbon-sulphur chains, but without certain knowledge of how the chain was formed. In the reaction system for HET in figure 21, the existence of the 86 m/z peak from the disintegration of dithiazine imposed an interesting implication; namely, the formation of methanedithiol. If it is assumed that dithiazine will continue to react with hydrogen sulphide, but without being able to convert to s-trithiane, then the opened structure of dithiazine could react with methanedithiol via condensation reactions as shown in figure 24, and this leads to a polymer with an empirical formula of $(C_7H_{15}S_{4.5}NO)_n$, which is equal to the experimentally determined empirical formula reported in literature.

In total the predicted results showed that the approach of using direct injection on ESI-MS can be successfully used to detect and identify reaction products in aqueous solutions. However, because only molar masses are given, it is very much up to the operator to determine the nature of the reaction products, and the use of complicated procedures such as the described combinatorial algorithm may be necessary. Detection is also dependent on the ability of the molecules to acquire charge and it is necessary to account for both protonated species and cation complexes. To obtain higher sensitivity, remove the influence of the solution composition and collect additional information about the molecules that may ease identification, ESI-MS can be coupled to a HPLC/UV system.

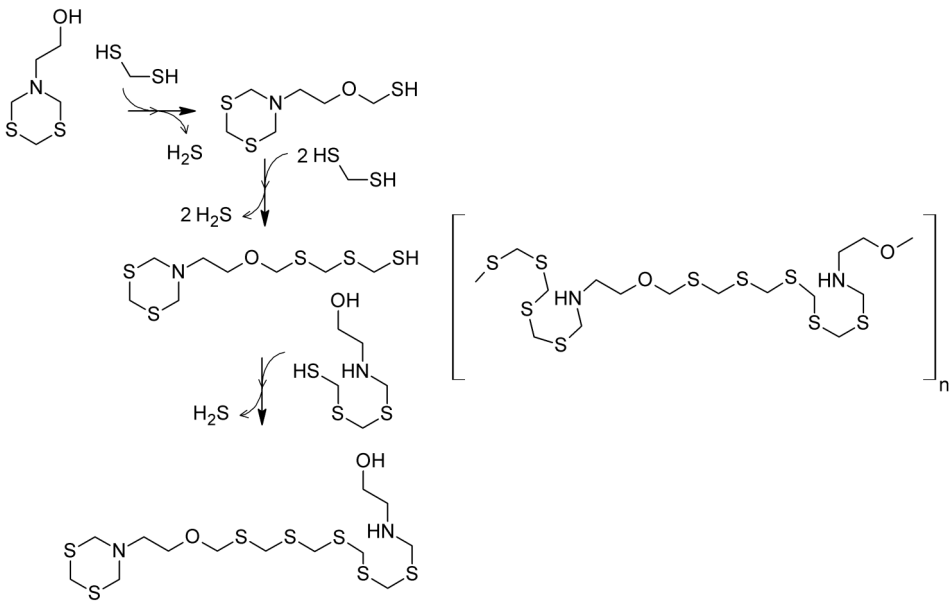

Figure 24 Mechanism for formation of fouling from with methanedithiol (left) and the predicted molecular structure of the polymer (right). Both are based on the use of HET in the scavenging process.

5.2 Use of HPLC/UV/ESI-MS to determine degradation pathway for EO of BAM

This section of the chapter refers to the methods used in papers IX and X, and where the specific method was explained in detail in paper IX. As already mentioned, there are only limited amounts of information available in literature on how to map unknown reaction systems, especially for studies relating to degradation of micropollutants, and the overall purpose of these subparts of the papers IX and X was to develop a methodology for detecting DIs that could be readily applied in other studies.

Specifically the study addressed two questions:

1. How can UV and ESI-MS detectors be used in combination to perform a qualitative investigation into the nature of the DIs formed during electrochemical oxidation?
2. Which supporting parameters can be successfully applied in unison with the data from the UV and ESI-MS detectors?

5.2.1 Background

Compared to the scavenging reaction system just described, the analysis of the degradation of micropollutants such as pesticides faces a different challenge. Where reactants and products were the main components of the scavenging system, pesticides only make up a minor component of samples of polluted groundwater and on direct injection on an ESI-MS the pesticide peak would not be distinguishable from the background. Therefore, it is necessary to separate the pesticide from the background solution, which can be achieved by combining ESI-MS with HPLC. However, even when HPLC is used there are a number of challenges regarding the detection and identification of DIs.

First of all, because the pesticides are only present in low concentrations and because of the parallel formation and degradation of DIs, they will most often be present in concentrations much lower than the original pesticide. Also, because the DIs are unknown by nature of the study, it is not possible to make a standard method based on known standard compounds, and because of the lack of libraries for HPLC/MS systems, fragmentation patterns cannot be compared against a library as is done in the case of GC/MS. Finally, a specific challenge for the use of HPLC/ESI-MS to study electrochemical oxidation reactions is the high electrolyte concentration, which may influence the charge formation during the ESI process, giving rise to peaks where the ionisation is not only due to protonation/deprotonation, but also cation/anion complexation.

5.2.2 Detection of peaks

In general, the same detection principles are in force for HPLC/ESI-MS as in direct ESI-MS. The main challenge lies in detecting the peak of a given DI due to its relatively low concentration. In the HPLC/ESI-MS chromatogram, the large amount of molecules from the background eluent makes it difficult to observe a peak of a compound only present in very low concentration. Here it can be advantageous to couple an UV detector to the system. UV detectors are generally less sensitive, but they give a stable background signal, which makes it easier to locate a potential peak. Afterwards, the compound responsible for the peak can be located in the HPLC/ESI-MS chromatogram. This will give the m/z ratio of the compound, and the MS can then be set to isolate this peak to get a

higher sensitivity that can be used in monitoring the development in peak intensity during the course of the reaction.

It is also necessary to choose whether to run the ESI-MS in positive or negative mode. Usually positive mode is preferred since it gives the most intense signals, but it depends on the functional groups of the analyte molecules. Molecules containing groups capable of protonation (amine, amide etc.) can be detected in positive mode, while groups capable of deprotonation (-OH, -COOH, etc.) allow for detection in negative mode. Because of the resistance of the amide group to hydroxyl radical oxidation, positive mode could be used to analyse the entire oxidation process of the EOTR process of the PTP BAM, while the initial oxidation of the amide group and the hydroxylation observed in the chloride medium made negative mode more applicable here. Furthermore, since the background sodium concentration was significantly higher when using the chloride medium (270 mM compared to 100 mM) due to the need of adding sodium thiosulphate, the mass spectra in the positive mode were more heavily influenced by ionic adducts.

5.2.3 Identification of degradation intermediates

For electrochemical oxidation, especially the EOTR process, which is mediated by hydroxyl radical reactions, a number of typical reactions are often encountered as described in section 3.2.1. As such certain changes in the chemical structure of the initial pesticide can be expected, and to investigate the effect of these changes on the relative HPLC retention time, a series a standard compounds can be analysed with the same instrument method. This principle was applied in paper IX, where the effect of oxidising the amide group of BAM to either a carboxylic acid or a hydroxy group was investigated by analysing 2,4-dichlorobenzoic acid and 3,5-dichlorophenol and comparing their retention times with the retention time of BAM. Also, the effect of losing the chloro groups was investigated. By doing this it could be shown that the amide group was stable towards EOTR mediated oxidation, and that the pure EOTR degradation occurred via hydroxylation and dechlorination leading to an opening of the aromatic ring. The stability of the amide group could also be inferred from the fact that the peaks were seen in positive mode, which as discussed previously indicated the presence of a protonisable functional group like the amide group.

Following the same logic, the detection of peaks in negative mode during the oxidation in the chloride medium indicated that either a conversion of the amide group to a carboxylic acid or the addition of a hydroxyl group to the ring structure was occurring. To distinguish between the two possibilities, the nitrogen rule was inferred showing that the peaks with uneven m/z ratios had lost their nitrogen atom in the conversion to an acid group, while peaks with even m/z ratios represented molecules with an intact nitrogen atom and a hydroxyl group. The nitrogen rule could however not be used to deduce the specific functional group containing the nitrogen atom, and to distinguish these, differences in HPLC retention times were used. Peaks with retention time values close to that of BAM would probably have an intact amide group, while the significantly longer retention time of a second group of peaks indicated that the amide group had been oxidized to an amine group. These observations could as such be used to identify the functional groups of the DIs, and hereby their relative content of nitrogen and oxygen.

To estimate the number of chlorine atoms, the relative intensity between the molecular ion and the +2 isotope peak was used. This could be done due to the relative high abundance of the ^{37}Cl isotope (24.22%), and the data was used to estimate whether compounds had undergone chlorination, dechlorination or had the original two chlorine atoms of BAM intact.

With knowledge of the mass of the molecular ion and the number of nitrogen, oxygen and chlorine atoms, the same combinatorial algorithm introduced in the ESI-MS study could be used to predict possible empirical formulas, from which molecular structures were deduced.

5.3 Evaluation of detection and identification protocols

As have been shown in the presented examples, it is possible to deduce reaction pathways and the structure of reaction products by using either direct injection on ESI-MS or HPLC/ESI-MS. At this point though, it is appropriate to comment on the uncertainty related to the proposed molecular structures.

By following the outlined methodology, it is possible that more than one structure will fit the data, and therefore one should preferably find ways to verify the proposed structure. The obvious experimental method to do this is to use GC/MS where a higher certainty of the structure can be obtained through comparison with fragmentation spectra, but as already mentioned this might not always be possible. A second approach is to compare the proposed structure to the rest of the model. There should be reasonable connections to the other molecular structures in the reaction pathway, and the reaction steps should follow mechanisms that are reasonably acceptable within the existent body of theory. In EOTR reactions, one should look for reaction steps involving hydrogen abstraction and substitution with hydroxy groups, and in a reaction system such as the one presented in the scavenging case, it is obvious to look at reaction steps involving protonation. A third approach that could become increasingly important in the coming years is the use computational chemistry software packages such as Gaussian. These can be used to calculate thermodynamic properties of the compounds predicted to be formed and to predict structures for activated complexes. With these numbers and structures, the activation energy and change in free energy for a proposed reaction step can be determined and used to evaluate its probability. Finally, if possible and following good scientific conduct, the proposed model should be used to make predictions that can be experimentally verified.

Chapter 6 Non-chemical pre-treatment strategies for NF/RO membranes

This chapter presents the main results from paper V. The work was an initial study that aimed at investigating both the fate of pesticides through the current Danish drinking water system and the possibility of using the existing drinking water treatment technology to pre-treat the groundwater before the filtration with NF/RO membranes.

Specifically the study addressed two questions:

1. How are pesticides and PTPs affected by the current aeration/sand filtration treatment as well as the alternative aeration/ceramic micro-/ultrafiltration?
2. How efficient are both the aeration/sand filtration and aeration/ceramic micro-/ultrafiltration methods as non-chemical pre-treatment strategies for NF/RO membranes?

6.1 Background

Although a previous study had found no effect of rapid sand filtration on pesticides [19], we experienced doubt about this outside literature. Therefore, we wanted to give the sand filtration system optimal conditions for removal of pesticides to be able to conclusively state whether or not pesticides can be removed with rapid sand filtration. Furthermore, because of the strict regulations on the methods used in drinking water production in Denmark, we were interested in investigating the use of sand filtration as a non-chemical pre-treatment strategy and comparing it to the use of low pressure MF/UF membranes that are often used as pre-treatment methods for NF/RO filtration.

To ensure optimal operating conditions and to improve the lifetime of a NF/RO membrane, it is often necessary to pre-treat the feed water to avoid fouling and scaling. For groundwater the main issues are usually related to hardness and ionic species that becomes insoluble when they are transported from the reductive conditions in the groundwater to the oxic environment in the drinking water treatment system. Typical species that can give problems are iron and manganese. Because of differences in exposure to the surroundings, the fouling from organic and biological matter can often be much lower for groundwater compared to river water, although this may vary from well to well.

Previously the use of polymeric MF/UF membranes in combination with different oxidation techniques had been investigated for removal of iron and manganese [141,142]. In general these had been found to be effective for removal of iron, but due to the higher reduction potential of manganese, removal of this was only possible when stronger oxidants than O_2 were used. Examples could be chlorine and permanganese. The main challenge when using MF/UF membranes to remove iron colloids from groundwater is colloidal fouling of the membranes [143,144], which for polymeric membranes necessitates the use of anti-scalants and/or chemicals for cleaning. If ceramic membranes are used instead of polymeric membranes, it is possible to use more powerful physical

techniques such as a high pressure back flush to clean the membrane, due to the higher mechanical strength of these membranes. As such it was decided to compare a series of ceramic membranes with the sand filtration, both following an aeration step, as possible non-chemical pre-treatment techniques. To compare the ability of the four ceramic membranes and the sand filter to pre-treat groundwater, their ability to lower key fouling parameters was investigated. These parameters were:

- Iron
- Manganese
- Organic matter measured as absorbance at 254 nm
- Particulate matter measured as turbidity and average particle size
- Biological matter measured as colony forming units (CFU)
- Overall fouling potential measured as the Unified Membrane Fouling Index (UMFI)

6.2 Results

In figure 25 the measured rejection values for all filtration systems can be seen, and for perspective they are compared to rejection results of a NF membrane, NF99HF, and a LPRO membrane, NF90. These will be more thoroughly investigated in the next chapter. The results showed that none of the pre-treatment techniques could be expected to remove any significant amount of the four compounds investigated in this study. It is possible that under certain conditions some pesticides may be removed partially as indicated by Søgaard et al. [19], but these will be special cases.

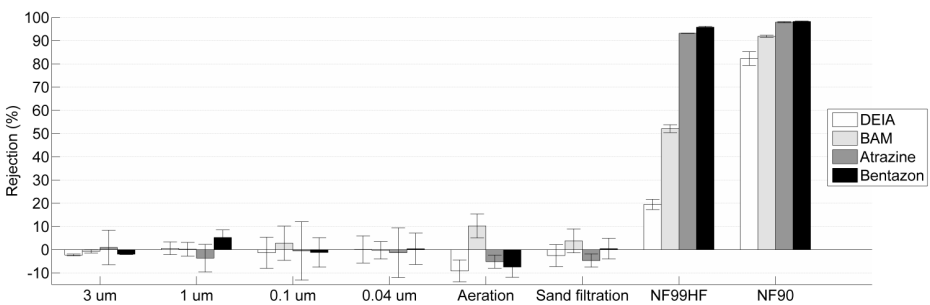

Figure 25 Measured rejection values for the four ceramic membranes and each of the unit operations in the sand filtration system. The values are compared with that of a NF membrane, NF99HF, and a LPRO membrane, NF90. The error bars represents the standard deviation for the measured triplicate samples.

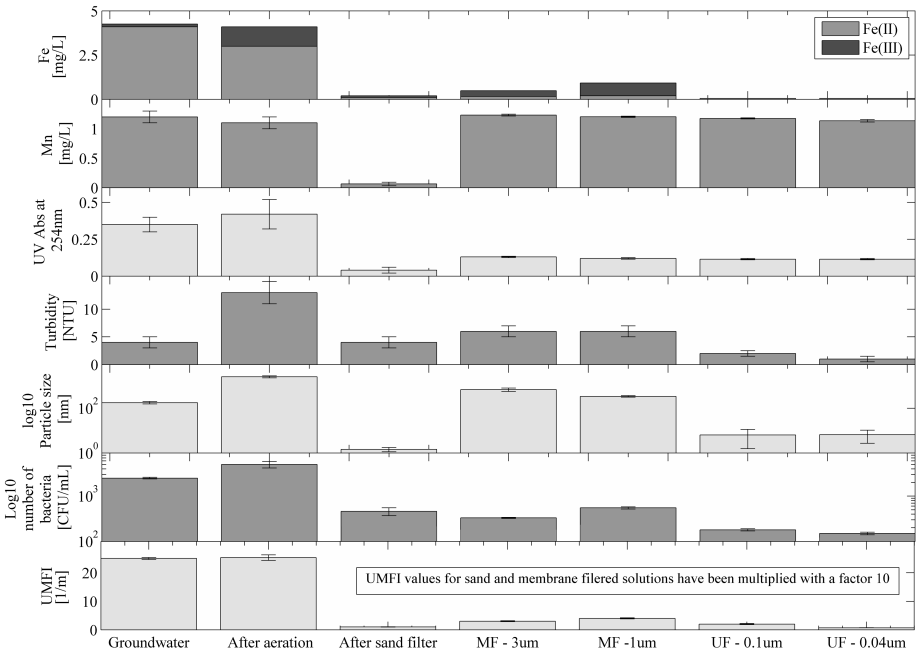

Figure 26 Comparison of the effect of each of the techniques on key fouling parameters. The error bars indicate the standard deviation of the determinations. Also to be comparable with the raw groundwater and the water after aeration, the UMFI index of the sand filter and the four ceramic membranes have been multiplied by a factor ten. For iron, the distribution between Fe(II) and Fe(III) is shown.

The results from the pre-treatment experiment are collected and compared in figure 26. These showed that in general the 0.04 µm UF membrane gave the best results, as indicated particularly by the UMFI value, which can be taken as a collective fouling indicator. It should however also be noted that the sand filter performed better both with respect to manganese removal and the organic matter measured as 254 nm absorbance.

6.3 Evaluation

The results from this study should conclusively show that pesticides and PTPs are not affected by the current sand filtration treatment. In this particular experiment the sand filter was given optimal conditions by allowing the pesticide mixture to recirculate through the system instead of the traditional continuous mode, and pesticide concentrations were chosen to be close to the actual values found in polluted groundwaters to ensure that the filter was not saturated by high concentrations. In total, if the pesticides/PTPs were affected by the sand filtration it should have been observed in this setup.

With respect to the pre-treatment strategy, the 0.04 µm UF membrane was the best option for the investigated groundwater. However, because the sand filter gave better removals of manganese and

organics, this may not always be the case, and the best strategy could be a combination of the two techniques with a sand filter followed by a ceramic membrane like the 0.04 µm membrane. The sand filter would remove the bulk of the iron, together with manganese and some of the biological matter, and the ceramic membrane could then ensure an even higher removal of iron together with a reduction of particulate and biological matter.

Chapter 7 Applicability of NF/LPRO/RO membranes for pesticide removal

This chapter presents the main results from paper VI. The main purpose of the study was to determine how the presence of PTPs in pesticide polluted groundwaters affected the remediation with membrane filtration, and in this way investigate the prevailing opinion that NF membranes are sufficient for treatment of pesticide polluted water. Specifically the study addressed three questions:

1. How applicable are existing NF/LPRO/RO membranes for treatment of groundwater polluted with not only pesticides, but also PTPs?
2. How is the filtration affected by the groundwater and in what range can the effects be expected to be for Danish groundwater?
3. Can the rejection be modelled with the pore flow model by Kiso et al. presented in section 2.3, and if so what are the expected rejections for all compounds in the Danish groundwater monitoring program?

7.1 Background

During the study of the existing literature, it was found that there was a discrepancy between the pesticides used in experimental membrane studies and the pesticides found in real groundwaters. The body of research on pesticide removal focused on the pesticides as they are applied in the pest control, but as was shown in section 1.1, PTPs constitute a significant part of the pesticide pollution. This created two problems:

1. The exact applicability of NF/LPRO membranes for treatment of real polluted groundwaters was unknown.
2. The actual pollution was more diverse, and it would require a huge amount of experiments to determine rejections of all compounds for each membrane.

The existing scientific literature had found NF membranes to be a viable treatment method for pesticide removal [21,36–39], but because of the PTPs there was a need to investigate whether NF membranes were also applicable for treatment of groundwater polluted with PTPs. Therefore, the rejection of the four selected pesticides/PTPs, described in section 4.1.1, for the five commercial membranes: NF99, NF99HF, NF90, XLE and BW30, described in section 4.1.3, were investigated. These membranes span the range from NF to loose RO and could as such be used to give an estimate for the removal efficiency that could be expected with the different types of membranes.

To be able to evaluate the applicability of the membranes in real groundwaters, two groundwaters from Astrup and Hvidovre, Denmark, representing the softest and hardest water in Denmark and described in section 4.1.2, were used in the experiments along with laboratory grade demineralised water. In general, rejection had been found to increase when going from laboratory grade water to real waters [46], but other studies had shown that an increasing ionic content could lead to both

increases and decreases in rejection depending on the specific ions and membranes. [56]. Hence, the overall effect of the groundwater was complex, and difficult to predict. These experiments therefore served to both investigate the effect of groundwaters with varying ionic strength and to investigate if previously reported results on the effect of the ionic environment on the filtration could be supported.

To account for the diverse pollution, it was investigated whether the removal of the pesticides/PTPs could be modelled with a relatively simple steric model, as described in section 2.3 [61]. From an engineering perspective, the application of such a model would be very interesting since it would make it possible to predict the rejection of a large number of pesticides for a given membrane while only experimentally investigating a small carefully selected subset of these. With the subset, a pore size could be determined for the membrane, after which rejection values for the remaining compounds could be calculated, by using their spatial geometries. These parameters could be easily determined by using computational chemistry software, and needed only be done once.

7.2 Results

As can be seen in figure 27, the two NF membranes were found to give reasonably high rejections (>88%) for the two investigated pesticides atrazine and bentazon, while only partial rejection could be obtained for the two PTPs BAM and DEIA. The membrane that gave the highest rejection was the LPRO membrane XLE.

It was found that the NF membranes could be modelled with the steric model of Kiso et al. [61], underlining the observation that the relative size between molecules and pores is the most important parameter determining pesticide rejection for NF membranes. The results also showed that it was the reduction in molecular size that was the main cause of the lower rejection values for the PTPs for these particular membranes and compounds.

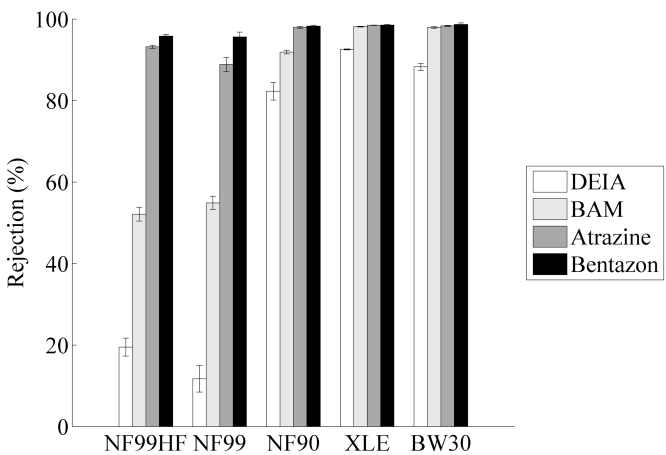

Figure 27 Rejection of the atrazine, bentazon, BAM and DEIA in demineralised water. Error bars represents the standard deviation of triplicate samples.

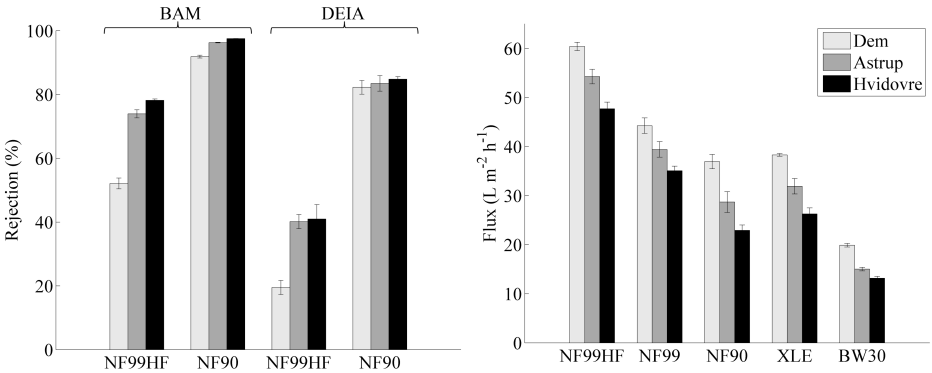

Figure 28 Effect of groundwater on rejection and flux. To the left, the rejection of BAM and DEIA in demineralised (Dem) and groundwater (Astrup and Hvidovre) are compared, while to the right the measured water fluxes of the five membranes for each of the three water types are compared. Error bars represent the standard deviation measured for four samples.

For the LPRO/RO membranes, the model could not immediately be used to fit the rejection data. However, when the molecular width in model was changed from being the average of the width and height of the molecules to being the longer of the two, the rejection data could be fitted. The reason for this was not discovered, but it was hypothesised that the affinity was higher between the molecules and the LPRO/RO membranes compared to the NF membranes, and that this affinity was correlated to the use of the longest side length. This could be argued because the affinity would be highest for the largest contact area of the molecules, which would be correlated to the longest side length. Due to the uncertainty of this hypothesis, the model was used to predict rejections obtained by a different research group for two different pesticides [56]. Here good agreement was found between the experimental and the modelled results, which strengthened the belief in the model.

As can be seen in figure 28, the effect of the groundwater was to increase rejection and lower flux, which was in accordance with previous findings of higher rejections in real waters compared to laboratory grade water [46]. Through comparison with the modelled results, these effects seemed to be caused by a decreasing pore size. This again seemed to be caused by ion adsorption on the membrane surface where the ions blocked or reduced the pore entrance, which could be seen from an increasing zeta potential for the membranes.

Finally, by determining the spatial geometries of the remaining pesticides and PTPs included in the Danish groundwater monitoring program and using these together with the measured pore sizes of the best NF membrane (NF99HF) and the best overall membrane (XLE) to calculate, an overview of the expected rejections could be made, see figure 29. In general this showed that the XLE membrane could be successfully used for most of the compounds, but also that the NF membrane could be used in some cases, depending on the specific composition of the pollution.

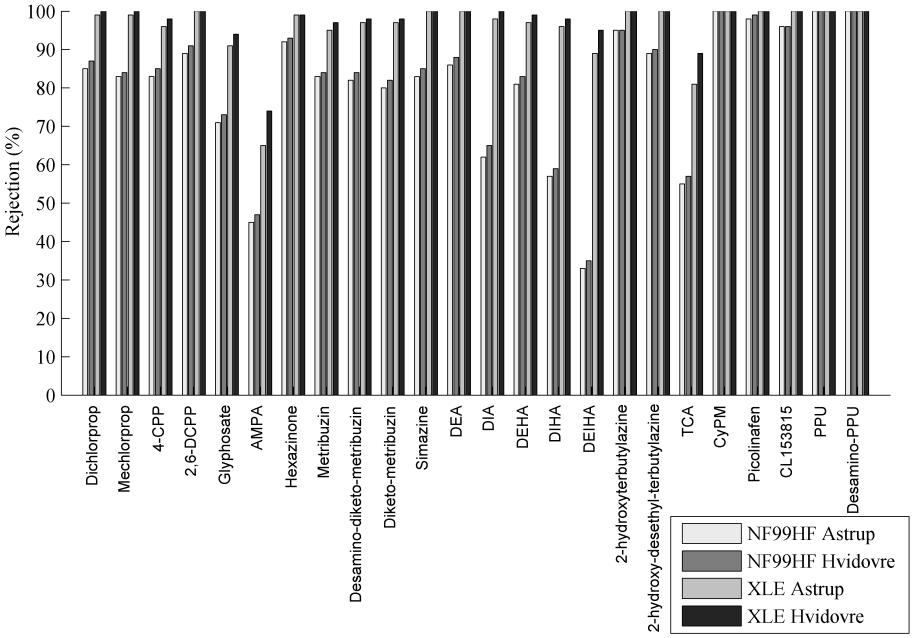

Figure 29 Potential of membranes to treat pesticide/PTP polluted groundwater. The figure presents an overview of the predicted rejections for a NF membrane (NF99HF) and a LPRO membrane (XLE), in the two groundwaters, Astrup and Hvidovre. Hereby, the potential difference of Danish groundwater is spanned.

7.3 Evaluation

The apparent conclusion from these experiments is that NF membranes are not suitable for removal of PTPs and that LPRO membranes should be used instead. This may however be stretching the empirical evidence. There may be NF membranes available that give higher rejections, and BAM and DEIA cannot be taken as representative for all PTPs. What the experiments do show is that it is dangerous to disregard the existence of PTPs when evaluating the applicability of a membrane. If the evaluation is purely based on the pesticides applied for pest control, the choice of membrane may be misguided. This is most clearly shown by comparing the measured rejections for atrazine and DEIA. Here the transformation of atrazine to DEIA greatly influences the rejection that can be obtained with the membrane as seen for the NF99 and NF99HF membranes. The modelling also shows that for smaller neutral organic pollutants such as DEIA, desethyl-desisopropyl-hydroxy-atrazine (DEIHA), glyphosate, AMPA and trichloro acetic acid (TCA), it may generally be difficult to get rejections above 95% with NF/LPRO membranes.

Chapter 8 Advanced membrane filtration for pesticide removal

This chapter is based on papers VII and VIII, where the work was performed at the research group of Professor Bart Van der Bruggen, at KU Leuven, Belgium. The papers were focused on how existing membrane technology could be improved for pesticide removal by adding different types of particles to the membrane matrix.

Specifically the studies aimed at investigating the following questions:

1. How can adsorptive particles be added to a membrane to increase rejection by combining adsorption and steric exclusion, and how will this affect the overall performance of the membrane?
2. How effective in rejecting pesticides is the use of a biomimetic membrane where transport of water is facilitated through aquaporin protein channels?

8.1 Background

In the previous chapter it was shown that existing commercial NF membranes might not be sufficient for filtration of water polluted with pesticides and PTPs, and that instead it may be necessary to use LPRO/RO membranes. These come at the expense of lower flux, which will increase cost of filtration. The next logical step was therefore to either: Improve the rejection capabilities of NF membranes or increase the flux of the RO membranes.

To do the first it was investigated how adsorptive particles could be implemented in the structure of NF membranes. The idea behind this approach was to let the membrane reject the main part of the pesticides/PTPs and then adsorb the fraction of the pollutants that moved through the membrane. To ensure that the adsorptive capacity of the membranes was only used for pesticides/PTPs actually penetrating the membrane, the particles were placed in the PES support layer in between the non-woven back layer and the selective polyamide layer. Potentially this approach could be the first step towards a complete rejection membrane. As could be seen from the previous chapter and in literature, existing membranes never obtain a complete removal, which may be a problem if the goal is completely pesticide free waters.

The second approach was based on collaboration with the Danish company Aquaporin A/S (AqP), who manufactures biomimetic membranes with aquaporin proteins embedded in the membrane. These protein channels offer a highly efficient specific transport of water molecules and could as such increase the flux of RO membranes without compromising the rejection. In this work, their membrane was tested in forward osmosis (FO) mode, and compared to an existing cellulose acetate FO membrane from Hydration Technology Innovations (HTI) for the removal of atrazine, DEIA and BAM. The idea behind this was that the HTI membrane had been used in almost all work on

trace organic removal with FO membranes, and through comparison with this membrane, the performance of the AqP membrane could be compared across studies.

8.2 Results

8.2.1 Adsorbing particles

As can be seen in figure 30, the introduction of adsorptive particles, in this case powderised activated carbon, significantly increased the amount of pesticide/PTP that could be adsorbed in the membrane. Especially for atrazine, where the amount of adsorbed atrazine increased with a factor of four after the activated carbon was introduced. But as figure 30 also shows, the increase in degree of adsorption for BAM and DEIA were more modest compared to that of atrazine. It was also found that the percentage of the permeating pesticides/PTPs that was adsorbed in the membrane decreased as a function of the total amount of pesticide/PTP that had permeated the membrane, see figure 30, and this highlighted one of the challenges when using adsorbents in membrane; namely that only a low adsorbent load was possible due to the limited volume of membrane. However, with a very high rejection and with the low pesticide/PTP concentrations seen in environmental samples it was estimated that a treatment capacity of >1000 m^3/m^2 (water/membrane) would be possible.

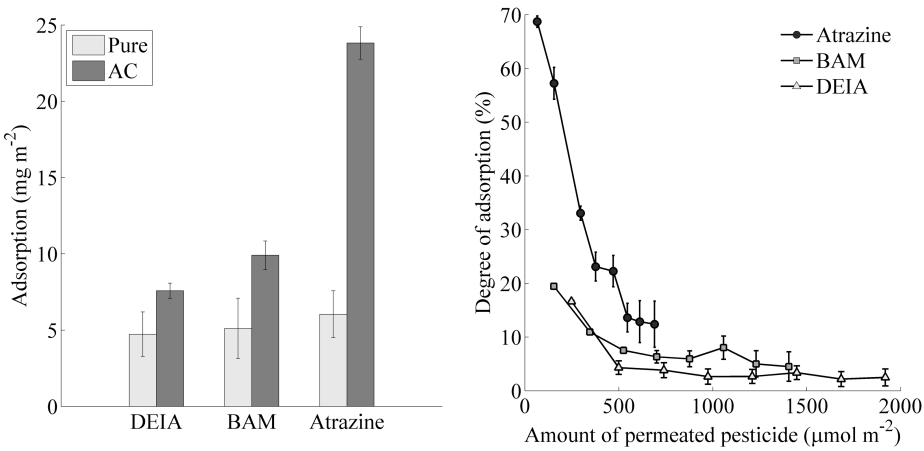

Figure 30 Adsorption of pesticide/PTP with membranes. To the left the amount of pesticide/PTP adsorbed by the membrane with added activated carbon (AC) is compared to a membrane with no activated carbon (Pure). The adsorption degree was measured as mg pesticide/PTP adsorbed per m^2 membrane after filtration of 100 mL solution. To the right the long term adsorption capacity for each of the three pesticides/PTPs is evaluated. This is done by measuring the percentage of the pesticides that permeates the membrane that are adsorbed as a function of the amount of pesticides that has permeated the membrane. Due to the difference in rejection for each of the three compounds, it is necessary to compare them with respect to the number of pesticide/PTP molecules passing the membrane rather than the volume of solution passing the membrane.

Finally, it was also shown how the addition of adsorbents to the PES support altered the membrane characteristics. The adsorbent load (mass of adsorbent relative to mass of polymer) decreased the stability of the membrane when it came above 1%, and if the adsorbents were not efficiently separated from the polyamide top layer they could have detrimental effects on both flux and rejection. As a result, a sandwich membrane of: non-woven polyester – PES (with adsorbent) – PES (no adsorbent) – polyamide was designed, with which it was possible to overcome these challenges.

8.2.2 Biomimetic membrane

For the biomimetic membrane it was found that significantly higher rejections for all three investigated compounds could be obtained with this membrane compared to the standard cellulose acetate membrane, see figure 31. This could be done without compromising flux, which was actually higher for the aquaporin membrane.

The reason for this difference was hypothesized to be due to the different transport mechanisms. For the HTI membrane it was shown that the rejections occurred because of steric hindrance whereas for the aquaporin membrane rejection was due to competitive diffusion of water and pesticide/PTP. That the aquaporin membrane was still capable of obtaining a higher flux may be due to the specific transport of water molecules via the aquaporin protein channels while the pesticides/PTPs must diffuse through the dense membrane matrix.

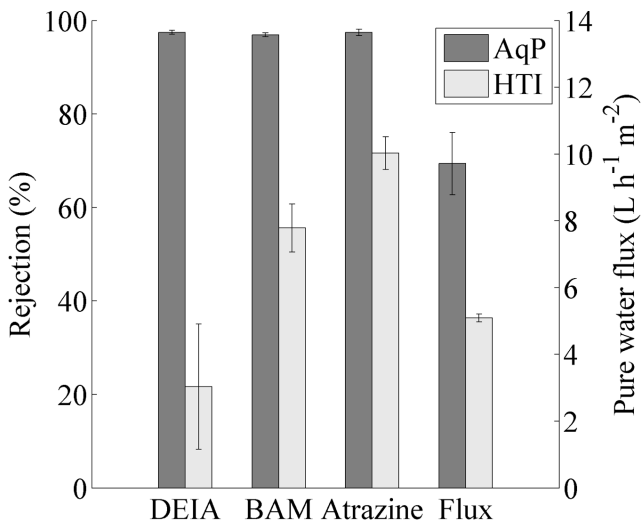

Figure 31 Removal of pesticide/PTP with aquaporin membrane. The bar plot compares the measured rejections and flux for the aquaporin (AqP) and the reference cellulose acetate (HTI) membrane. Error bars represents standard deviations based on triplicate samples.

8.3 Evaluation

In these experiments it was shown that it is possible to improve the filtration capacity of existing membranes with respect to pesticide removal by addition of particles to the membranes.

The use of adsorbents is an interesting and promising technology, but as was shown in this study much work is needed here. Active carbon was not an effective adsorbent for removal of small polar pesticides/PTPs such as BAM and DEIA. Since these compounds can be expected to be rejected the least, it will be important to develop adsorbents with a higher affinity for these compounds. Because the adsorbents affected the flux and rejection of the membrane negatively when in contact with the polyamide layer, it will also be necessary to design better methods to obtain the desired sandwich structure. The method used in this study was acceptable for laboratory investigations, but lead to relatively heterogeneous PES layers and a high percentage of malfunctioning membranes.

Aquaporins also represent a very interesting technology, but the experiments performed in this study only showed the potential of the aquaporin membrane, and did not clarify the exact importance of the proteins. To be able to conclusively state that aquaporins can be used to make membranes with high rejections of pesticides, it will be necessary to investigate their influence in greater detail.

Chapter 9 Degradation of BAM with electrochemical oxidation

This chapter presents the main results from papers IX and X. The papers focused on the electrochemical oxidation of BAM with an overall purpose of determining degradation pathways for both the EOTR and the indirect chloride mediated oxidation.

Specifically the study aimed at investigating the following questions:

1. What is the degradation pathway for the electrochemical oxidation of BAM for both the EOTR and the chloride mediated oxidation?
2. How many degradation intermediates are formed, and how does this depend on the type of electrolyte and electrode?

9.1 Background

At the time of this study, the really interesting question when it came to electrochemical oxidation of pesticides, was not so much as whether the process would be effective in degrading the pesticides or not. The existing literature had shown it would be. Instead the interesting questions were rather, which DIs would be formed and in how large quantities. Also the question of energy consumption was interesting, and we will return to this in the next chapter. As shown in section 3.2.1 degradation pathway had been mapped for a number of pesticides, but almost exclusively for the EOTR process. Very little work had been attempted in cases with an active electrolyte such as chloride, although the omnipresence of chloride made it unlikely not to encounter this ion in real cases. Furthermore, in none of the studies had it been attempted to quantify the DIs.

Based on these observations it was decided to investigate the degradation of the PTP BAM, in both an inert (sodium sulphate) and an active (sodium chloride) electrolyte environment. As was outlined in the introduction, BAM is the single most important groundwater pollutant in the Danish pesticide surveillance, but in spite of this no work on electrochemical oxidation or other AOPs with BAM as the target pollutant had been undertaken. In line with other studies on degradation of pesticides, the EOTR mediated degradation pathway was investigated, and to investigate the importance of chloride, the degradation pathway in the presence of chloride was determined for comparison. To quantify the DIs, a new method based on the concentration of BAM and TOC were developed, where the carbon bound in BAM was subtracted from the total amount of organic carbon, to get the amount of carbon bound in DIs.

9.2 Results

As expected, BAM was found to be efficiently degraded in both the sulphate and chloride solutions; however, the two electrolytes resulted in markedly different degradation pathways as seen in figure 32 and figure 33. In the inert sulphate solution, the degradation occurred by hydroxylation of the aromatic ring, and dechlorination as a parallel pathway when using the BDD cell. One of the key observations was that the amide group was not affected by the EOTR process.

When chloride was used as the electrolyte, the formation of active chlorine resulted in oxidation of the amide group as the initial step. Here two parallel routes were observed, one in which the amide group was oxidised to an amine group, and a second in which it was oxidised to a carboxylic acid group. By comparing the rate of degradation in solutions of varying volume, it could be seen that this initial oxidation was mainly driven by the active chlorine; especially for the Pt anode while the EOTR oxidation also played a role for the BDD anode. After the initial oxidation, parallel oxidation by active chlorine and the anode led to a mixture of chlorinated and hydroxylated DIs. Here one of the most significant findings was that when using the active Pt anode, some of the chlorinated DIs were difficult to degrade, while the higher oxidation potential of the BDD anode allowed for an easier removal of these recalcitrant DIs.

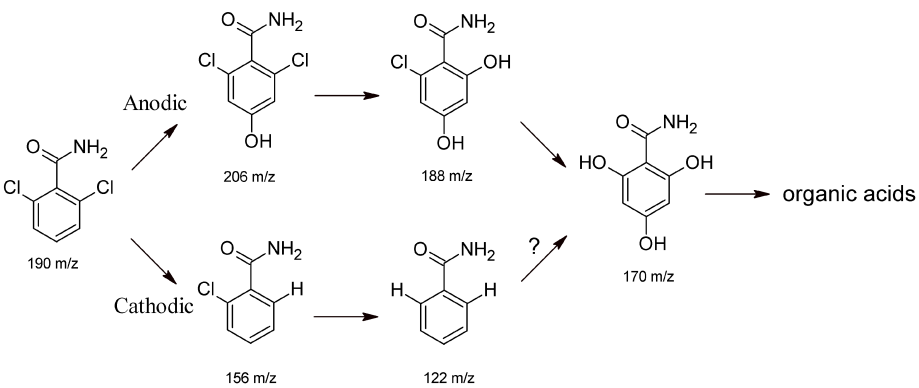

Figure 32 Degradation pathway for the EOTR mediated oxidation.

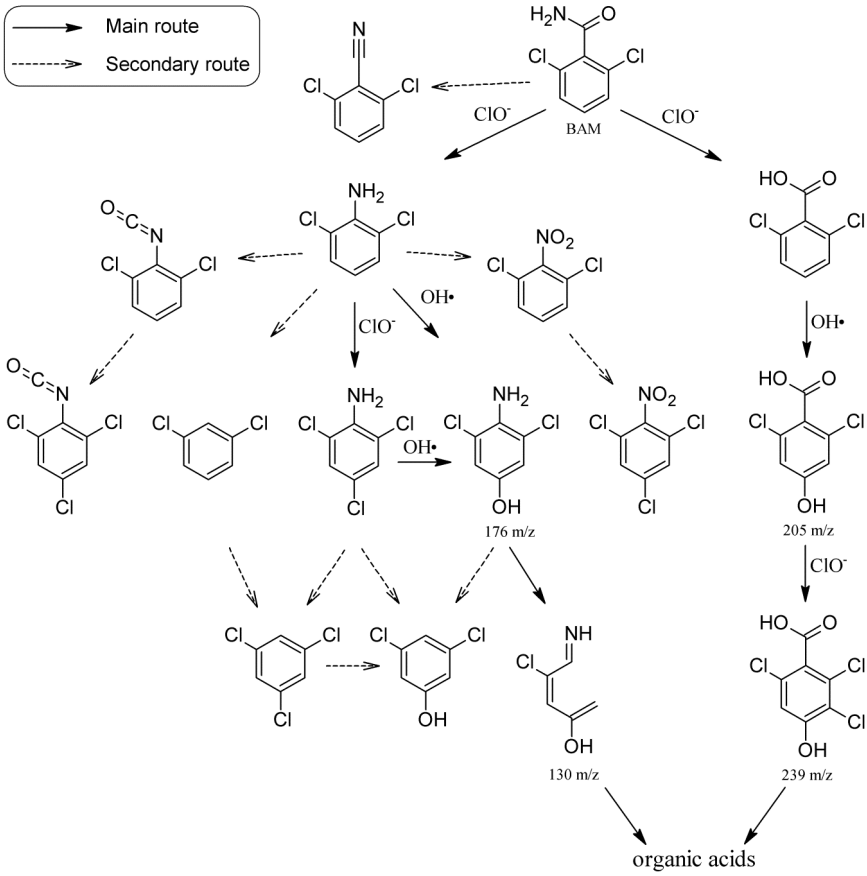

Figure 33 Degradation pathway for the chloride mediated oxidation. The compounds detected with HPLC/ESI-MS are highlighted with the m/z values. The remaining compounds were detected with GC/MS. The secondary routes represented compounds that were formed in much lower amounts and for which the development in intensity over time was not determined.

Since a more diverse mixture of DIs was found when using chloride as the electrolyte, it could be expected that this would also correspond to a higher total number of DIs. In figure 34 it can be seen that this was not the case. Actually, the opposite trend was seen with a significant reduction in the total number of DIs for the Pt anode when using chloride compared to sulphate. For the BDD anode, a comparable amount was seen, although the DIs were degraded more efficiently with respect to the specific charge when using chloride as the electrolyte. From these results it seems reasonable to hypothesise that it is the most powerful oxidant that determines the total amount of DIs. In these experiments the following oxidants were present HO• (BDD) > active chlorine > MO (Pt). Because active chlorine has a higher reduction potential compared to the metal oxide (MO) of the Pt anode, a significant reduction in the total quantity of DIs was seen when shifting from

sulphate to chloride. On the other hand, no significant change was seen for the BDD anode since the hydroxyl radical continued to be the strongest oxidant here.

Finally, it was also interesting to investigate the effect of the two anodes and electrolytes on the energy consumption. Since the synthetic solutions were not representative of real waters and because different cells were used in the two sets of experiments, the specific energy consumption was not particularly interesting to compare. Instead, the ability of the setups to use the electrical energy for BAM and DI oxidation measured as the mineralization current efficiency (MCE), see section 3.1, was compared.

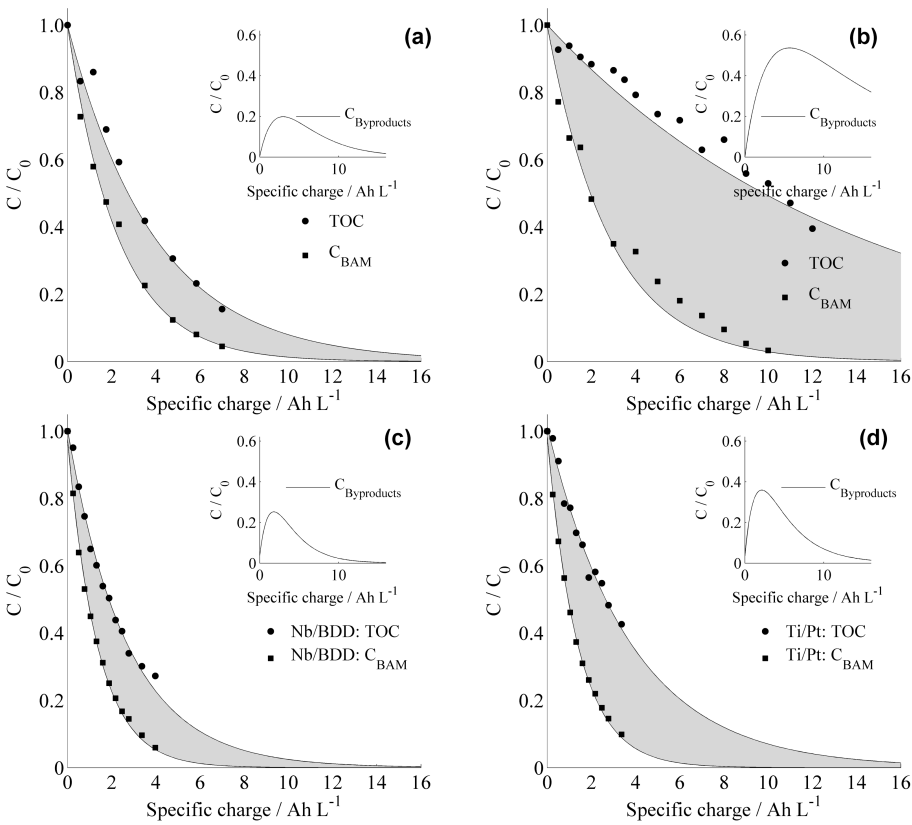

Figure 34 Quantitative DI plots. (a) BDD sulphate, (b) Pt sulphate, (c) BDD chloride, (d) Pt chloride. The difference between the BAM and the TOC curves represents the remaining organic carbon, which is the DIs. The integrated areas are plotted in the subplots.

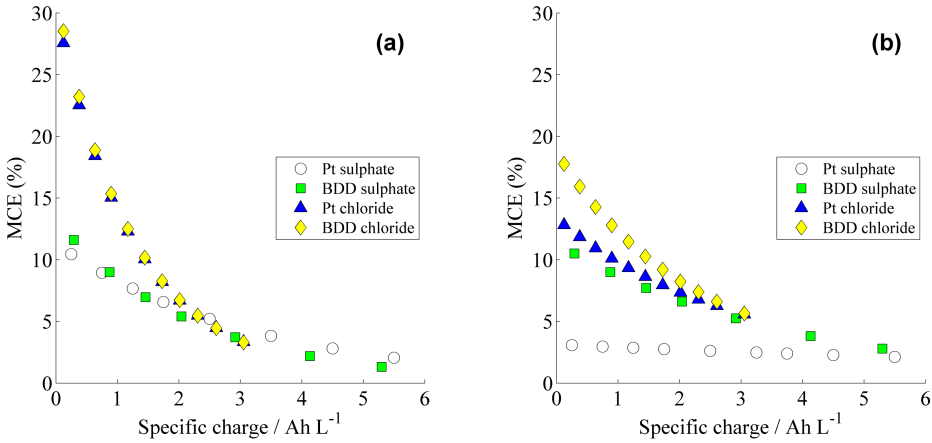

Figure 35 Comparison of the MCE for BAM (a) and TOC (b) removal.

From the plots in figure 35 it can be seen that the efficiency of the removal of BAM was enhanced with almost a factor 3 when shifting from the inert sulphate electrolyte to the active chloride electrolyte, while the effect of the different anode materials was of insignificant importance. The reason for this behaviour was that BAM was relatively easily degraded by both active chlorine, the Pt anode and the BDD anode. Because of the high chloride concentration relative to BAM, a higher efficiency could be obtained because chloride ensured that a higher proportion of the current was used to generate oxidants rather than water splitting. From the TOC plots, it is seen that here both anodes and electrolyte determined the overall efficiency. The reason for the influence of the anodes was that some of the DIs were more efficiently degraded by the BDD anode compared to the Pt anode and active chlorine.

9.3 Evaluation

In general these experiments showed the importance of investigating both the EOTR mediated degradation pathway and the pathways mediated by electroactive ions. The presence of chloride led to a completely different set of DIs, and if decisions regarding DIs in the design process of an electrochemical oxidation system are based solely on experiments with inert electrolytes, these will not stand the test of reality. Actually, based on these experiments, it may be more important to investigate the degradation pathway mediated by chloride since active chlorine may completely dominate the initial step in the oxidation. It is of course necessary to mention that these effects are only strictly valid for BAM. If another compound that is more resistant towards oxidation by active chlorine is to be degraded, then it may be the EOTR pathway that will be dominant. However, in the studies where chloride have been used, the rate of degradation is to the best of our knowledge almost always found to increase, indicating that pesticides generally are susceptible to active chlorine oxidation.

In general BDD was found to be the most efficient of the two anodes both with respect to efficiency and total amount of DIs, but a closer examination showed that active anodes such as Pt may still be attractive. Although a higher rate of removal of BAM was obtained with BDD in the sulphate solution, the rate constants for the BDD and Pt anodes were not very different, and when chloride was used as the electrolyte there was no difference. Furthermore, although BDD resulted in a smaller amount of total DIs, the difference may be due to carboxylic acids. When the plots of total DIs are compared with the plots of intensities for the individual DIs found in the papers, it can be seen that the amount of DIs left when using the Pt anode is still high when the individual DIs have been degraded, indicating that the remaining DIs are primarily carboxylic acids. These are usually considered to be less toxic and more biodegradable, and therefore less problematic. Active anodes such as Pt may as such allow for a more specific oxidation, where the current is primarily used to oxidise the parent compounds prior to formation of carboxylic acids, and this could make the overall process more economical. Finally, one aspect that was not looked at in the studies with chloride, and which could make active anodes more competitive with BDD, was the formation of the inorganic byproducts, chlorate and perchlorate. These compounds are starting to attract attention since they may be formed in concentrations that are in violation with the drinking water guidelines, and BDD is usually found to generate higher amounts of these compared to active anodes [34]. In total, these considerations show that active anodes should not be immediately ruled out as potential candidates for electrochemical pesticide oxidation.

Chapter 10 Combined use of electrochemical oxidation and membrane filtration

This chapter presents the main results from paper XI. The paper focused on how electrochemical oxidation could be combined with membrane filtration to reduce the energy consumption of pesticide removal.

Specifically the study aimed at investigating the following questions:

1. How was the degradation/energy efficiency of the electrochemical oxidation affected by NF/RO membrane filtration?
2. How was the overall energy consumption affected by the combined use of electrochemical oxidation and NF/RO membrane filtration?

10.1 Background

In the previous chapters, it was shown how pesticides could be removed with either membrane filtration or electrochemical oxidation. However, both of these techniques suffered from certain disadvantages. For membrane filtration the most obvious problem was that it was a non-destructive technique that did not degrade and hereby remove the pesticides, but transferred them from the feed to the concentrate. Although smaller in volume, the pesticide concentration in the concentrate would be higher, and thus the membrane filtration could be said to merely move the problem, not remove it. Electrochemical oxidation was capable of removing the pesticides, but the energy requirement for this would be high. Therefore, it was investigated whether it was possible to overcome the challenges of both techniques through a combinatorial scheme, in which the electrochemical oxidation was applied to the membrane concentrate as outlined in figure 36.

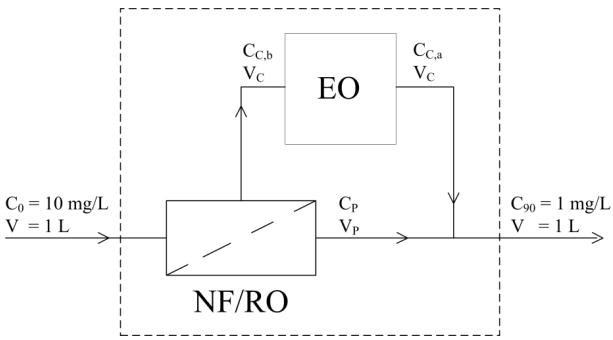

Figure 36 Conceptual scheme for the combination of electrochemical oxidation and membrane filtration.

The underlying hypothesis was that the energy consumption of the electrochemical oxidation could be lowered by applying it to the membrane concentrate since this would have a higher conductivity and thus a lower ohmic resistance. The higher pesticide concentration could also potentially lead to a faster and more efficient removal as was discussed in chapter 3. Finally, the fact that the electrochemical oxidation would only have to be applied to the fraction of the incoming water (V) that was left in the concentrate (V_c) could reduce the overall energy consumption. However, the reduction in energy would be a combination of the membrane's rejection of the pesticide and the energy consumption of the membrane filtration itself. A low rejection would require a higher degree of removal of pesticide/PTP from the concentrate to allow the final concentration to get below the required level. High rejection could on the other hand come at the expense of a higher energy consumption by the membrane.

To evaluate the energy consumption of the degradation, the IUPAC definition for AOP energy consumption was used.

$$EE_V = \frac{P \cdot t_{90}}{V \cdot \log\left(\frac{C_0}{C}\right)} \tag{23}$$

This describes the energy (kWh/m^3) required to obtain a 1-log removal (90%) of the pollutant. In this work BAM was used as the chosen pesticide/PTP. This was done both to link this study to the rest of the work in this thesis and because of BAM's importance in the Danish groundwater pollution. The experiments were performed in tap water to provide realistic estimates of the energy consumption.

10.2 Results

In figure 37 the respective effect of a NF (NF99HF) and a RO membrane (XLE) at two different recoveries (80 and 90%) on the degradation efficiency are compared. The experiments showed that although the NF membrane increased the conductivity, the reduction in the energy consumption of the electrochemical oxidation was small. This was due to a reduction in the rate of degradation, possibly because of the increased concentration of bicarbonate, which could act as a hydroxyl radical scavenger [145–148]. For the RO membrane a significant reduction in the energy consumption was observed. This was explained by the high rejection of chloride by the RO membrane. The increased concentration of chloride in the RO concentrates allowed for the formation of active chlorine, which benefited the degradation. Another interesting observation was that the increase in BAM concentration by the membrane filtration affected the degradation efficiency negatively. From traditional kinetic theory, the initial concentration is expected to have no influence on first order rate constants, which is the assumption that most AOP experiments, in which higher pollutant concentrations are used to facilitate analysis, is based upon. In this study a negative influence on the rate constant, most pronounced in the RO concentrates, was found, which is in contrast to both traditional theory and other results reported in literature as discussed in chapter 3.

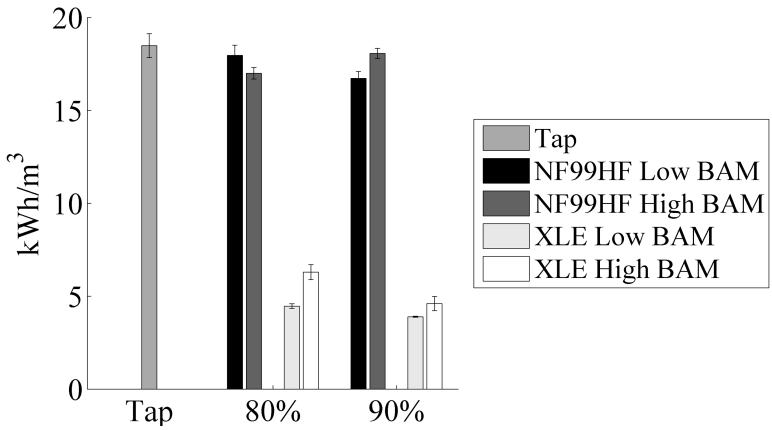

Figure 37 Effect of membrane filtration on degradation efficiency. Degradation efficiency here is defined as the energy consumption required to obtain a 1-log removal of BAM in 1 m^3 of the water (tap water or membrane concentrate).

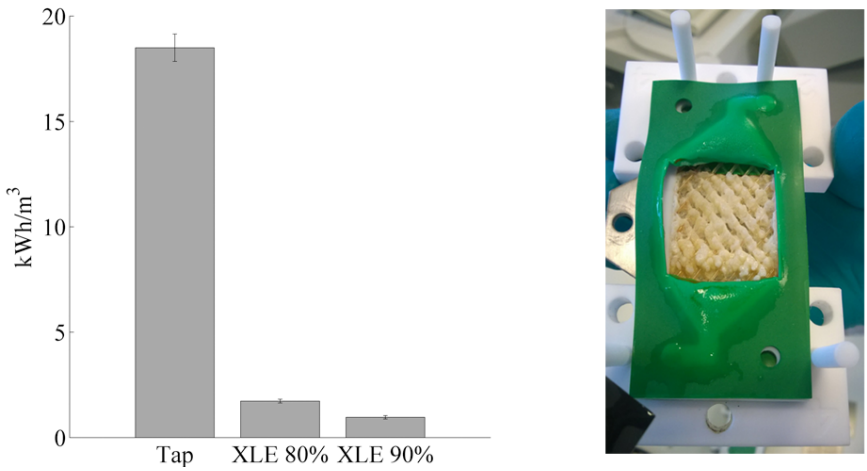

Figure 38 Energy reduction and scaling issues. The bar plot on the left shows the effect of membrane filtration with the LPRO membrane XLE on the total energy consumption of a setup where the electrochemical oxidation is applied to the membrane concentrate. The "tap water" bar illustrates the scenario with no membrane (recovery = 0%). The error bars represent the standard deviation measured from duplicate experiments. The picture to the right shows an example of $CaCO_3$ scaling on the cathode. This particular photo was taken after two experiments with tap water and three experiments with 90% NF99HF recovery. It can be seen how the $CaCO_3$ has precipitated on the cathode and the threaded spacer from where it has grown towards the anode. The green spacer is a Viton gasket used to separate the electrodes and seal the setup.

With respect to the overall energy consumption of the combined membrane/EO system, the NF membrane was found to be unsuitable for the specific case of BAM. The low rejection of BAM, see chapter 7, ensured that it was not possible to obtain a 1-log removal in either the 80% recovery or the 90% recovery scheme because of too much BAM passing through the membrane and into the permeate. The RO membrane could be used, and here a significant reduction in energy was found, see figure 38. The reason for this reduction was a combination of both the increased degradation efficiency as seen in figure 37, and the decrease in the volume in need of electrochemical treatment. The membrane filtration was significantly less energy intensive (0.2 kWh/m^3) compared to the electrochemical oxidation (18.5 ± 0.7 kWh/m^3, tap water), which meant that the energy consumption decreased with increasing recovery. The highest energy reduction was observed for the 90% recovery solution, where a reduction of 94.8% was obtained.

10.3 Evaluation

By combining electrochemical oxidation with membrane filtration, it is possible to significantly reduce the overall energy consumption. Because of the large difference in the energy consumption by the electrochemical oxidation and the membrane filtration, the results indicated that it would be beneficial to increase the level of recovery even more than the 90% used in this study. Two factors may however affect this. First, because rejection is a ratio of the permeate concentration and the average concentration of feed and concentrate, increasing the recovery will lead to an increased permeate concentration of BAM. This will require a prolonged electrochemical oxidation to lower the BAM concentration in the concentrate sufficiently to obtain the 1-log removal in the final mixed stream, and may make the process less energy efficient. Secondly, by increasing recovery in general, the solubility of several ionic species may be exceeded leading to scaling of the membrane. In these experiments, $CaCO_3$ was found to precipitate from the concentrates. Due to the alkaline conditions at the cathode, precipitation of $CaCO_3$ was especially pronounced here as seen from the picture in figure 38. The precipitation was not found to affect the efficiency of the electrochemical oxidation, but the additional costs of the required cleaning or use of anti-scalants should be included into the overall economic evaluation of the process and may constitute a limitation to the general applicability of electrochemical oxidation of pesticides in groundwater.

Finally, the water used in these experiments came from South Western Denmark and was relatively soft. Harder water would lower the possible level of recovery, and since the volume reduction was a significant part of the total reduction in energy consumption, the reduction in energy could be lower for harder waters.

Despite these further challenges, the energy reduction obtained through combining electrochemical oxidation and membrane filtration was substantial, and could be a significant step on the path to making electrochemical oxidation cost competitive with other treatment options.

Conclusion

In this study pesticides and pesticide transformation products have been shown to have a major impact on Danish drinking water production, resulting in many closed wells and delocalisation of the drinking water structure. The current scheme of aeration and sand filtration was found not to remove the pesticides and transformation products, and therefore membrane filtration and electrochemical oxidation was investigated as alternative methods for treatment. Based on the experimental results, it can be concluded that:

- Aeration/sand filtration can be used as a pre-treatment for a subsequent NF/RO membrane filtration, as it lowered the fouling index from 25 m^{-1} to 0.11 m^{-1}. However, an even lower fouling index of 0.066 m^{-1} was obtained using a ceramic UF membrane, which might offer a better treatment option. Overall, sand filtration and/or ceramic membranes offer ways of pre-treating groundwater without the addition of chemicals.
- Existing commercial NF/RO membranes can be used to give high removals of pesticides. However, the presence of transformation products in the groundwater can make NF membranes insufficient, requiring the use of more energy intensive RO membranes that will also desalinate the water to a larger extent.
- Rejections will be higher in groundwater compared to laboratory grade water because the pore size of the membranes is reduced, most likely due to ion adsorption to the membrane surface. When the pore size is known, rejection can be predicted based on the spatial geometry of the pesticides/PTPs, allowing for the use of steric models as a tool for evaluating the applicability of a given membrane to remediate a polluted groundwater.
- By incorporating adsorbents in the support layers of a thin film composite membrane, adsorption of the pesticides permeating the membrane can be increased. In this way the perceived rejection of a membrane can be increased, giving higher removals of pesticides. Neither active carbon, carbon nanotubes nor acid activated clay are efficient adsorbents for small polar PTPs such as BAM and DEIA.
- High rejections (>97%) can be obtained by using biomimetic membranes, where the water transport is facilitated by aquaporins. Use of aquaporins in membranes allows for the design of membranes with dense active layers, where water is transported through the membrane by aquaporins while pesticides can only be transported by diffusion through the dense active layer.
- The most widely detected pollutant BAM, can be efficiently degraded by both Pt and BDD anodes, but with BDD yielding the highest rate of removal and fewest degradation intermediates. When chloride is used as the supporting electrolyte, the difference in efficiency between the two anode materials is smaller, but BDD is better at obtaining a complete mineralization. In general the degradation pathway will be very dependent on whether an inert or an electroactive electrolyte is used.

- By combining RO membrane filtration with electrochemical oxidation, the overall energy consumption of the process can be lowered. Electrochemical oxidation required 93 times as much energy as the membrane filtration, and by only applying the electrochemical oxidation to the membrane concentrate the total energy consumption could be significantly reduced. Increased chloride content and conductivity further improved the energy efficiency of the process.

The overall objective of this thesis was to investigate how membranes and electrochemical oxidation could be used as non-chemical methods to remove pesticides and PTPs from groundwater. Summing up the results of the thesis, this removal can be achieved by implementing a membrane filtration step after the existing aeration and sand filtration, with an electrochemical cell added to the concentrate stream. To ensure sufficient removal of even small PTPs, LPRO/RO membranes should be used, and compared to NF membranes these membranes will also give a larger reduction of the energy consumption of the electrochemical oxidation.

Future perspectives

As it has been shown in this work, there are great possibilities and advantages to be obtained by combining membranes and electrochemical oxidation for the removal of pesticides. I will end the thesis by both highlighting some of the areas where further research could be made, and with some general thoughts about how membranes and AOPs could be implemented to remove pesticides and other micropollutants as well as to generally improve water quality.

Areas of further research

In the study of the applicability of commercial membranes presented in paper VI, it was shown that the rejection of the pesticides/PTPs could be reasonably modelled for each of the three water types. It would be interesting to investigate how much this model could be improved by including other aspects such as diffusion. However, part of the attractiveness of the model from an engineering point of view is that it does not require time-consuming experimental work to determine diffusion coefficients, and although inclusion of diffusion might improve the model, it might also complicate it unnecessarily. What would be really interesting would be to include the effect of the ionic environment into the model. The experiments showed that there was a large difference between the rejections observed in demineralised water and real groundwater, and that this difference was caused by ion adsorption to the membranes. By investigating the relative influence of each ion on the change in rejection, it could become possible to predict the effect of a given water source on rejection.

The use of adsorbents in TFC membranes represented a completely new approach within pesticide removal with membranes. The general applicability of the approach was shown, but the study was left with many unanswered questions. One of these was the need for better adsorbents. The use of active carbon was not an effective solution for the small polar PTPs BAM and DEIA, and adsorbents need to be tailored towards compounds such as these. A possible strategy could be to produce silica nanoparticles and then alkylate them with silane coupling agents with variable functional groups. Also, a better casting technique needs to be developed, which will keep the adsorbents separated from the polyamide layer and homogenously dispersed in the support layer.

The use of aquaporins in the removal of pesticides also represented a new approach where more work is necessary. Of highest importance is the verification of the effect of the aquaporins on the rejection. This can be done by testing the performance of a membrane without aquaporins or with inactive aquaporins and comparing it with the results of a membrane with active aquaporins. The use of DEIA ensured that the rejection of even small micropollutant was shown, but it will be interesting to investigate how far down in molecular size high rejection is obtainable. When the use of aquaporins has been established, the addition of ion specific protein channels would represent a highly interesting area. If calcium ion channels were incorporated in the membrane structure, calcium scaling could be reduced allowing for higher recoveries.

In the area of electrochemical oxidation there will be a need to continue the work on degradation pathways, and here focus should also be on PTPs due to their importance in groundwater pollution. As was shown, it will be important to also investigate the chloride mediated degradation pathways since these can be completely different from the EOTR mediated pathways.

Lastly, in the area of membrane and AOP combination, I will highlight two focus points. First, it will be necessary to investigate methods that can reduce the scaling on the cathode due to the alkaline environment formed here. One possibility could be the use of an ion exchange membrane. A highly conductive solution could then be kept on the cathode side, while the membrane concentrate was kept on the anode side. Secondly, only the effect on electrochemical oxidation was investigated. It would be interesting to also investigate the effect on other AOPs such as photocatalysis, and to compare the effectiveness of different AOPs for a given water type.

Areas of applications for membranes and AOPs in micropollutant abatement

Due to the simultaneous removal of pesticides and ionic species, the combination of membranes and AOPs will make it possible to produce "designed water" in which pesticides are removed and a desired ionic content is reached. Systems like the one outlined in chapter 10 could be used to first separate the water in a "clean" permeate and a polluted concentrate stream. After being depolluted, softened etc., the concentrate stream could be dosed back into the permeate to obtain the desired ionic composition of the treated water.

The use of membranes and AOPs could also find use in other areas where micropollutants are a problem. Examples of these are: Municipal wastewater, landfill percolate and industrial wastewater. Municipal wastewater represents an interesting opportunity to apply osmotic membranes. These could be implemented as a final polishing step in the wastewater treatment, and would ensure that micropollutants such as endocrine disruptors would not be discharged into the environment. By applying osmotic membranes, seawater could be used as the driving force, which would significantly reduce the expenses for pumping. The polishing would in this way almost become self-propelling, and the controlled mixing would reduce the environmental impact of discharging fresh water into seawater. If the osmotic membranes were applied in a pressure retarded osmosis scheme, the energy generated could be used to drive the electrochemical treatment of the concentrate.

A third idea could be to turn the application of membranes for pesticide removal upside down. Instead of focusing on the use of membranes to clean up water after it has been polluted, membranes could be used to avoid pollution in the first place, and at the same time make the agriculture business more efficient. As it was discussed in the introduction, pesticides are used because we need them. It is unrealistic to imagine a world in which all agriculture is based on organic farming. Such a practice would lead to widespread famine and hunger. Therefore, instead of putting restrictions on how many pesticides a farmer can use, restrictions could be put on how many pesticides he was allowed to discharge to the environment. In the same way as it is done for other industries. In such a scenario, it might become beneficial for the farmer to establish a system in which all water that percolates through the soil is collected and treated with a membrane. The

pesticides can then be recirculated back into use and the clean water discharged to the environment. The pesticide collection system would enable the farmer to decide how many pesticides and nutrients to use, and hereby potentially increase the output per hectare, which could mean less farming and hereby a reduced effect of agriculture on the environment.

Bibliography

1. Ware G, Whitacre D. The Pesticide Book. 6th ed. Meister Media; 2008.

2. Srivastava S, Goyal P, Srivastava MM. Pesticides: Past, Present and Future. In: Nollet LML, Rathore HS, editors. Handbook of Pesticides - Methods of Pesticide Residue Analysis. CRC Press; 2010. p. 47–65.

3. McKinlay R, Plant JA, Bell JNB, Voulvoulis N. Endocrine disrupting pesticides: Implications for risk assessment. Environ Int. 2008;34:168–83.

4. Skinner JA, Lewis KA, Bardon KS, Tucker P, Catt JA, Chambers BJ. An Overview of the Environmental Impact of Agriculture in the U.K. J Environ Manage. 1997;50:111–28.

5. Sanborn M, Bassil K, Vakil C, Kerr K, Ragan K. 2012 Systematic Review of Pesticide Health Effects. 2012.

6. Global Environment Outlook 5, United Nations Environment Programme. 2012.

7. Guldagger M. Danske børn har sprøjtegifte i urinen (Danish children have pesticides in the urin). Politiken [Internet]. 2013; Available from: http://politiken.dk/forbrugogliv/sundhedogmotion/forbrugerkemi/ECE1960165/danske-boern-har-sproejterester-i-urinen/

8. Mage DT, Allen RH, Gondy G, Smith W, Barr DB, Needham LL. Estimating pesticide dose from urinary pesticide concentration data by creatinine correction in the Third National Health and Nutrition Examination Survey (NHANES-III). J Expo Sci Environ Epidemiol. 2004;14:457–65.

9. Thorling L, Brüsch W, Hansen B, Larsen CL, Mielby S, Troldnorg L, et al. Grundvand - Status og udvikling 1989 – 2012 (Groundwater: Status and development 1989 - 2012). Technical report, Geological Survey of Denmark and Greenland, 2013.

10. Danmarks Statistik [Internet]. Available from: http://www.statistikbanken.dk/statbank5a/default.asp?w=1600

11. Thorling L, Hansen B, Larsen CL, Brüsch W, Møller RR, Mielby S, et al. Grundvand - Status og udvikling 1989 – 2009 (Groundwater: Status and development 1989 - 2009). Technical report, Geological Survey of Denmark and Greenland, 2010.

12. Søgaard EG, Madsen HT. Groundwater Chemistry and Treatment: Application to Danish Waterworks. In: Elshorbagy W, Chowdhury RK, editors. Water Treatment. 1st ed. InTech; 2013. p. 223–46.

13. Kjær J, Rosenbom AE, Brüsch W, Juhler RK, Gudmundsson L, Plauborg F, et al. The Danish Pesticide Leaching Assessment Programme. Technical report, Geological Survey of

Denmark and Greenland, Department of Agroecology and Department of Bioscience Aarhus Univerisity, 2010. Control.

14. Thorling L, Hansen B, Langtofte C, Brüsch W, Møller RR, Mielby S. Grundvand: Status og udvikling 1989 – 2011 (Groundwater: Status and development 1989 - 2011). Technical report, Geological Survey of Denmark and Greenland, 2012.

15. Lindhart B, Kjær J. Overvågning af pesticider i grundvand (Surveillance of pesticides in groundwater), Geological Survey of Denmark and Greenland, Årsberetning, 2000.

16. Nyegaard P, Larsen CL, Brüsch W, Rasmussen P, Højberg AL. Grundvandsovervågningen 1998-2003 (The groundwater monitoring 1998-2003). Technical report, Geological Survey of Denmark and Greenland, 2004.

17. Grant R, Blicher-Mathiesen G, Pedersen LE, Jensen PG, Madsen I, Hansen B, et al. Landovervågningsoplande 2006 - NOVANA (Land surveillance catchment areas 2006 - NOVANA). Technical report, Danish Environmental Investigation, Aarhus Univerisity, 2007.

18. Juhl MM, Bjerg B. Økonomisk vurdering af forskellige strategier til at imødegå BAM-problemer på vandværker (Economic evaluation of different strategies to counter BAM-problems at waterworks). Technical report, Danish Environmental Protection Agency , 2004.

19. Søgaard EG, Aruna R, Abraham-Peskir J, Koch CB. Conditions for biological precipitation of iron by Gallionella ferruginea in a slightly polluted ground water. Appl Geochemistry. 2001;16:1129–37.

20. Kowalski KP, Madsen HT, Søgaard EG. Comparison of sand and membrane filtration as non-chemical pre-treatment strategies for pesticide removal with nanofiltration/low pressure reverse osmosis membranes. Water Sci Technol Water Supply. 2014;14(4):532.

21. Plakas K V., Karabelas AJ. Removal of pesticides from water by NF and RO membranes - A review. Desalination. 2012;287:255–65.

22. Muff J. Applications of Electrochemical Oxidation for Degradation of Aqueous Organic Pollutants. Aalborg University; 2010.

23. Comninellis C, Kapalka A, Malato S, Parsons SA, Poulios I, Mantzavinos D. Advanced oxidation processes for water treatment: advances and trends for R&D. J Chem Technol Biotechnol. 2008;83:769–76.

24. Ijpelaar GF, Groenendijk M, Hopman R, Kruithof JC. Advanced oxidation technologies for the degradation of pesticides in ground water and surface water. Water Sci Technol Water Supply. 2002;2(1):129–38.

25. Quiroz MA, Bandala ER, Martínez-huitle CA. Advanced Oxidation Processes (AOPs) for Removal of Pesticides from Aqueous Media. In: Stoytcheva M, editor. Pesticides - Formulations, Effects, Fate. InTech; 2011. p. 685–730.

26. Poyatos JM, Muñio MM, Almecija MC, Torres JC, Hontoria E, Osorio F. Advanced Oxidation Processes for Wastewater Treatment: State of the Art. Water Air Soil Pollut. 2010;205:187–204.

27. Lazarova Z, Spendlingwimmer R. Treatment of yellow water by membrane separations and advanced oxidation methods. Water Sci Technol. 2008;58:419–26.

28. Kwon M, Yoon Y, Cho E, Jung Y, Lee B-C, Paeng K-J, et al. Removal of iopromide and degradation characteristics in electron beam irradiation process. J Hazard Mater. 2012;227-228:126–34.

29. Rozen AE, Kamyshanskii SI, Vorob'ev E V., Usin V V., Raevskaya EG. Physicochemical foundations and specificity of the practical application of supercritical water oxidation to the destruction of persistent organic pollutants. Russ J Phys Chem B. 2012;6:744–9.

30. Remya N, Lin J-G. Current status of microwave application in wastewater treatment - A review. Chem Eng J. 2011;166:797–813.

31. Madsen HT, Søgaard EG. Case study of treatment of waste water for 17α-ethinylestradiol and microorganisms with UV and photocatalysis in an on-going process of introducing AOP techniques in the Danish water sector. Water Pract Technol. 2012;7(4).

32. Boye B, Brillas E, Marselli B, Michaud P, Comninellis C, Farnia G, et al. Electrochemical incineration of chloromethylphenoxy herbicides in acid medium by anodic oxidation with boron-doped diamond electrode. Electrochim Acta. 2006;51:2872–80.

33. Cavalcanti EB, Garcia-Segura S, Centellas F, Brillas E. Electrochemical incineration of omeprazole in neutral aqueous medium using a platinum or boron-doped diamond anode: Degradation kinetics and oxidation products. Water Res. 2013;47:1803–15.

34. Bergmann MEH, Koparal AS, Iourtchouk T. Electrochemical Advanced Oxidation Processes, Formation of Halogenate and Perhalogenate Species: A Critical Review. Crit Rev Environ Sci Technol. 2014;44:348–90.

35. Miralles-Cuevas S, Arques A, Maldonado MI, Sánchez-Pérez JA, Rodriguez SM. Combined nanofiltration and photo-Fenton treatment of water containing micropollutants. Chem Eng J. 2013;224:89–95.

36. Van der Bruggen B, Vandecasteele C. Removal of pollutants from surface water and groundwater by nanofiltration: overview of possible applications in the drinking water industry. Environ Pollut. 2003;122:435–45.

37. Moons K, Van der Bruggen B. Removal of micropollutants during drinking water production from surface water with nanofiltration. Desalination. 2006;199:245–7.

38. Sanches S, Penetra A, Rodrigues A, Ferreira E, Cardoso VV, Benoliel MJ, et al. Nanofiltration of hormones and pesticides in different real drinking water sources. Sep Purif Technol. 2012;94:44–53.

39. Bellona C, Drewes JE, Xu P, Amy G. Factors affecting the rejection of organic solutes during NF/RO treatment - a literature review. Water Res. 2004;38:2795–809.

40. Turner AG. Operational experience of a nanofiltration plant for pesticide removal. Membr Technol. 1998;1988(104):7–9.

41. Ventresque C, Gisclon V, Bablon G, Chagneau G. An outstanding feat of modern technology: the Mery-sur-Oise Nanofiltration Treatment Plant (340,000 m3/day). Desalination. 2000;131:1–16.

42. Majamaa K, Warczok J, Lehtinen M. Recent operational experiences of FILMTEC ™ NF270 membrane in Europe. Water Sci Technol. 2011;64(1):228–32.

43. Wijmans JG, Baker RW. The solution-diffusion model: a review. J Memb Sci. 1995;107:1–21.

44. Kiso Y, Muroshige K, Oguchi T, Yamada T, Hhirose M, Ohara T, et al. Effect of molecular shape on rejection of uncharged organic compounds by nanofiltration membranes and on calculated pore radii. J Memb Sci. Elsevier B.V.; 2010;358:101–13.

45. Košutić K, Furač L, Sipos L, Kunst B. Removal of arsenic and pesticides from drinking water by nanofiltration membranes. Sep Purif Technol. 2005;42:137–44.

46. Zhang Y, Van der Bruggen B, Chen G, Braeken L, Vandecasteele C. Removal of pesticides by nanofiltration: effect of the water matrix. Sep Purif Technol. 2004;38:163–72.

47. Boussahel R, Bouland S, Moussaoui KM, Montiel A. Removal of pesticide residues in water using the nanofiltration process. Desalination. 2000;132:205–9.

48. Boussahel R, Montiel A, Baudu M. Effects of organic and inorganic matter on pesticide rejection by nanofiltration. Desalination. 2002;145:109–14.

49. Mohammad AW, Ali N. Understanding the steric and charge contributions in NF membranes using increasing MWCO polyamide membranes. Desalination. 2002;147:205–12.

50. Van der Bruggen B, Schaep J, Maes W, Wilms D, Vandercasteele C. Nanofiltration as a treatment method for the removal of pesticides from ground water. Desalination. 1998;117:139–47.

51. Berg P, Hagmeyer G, Gimbel R. Removal of pesticides and other micropollutants by nanofiltration. Desalination. 1997;113:205–8.

52. Kiso Y, Nishimura Y, Kitao T, Nishimura K. Rejection properties of non-phenylic pesticides with nanofiltration membranes. J Memb Sci. 2000;171:229–37.

53. Kiso Y, Sugiura Y, Kitao T, Nishimura K. Effects of hydrophobicity and molecular size on rejection of aromatic pesticides with nanofiltration membranes. J Memb Sci. 2001;192:1–10.

54. Plakas K V., Karabelas AJ. Triazine retention by nanofiltration in the presence of organic matter: The role of humic substance characteristics. J Memb Sci. 2009;336:86–100.

55. Plakas K V., Karabelas AJ. A systematic study on triazine retention by fouled with humic substances NF/ULPRO membranes. Sep Purif Technol. 2011;80:246–61.

56. Plakas KV, Karabelas AJ. Membrane retention of herbicides from single and multi-solute media: The effect of ionic environment. J Memb Sci. 2008;320:325–34.

57. Elimelech M, Chen WH, Waypa JJ. Measuring the zeta (electrokinetic) potential of reverse osmosis membranes by a streaming potential analyzer. Desalination. 1994;95:269–86.

58. Szymczyk A, Fievet P, Bandini S. On the amphoteric behavior of Desal DK nanofiltration membranes at low salt concentrations. J Memb Sci. Elsevier B.V.; 2010;355:60–8.

59. Nghiem LD, Shäfer AI. Trace contaminant removal with nanofiltration. In: Shäfer AI, Fane AG, Waite TD, editors. Nanofiltration, Principles and Applications. Oxford, UK: Elsevier Advanced Technology; 2005. p. 479–520.

60. Karabelas A, Plakas K. Membrane Treatment of Potable Water for Pesticides Removal. In: Larramendy PM, editor. Herbicides, Theory and Applications. InTech; 2011. p. 369–408.

61. Kiso Y, Muroshige K, Oguchi T, Hirose M, Ohara T, Shintani T. Pore radius estimation based on organic solute molecular shape and effects of pressure on pore radius for a reverse osmosis membrane. J Memb Sci. 2011;369:290–8.

62. Deen WM. Hindered Transport of Large Molecules in Liquid-Filled Pores. AIChE J. 1987;33(9):1409–25.

63. Otero J a., Mazarrasa O, Villasante J, Silva V, Prádanos P, Calvo JI, et al. Three independent ways to obtain information on pore size distributions of nanofiltration membranes. J Memb Sci. 2008;309:17–27.

64. Bowen WR, Sharif AO. Transport through Microfiltration Membranes - Particle Hydrodynamics and Flux Reduction. J Colloid Interface Sci. 1994;168:414–21.

65. Bowen WR, Mohammad AW, Hilal N. Characterisation of nanofiltration membranes for predictive purposes - use of salts , uncharged solutes and atomic force microscopy. J Memb Sci. 1997;126:91–105.

66. Van Der Bruggen B, Schaep J, Wilms D, Vandecasteele C. A Comparison of Models to Describe the Maximal Retention of Organic Molecules in Nanofiltration. Sep Sci Technol. 2000;35(2):169–82.

67. Ng LY, Mohammad AW, Leo CP, Hilal N. Polymeric membranes incorporated with metal/metal oxide nanoparticles: A comprehensive review. Desalination. Elsevier B.V.; 2013;308:15–33.

68. Kim J, Van der Bruggen B. The use of nanoparticles in polymeric and ceramic membrane structures: Review of manufacturing procedures and performance improvement for water treatment. Environ Pollut. 2010;158:2335–49.

69. Taurozzi JS, Arul H, Bosak VZ, Burban AF, Voice TC, Bruening ML, et al. Effect of filler incorportation route on the properties of polysulfone-silver nanocomposite membranes of different porosities. J Memb Sci. 2008;325(1):58–68.

70. Balta S, Sotto A, Luis P, Benea L, Van der Bruggen B, Kim J. A new outlook on membrane enhancement with nanoparticles: The alternative of ZnO. J Memb Sci. 2012;389:155–61.

71. Rajaeian B, Rahimpour A, Tade MO, Liu S. Fabrication and characterization of polyamide thin film nanocomposite (TFN) nanofiltration membrane impregnated with TiO2 nanoparticles. Desalination. 2013;313:176–88.

72. Bowen WR. Biomimetic separations - learning from the early development of biological membranes. Desalination. 2006;199:225–7.

73. Tang CY, Zhao Y, Wang R, Hélix-Nielsen C, Fane AG. Desalination by biomimetic aquaporin membranes: Review of status and prospects. Desalination. 2013;308:34–40.

74. Wang HL, Chung T-S, Tong YW, Jeyaseelan K, Armugam A, Duong HHP, et al. Mechanically robust and highly permeable AquaporinZ biomimetic membranes. J Memb Sci. Elsevier; 2013;434:130–6.

75. Buonomenna MG. Nano-enhanced reverse osmosis membranes. Desalination. 2013;314:73–88.

76. Wang H, Chung T-S, Tong YW, Meier W, Chen Z, Hong M, et al. Preparation and characterization of pore-suspending biomimetic membranes embedded with Aquaporin Z on carboxylated polyethylene glycol polymer cushion. Soft Matter. 2011;7:7274–80.

77. Sun G, Chung T-S, Jeyaseelan K, Armugam A. Stabilization and immobilization of aquaporin reconstituted lipid vesicles for water purification. Colloids Surfaces B Biointerfaces. Elsevier B.V.; 2013;102:466–71.

78. Zhao Y, Qiu C, Li X, Vararattanavech A, Shen W, Torres J, et al. Synthesis of robust and high-performance aquaporin-based biomimetic membranes by interfacial polymerization-membrane preparation and RO performance characterization. J Memb Sci. 2012;423-424:422–8.

79. Elimelech M, Phillip WA. The Future of Seawater Desalination: Energy, Technology, and the Environment. Science. 2011;333(6043):712–717.

80. Martínez-Huitle CA, Ferro S. Electrochemical oxidation of organic pollutants for the wastewater treatment: direct and indirect processes. Chem Soc Rev. 2006;35:1324–4130.

81. Martínez-Huitle CA, Brillas E. Decontamination of wastewaters containing synthetic organic dyes by electrochemical methods: A general review. Appl Catal B Environ. 2009;87:105–45.

82. Anglada A, Urtiaga A, Ortiz I. Contributions of electrochemical oxidation to waste-water treatment: fundamentals and review of applications. J Chem Technol Biotechnol. 2009;84:1747–55.

83. Sirés I, Brillas E, Oturan MA, Rodrigo MA, Panizza M. Electrochemical advanced oxidation processes: today and tomorrow. A review. Environ Sci Pollut Res Int. 2014;21:8336–67.

84. Chaplin BP. Critical review of electrochemical advanced oxidation processes for water treatment applications. Environ Sci Process Impacts. 2014;16:1182–203.

85. Panizza M, Cerisola G. Direct And Mediated Anodic Oxidation of Organic Pollutants. Chem Rev. 2009;109:6541–69.

86. Muff J, Andersen CD, Erichsen R, Soegaard EG. Electrochemical treatment of drainage water from toxic dump of pesticides and degradation products. Electrochim Acta. 2009;54:2062–8.

87. Comninellis C. Electrocatalysis in the electrochemical conversion/combustion of organic pollutants for waste water treatment. Electrochim Acta. 1994;39(11-12):1857–62.

88. Bonfatti F, Ferro S, Lavezzo F, Malacarne M, Lodi G, De Battisti A. Electrochemical Incineration of Glucose as a Model Organic Substrate II. Role of Active Chlorine Mediation. J Electrochem Soc. 2000;147(2):592–6.

89. Brillas E, Boye B, Sirés I, Antonio J, Mar R, Arias C, et al. Electrochemical destruction of chlorophenoxy herbicides by anodic oxidation and electro-Fenton using a boron-doped diamond electrode. Electrochim Acta. 2004;49:4487–96.

90. Yoshihara S, Murugananthan M. Decomposition of various endocrine-disrupting chemicals at boron-doped diamond electrode. Electrochim Acta. 2009;54(7):2031–8.

91. Arapoglou D, Vlyssides A, Israilides C, Zorpas A, Karlis P. Detoxification of methyl-parathion pesticide in aqueous solutions by electrochemical oxidation. J Hazard Mater. 2003;98(1-3):191–9.

92. Polcaro AM, Mascia M, Palmas S, Vacca A. Electrochemical degradation of diuron and dichloroaniline at BDD electrode. Electrochim Acta. 2004;49(4):649–56.

93. Vlyssides A, Barampouti EM, Mai S, Arapoglou D, Kotronarou A. Degradation of Methylparathion in Aqueous Solution by Electrochemical Oxidation. Environ Sci Technol. 2004;38(22):6125–31.

94. Da Pozzo A, Merli C, Sirés I, Garrido JA, Rodríguez RM, Brillas E. Removal of the herbicide amitrole from water by anodic oxidation and electro-Fenton. Environ Chem Lett. 2005;3(1):7–11.

95. Polcaro AM, Vacca A, Mascia M, Palmas S. Oxidation at boron doped diamond electrodes: an effective method to mineralise triazines. Electrochim Acta. 2005;50(9):1841–7.

96. Vlyssides A, Arapoglou D, Mai S, Barampouti EM. Electrochemical detoxification of four phosphorothioate obsolete pesticides stocks. Chemosphere. 2005;58(4):439–47.

97. Flox C, Cabot PL, Centellas F, Garrido JA, Rodríguez RM, Arias C, et al. Electrochemical combustion of herbicide mecoprop in aqueous medium using a flow reactor with a boron-doped diamond anode. Chemosphere. 2006;64(6):892–902.

98. Malpass GRP, Miwa DW, Machado SAS, Olivi P, Motheo AJ. Oxidation of the pesticide atrazine at DSA electrodes. J Hazard Mater. 2006;137(1):565–72.

99. Miwa DW, Malpass GRP, Machado SAS, Motheo AJ. Electrochemical degradation of carbaryl on oxide electrodes. Water Res. 2006;40(17):3281–9.

100. Hachami F, Salghi R, Mihit M, Bazzi L, Serrano K, Hormatallah A, et al. Electrochemical Destruction of Methidathion by Anodic Oxidation Using a Boron-Doped Diamond Electrode. Sol Energy. 2008;62(6):35–40.

101. Martínez-Huitle CA, De Battisti A, Ferro S, Reyna S, Cerro-Lopez M, Quiro MA. Removal of the Pesticide Methamidophos from Aqueous Solutions by Electrooxidation using Pb/PbO_2, $TiSnO_2$ and Si/BDD Electrodes. Environ Sci Technol. 2008;42(18):6929–35.

102. Ozcan A, Sahin Y, Koparal AS, Oturan MA. Propham mineralization in aqueous medium by anodic oxidation using boron-doped diamond anode: Influence of experimental parameters on degradation kinetics and mineralization efficiency. Water Res. 2008;42:2889–98.

103. Sirés I, Brillas E, Cerisola G, Panizza M. Comparative depollution of mecoprop aqueous solutions by electrochemical incineration using BDD and PbO_2 as high oxidation power anodes. J Electroanal Chem. 2008;613(2):151–9.

104. Abdessalem AK. Treatment of an aqueous pesticides mixture solution by direct and indirect electrochemical advanced oxidation processes. Int J Environ Anal Chem. 2010;90:468–77.

105. Borràs N, Oliver R, Arias C, Brillas E. Degradation of Atrazine by Electrochemical Advanced Oxidation Processes Using a Boron-Doped Diamond Anode. J Phys Chem A. 2010;114(24):6613–21.

106. Liu L, Zhao G, Pang Y, Lei Y, Gao J, Liu M. Integrated Biological and Electrochemical Oxidation Treatment for High Toxicity Pesticide Pollutant. Ind Eng Chem Res. 2010;49(12):5496–503.

107. Samet Y, Agengui L, Abdelhédi R. Electrochemical degradation of chlorpyrifos pesticide in aqueous solutions by anodic oxidation at boron-doped diamond electrodes. Chem Eng J. 2010;161(1-2):167–72.

108. Errami M, Salghi R, Abidi N, Bazzi L, Hammouti B, Chakir A, et al. Electrooxidation of Bupirimate: A Comparative Study of SnO2 and Boron Doped Diamond Anodes. J Electrochem Sci. 2011;6:4927–38.

109. Oturan N, Brillas E, Oturan M a. Unprecedented total mineralization of atrazine and cyanuric acid by anodic oxidation and electro-Fenton with a boron-doped diamond anode. Environ Chem Lett. 2011;10(2):165–70.

110. Oturan N, Hamza M, Ammar S, Abdelhédi R, Oturan MA. Oxidation/mineralization of 2-Nitrophenol in aqueous medium by electrochemical advanced oxidation processes using Pt/carbon-felt and BDD/carbon-felt cells. J Electroanal Chem. 2011;661(1):66–71.

111. Wei J, Feng Y, Sun X, Liu J, Zhu L. Effectiveness and pathways of electrochemical degradtion of pretilachlor herbicides. J Hazard Mater. Elsevier B.V.; 2011;189(1-2):84–91.

112. Bouya H, Errami M, Salghi R, Zarrouk A, Hammouti B, Bazzi L, et al. Electrochemical Degradation of Cypermethrin Pesticide on a SnO_2 Anode. Int J Electrochem Sci. 2012;7:3453–65.

113. Errami M, Salghi R, Zarrouk A, Chakir A, Hammouti B, Bazzi L, et al. Electrochemical Combustion of Insecticides Endosulfan and Deltamethrin in Aqueous Medium Using A Boron-Doped Diamond Anode. J Electrochem Sci. 2012;7:4272–85.

114. Errami M, Salghi R, Zougagh M, Zarrouk A, Bazzi EH, Chakir A, et al. Electrochemical degradation of buprofezin insecticide in aqueous solutions by anodic oxidation at boron-doped diamond electrode. Res Chem Intermed. 2012;39(2):505–16.

115. Lazarević-Pašti TD, Bondžić AM, Pašti I a., Mentus S V., Vasić VM. Electrochemical oxidation of diazinon in aqueous solutions via electrogenerated halogens – Diazinon fate and implications for its detection. J Electroanal Chem. 2013;692:40–5.

116. Malpass GRP, Salazar-Banda GR, Miwa DW, Machado SAS, Motheo AJ. Comparing atrazine and cyanuric acid electro-oxidation on mixed oxide and boron-doped diamond electrodes. Environ Technol. 2013;34(8):1043–51.

117. Rabaaoui N, Saad MEK, Moussaoui Y, Allagui MS, Bedoui A, Elaloui E. Anodic oxidation of o-nitrophenol on BDD electrode: Variable effects and mechanisms of degradation. J Hazard Mater. Elsevier B.V.; 2013;250-251:447–53.

118. Pipi ARF, Sirés I, De Andrade AR, Brillas E. Application of electrochemical advanced oxidation processes to the mineralization of the herbicide diuron. Chemosphere. 2014;109:49–55.

119. Zaviska F, Drogui P, Blais J-F, Mercier G, Lafrance P. Experimental design methodology applied to electrochemical oxidation of the herbicide atrazine using Ti/IrO_2 and Ti/SnO_2 circular anode electrodes. J Hazard Mater. 2011;185:1499–507.

120. Radjenovic J, Bagastyo A, Rozendal RA, Mu Y, Keller J, Rabaey K. Electrochemical oxidation of trace organic contaminants in reverse osmosis concentrate using RuO_2/IrO_2-coated titanium anodes. Water Res. 2011;45(4):1579–86.

121. Pérez G, Fernández-Alba AR, Urtiaga AM, Ortiz I. Electro-oxidation of reverse osmosis concentrates generated in tertiary water treatment. Water Res. 2010;44(9):2763–72.

122. Dialynas E, Mantzavinos D, Diamadopoulos E. Advanced treatment of the reverse osmosis concentrate produced during reclamation of municipal wastewater. Water Res. Elsevier Ltd; 2008;42(18):4603–8.

123. Bagastyo AY, Radjenovic J, Mu Y, Rozendal RA, Batstone DJ, Rabaey K. Electrochemical oxidation of reverse osmosis concentrate on mixed metal oxide (MMO) titanium coated electrodes. Water Res. 2011;45(16):4951–9.

124. Bagastyo AY, Batstone DJ, Kristiana I, Gernjak W, Joll C, Radjenovic J. Electrochemical oxidation of reverse osmosis concentrate on boron-doped diamond anodes at circumneutral and acidic pH. Water Res. Elsevier Ltd; 2012;46(18):6104–12.

125. Bagastyo AY, Batstone DJ, Rabaey K, Radjenovic J. Electrochemical oxidation of electrodialysed reverse osmosis concentrate on Ti/Pt-IrO_2, Ti/SnO_2-Sb and boron-doped diamond electrodes. Water Res. Elsevier Ltd; 2013;47(1):242–50.

126. Van Hege K, Verhaege M, Verstraete W. Indirect electrochemical oxidation of reverse osmosis membrane concentrates at boron-doped diamond electrodes. Electrochem commun. 2002;4(4):296–300.

127. Zhou M, Liu L, Jiao Y, Wang Q, Tan Q. Treatment of high-salinity reverse osmosis concentrate by electrochemical oxidation on BDD and DSA electrodes. Desalination. Elsevier B.V.; 2011;277(1-3):201–6.

128. Tomlin CDS. The Pesticide Manual : A World Compendium. 15th ed. British Crop Production Council; 2011.

129. Nakagawa Y, Izumi K, Oikawa N, Sotomatsu T, Shigemura M, Fujita T. Analysis and prediction of hydrophobicity parameters of substituted acetanilides, benzamides and related aromatic compounds. Environ Toxicol Chem. 1992;11(7):901–16.

130. Sotto A, López-Muñoz MJ, Arsuaga JM, Aguado J, Revilla A. Membrane treatment applied to aqueous solutions containing atrazine photocatalytic oxidation products. Desalin Water Treat. 2010;21(1-3):175–80.

131. Geyer H, Viswanathan R, Freitag D, Korte F. Relationship between water solubility of the organic chemicals and their bioaccumulation by the alga chlorella. Chemosphere. 1981;10(11/12):1307–13.

132. Jensen GG, Björklund E, Simonsen A, Halling-Sørensen B. Determination of 2,6-dichlorobenzamide and its degradation products in water samples using solid-phase

extraction followed by liquid chromatography-tandem mass spectrometry. J Chromatogr A. 2009;1216(27):5199–206.

133. Purvis GD. On the use of isovalued surfaces to determine molecule shape and reaction pathways. J Comput Aided Mol Des. 1991;5(1):55–80.

134. Rodrigues AM, Ferreira V, Cardoso VV, Ferreira E, Benoliel MJ. Determination of several pesticides in water by solid-phase extraction, liquid chromatography and electrospray tandem mass spectrometry. J Chromatogr A. 2007;1150(1-2):267–78.

135. Smith GA, Pepich B V., Munch DJ. Determination of triazine pesticides and their degradates in drinking water by liquid chromatography electrospray ionization tandem mass spectrometry (LC/ESI-MS/MS). Technical report, United States Environmental Protection Agency, 2007.

136. Beck J. Analysis of Triazine Pesticides in Drinking Water Using LC-MS/MS (EPA Method 536.0) [Internet]. North. Available from: http://www.thermo.com.cn/Resources/201303/5113410468.pdf

137. Zhang R-X, Vanneste J, Poelmans L, Sotto A, Wang X-L, Van der Bruggen B. Effect of the Manufacturing Conditions on the Structure and Performance of Thin-Film Composite Membranes. J Appl Polym Sci. 2012;135:3755–69.

138. Bakke JM, Buhaug JB. Hydrogen Sulfide Scavenging by 1,3,5-Triazinanes. Comparison of the Rates of Reaction. Ind Eng Chem Res. 2004;43(9):1962–5.

139. Bakke JM, Buhaug J, Riha J. Hydrolysis of 1,3,5-Tris(2-hydroxyethyl)hexahydro-s-triazine and Its Reaction with H_2S. Ind Eng Chem Res. 2001;40(26):6051–4.

140. Taylor GN, Matherly R. Structural Elucidation of the Solid Byproduct from the Use of 1,3,5-Tris(hydroxyalkyl)hexahydro-s-triazine Based Hydrogen Sulfide Scavengers. Ind Eng Chem Res. 2011;50(2):735–40.

141. Ellis D, Bouchard C, Lantagne G. Removal of iron and manganese from groundwater by oxidation and microfiltration. Desalination. 2000;130(3):255–64.

142. Choo K, Lee H, Choi S. Iron and manganese removal and membrane fouling during UF in conjunction with prechlorination for drinking water treatment. J Memb Sci. 2005;267(1-2):18–26.

143. Soffer Y, Adin A, Gilron J. Threshold flux in fouling of UF membranes by colloidal iron. Desalination. 2004;161:207–21.

144. Korchef A, Kerkeni I, Amor M Ben, Galland S, Persin F. Iron removal from aqueous solution by oxidation, precipitation and ultrafiltration. Desalin Water Treat. 2009;9(1-3):1–8.

145. Andreozzi R. Advanced oxidation processes (AOP) for water purification and recovery. Catal Today. 1999;53(1):51–9.

146. Chiron S, Fernandez-Alba A, Rodriguez A, Garcia-Calvo E. Pesticide Chemical Oxidation: State-of-The-Art. Water Res. 2000;34(2):366–77.

147. Linden KG. Experimental and Model Comparisons of Low- and Medium-Pressure Hg Lamps for the Direct and H_2O_2 Assisted UV Photodegradation of N-Nitrosodimethylamine in Simulated Drinking Water. Environ Sci Technol. 2003;37:1933–40.

148. Wu C, Linden KG. Phototransformation of selected organophosphorus pesticides: Roles of hydroxyl and carbonate radicals. Water Res. 2010;44(12):3585–94.

149. Madsen HT. Membrane Filtration in Water Treatment - Removal of Micropollutants. In: Søgaard EG, editor. Chemistry of Advanced Environmental Purification Processes of Water. 1st ed. Elsevier; 2014. p. 199–248.

Appendix A1 Modelling steric rejection of non-spherical molecules

In this appendix an example of a script file, developed in Matlab, showing how to use the non-spherical steric model described in chapter 2.

```
clear
clc

x = [0.3:0.001:1];                                          % Investigated span for pore radius (nm)
r_p = x*10.^-9;                                             % Pore radius (m)

Rm   = [0.7561 0.8773 0.7239 0.8431 0.9283 0.9746 0.9889];  % Measured rejection
MWd  = [0.2511 0.2720 0.2555 0.2580 0.2776 0.3130 0.3087]*10^-9;    % Calculated molecular width
L    = [0.7769 0.7340 0.7058 0.9052 0.8602 0.7771 0.7346]*10^-9;    % Calculated molecular length

for i = 1:length(Rm)
% Constants used in the model
n      = 1.002 * 10^-3;                                     % Viscosity (Pa s)
t      = 298;                                               % Temperature (K)
P      = 1*10^6;                                            % Applied pressure (Pa)
R      = 8.314;                                             % Gas constant (J/mol*K)
c      = 2.14;                                              % Concentration (mol/m^3)
P_pi   = c*R*t;                                             % Osmotic pressure (Pa)
k      = 1.3806*10^-23;                                     % Boltzmann's constant
r_s    = 1.42*MWd(i) - 0.142*10^-9;                         % Solute radius
D      = k*t/(6*pi*n*(r_s));                                % Diffusion coefficient
lambda = r_s./r_p;

% Calculation of steric partition factor, T, - Non-spherical model
T describes the ratio of the area of the molecule when projected down upon the membrane relative to
the area of the pore entrance. Since the molecule is allowed to rotate it is necessary to calculate
the area from an angle (A) of 0 to an angle of pi/2, and multiply each of the numbers with a
probability function (in this case sinus to the angle). T is found by integrating the area
multiplied with the probability over the angles of rotation. Some of the results may however yield
non-real values, and these need to be discarded. The following equations are best understood by
comparing with literature (see references in chapter 2).

dA = 0.001;                                         % Step size for integration with respect to A
A = [0:dA:pi/2];                                    % Angle of rotation for the molecule
        for K = 1:length(A)
        Lp     = L(i).*cos(A(K)) + 2*MWd(i).*sin(A(K));             % Effective molecular length
        f   = (((r_p.^2-(Lp./2).^2).^(1/2)-MWd(i))./r_p).^2.*sin(A(K));% ratio of molecule and pore
        area
        a      = (r_p.^2 - (Lp./2).^2).^(1/2) - MWd(i);      % Radius of pore available to the
molecule
        f1     = f.*dA;                                      % Area of f at K(A)
        F(K,:) = f1;                                    % Inclusion of calculated f1 value in a F
matrix
        a1     = a*dA;                                  % Area of a at K(A)
        AA(K,:)= a1;                                    % Inclusion of calculated a1 value in a AA
matrix
        end

% Removal of none-real values
        Q      = find(AA<0);   % In the physical interpretation of the model, a cannot be < 0
        F(Q)   = 0;            % For values of a<0, f1 = 0
        T      = sum(F);       % T = Sum of all f1 values at a specific r_p

% Calculation of hindrance factors and parameters dependent on T.
G     = 1 + 0.054*lambda - 0.988*lambda.^2 + 0.441*lambda.^3;% The lag coefficient
Kc    = (2 - T).*G;                                         % Solute hindrance factor for convection
Kd    = 1 - 2.30*lambda + 1.154*lambda.^2 + 0.224*lambda.^3;% Solute hindrance factor for diffusion
D_p   = Kd*D;                                                          % Diffusivity in a pore
u     = T.*Kc;
```

```
v     = Kc./Kd;
Pe    = ((r_p.^2.*(P-P_pi)*6*pi.*r_s)/(8*k*t)) .* v;                                % Peclet number

% Calculation of rejections based on the current guess for pore radius (x)
Rc    = 1 - u./(1 - (1 - u).*exp(-Pe));

Delta = (Rm(i)- Rc).^2;               % Squared difference between measured and calculated rejection
DELTA(i,:) = Delta;                   % Save calculated delta value in a matrix
end

% To find the pore radius that best describes the rejection, a sum of squares analysis is performed
in which the pore radius that gives the lowest squared difference between measured and calculated
rejection is taken to be the pore radius of the membrane.

SUM = sum(DELTA);                                          % Sum of all delta values for each r_p
SSy = (SUM./(length(Rm)-1)).^(1/2);                        % Sum of squares as a function of r_p

[minVal minInd] = min(SSy);                   % Identification of minimum value of SSy and its index
RP = x(minInd)                                                  % Pore radius (nm) with minimum
SSy
RP_opt = RP*10^-9;            % Pore radius to be used in calculation of optimal rejection values


% To find the optimized values, the calculation is performed again, but only with the modelled pore
radius.
for i = 1:length(Rm)
r_s             = 1.42*(MWd(i)) - 0.142* 10^-9;
D               = k*t/(6*pi*n*(r_s));
lambda_opt      = r_s./(RP_opt);

        dA = 0.001;
        A = [0:dA:pi/2];
        for w = 1:length(A)
                Lpopt  = L(i).*cos(A(w)) + 2*MWd(i).*sin(A(w));
                f_opt  = (((RP_opt.^2-(Lpopt./2).^2).^(1/2)-MWd(i))./RP_opt).^2.*sin(A(w));
                a_opt  = (RP_opt.^2-(Lpopt./2).^2).^(1/2)-MWd(i);
                f1_opt = f_opt.*dA;
                F_opt(w,:) = f1_opt;
                a1_opt = a_opt*dA;
                AA_opt(w,:) = a1_opt;
        end
        Q_opt = find(AA_opt<0);
        F_opt(Q_opt) = 0;
        T_opt = sum(F_opt);

G_opt     = (1 + 0.054*lambda_opt - 0.988*lambda_opt.^2 + 0.441*lambda_opt.^3);
Kc_opt    = (2 - T_opt).*G_opt;
Kd_opt    = (1 - 2.30*lambda_opt  + 1.154*lambda_opt.^2 + 0.224*lambda_opt.^3);
D_p_opt   = Kd_opt*D;
a1_opt    = T_opt.*Kc_opt;
b_opt     = (Kc_opt)./(lambda_opt.^2 .* Kd_opt);
Pe_opt    = ((P-P_pi)*6*pi*(r_s).^3)/(8*k*t) * b_opt;
Rc_opt    = 1 - a1_opt./(1 - (1 - a1_opt).*exp(-Pe_opt));

RC_opt(i,:) = Rc_opt;                         % Save of Rc values for each set of MWd and L values

end
disp('Calculated rejection');
disp(RC_opt)

hold on

% To compare the results, the calculated rejections are plotted as a function of the measured. In a
perfect fit they would lie on a Rc = Rm line, and to compare the modelled results to this ideal
scenario, the line is also plotted.
y   = [0.5:0.1:1];
plot(y,y)
scatter(Rm,RC_opt)
```

Appendix A2 Log-normal model for rejection of molecules

In this appendix an example of a script file, developed in Matlab, showing how to use the log-normal model described in chapter 2 to describe pore size and pore size distribution of a membrane.

```
clear
clc


d = [6.86 9.67 7.78 8.66 8.51 9.92]; %Mean height in projection of molecules, calculation can be
found in literature
Rm = [0.409 0.947 0.782 0.92 0.91 0.99];                                    % Measured rejection
values

mu = [log(3):0.01:log(15)]';     % Logarithmic values of average pore size in angstroms
std = [0.001:0.005:1]';          % Logarithmic standard deviations (Ln(std dev))
x = (0:0.1:15)';                 % X values representing pore sizes in angstroms

% In this script file, the model is solved by preparing a matrix of all possible combinations of
pore sizes (mu) and standard deviations (std), and then calculating a theoretical rejection for each
pair of values. The calculated values are then compared to the measured values to find the best fit.

std1 = kron(std, ones(length(mu),1)); % Creates a column vector standard deviation with each
standard deviation being replicated mu times.
mu1 = repmat(mu,length(std),1); % Creates a column vector where the column vector mu is repeated.

A = [std1 mu1];                  % Matrix of the total set of mu and std combinations
mu = A(:,2);                     % Vector for the average pore size
s  = A(:,1);                     % Vector for the log standard deviation

% Calculation of the sum of squares between the calculated rejection and the measured rejection for
all mu/std combinations

    for i = 1:length(mu)

        for j = 1:length(d)
            Y = logncdf(d(j),mu(i),s(i));   % The calculated rejections
            Rc(j,:) = Y;
        end

        Delta = (Rm' - Rc).^2;
        SUM = sum(Delta);
        SSy = (SUM./(length(Rm)-1)).^(1/2); % Sum of squares
        SSY(i,:) = SSy;
    end

[minVal minInd] = min(SSY);      % The minimum sum of squares
RP = exp(mu(minInd))             % The pore radius of the optimised solution [Å]
mu = log(RP);                    % Logarithmic value of the pore radius
S  = s(minInd)                   % The log standard deviation of the optimised solution [Å]

% Plotting the cumulative distribution, that is the change rejection as a function of size (d) of
the molecules. The curve is dependent on the parameters determined in the model, and to compare the
model to the measured values, these are plotted alongside.

subplot(1,2,1)
y = logncdf(x,mu,S);
plot(x,y)
hold on
plot(d,Rm,'ro')
xlabel('Solute size (Å)')
ylabel('Rejection')
title('Cumultative PSD')
```

```
% Plotting the pore size distribution
subplot(1,2,2)
y2 = lognpdf(x,mu,S);
plot(x,y2)
hold on
xlabel('Pore diameter (Å)')
title('PSD')
```

Paper I

Henrik Tækker Madsen and Erik G. Søgaard

Case study of treatment of waste water for 17α-ethinylestradiol and microorganisms with UV and photocatalysis in an on-going process of introducing AOP techniques in the Danish water sector

Water Practice & Technology, **7** (2012)

Reprinted with permission from IWA Publishing

© IWA Publishing 2012

Water Practice & Technology Vol 7 No 4
doi: 10.2166/wpt.2012.080

Case study of treatment of waste water for 17α-ethinylestradiol and microorganisms with UV and photocatalysis in an on-going process of introducing AOP techniques in the Danish water sector

H. T. Madsen* and E. G. Søgaard

Department of Biotechnology, Chemistry and Environmental Engineering, Aalborg University Esbjerg, Niels Bohrs Vej 8, 6700 Esbjerg, Denmark.

* Corresponding author. E-mail: htm@bio.aau.dk

Abstract

Failure to obtain a sufficient disinfection of waste water, initiated an investigation of the use of UV light and photocatalysis with TiO_2 for treating the waste water. Furthermore, the ability of such a system to degrade endocrine disrupting chemicals was investigated through experiments with the estrogen 17α-ethinylestradiol (EE2). This study found LP UV lamps to be the optimal solution for disinfection, while photocatalysis with TiO_2 was found to be the best method for removal of EE2. The experiments were carried out in a mobile test unit with solution volumes of 30 L. By use of data from the real UV system, the effect found in the experiments were extrapolated and used to evaluate the efficiency of the current system.

Key words: AOPs, disinfection, endocrine disrupters, photocatalysis, waste water

INTRODUCTION

Current Danish waste water treatment consists of mechanical, chemical and biological processes depending on the size of the plant. Because Denmark is heavily populated and cultivated, the treated waste water is often discharged to recreational areas, which demands a heightening of the standards for the water with respect to the content of microorganisms (European Union 2006). To meet these standards, a number of waste water treatment plants (WWTP) have invested in low pressure (LP) UV equipment for disinfection, which has been found to be an effective method against all waterborne pathogens (Hijnen *et al*. 2006). One of these plants is Vejle Central Waste Water Treatment Plant (CWWTP). In Vejle, the waste water is discharged to the nearby fjord, which also functions as the local bathing area. However, recently the water quality has not been able to meet the bacteriological standards for bathing water, and as a result of this, an investigation was initiated to evaluate the possibility for optimization of the UV system.

A second concern in the Danish waste water industry is the amounts of endocrine disruptors in the waste water. These substances are not affected by the current treatment procedure, and they are suspected of causing the observed feminization in certain fish species (Christiansen & Plesner 2001; Christiansen *et al*. 2002). In Table 1, an assessment of the amount of endocrine disrupting chemicals discharged into the Danish environment along with concentrations, which have been found to induce feminization in male fish, is shown. Signs of feminization is the production of female yolk protein, and the occurrence of hermaphroditism; intersex. As a result, it was desired to assess the ability of the UV system to remove endocrine disrupting chemicals from the waste water.

To assess the possibility of optimizing the UV system at the waste water treatment plant, the current disinfection ability was investigated with *E. coli*, which is a commonly used indicator microorganism,

Table 1 | Total daily discharge and concentrations of water with hormonal effect of endocrine disruptors in Denmark. (Christiansen *et al.* 2002)

Endocrine disruptor	Daily discharge	Yolk protein	Intersex
Estrone	36 g	10 ng/L	30 ng/L
Estriol	69 g	500 ng/L	1,000 ng/L
17β-estradiol	340 g	5 ng/L	10 ng/L
17α-ethinylestradiol	3.2	0.1 ng/L	0.1 ng/L
Nonylphenols	0.1–2.73 tonnes	5 μg/L	30–100 μg/L
Bisphenol A	~2 kg	10–40 μg/L	10–40 μg/L

and then it was compared to the use of medium pressure (MP) UV lamps, which have a broader emission spectrum. One of the concerns about the use of LP UV light is that the bacteria might be able to repair the damaged DNA and reactivate. When using MP UV light, the degree of reactivation has been found to be smaller (Hu & Quek 2008). The effect of the current system on endocrine disrupting chemicals was investigated by degradation of the most potent endocrine disruptor in the above mentioned survey, 17α-ethinylestradiol (EE2). Photolysis has been shown to degrade a wide range of endocrine disruptors, including the natural estrogens and EE2 (Coleman *et al*. 2004; Rosenfeldt *et al*. 2007), but the rate of degradation is very dependent on the UV source (LP/MP, UVC/UVA), and investigations seldom consider the costs of the process. A reduction of one decade in concentration of EE2 by photolysis has been found to require 6.1 ± 0.7 kWh/m^3, and even higher amounts for other endocrine disruptors (Andersen *et al*. 2008). State of the art in degradation of organic micropollutants is the use of advanced oxidation processes (AOPs), and techniques such as TiO_2 photocatalysis, UV/H_2O_2 and UV/O_3, have been found to degrade endocrine disruptors more effectively compared to photolysis (Coleman *et al*. 2000, 2004, 2005; Rosenfeldt *et al*. 2007; Andersen *et al*. 2008). The use of TiO_2 is especially interesting since the technique does not require addition of extra chemicals, and TiO_2 may be immobilized allowing for its use in flow systems without need for additional separation steps. Also, TiO_2 has been found to be effective for disinfection (Gumy *et al*. 2006; Chen *et al*. 2010; Acevedo *et al.* 2012). As a result, the possibility of introducing immobilized TiO_2 was assessed both with respect to disinfection and removal of EE2. Furthermore, data was collected from the actual UV system over two seasons and compared to the laboratory results to evaluate the effect of the system.

METHODS

Materials

E. coli from Leibniz-Institut DSMZ-German Collection of Microorganisms and Cell Cultures was inoculated in the laboratory. Acetic acid (>99%), nitric acid (67%), titanium(IV)isopropoxide, NaCl, agar, glucose (analytical grade) and 17α-ethinylestradiol (98% HPLC grade) were purchased from Sigma Aldrich. Demineralized water was produced with a Silex II ion exchanger from SILHORKO.

Philips 16 W LP UV lamps (3.9 W UVC output), and Aqua System 400 W MP UV lamp were used for the experiments. TiO_2 coated quartz tubes were produced according to a microwave assisted sol-gel method (Simonsen *et al*. 2009). A 9 L UV flow reactor in AISI 316 L from Aqua System A/S was used for both the UV and photocatalysis experiments. The reactor has room for one UV lamp centered in the reactor along the flow direction.

Methods of analysis

E. coli concentration was measured and PCA plates were produced according to DS 2254. To evaluate EE2 degradation, a solid phase extraction HPLC method with fluorescence detection was developed in the laboratory (Perkin Elmer HPLC (model 250 isocratic LC pump, 100–240 V, 50/60 Hz), C18 Column (Varian, ChromSpher 5 PAH VARIAN, VF-5sms-General Purpose FactorFourTM Column CP8944 (0.25 mm × 30 m × 0.25 μm)), 32% acetonitrile in water as eluent, water flow of 7 psi, HP 1100 Fluorescence detector, $\lambda_{ex} = 280$ nm, $\lambda_{em} = 310$ nm, calibration curve: $c(EE2) = 187.25 \times \text{Area} + 3.828$, $R^2 = 0.9993$). For the solid phase extraction a C18 column equal to the one in the HPLC was used. The column was first activated with 1 ml methanol, then eluated with the sample, after which the analytes were washed out with 1 ml acetonitrile and diluted with 2 ml distilled water.

Experimental design

The experiments were carried out in a mobile lab unit with 30 L volume of solution. The solution was pumped through the UV reactor with a flow of 40 L/min, and samples were taken from a holding tank. The UV lamps were placed in a quartz tube in the reactor. For the experiments with TiO_2, a coated quartz tube was used. For *E. coli* experiments the water was prepared with a physiological NaCl concentration of 0.9% weight, 5 ml of the *E. coli* stock solution was added and the solution was left to recirculate for 15 minutes to ensure homogenization of the solution. For the EE2 experiments, EE2 was initially dissolved in acetonitrile, which was then added to the water to obtain a concentration of 2 mg/l EE2. The EE2 solution was left to recirculate over night to ensure a complete dissolution.

To investigate the possibility for optimizing the system with MP lamps, the amount of electrical energy per volume (kWh/m^3) was used. This is done because LP and MP UV lamps do not emit radiation at the same wavelength, and therefore cannot be compared at a given wavelength. Furthermore, it is the amount of spent energy that determines, which of the two options is the most cost efficient. To investigate the efficiency of the current system with respect to both disinfection and removal of endocrine disruptors, the amount of UVC radiation deposited per volume (kWh UVC/m^3) was used. This allows for comparison with other studies where different LP lamps have been used, and enabled the use of the laboratory results to evaluate the UV system at Vejle CWWTP. The lamps used at the WWTP have a more efficient conversion of electrical to UVC energy compared to the laboratory UV lamp (275 W/175 W) and (16 W/3.9 W). The UV system at the waste water facility consists of 108 lamps. The amount of UVC energy was also applied for the evaluation of photocatalytic surfaces.

RESULTS AND DISCUSSION

Germicidal effect

By applying 0.075 kWh/m^3 of LP UV energy (1.85×10^{-2} kWh UVC/m^3), a 3-log reduction (99.9%) in the *E. coli* concentration was achieved. When using the MP UV lamp, 0.075 kWh/m^3 MP UV energy gave a reduction of 89.8%. The use of LP UV lamps does as such seem to be more effective for killing *E. coli*, and the MP UV lamps should not be used for optimization of the UV system. The reason for the higher effectiveness of the LP UV lamps, is thought to be due to the absorption of UV light by the nucleic acids of DNA, which all show a high absorption around the emission wavelength of LP UV lamps (254 nm) (EPA 2006). The photochemical reactions induced by the MP light do not seem to be able to compete with this reaction. The killing of *E. coli* with LP UV light was found to follow first

order kinetics with respect to the concentration of *E. coli*, with a rate constant $k = 3.66 \times 10^2\ m^3/kWh$ UVC.

To investigate if the removal of *E. coli* can be improved by applying photocatalytic surfaces, the quartz tube for the UV lamp was exchanged with a TiO_2 coated quartz tube. It is found that to achieve a 3-log removal of *E. coli*, 2.23×10^{-2} kWh UVC/m^3 was required. The degradation is however not as simple to describe as when only the LP UV lamp is used. The *E. coli* concentration does initially decrease following first order kinetics, but above 1.00×10^{-2} kWh UVC/m^3 the data are better described with second order kinetics. Presently, the reason for this relation is unknown. One possibility could be that since the photocatalytic process is mediated by hydroxyl radicals, oxidation by-products toxic to *E. coli* are formed. This has not been confirmed. The overall result of the experiment is that by coating the quartz tube, the killing of *E. coli* becomes less efficient.

Since coating the quartz tube surrounding the LP UV lamp inhibits the degradation of *E. coli*, it was attempted to apply the coated TiO_2 differently, by placing the TiO_2 surface away from the UV lamps to allow the UV light to radiate the solution while maintaining the photocatalytic effect. To do so, a second reactor with room for four UV lamps was used. Two of the tubes were coated with TiO_2 and left containing no UV lamps to contribute with TiO_2 surfaces, and the remaining two tubes were left uncoated, each containing a LP UV lamp. Also, the wall of the reactor was coated with TiO_2. In this way, the direct LP UV light effect is present as well as the photocatalytic effect. The energy required to achieve a 3-log removal with this reactor design was found to be 2.77×10^{-2} kWh UVC/m^3. This relatively high amount of energy compared to the pure LP UV lamp may be caused by shadow effects of the coated tubes. By plotting the logarithmic removal as a function of UVC dose, the three techniques may be compared graphically, see Figure 1. It is evident that the two designs with TiO_2 results in less efficient disinfection compared to the use LP UV lamps without TiO_2. Initially, the setup with TiO_2 surfaces placed out in the reactor resulted in a level of disinfection efficiency between that of the pure UVC light and the TiO_2 coated quartz tube. This is to be expected since the UV light is not constricted by surrounding TiO_2, but the TiO_2 surfaces in the reactor may absorb some of the UV light, resulting in an overall less efficient disinfection compared to the pure UVC light.

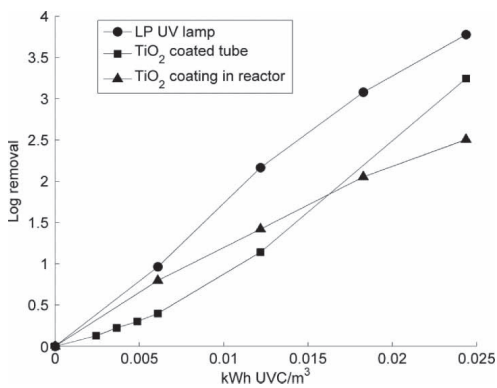

Figure 1 | Plot of the logarithmic degradation of *E. coli* for the three experiments.

It was also tested if the use of MP lamps in connection with TiO_2 could improve the removal of *E. coli*. However, when the same TiO_2 coated quartz tube was applied, no elimination was observed. This may be due to the high power (400 W) of the MP lamp compared to the LP lamp (16 W). Because of the relative high power, the same energy per volume is deposited 25 times as quickly.

Since photocatalysis is a surface catalyzed process, the *E. coli* bacteria must diffuse close to the surface for reaction to occur, and with only a short time available, limited diffusion is possible. The reaction may as such be severely limited by mass transport to the TiO_2 surface. A second possibility is that the amount of hydroxyl radicals on the TiO_2 surface reaches a saturation level, and that additional UV energy therefore is lost as heat.

Degradation of EE2

EE2 was found to be degraded according to first order kinetics by both pure LP UV light and with photocatalysis. A rate constant $k = 0.685\ m^3/kWh$ UVC was found for the photolytic degradation, while the photocatalytic degradation had a rate constant $k = 1.14\ m^3/kWh$ UVC.

The use of a TiO_2 coated quartz tube did as such increase the rate of degradation with 66%. The two processes are compared graphically in Figure 2.

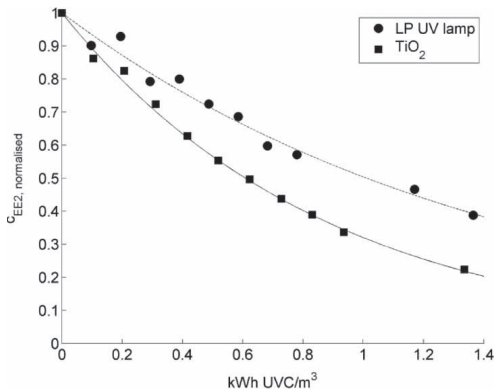

Figure 2 | Normalized degradation curves for EE2 with best fit.

Full scale system performance

The system installed at Vejle CWWTP has been in use from May to September since 2007, where data has been collected on a regular basis. As seen in Figure 3, the number of cfu/100 ml for both coliforms and thermo coliforms have been reduced below the threshold limits most of the time, but also occasionally exceeding the limits.

The system is equipped with a control system, which regulates the UV dose by adjusting the lamp power consumption. To evaluate the system performance, the maximum energy deposited as a function of flow is plotted in Figure 4. Also plotted are the amounts of UVC energy required to achieve 3-log, 2-log and 1-log degradation, as found in the experiments. When compared to the results from the laboratory, it is seen that at flows $>1{,}020\ m^3/h$, the system does not deliver the 1.85×10^{-2} kWh UVC/m^3 necessary for a 3-log removal of *E. coli*. By plotting the actual power consumption of the UV lamps as a function of the flow, it is seen that at flows above $1{,}100\ m^3/h$, the control system sets the lamps at their maximum capacity, which might explain the issues with disinfection, see Figure 4 (right). When the flow is above $1{,}100\ m^3/h$, the system cannot deliver a sufficient UV dose, and if the amount of microorganisms present in the waste water is large, the disinfection may be inefficient. However, as seen from the correlation table, Table 2, there is no correlation between the flow and the amount of bacteria in the water, and the flow alone cannot be used to assess the

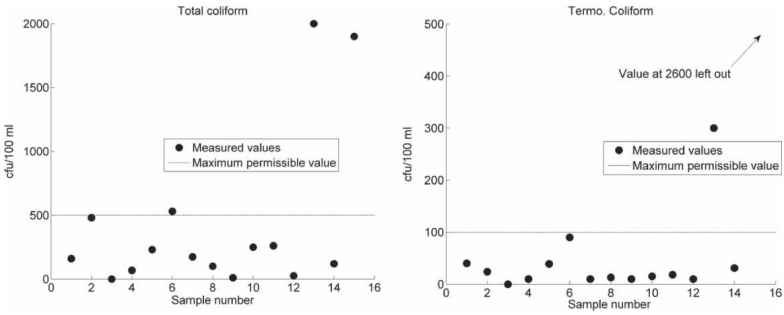

Figure 3 | Measured amounts of total and termo coliforms after the UV treatment in Vejle.

disinfection requirement. It can also be seen that there is a medium negative correlation between flow and the UV dose as measured by the UV system. This indicates that the system is not capable of fully compensating for increasing flow.

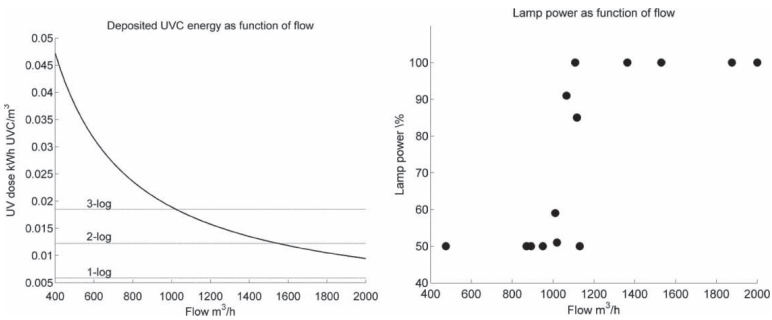

Figure 4 | Plots of deposited UVC energy as a function of the flow (left), and the percentage of the total lamp power as regulated by the system as a function of the flow (right). Also plotted in the graph for the deposited UVC energy are the amounts of UVC energy required to achieve a 3-log, 2-log and 1-log degradation as found in the experiments with the LP UV lamp.

Table 2 | Correlation table for performance of UV system at Vejle CWWTP

		UV dose (mJ/cm^2)	Lamp output (%)	Flow (m^3/h)	Coliform cfu/100 ml Before UV	Coliform cfu/100 ml After UV	Termo. coliform cfu/100 ml Before UV	Termo. coliform cfu/100 ml After UV
UV dose (mJ/cm^2)		1	−0.71	−0.63	0.03	−0.31	0.03	−0.50
Lamp outout (%)		−0.71	1	0.75	0.09	0.02	0.10	0.24
Flow (m^3/h)		−0.63	0.76	1	−0.08	−0.15	−0.07	−0.10
Coliform cfu/100 ml	Before UV	0.03	0.09	−0.08	1	−0.11	0.99	−0.08
	After UV	−0.31	0.02	−0.15	−0.11	1	−0.11	0.72
Termo. Coli cfu/100 ml	Before UV	0.03	0.10	−0.07	0.99	−0.11	1	−0.06
	After UV	−0.50	0.24	−0.10	−0.08	0.72	−0.06	1

With respect to endocrine disruptors, the data show that the system will not remove these compounds. By applying photocatalytic surfaces, the degradation is improved, but with 0.61 kWh UVC/m^3 required to halve the concentration, the effect is limited. At a flow of 1,000 m^3/h, the

maximum UVC dose given off by the UV system will only result in a reduction of 1.29% in the concentration of EE2. Furthermore, if the quartz tubes are coated to improve degradation of endocrine disruptors, it will reduce the efficiency of an already struggling disinfection system. This highlights the need for separating the disinfection process and the degradation of organic micropollutants. The treatment of micropollutants requires more energy per volume, and is as a result more costly. It will therefore be necessary to concentrate the micropollutants prior to AOP treatment, since this will result in a smaller volume in need of treatment, and allow for the possibility of adjusting the retention time because the smaller volume with the micropollutants may be transferred to a holding tank or a recirculation system, separate from the flow through system. One way of achieving this separation is by applying nanofiltration (NF) followed by an AOP reactor. NF membranes will separate organics, while allowing for passage of macro ions, and the AOP reactor may then degrade the micropollutants. Such a system would ideally be placed after the current UV system, since the UV system could reduce biofouling of the membranes. The NF process could also completely remove the remaining microorganisms.

CONCLUSIONS

LP UV lamps were found to be superior to MP UV lamps in killing *E. coli* bacteria, and by applying 1.85×10^{-2} kWh UVC/m^3 a 3-log removal was achieved. The introduction of photocatalytic TiO_2 surfaces were found to reduce the disinfection effectiveness of the LP UV lamps, both when the TiO_2 was used to coat the quartz tubes containing the UV lamps, and when the coated surfaces were placed elsewhere in the reactor. The TiO_2 surfaces were found to increase the degradation of EE2 with 66% compared to the pure photolytic reaction.

The analysis of the data from Vejle Central Waste Water Treatment Plant showed that the UV system is not well controlled, and that at flows above 1,020 m^3/h it does not deliver a sufficient UVC dose to achieve a 3-log removal of *E. coli*. Also, the energy required to degrade micropollutants such as EE2, is so great that a secondary treatment is necessary. Here nanofiltration could be used to produce a smaller volume, which could be more easily managed and treated with AOPs.

REFERENCES

Acevedo, A., Carpio, E. A., Rodriguez, J. & Manzano, M. A. 2012 Disinfection of natural water by solar photocatalysis using immobilized TiO_2 devices: efficiency in elimination indicator bacteria and operating life of the system. *Journal of Solar Energy Engineering* **134**.

Andersen, H. R., Hansen, K. M. S., Hey, T. & Ledin, A. 2008 Photochemical treatment of estrogenic chemicals. Proceedings of IWA World Water Congress, Vienna, Austria.

Chen, C. Y., Wu, L. C., Chen, H. Y. & Chung, Y. C. 2010 Inactivation of *Staphylococcus aureus* and *Escherichia coli* in water using photocatalysis with fixed TiO_2. *Water Air Soil Pollution* **212**, 231–238.

Christiansen, L. B. & Plesner, T. 2001 Intersex og andre effecter på reproduktionssytemet i skalle og bækørred – relationer til østrogener og østrogenligende stoffer (Intersex and other effects on the reproductional system of roach and brown trout). Report for Aarhus county, Denmark.

Christiansen, L. B., Winther-Nielsen, M. & Helweg, C. 2002 Feminisation of fish – The effect of estrogenic compounds and their fate in sewage treatment plants and nature. Report for Danish EPA project no. 729.

Coleman, H. M., Abdullah, M. I., Eggins, B. R. & Palmer, F. L. 2005 Photocatalytic degradation of 17β-oestradiol, oestriol and 17α-ethynyloestradiol in water monitored using fluorescence spectroscopy. *Applied Catalysis B: Environmental* **55**, 23–30.

Coleman, H. M., Eggins, B. R., Byrne, J. A., Palmer, F. L. & King, E. 2000 Photocatalytic degradation of 17-β-oestradiol on immobilised TiO_2. *Applied Catalysis B: Environmental* **24**, L1–L5.

Coleman, H. M., Routledge, E. J., Sumpter, J. P., Eggins, B. R. & Byrne, J. A. 2004 Rapid loss of estrogenicity of steroid estrogens by UVA photolysis and photocatalysis over an immobilised titanium dioxide catalyst. *Water Research*. **38**, 3233–3240.

European Union. 2006 Directive 2006/7/EC of the European Parliament and of the council of 15 February 2006 concerning the management of bathing water quality and repealing Directive 76/160/EEC.

Gumy, D., Rincon, A. G., Hajdu, R. & Pulgarin, C. 2006 Solar photocatalysis for detoxification and disinfection of water: Different types of suspended and fixed TiO_2 catalysts study. *Solar Energy* **80**, 1376–1381.

Hijnen, W. A. M., Beerendonk, E. F. & Medema, G. J. 2006 Inactivation credit of UV radiation for viruses, bacteria and protozoan (oo)cysts in water: A review. *Water Research* **40**, 3–22.

Hu, J. & Quek, P. H. 2008 Effects of UV radiation on photolyase and implications with regards to photoreactivation following low- and medium pressure UV disinfection. *Applied and Environmental Microbiology*. **74** (1), 327–328.

Rosenfeldt, E. J., Chen, P. J., Kullman, S. & Linden, K. G. 2007 Destruction of estrogenic activity in water using UV advanced oxidation. *Science of the Total Environment* **377**, 105–113.

Simonsen, M. E., Zheshen, L. & Søgaard, E. G. 2009 Influence of the OH groups on the photocatalytic activity and photoinduced hydrophilicity of microwave assisted sol-gel TiO_2 film. *Applied Surface Science* **255** (18), 8054–8062.

Ultraviolet disinfection guidance manual for the final long term 2 enhanced surface water treatment rule. 2006 United States Environmental Protection Agency, Office of Water, Washington, DC, USA.

Paper II

Henrik Tækker Madsen and Erik G. Søgaard

Use of ESI-MS to determine reaction pathway for hydrogen sulphide scavenging with 1,3,5-tri-(2-hydroxyethyl)-hexahydro-s-triazine

European Journal of Mass Spectrometry, **18** (2012), 377-383

Reprinted with permission from IM Publications LLP

H.T. Madsen and E.G. Søgaard, *Eur. J. Mass Spectrom.* **18,** 377–383 (2012)
Received: 7 May 2012 ■ Revised: 8 August 2012 ■ Accepted: 10 August 2012 ■ Publication: 12 September 2012

EJMS EUROPEAN JOURNAL OF MASS SPECTROMETRY

Use of ESI-MS to determine reaction pathway for hydrogen sulphide scavenging with 1,3,5-tri-(2-hydroxyethyl)-hexahydro-*s*-triazine

Henrik T. Madsen* **and Erik G. Søgaard**

Aalborg University Esbjerg, Section for Chemical Engineering, Niels Bohrs Vej 8, 6700 Esbjerg, Denmark. E-mail: htm@bio.aau.dk

To study the reaction between hydrogen sulphide and 1,3,5-tri-(2-hydroxyethyl)-hexahydro-*s*-triazine, which is an often used hydrogen sulphide scavenger, electrospray ionisation mass spectrometry (ESI-MS) was used. The investigation was carried out in positive mode and tandem mass spectrometry was used to investigate the nature of unknown peaks in the mass spectra. The reaction was found to proceed as expected from theory with the triazine reacting with hydrogen sulphide to form the corresponding thiadiazine. This species subsequently reacted with a second hydrogen sulphide molecule to form the dithiazine species, thereby confirming previously obtained results and showing the ability of the ESI-MS method for studying the scavenging reaction. The final theoretical product *s*-trithiane was not detected. Furthermore, fragmentation products of thiadiazine and dithiazine were detected in the solution and possible pathways and structures were suggested to describe the observed fragments. In these, thiadiazine fragmented to 2-(methylidene amino)-ethanol and 2-(1,3-thiazetidin-3-yl)-ethanol and *N*-(2-hydroxyethyl)-*N*-(sulfanylmethyl)-ethaniminium, which underwent a further fragmentation to *N*-methyl-*N*-(2-oxoethyl)-methaniminium. Dithiazine fragmented to *N*-methyl-*N*-(2-oxoethyl)-methaniminium as well. The by-product from this reaction is methanedithiol, which was not detected due to its low polarity.

Keywords: hydrogen sulphide, scavenging, triazines, reaction pathway, by-products

Introduction

During production of oil and gas, a commonly encountered pollutant is hydrogen sulphide gas. Hydrogen sulphide is both highly toxic and corrosive and must therefore be removed.[1,2] In general, two strategies exist for this: regenerative and non-regenerative. For fields with H_2S concentrations below a few hundred ppm, the most economical solution is the non-regenerative one and the triazine-based molecules are among the most frequently used scavengers.[3] Triazines have the advantage that they can be modified to become more or less hydrophilic by using different functional groups on the nitrogen atoms. Often, a polar functional group is used but also purely nonpolar alkyl side groups have been investigated.[4] The reasons why triazines are so widely used are that they are H_2S-selective because of their tertiary nitrogen atoms, the reactions products are corrosion inhibitors and the spent material has a low toxicity, making waste management easier.[3] When applied after extraction from the well during the separation process on the platform, a water soluble triazine is chosen to ensure that the reaction products are disposed of with the produced water. One of the most commonly chosen water soluble triazines is 1,3,5-tri-(2-hydroxyethyl)-hexahydro-*s*-triazine (triazine).

The accepted theoretical reaction pathway for the reaction between triazine and H_2S is shown in Figure 1. Triazine reacts with H_2S in an S_N2 reaction, where a nitrogen atom is substituted with a sulphur atom forming 3,5-di-(2-hydroxyethyl)-hexahydro-1,3,5-thiadiazine (thiadiazine). Thiadiazine may then further react with H_2S forming 5-(2-hydroxyethyl)-hexahydro-1,3,5-dithiazine (ditihiazine), which may, in theory, finally form *s*-trithiane (trithiane) via a final reaction with H_2S.[4,5]

ISSN: 1469-0667
doi: 10.1255/ejms.1192
© IM Publications LLP 2012
All rights reserved

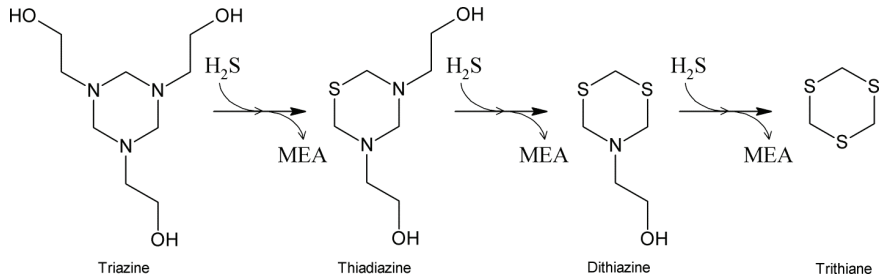

Figure 1. Reaction system for the scavenging process. Triazine may react with H_2S forming the scavenging products: thiadiazine, dithiazine and trithiane under loss of monoethanolamine molecules.

The final conversion to trithiane is not usually observed. The reaction has previously been studied with ^{1}H NMR,[5] where it was found to terminate at dithiazine. In Figure 2, the reaction mechanism, as described by Buhaug and Bakke,[5] is given. The mechanism is the same for all three steps in the reaction, but the rate of reaction is expected to decrease due to the polarisability of sulphur atoms. Sulphur atoms contribute with more electrons to the ring structure compared to nitrogen atoms and, because these are found further away from the sulphur nucleus, they will be shared more efficiently within the molecule. This will allow the presence of S-atoms in the ring structure to increase the stability and decrease the reactivity of the molecules from triazine to trithiane.

During the scavenging reaction, a solid precipitate with a high content of sulphur and carbon has been observed, which has been thought to be trithiane formed by an overspending of

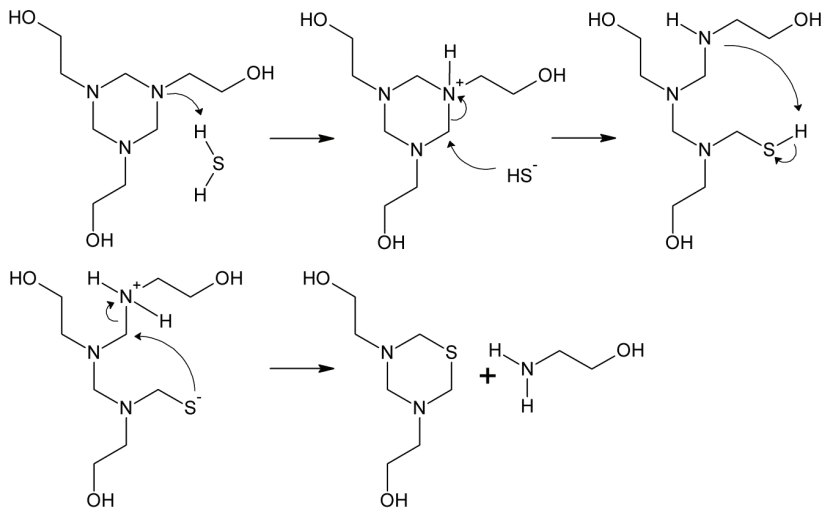

Figure 2. Reaction mechanism for the scavenging process. To react with H_2S, the scavenger will revert to an open ring form, and upon ring re-formation, monoethanolamine will act as a leaving group.

Table 1. ESI-MS settings during experiments.

Parameter		Parameter	
Mass range mode	Std/normal	Skimmer	40.0 V
Ion polarity	Positive	Oct 1 DC	12.00 V
Ion source type	ESI	Oct 2 DC	1.70 V
Dry gas temperature	325°C	Scan begin	50 *m/z*
Nebulizer	15 psi	Scan end	2200 *m/z*
Dry gas flow	5.00 L min^{-1}	Averages	7 spectra
Trap drive	45.8	Maxx accu time	20000 µs
Octopole RF amplitude	135.6 Vpp	ICC target	–1
Capillary exit	107.4 V	Charge control	On

the scavenger, or an amorphous dithiazine polymer for which strong evidence has been produced.[6–8] The formation of the precipitate must originate from compounds initially present or formed in the scavenging mixture, but none of the previously detected compounds seems to be able to explain how the precipitate is formed. As a result, it was desired to investigate the composition of the mixture at different stages of scavenging and, to do this, electrospray ionisation mass spectrometry (ESI-MS) was employed. ESI-MS is a highly sensitive method of analysis, capable of detecting compounds in concentration as low as ng L^{-1}. Furthermore, ESI has the benefit over other ionisation techniques that it produces spectra with only very limited fragmentation. It is therefore possible to study the entire composition of even complex reaction mixtures in a single spectrum.

Material and methods

Materials

1,3,5-tri-(2-hydroxyethyl)-hexahydro-*s*-triazine (51 mass%, dissolved in water), equal to what is injected in the gas stream offshore, was supplied by Maersk Oil. NaHS and HCl (37%) were purchased at Sigma–Aldrich Chemical Co. Demineralised water was produced with a Silex II ion exchanger from SILHORKO.

ESI-MS analysis of H_2S scavenging

25 mL triazine (0.064 moles) were filled in a 250 mL gas washing bottle together with a stirring magnet. The washing bottle was connected to a two-neck, pear-shaped boiling flask in which 1.8048 g (0.032 moles) NaHS were kept. A dripping funnel with HCl was attached to the boiling flask. By allowing HCl to slowly drip down on the NaHS, gaseous H_2S was formed and bubbled through the triazine solution. Eight batches of 0.032 moles each were used consecutively, so ratios of H_2S to triazine from 1 : 2 up to 4 : 1 could be examined. After each batch, a sample of 0.1 mL solution was extracted, diluted 1:10000 in demineralised water and analysed by ESI-MS. In this way, the composition of the mixture was analysed from the initial triazine solution to the overspend solution. Experiments were carried out at room temperature and atmospheric pressure.

Instrumental analysis

Mass spectra were obtained using ESI-MS with an ion trap, 1100 series LC/MSD Trap (Agilent). Prior to injection, samples were diluted 1 : 10,000 with demineralised water to avoid overloading the trap. The diluted solution was sampled with a syringe, which was subsequently attached to a syringe pump for injection into the ESI-MS. Between measurements, the MS was cleaned with a 1 : 1 : 1 mixture of demineralised water, isopropanol and methanol. The settings for the ESI-MS during experiments are shown in Table 1. Tandem mass spectrometry (MS/MS) was performed by isolating a given peak and then fragmenting it via collisions with He gas.

Results

The mass spectrum in Figure 3 displays the composition of the scavenger mixture reaction with H_2S after a ratio of 1 : 2 H_2S to triazine. The main peak in the spectrum is protonated thiadiazine (*m/z* = 193), with a small peak of the sodiated molecule (*m/z* = 215). The protonated dithiazine (*m/z* = 166) only gives a very small peak, which is a result of the amount of H_2S used relative to the amount of scavenger. Triazine was only detected as the triazine–Na adduct (*m/z* = 242) and trithiane was not detected, even after completely spending the scavenger with a ratio of 4 : 1. In the completely spent mixture, the only scavenger product found was dithiazine.

As well as the expected triazine, thiadiazine and dithiazine peaks, two other main peaks were present at 86.4 *m/z* and 120.3 *m/z*. The ESI-MS operated with a small offset of 0.2–0.3 *m/z* and was only calibrated down to *m/z* values of 118 *m/z*. Close to or below the lower calibration limit, the offset is increased up to 0.4 *m/z* for 86 *m/z* peak and 0.5 *m/z* for the 74 *m/z* peak. The real nominal mass of the two peaks is, therefore, 86 *m/z* and 120 *m/z*. Both peaks were absent in a spectrum of the pure triazine. By analysing the composition as more H_2S was bubbled through the scavenger solution, it was found that the 120 *m/z* peak is formed alongside with thiadiazine and as the intensity of thiadiazine decreased, so did the intensity of the 120 *m/z* peak. After a complete spending of the scavenger, the 120 *m/z* peak had disappeared. The 86 *m/z* peak was also formed alongside thiadiazine, but it did not disappear

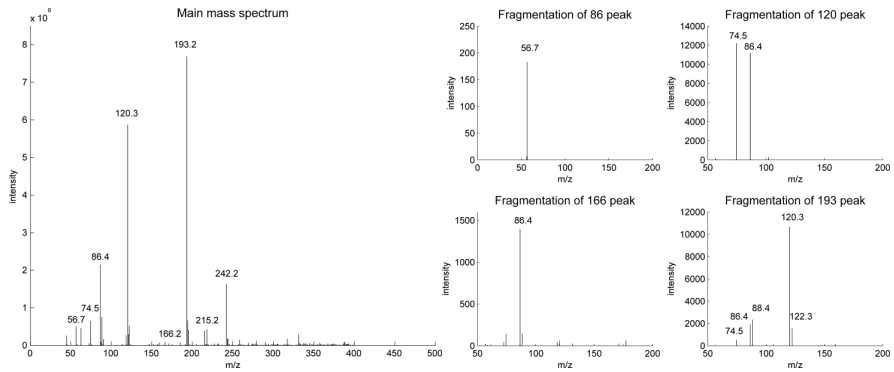

Figure 3. Mass spectra from the experiments. To the left, the spectrum of the scavenger mixture after reaction with H_2S is shown, and to the right, fragmentation spectra of the peaks from the main mass spectrum are shown.

with thiadiazine and it was present as the only peak other than dithiazine after a complete spending of the scavenger.

Fragmentation spectra from the MS/MS analyses of thiadiazine, dithiazine, the 120 *m/z* peak and the 86 *m/z* peak are shown in Figure 3. Upon fragmentation, the 120 *m/z* peak yielded the 86 *m/z* peak and a peak at 74 *m/z*. The 86 *m/z* peak yielded a peak at 56 *m/z*. The fragmentation of thiadiazine yielded both the 120 *m/z* peak and the 86 *m/z* peak, as well as peaks at 74 *m/z*, 88 *m/z* and 122 *m/z*, while the fragmentation of dithiazine mainly yielded the 86 *m/z* peak, but also peaks at 74 *m/z* and 88 *m/z* with lower intensity. Fragmentation of triazine did yield peaks at 84 *m/z*, 96 *m/z*, 169 *m/z* and 181 *m/z*.

Discussion

In general, the mass spectrum confirms the overall features of the reaction. Triazine is first converted to thiadiazine and then to dithiazine, where the reaction terminates. Even after completely spending the scavenger, no trithiane is formed. This strongly indicates that the scavenging reaction at the investigated conditions does not yield trithiane. It is possible that trithiane was not detected by the ESI-MS due to its relatively low dipole moment, but viewed in the context of experiments by Bakke *et al.*,[4,5] where ^{1}H NMR was used and no trithiane detected, this does not seem to be a likely explanation. Furthermore, the experiment shows the applicability of the ESI-MS technique for the study of the scavenging reaction, since it is able to reproduce previously reported observations.

The MS/MS analyses show that the two peaks at 120 *m/z* and 86 *m/z* are products of a fragmentation of thiadiazine and that 86 *m/z* is a fragmentation product of dithiazine as well; this may explain the observations made during the scavenging reaction. When thiadiazine is formed, some of the molecules may undergo a natural fragmentation, not induced by the MS, and form the 120 *m/z* peak, which will further react and form the 86 *m/z* peak. To distinguish between fragmentation processes occurring inside the mass spectrometer, and fragmentation processes occurring in the liquid scavenger solution phase, the solution phase fragmentation will be termed decomposition from here on. When thiadiazine has been completely spent and converted to dithiazine, the 120 *m/z* peak will disappear since its source is no longer present. The 86 *m/z* peak will still be present since it is formed by decomposing dithiazine molecules. The interesting question at this point is whether the fragmentation of thiadiazine and dithiazine is a naturally occurring decomposition process taking place in the solution, or if it is a reaction taking place inside the mass spectrometer. Triazine and thiadiazine have previously been found to undergo an acid catalysed hydrolysis, whereas dithiazine has been found to be stable,[5] and it would therefore not seem obvious that dithiazine should naturally decompose in the solution. However, ionisation via ESI is a very gentle technique under which no, or only very little, fragmentation in the mass spectrometer is usually observed and, upon inspection of the mass spectrum in Figure 3, none of the MS/MS induced fragmentation products of triazine is seen. With no fragmentation of the least stable of the three compounds—triazine, thiadiazine and dithiazine—found to occur inside the mass spectrometer, it does not seem obvious that the fragmentation of thiadiazine and dithiazine should be caused by the MS. As such, the two peaks at 86 *m/z* and 120 *m/z* seem to be by-products of the scavenging reaction instead. Also, even if the compounds were a product of the relatively mild ESI, it would only show that thiadiazine and dithiazine will fragment if subjected to ionisation. Since ionisation is thought to be the first step in the scavenging reaction mechanism, as seen in Figure 2, the compounds do seem

to be important to consider when describing the complete scavenging system. As a result, the fragmentation is believed to occur in the solution, and the reaction pathways given in Figure 4 describe processes occurring in the solution phase and not the mass spectrometer.

Identification of peaks and suggested reaction pathway

The 120 *m/z* and 86 *m/z* peaks are products of thiadiazine and dithiazine; therefore, the differences in mass between the peaks may be calculated to determine the reaction mechanism. The difference between protonated thiadiazine and the 120 *m/z* peak is 73 Da and the difference between the 120 *m/z* peak and the 86 *m/z* peak is 34 Da. The difference between protonated dithiazine and the 86 *m/z* peak is 80 Da and the difference between the 86 *m/z* and 56 *m/z* peaks is 30 Da. The difference of 73 Da maybe explained by the 74 *m/z* peak, which would correspond to a molecule with a nominal mass of 73 Da that has been protonated.

Assuming that the only elements present in the molecular structure of these peaks are carbon, hydrogen, oxygen, nitrogen and sulphur, the possible empirical formulae that give the correct *m/z* ratio may be calculated. This was done with a Matlab script file. The only realistic combinations that give 30 Da and 34 Da are CH_2O/C_2H_6 and H_2S. This means that the 120 *m/z* peak is probably converted to the 86 *m/z* peak through the loss of a H_2S molecule and the 86 *m/z* peak is converted to the 56 *m/z* peak through the loss of a formaldehyde molecule. Since the 120 *m/z* peak originates from thiadiazine, which contains only one sulphur atom, the fact that the difference of 34 *m/z* corresponds to a H_2S molecule also shows that the sulphur atom must be retained in the 120 *m/z* compound. Investigation of possible empirical formulae for the 73 Da compound confirms this since there is no combination with sulphur that has a nominal mass of 73 Da. From the script file, it is found that there are three possible empirical formulae for the 73 Da compound: $C_2H_7N_3$, $C_4H_{11}N$ and C_3H_7ON. The first one may be ruled out since thiadiazine only contains two nitrogen atoms. The second option does not seem likely either, since it would require a shift in the placement of one of the hydroxyl groups to get a compound with four carbon atoms and one nitrogen atom. Instead, the third option seems to be more likely. Based on these considerations, a reaction scheme showing how thiadiazine may decompose in the solution to compounds with the correct molecular weights is proposed in Figure 4. These compounds are 2-(methylidene amino)-ethanol (73 Da, MAE) and 2-(1,3-thiazetidin-3-yl)-ethanol (119 Da, TYE). In the ESI-MS, these will appear as peaks at 74 *m/z* and 120 *m/z* when protonated. Thiadiazine may also decompose to *N*-(2-hydroxyethyl)-*N*-(sulfanylmethyl)-methaniminium (120 Da, HSMI), which is a protonated open variant of TYE.

As the general scavenging reaction is initiated by protonation, it is assumed that the same holds for the decomposition process. The protonation of thiadiazine may occur on either one of the nitrogen atoms or the sulphur atom. Instead of leading to the formation of dithiazine, protonation of one of the nitrogen atoms may result in reconfigurations in the electronic structure, resulting in dissociation into protonated MAE and TYE. If the protonation occurs on the sulphur atom, the positive charge on the sulphur atom may attract electrons and lead to an opening of the ring structure. From here, the electrons may be redistributed, thereby dissociating the molecule into MAE and HSMI. HSMI will also be formed if the sulphur atom in TYE is protonated. HSMI may then undergo a final reconfiguration to form *N*-methyl-*N*-(2-oxoethyl)-methaniminium (MOM, 86 Da). During the reconfiguration from HSMI to MOM, H_2S is lost, which is equal to the mass difference between the 120 *m/z* and 86 *m/z* peaks. The removal of H_2S will lead to the formation of a carbocation that will allow a hydride shift to take place, which will enable the negative charge on the oxygen atom to stabilise as a double bond between carbon and oxygen. MOM may also be formed as a result of protonation of the nitrogen atom in TYE. The hydride here shift will be from the nitrogen atom to the carbocation left when H_2S is lost, see Figure 4.

Whether the protonation occurs on one of the nitrogen atoms or the sulphur atom in thiadiazine is not known. Due to their electronegativity, the nitrogen atoms are likely to be the ones with the highest proton affinity, but the 2-hydroxyethyl groups will result in some degree of shielding. The sulphur atom will, on the other hand, stabilise the positive charge more efficiently due to its polarisability. As the protonation results in the same compounds or molecules with identical *m/z* ratios, it is not possible to exclude one of the protonations based on these experimental results and it is possible that both reaction pathways occur.

If this theory is to be valid, MOM must also be formed when dithiazine decomposes in the solution. This is shown in Figure 4. As for thiadiazine, both the nitrogen atom and the sulphur atoms may become protonated. Protonation of the nitrogen atom may, theoretically, lead to formation of *s*-trithiane, but since this is found not to occur, the reaction pathway is not viable. If one of the sulphur atoms is protonated, the positive charge may lead to a ring opening as with thiadiazine. From this open form, the molecule may undergo a reconfiguration to form MOM. The reconfiguration is similar to the one described for HSMI, but with methanedithiol as the leaving group instead of H_2S. Methanedithiol will only be very weakly polar and will not, as such, be expected to give a significant peak in the ESI-MS analysis since it must become charged to be detected.

The proposed reaction pathways do not aim at excluding other possibilities, but do seem to be able to explain the observations very well. They account for all the observed peaks and show high symmetry in that both reaction pathways may explain how the same structure for the 86 *m/z* peak is formed through simple reconfigurations.

For both thiadiazine and dithiazine, another theoretical reaction pathway leads to (dimethylidene-λ^5-amino)-ethanal (DMAE) formation. DMAE has a nominal mass of 85 Da and a protonated form would therefore fit with the observed 86 *m/z* peak. However, DMAE includes a penta valent nitrogen atom with ten valence electrons, which is not commonly observed under these experimental conditions. Also, the reaction

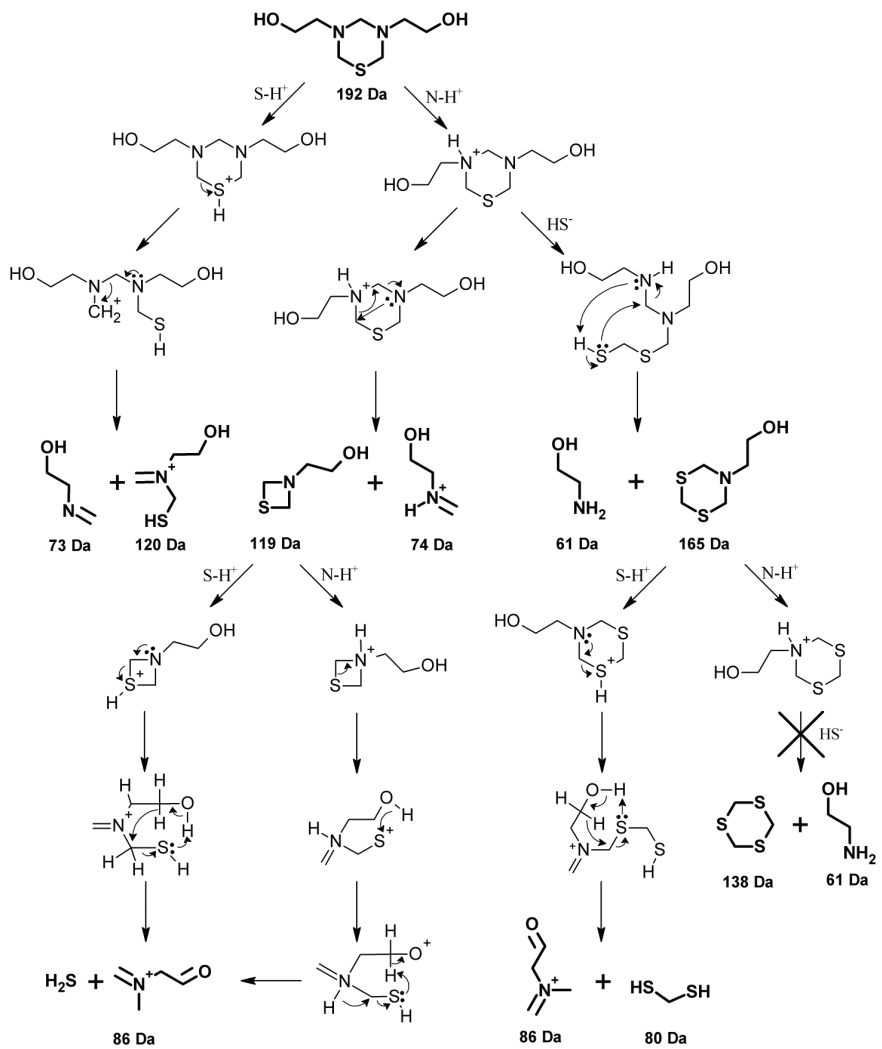

Figure 4. Proposed fragmentation pathway for thiadiazine and dithiazine in solution phase. Products are in bold, while intermediate states are not. These intermediate states are used as descriptors for how the reconfigurations can be thought to occur, and the electronic changes are shown with arrows. The nominal mass of the products are also shown. Since only charged species will occur in the mass spectra, the uncharged products occur in their protonated form (nominal mass + 1) in the mass spectra.

pathway includes a hydride shift to a neutral sulphur atom and, as such, we find this reaction pathway to be unlikely.

The proposed structure for the 86 *m/z* peak, MOM, carries a carbonyl group and should, as such, react with H_2S, resulting

in heavier compounds. No such compounds were detected with the ESI-MS, but this may be due to low polarity. The variety of compounds besides triazine, thiadiazine and dithiazine that are present in the reaction mixture may help explain the solid precipitate. In particular, methanedithiol could be interesting since it could contribute with sulphur and carbon to a precipitate.

Discussion about remaining peaks from fragmentation

It is interesting to notice that upon MS/MS fragmentation of TYE, the two peaks formed, 86 *m/z* and 74 *m/z*, have almost equal intensity. The difference in mass between 74 *m/z* and 120 *m/z* is 46 Da, which may correspond to ethanol or thioformaldehyde. However, when compared with the mass spectra of the reaction, the intensity of the 74 *m/z* peak is only around a third of the 86 *m/z* peak. This indicates that, although thioformaldehyde or ethanol may theoretically be formed from TYE, it does not seem to take place under the investigated conditions. The reason for the high intensity of the 74 *m/z* peak during MS/MS fragmentation may be that the high energy of the MS/MS fragmentation process allows the formation. Finally, the 88 *m/z* peak may be the reduced form of MOM, *N*-methyl-*N*-(2-hydroxyethyl)-methaniminium.

Conclusion

With the use of ESI-MS, the reaction pathway for the scavenging of H_2S with 1,3,5-tri-(2-hydroxyethyl)-hexahydro-*s*-triazine has been described. The general scavenging reaction, with triazine reacting with H_2S to form thiadiazine, which will then react with another H_2S molecule to form dithiazine, where the scavenging reaction terminates, has been confirmed and ESI-MS has been shown to be an effective way of analysing the reaction. Furthermore, additional reaction products originating from thiadiazine and dithiazine were detected and molecular structures proposed. Thiadiazine may decompose to 2-(methylidene amino)-ethanol and 2-(1,3-thiazetidin-3-yl)-ethanol and *N*-(2-hydroxyethyl)-*N*-(sulfanylmethyl)-methaniminium, which may further decompose to *N*-methyl-*N*-(2-oxoethyl)-methaniminium. Dithiazine may decompose to *N*-methyl-*N*-(2-oxoethyl)-methaniminium in which the by-product is methanedithiol. The decomposition may be occurring inside the mass spectrometer as a gas-phase fragmentation process but, due to the facts that the ionisation with electrospray is a gentle process and that pure triazine was not found to fragment in the mass spectrometer, it is expected that the formation of the additional reaction products takes place in solution and not in the mass spectrometer.

References

1. World Health Organisation, Environmental Health Criteria 19: Hydrogen Sulfide (1981).
2. Sikkerhedsstyrelsen, Bekendtgoerelse nr 4009, gasreglementet—afsnit a (Executive order no. 4009, Danish gas regulations – section a) (1981).
3. M.A. Kelland, *Production Chemicals for the Oil and Gas Industry*, 1st Edition, CRC Press, Boca Raton, Florida, USA (2009). doi: 10.1201/9781420092974
4. J. Bakke and J. Buhaug. "Hydrogen sulfide scavenging by 1,3,5-triazinanes. Comparison of the rates of reaction", *Ind. Eng. Chem. Res.* **43,** 1962–1965, doi: 10.1021/ie030510c
5. "Hydrolysis of 1,3,5-tris(2-hydroxyethyl)-hexahydro-*s*-triazine and its reaction with H_2S", *Ind. Eng. Chemi. Res.* **40,** 6051–6054, (2001). doi: 10.1021/ie010311y
6. G.N. Taylor and R. Matherly, "Structural elucidation of the solid byproduct from the use of 1,3,5-tris(hydroxyethyl)hexahydro-*s*-triazine based hydrogen sulfide scavengers", *Ind. Eng. Chem. Res.* **50,** 735–740, (2011). doi: 10.1021/ie101985v
7. R.L. Horton, R. Stoker and P. Davis, *Process for Preventing or Remediating Trithiazine Deposition in High H2S Wells*,. United States Patent, Pub. No.: US 2010/016/0163255 A1 (2010).
8. C. W. Titley and P. H. Wieninger. *Method and Composition for Removing Sulfides from Hydrocarbon Streams*, United States Patent, Pub. No.: US 2003/0234383 A1 (2003).

Paper III

Henrik Tækker Madsen and Erik G. Søgaard

Fouling Formation During Hydrogen Sulfide Scavenging With 1,3,5-tri-(hydroxyethyl)-hexahydro-s-triazine

Petroleum Science and Technology, **32** (2014), 2230-2238

Reprinted with permission from Taylor & Francis LLC

Petroleum Science and Technology, 32:2230–2238, 2014
Copyright © Taylor & Francis Group, LLC
ISSN: 1091-6466 print / 1532-2459 online
DOI: 10.1080/10916466.2013.783066

Downloaded by [Aalborg University Library] at 23:08 14 July 2014

Fouling Formation During Hydrogen Sulfide Scavenging With 1,3,5-tri-(hydroxyethyl)-hexahydro-s-triazine

H. T. Madsen[1] and E. G. Søgaard[1]

[1]*Department of Biotechnology, Chemistry and Environmental Technology, Aalborg University, Esbjerg, Denmark*

To investigate if the hydrogen sulfide scavenger, 1,3,5-tri-(hydroxyethyl)-hexahydro-s-triazine, could explain a severe carbon/sulfur rich fouling found at a refinery, experiments were conducted to study the scavenging process and the composition of the fouling. The reaction was analyzed with electro spray ionization mass spectrometry (ESI-MS), and the fouling with infrared spectroscopy and X-ray diffraction. The fouling was found to be a by-product of the scavenging reaction, and to consist of dithiazine molecules with linking carbon-sulfur chains. ESI-MS analysis strongly indicates that these chains are generated when dithiazine decomposes to smaller molecules, which through condensation reactions with dithiazine forms the fouling.

Keywords: Fouling, hydrogen sulfide, scavenging processes, triazine

INTRODUCTION

Sulfur fouling during oil production and refining can be a major problem. Fouling may occur along the entire production train from formation to production facilities, leading to reduced permeability and production flow (Hyne, 1983; Elsamimanesh et al., 2011).

At a Danish refinery using North Sea oil, severe fouling in the water system after the distillation column has been encountered, and it has often been necessary to stop the refining process to clean the system. Elemental analyses have shown the fouling to consist mainly of carbon and sulfur in a 1:1 ratio along with hydrogen and trace amounts of nitrogen and oxygen, and it has been speculated that the fouling originates from the offshore hydrogen sulfide (H_2S) scavenging process, where 1,3,5-tri-(hydroxyethyl)-hexahydro-s-triazine (triazine) is used.

It has been reported that the use of triazines for H_2S scavenging may result in the deposition of a solid material (Sullivan et al. 1997; Titley and Wieninger, 2003; Horton et al., 2010), and due to the high content of carbon and sulfur, it has been speculated that it is the theoretical final product of the scavenging process, s-trithiane, which should be involved. However, laboratory studies have found dithiazine to be the final reaction product and not s-trithiane (Bakke et al., 2001; Bakke and Buhaug, 2004; Madsen and Søgaard, 2012). To explain both observations, it has been hypothesized that the precipitate is a dithiazine polymer with C-S chains linking the dithiazine molecules (Taylor and Matherly, 2011). It was postulated that thioformaldehyde was causing the formation of the C-S chains, and that it might be formed through hydrolysis of the triazine into monoethanolamine (MEA) and formaldehyde. However, to explain the observed elemental composition, a comparable

Address correspondence to H. T. Madsen, Department of Biotechnology, Chemistry and Environmental Engineering, Aalborg University, Niels Bohrs Vej 8, Esbjerg 6700, Denmark. E-mail: htm@bio.aau.dk

high amount of thioformaldehyde must be produced and whether this happens may be considered as doubtful.

Based on these considerations, two hypotheses were propounded to explain the fouling encountered at the refinery: (a) during the industrial conditions, s-trithiane would formed and causes the fouling; (b) the reaction terminates at dithiazine, but would form a bridging agent that causes a polymerization. These hypotheses were assessed with infrared spectroscopy (IR) and X-ray diffraction (XRD) analyses of the fouling. To understand how the fouling is formed, the reaction mixture composition was analyzed by help of electro spray ionization mass spectrometry (ESI-MS). To approach industrial conditions, scavenging experiments with spent scavenger solution and pure triazine were performed.

In this study, the nature of the fouling found at the refinery was identified by a comparison of IR and XRD spectra of reference compounds and the fouling. ESI-MS spectra from scavenging experiments using HS^-/triazine, H_2S/triazine, and H_2S/spent scavenger are compared to investigate the link between controlled laboratory experiments and conditions experienced in industry. The results from the IR investigations of the fouling are evaluated together with the ESI-MS spectra and used to develop a model for the fouling phenomenon that is validated by previously obtained results (Taylor and Matherly, 2011).

Downloaded by [Aalborg University Library] at 23:08 14 July 2014

EXPERIMENTAL

Materials

1,3,5-tri-(hydroxyethyl)-hexahydro-s-triazine (51% weight, dissolved in water), equal to what is injected in the gas stream offshore, and spent scavenger solution was supplied by Maersk Oil. NaHS, HCl (37%), s-trithiane, NaCl, Na_2HPO_4, and NaH_2PO_4 were purchased at Sigma-Aldrich Chemical Co. Fouling was sampled from the refinery. Demineralized water was produced with a Silex II ion exchanger from SILHORKO.

Instrumental Analysis

Mass spectra were obtained using ESI-MS with an ion trap, 1100 series LC/MSD Trap (Agilent) as previously described (Madsen and Søgaard, 2012). IR spectra analyses were made with the ATR-FT-IR instrument Avatar 370 FT-IR (Thermo Nicolet). X-ray diffraction spectra were made using a Philips X'Pert X-ray diffractometer, with Co Kα (1.7890 Å) as X-ray source, scanning from 5° to 105°.

ESI-MS Experiments

Three model experiments aimed at investigating the reaction pathway were conducted to link laboratory results to industrial observations: 1) A study of the reaction between HS^- and diluted triazine, 2) a study of the reaction between triazine and gaseous H_2S, and 3) a study of the reaction between offshore spent scavenger and gaseous H_2S.

MS analysis of scavenging reaction, HS^-

The experimental procedure was based on a previous work made by Buhaug and Bakke (Bakke and Buhaug, 2004). 4.2140 g NaHS and 10.7855 g triazine solution were weighed off and dissolved in 40 mL buffered solution at pH 10, giving a final concentrations of c(triazine) = 0.5 M and

$c(HS^-) = 1.5$ M. The reaction was mixed with a magnet stirrer and kept at 25°C. 0.1 mL samples were extracted after: 0, 1, 2, 3, 4, 5, 24, 48, 72, 96, 168, and 192 h.

MS analysis: actual scavenging, H_2S, and triazine

25 mL triazine (0.064 mol) was filled in a 250 mL gas washing bottle, connected to a two neck pear shaped boiling flask in which batches of NaHS were stored. By allowing HCl to slowly drip down to the NaHS, gaseous H_2S was formed and bubbled through the triazine solution. Eight batches of 1.8048 g (0.032 mol) NaHS were used and samples of 0.1 mL were extracted after each batch.

Spent scavenger reaction with H_2S

The experiment was carried out analogous to the previous experiment. 50 mL of spent scavenger solution and only six batches of 1.8048 g NaHS were used. Parallel with this experiment a portion of the spent scavenger solution was brought to boil before H_2S was bubbled through the solution. This was done to investigate the effect of temperature on the fouling formation.

RESULTS AND DISCUSSION

Structural Analysis of Fouling

The IR spectrum for pure s-trithiane in Figure 1 has significant peaks at 2952, 1392, 1369, 1217, 1171, 1034, 907, 730, and 661 cm^{-1}. The peaks at 730 and 661 cm^{-1} are due to C—S stretching modes, while the remaining peaks are caused by methylene stretching and bending motions (Socrates, 2003). The 730 cm^{-1} peak is caused by an asymmetric stretching of the C—S bond, while the smaller peak at 661 cm^{-1} is caused by a ring breath motion when the ring is in the chair conformation (Klaboe, 1969).

The IR spectrum of the fouling is clearly different from s-trithiane. It absorbs at 3400, 2956, 2923, 2867–2855, 1584, 1449, 1366, 1175, 1051, 880, 745, 734, and 707 cm^{-1}. As with s-trithiane, many of the peaks can be subscribed to methylene stretching and bending motion; however, the remaining peaks leave clues about the molecular structure of the fouling. The broad peak at 3400 cm^{-1} may be caused by H-bonding of either a hydroxyl or amine group (Socrates, 2003). The peaks 745, 734, and 707 cm^{-1} may all be caused by C—S stretching, indicating sulfur atoms with different molecular surroundings in the structure (Socrates, 2003). Furthermore, no peak is seen around 661 cm^{-1}, which could indicate a loss of ring structure.

In Figure 2 the X-ray diffraction spectra of the fouling and s-trithiane are shown. These also indicate that the fouling and s-trithiane are different compounds. The fouling has fewer peaks and with lower intensity, showing that the fouling has a more amorphous structure. When the X-ray diffraction spectrum for the fouling is compared to the X-ray diffraction spectrum recorded by Taylor and Matherly (2011) for the precipitate found in their experiment, it is seen that the two spectra are identical. This indicates that the fouling from the refinery, and the precipitate produced by Taylor and Matherly (2011) are the same compound.

The observations made for the IR spectrum of the fouling match well with the dithiazine polymer hypothesis (Taylor and Matherly, 2011). This would give an acyclic structure with different C—S bonds and a small amount of amine and hydroxyl groups as indicated by the IR analysis.

Downloaded by [Aalborg University Library] at 23:08 14 July 2014

Downloaded by [Aalborg University Library] at 23:08 14 July 2014

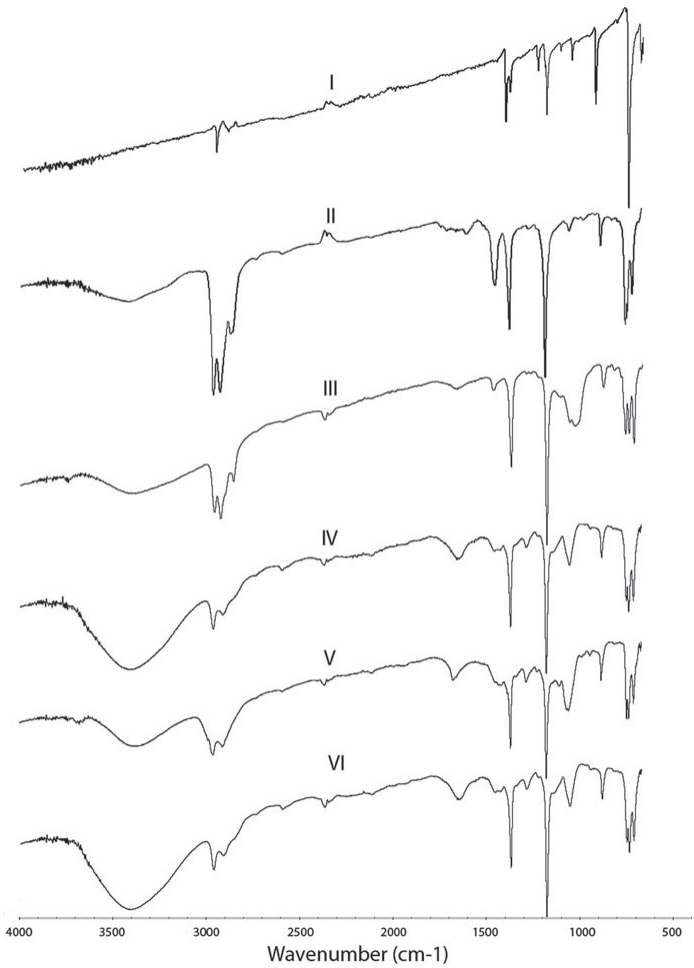

FIGURE 1 Infrared spectra. (I) s-trithiane, (II) fouling from refinery, (III) triazine + HS^-, (IV), triazine + H_2S, (V) spent scavenger + H_2S, (VI) heated spent scavenger + H_2S.

Origin of Fouling

In all three scavenging experiments a precipitate was formed. These were isolated and compared by help of IR spectroscopy. Looking at the three IR spectra in Figure 1, a high degree of overlap can be seen. Shared peaks are found at 3400, 2957, 1650, 1367, 1174, 1050, 880, 745, 734, and

Downloaded by [Aalborg University Library] at 23:08 14 July 2014

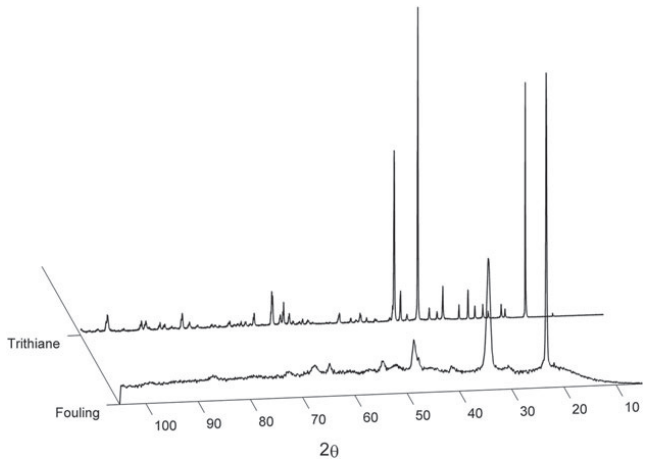

FIGURE 2 XRD spectra of s-trithiane and fouling from refinery.

708 cm^{-1}, which clearly indicates that the three precipitates have the same molecular structure. If the IR spectrum for the fouling is compared with these, overlapping peaks are found at 3400, 2957, 1367, 1174, 1050, 880, 745, 734, and 708 cm^{-1}. An overlapping peak is also found at 1449 cm^{-1}. The fouling exhibits a strong peak here, whereas the precipitates only show a weak peak. In total, the high degree of overlapping between the spectra strongly indicates that the industrial fouling and the laboratory produced precipitates are the same, and that the fouling is formed as a by-product of the scavenging reaction.

The time for the precipitation process was several hours in the experiments with H_2S and triazine/spent scavenger. However, if a precipitate should create a fouling problem at the refinery, a short reaction time will be necessary. By bringing the spent scavenger solution to boil, a precipitate could be seen within few minutes, and when it was investigated with IR, the precipitate was found to be identical to the previous obtained precipitates (see Figure 1). Therefore, the elevated temperatures experienced during the distillation process at the refinery may increase the kinetic energy of the molecules sufficiently for rapid fouling formation similar to the laboratory experiment.

Fouling Formation Mechanism

The time evolving mass spectra in Figures 3, 4, and 5, for the reaction between triazine and HS^-, triazine and H_2S, and spent scavenger and H_2S show that in all three cases the same reaction pathway is observed. The molecules associated with the peaks are given in Table 1. Triazine is first converted to thiadiazine and then to dithiazine, which completely dominates the final spectra. For the HS^- experiment the sodiated molecules dominate due to the presence of Na^+ ions from the NaHS and phosphate compounds. The experiments show that the spent scavenger matrix does not influence the scavenging reaction, and laboratory experiments with HS^- ions may therefore be considered representative for the scavenging reaction.

Downloaded by [Aalborg University Library] at 23:08 14 July 2014

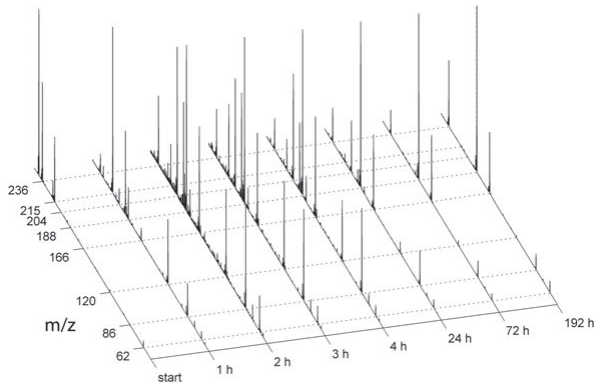

FIGURE 3 Normalized mass spectra from the reaction between triazine and HS^-, with samples taken at different times. The figure shows the composition of the reaction mixture at different times during the scavenging reaction.

Besides the triazine, thiadiazine and dithiazine peaks, two other main peaks are seen in the spectra, 86 m/z and 120 m/z, which are N-methyl-N-(2-oxoethyl)-methaniminium (MOM) and 2-(1,3-thiazetidin-3-yl)-ethanol (TYE) mixture (Madsen and Søgaard, 2012). Via MS/MS analyses they have been found to be fragmentation products of thiadiazine and dithiazine mixture (Madsen and

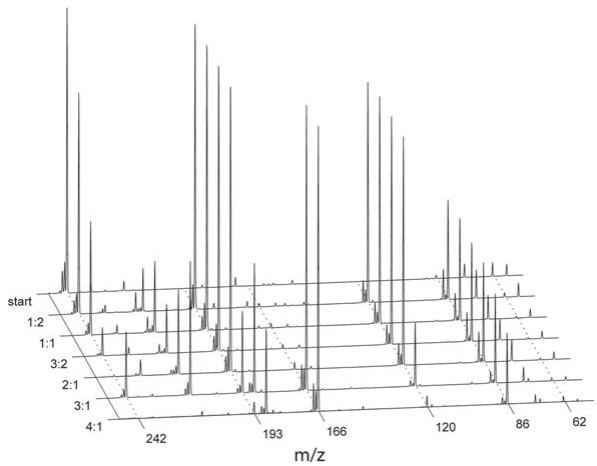

FIGURE 4 Normalized mass spectra from the reaction between triazine and H_2S, with samples taken after reaction with increasing amount of H_2S, showing how the composition of the reaction mixture changed with increasing amounts of H_2S. The mass spectrum of the initial solution is found furthest away, while the closest spectrum is for the final sample.

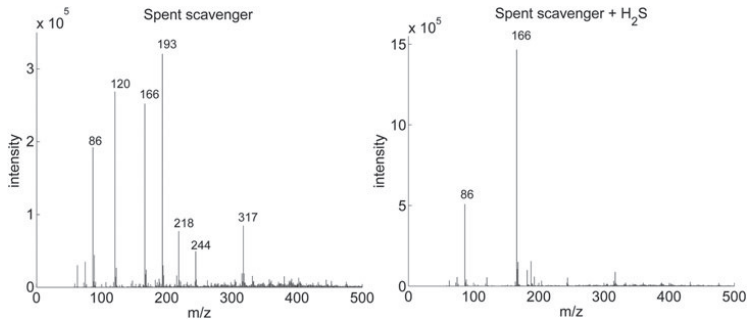

FIGURE 5 Mass spectra of spent scavenger mixture from offshore installation (left) and after it has been completely spent with H_2S (right).

Søgaard, 2012), and the overall reaction system can be described as in Figure 6. Most interestingly, the predicted by-product of the dithiazine decomposition is methanedithiol. The two thiol groups make it suitable as a bridging agent between dithiazine molecules. The polymerization may be explained by a dithiazine molecule reacting with a methanedithiol molecule in a condensation reaction, which would be in agreement with the findings of Taylor and Matherly (2011) that showed the need for a terminal hydroxyl group for polymerization to occur. The terminal thiol group may then react with other methanedithiol molecules in condensation reactions to form a C-S chain. To achieve a polymer with dithiazine molecules, the dithiazine molecule is believed to revert to an opened structure in which it has reacted with a H_2S molecule. The ring opening is a step in the general scavenging process mixture (Madsen and Søgaard, 2012), and it will result in a terminal thiol group, which may react with the C-S chain in a condensation reaction. The suggested polymerization reaction is illustrated in Figure 7, giving the polymer formula seen Figure 8, with an empirical formula of $(C_7H_{15}S_{4.5}NO)_n$, equal to the formula for the amorphous structure found by Taylor and Matherly (2011).

The methanedithiol model is in agreement with the observation that the precipitation first occurs in the final solution where only dithiazine and MOM are present. The compound causing the formation of C—S chains must as such originate from this mixture, and cannot be a

TABLE 1
Nominal Mass of Compounds Detected During the Scavenging Reaction (Madsen and Søgaard, 2012)

Compound	*Nominal Mass*	$+H^+$	$+Na^+$
Monoethanolamine	61	62	—
2-(Methylidene-amino)-ethanol	73	74	—
N-methyl-N-(2-oxoethyl)-methaniminium	86	—	—
2-(1,3-thiazetidin-3-yl)-ethanol	119	120	—
Triazine	219	—	242
Thiadiazine	192	193	215
Dithiazine	165	166	188
Trithiane	138	—	—

— = indicates that no peak is seen at this mass.

Downloaded by [Aalborg University Library] at 23:08 14 July 2014

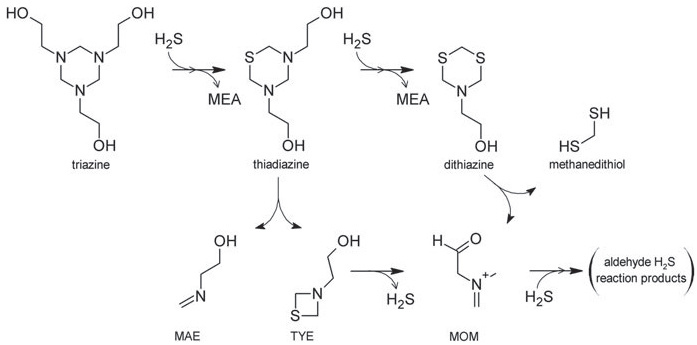

FIGURE 6 Reaction system for scavenging process, with detected by-products. MAE = 2-(methylidene-amino)-ethanol, TYE = 2-(1,3-thiazetidin-3-yl)-ethanol, MOM = N-methyl-N-(2-oxoethyl)-methaniminium.

triazine decomposition product. Methanedithiol has not been directly observed in the experiments, but this may be due to a high reactivity as well as a low dipole moment, which will make the sensitivity of the ESI-MS toward the compound low. Based on the ability of the proposed hypothesis to explain the observed results, it seems to be a likely model for the reaction system.

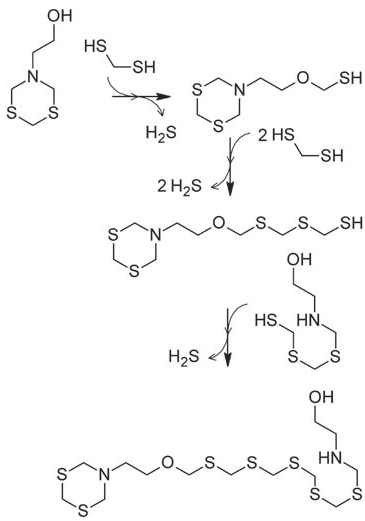

FIGURE 7 Suggested polymerization reaction between dithiazine and methanedithiol.

Downloaded by [Aalborg University Library] at 23:08 14 July 2014

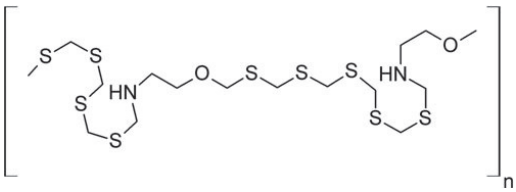

FIGURE 8 Suggested structure of polymer.

Downloaded by [Aalborg University Library] at 23:08 14 July 2014

CONCLUSION

The fouling problem found at an oil refinery has been shown to be caused by the use of 1,3,5-tri-(2-hydroxyethyl)-hexahydro-s-triazine for offshore H_2S scavenging. The triazine will react with H_2S forming first thiadiazine and then dithiazine after which the reaction terminates. The final theoretical product, s-trithiane, is not formed. Under further reaction with H_2S, a precipitate is formed from the spent scavenger solution. The rate of its precipitation can be greatly enhanced by increasing the temperature.

The precipitate is most likely a dithiazine polymer with connecting C—S chains. This is necessary in order to explain the high carbon and sulfur content, and is also strengthened by IR analyses, which indicate a ring opening and the presence of different C—S bonds. The polymerization is most likely caused by the decomposition of dithiazine to methanedithiol, which may react with dithiazine and other methanedithiol molecules in condensation reactions forming a dithiazine polymer with an empirical formula of $(C_7H_{15}S_{4.5}NO)_n$.

REFERENCES

Bakke, J. M., and Buhaug, J. (2004). Hydrogen sulfide scavenging by 1,3,5-triazinanes. Comparison of the rates of reaction. *Ind. Eng. Chem. Res.* 43:1962–1965.

Bakke, J. M., Buhaug, J., and Riha, J. (2001). Hydrolysis of 1,3,5-tris(2-hydroxyethyl)-hexahydro-s-triazine and its reaction with H_2S. *Ind. Eng. Chem. Res.* 40:6051–6054.

Eslamimanesh, A., Mohammadi, A. H., and Richon, D. (2011). Thermodynamic consistency test for experimental data of sulfur content of hydrogen sulfide. *Ind. Eng. Chem. Res.* 50:3555–3563.

Horton, R. L., Stoker, R., and Davis, P. (2010). *Process for preventing or remediating trithiazine deposition in high H_2S wells.* U.S. Patent No. ***5***,128,049.

Hyne, J. B. (1983). Controlling sulfur deposition in sour gas wells. *World Oil* 197/2:35–39.

Klaboe, P. (1969). The vibrational spectra of 1,4-dithiane and 1,3,5-trithiane. *Spectrochim. Acta Part A: Mol. Spectrosc.* 25:1437–1447.

Madsen, H. T., and Søgaard, E. G. (2012). Use of ESI-MS to determine reaction pathway for hydrogen sulfide scavenging with 1,3,5-tri-(2-hydroxyethyl)-hexahydro-s-triazine. *Eur. J. Mass Spectrom.* 18:377–383.

Socrates, G. (2003). *Infrared and Raman Characteristic Group Frequencies: Tables and Charts* (3rd ed.). New York: Wiley.

Sullivan, D. S., Thomas, A. R., Edwards, M. A., Taylor, G. N., Yon-Hin, P., and Garcia, J. M. (1998). *Method of treating sour gas and liquid hydrocarbon.* U.S. Patent No. ***5***,744,024.

Taylor, G. N., and Matherly, R. (2011). Structural elucidation of the solid byproduct from the use of 1,3,5-tris(hydroxyalkyl)hexahydro-s-triazine based hydrogen sulfide scavengers. *Ind. Eng. Chem. Res.* 50:735–740.

Titley, C. W., and Wieninger, P. H. (2003). *Method and composition for removing sulfides from hydrocarbon streams.* U.S. No. Patent. *6:582,624*.

Paper IV

Henrik Tækker Madsen, Carina V. Jensen and Erik G. Søgaard

Triazine based H_2S scavenging: Development of a conceptual model for understanding of fouling formation

Petroleum Science and Technology, **32** (2014), 2803-2806

Reprinted with permission from Taylor & Francis LLC

Petroleum Science and Technology, 32:2803–2806, 2014
Copyright © Taylor & Francis Group, LLC
ISSN: 1091-6466 print / 1532-2459 online
DOI: 10.1080/10916466.2014.915852

Downloaded by [Aalborg University Library], [Henrik Madsen] at 02:16 19 June 2015

Triazine-based H_2S Scavenging: Development of a Conceptual Model for the Understanding of Fouling Formation

H. T. Madsen,[1] C. V. Jensen,[1] and E. G. Søgaard[1]

[1]*Department of Biotechnology, Chemistry and Environmental Engineering, Aalborg University, Niels Bohrs Vej 8, 6700 Esbjerg, Denmark*

The authors studied the applicability of a previously suggested model to describe the reaction between 1,3,5-tri-(2-hydroxypropyl)-hexahydro-s-triazine and H_2S and thereby predict formation of fouling. To investigate the reaction system, electrospray ionization mass spectrometry was employed to analyze the composition of the generated mixture as H_2S is bubbled through the scavenger. The results of the study confirm that the suggested model is capable of explaining how the scavenger reacts with H_2S, which may be used to explain from where and how the fouling originates, and how a scavenging process can be designed to avoid fouling.

Keywords: hydrogen sulfide scavenging, triazines, fouling, modeling

INTRODUCTION

Hydrogen sulfide is a toxic and corrosive gas, which causes problems in both up- and down-stream processes. Once H_2S is generated, it must be removed from the oil and gas streams in order to avoid these H_2S-related problems. The removal of H_2S, often referred to as gas sweetening, and can be accomplished with the use of either regenerative or non-regenerative scavengers. When the concentration of H_2S is only a few hundred ppm, the use of nonregenerative H_2S scavengers is most economic, and one of the most widely used nonregenerative H_2S scavengers is triazines (Kelland, 2009). These compounds react rapidly with H_2S and can be modified for application both down- and up-stream of the borehole. For removal of H_2S from the produced gas, it is common to use a water-soluble triazine since its reaction products can be removed with the condensed water phase. Here the triazine 1,3,5-(2-hydroxyethyl)-hexahydro-s-triazine (HET) is often used. It has been found, however, that the use of this triazine may result in fouling further downstream during the refining process. The fouling has been identified to be a dithiazine polymer (Taylor and Matherly, 2011), which cannot readily be explained from the current known reaction pathway for the triazine, where the triazine first reacts to form the respective thiadiazine, and then further to the dithiazine where the reaction ends (Bakke et al., 2001; Bakke and Buhaug, 2004; Owens and Clark, 2010).

In a previous study, we found that alongside the formation of the thiadiazine and the dithiazine other by products were formed (Madsen and Søgaard, 2012), which may be some of the

Address correspondence to H. T. Madsen, Department of Biotechnology, Chemistry and Environmental Engineering, Aalborg University, Niels Bohrs Vej 8, 6700 Esbjerg, Denmark. E-mail: htm@bio.aau.dk

Downloaded by [Aalborg University Library], [Henrik Madsen] at 02:16 19 June 2015

unknown compounds that have been detected, but not identified by others (Owens and Clark, 2010). These by-products were identified as 2-(methylidene amino)-ethanol (MAE), 2-(1,3-thiazetidin-3-yl)-ethanol (TYE), and N-methyl-N-(2-oxoethyl)-methaniminium (MOM). MAE and TYE were found to originate from thiadiazine, while MOM could be formed from both TYE and dithiazine. It was suggested that the formation of these compounds occurred via a reaction pathway similar to the general reaction between H_2S and the triazine compounds, where the reaction is initiated by protonation. An interesting feature of this model was that it predicted the formation methanedithiol, which together with dithiazine is capable of explaining the observed dithiazine polymer.

To verify this model of the reaction between triazines and H_2S, we investigated the reaction between a similar triazine, 1,3,5-tri-(2-hydroxypropyl)-hexahydro-s-triazine (HPT), and H_2S. If the previously suggested reaction mechanism is applied on HPT it would be expected to result in compounds with nominal masses of 134 and 88 Da from thiadiazine. The 134 Da compound should further decompose to a compound with a nominal mass of 100, which should also be formed from the dithiazine. The 134 Da compound should be a protonated 1-(1,3-thiazetidin-3-yl)propan-2-ol (TYP), the 88 Da should be protonated 1-(methylideneamino)propan-2-ol (MAP), and the 100 Da should be N-methyl-N-(2-oxopropyl)methaniminium (MOPM) already carrying a positive charge. The predicted reaction system is shown in Figure 1.

METHODS

Materials

1,3,5-tri-(2-hydroxypropyl)-hexahydro-s-triazine was supplied by Schülke & Mayr GmbH. NaHS and HCl (37%) were purchased at Sigma-Aldrich Chemical Co. Demineralized water was produced with a Silex II ion exchanger from SILHORKO.

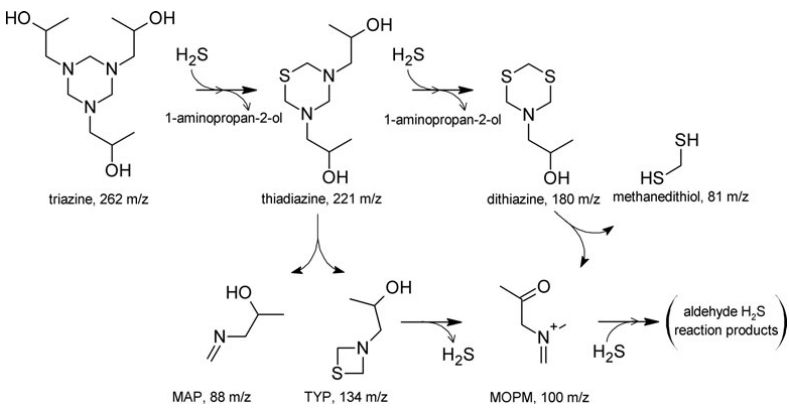

FIGURE 1 Proposed reaction system for H_2S scavenging with 1,3,5-(2-hydroxypropyl)-hexahydro-s-triazine. Compounds are labeled with m/z values for the protonated species, except for MOPM, which already bears a charge.

Downloaded by [Aalborg University Library], [Henrik Madsen] at 02:16 19 June 2015

Study of Reaction Pathway

The triazine solution was filled in a 250 mL gas washing bottle connected to a two-neck pear-shaped boiling flask in which batches of NaHS was stored. A dripping funnel with HCl was attached to the boiling flask, and by letting HCl react with NaHS, H_2S gas was produced and bubbled through the triazine solution. Batches of NaHS were used so that the composition of the triazine could be studied for molar ratios of H_2S to triazine up to 4:1. After each batch a sample of 0.1 mL solution was extracted, diluted 1:10000 in demineralized water and analyzed by ESI-MS equipped with an ion trap, 1100 series LC/MSD Trap (Agilent). The experiment was ended when precipitate formation prohibited extraction of additional samples.

RESULTS AND DISCUSSION

The overall reaction was found to take place as previously reported in literature with the triazine being converted to the thiadiazine and then the dithiazine, see Figure 2. As predicted by the model, peaks are also seen at 134 m/z, 100 m/z, and 88 m/z.

The by products are formed alongside the thiadiazine, and when thiadiazine starts to be consumed, the intensity of the 134 m/z peak decreases simultaneously. The intensity of the 100 m/z peak also decreases, but much less compared to the thiadiazine and the 134 m/z peak, and it may be within the limits of uncertainty. The apparent steady state can be explained by the increasing amount of dithiazine, from which the 100 m/z peak is also predicted to be formed.

Based on these observations it seems that the triazine follows the pathway predicted by the model, which may be generalized as shown in Figure 3.

As the model has only been applied to triazines with hydroxy functionality in their side groups, its validity for other triazines cannot be evaluated. Also since the formation of the by product from

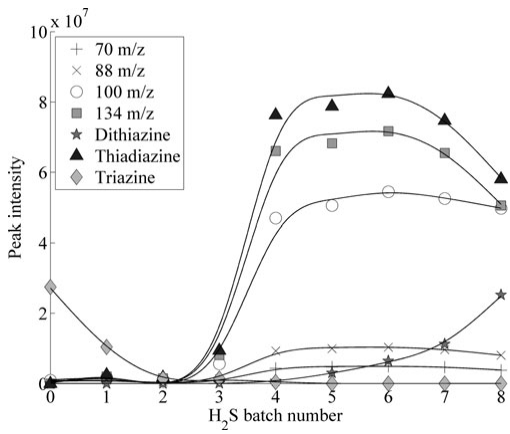

FIGURE 2 Composition of scavenger mixture after reaction with batches of H_2S. The plotted values are intensities from the mass spectra, and can as such not be directly converted to concentrations due to possible differences in sensitivity of the ESI-MS toward each compound.

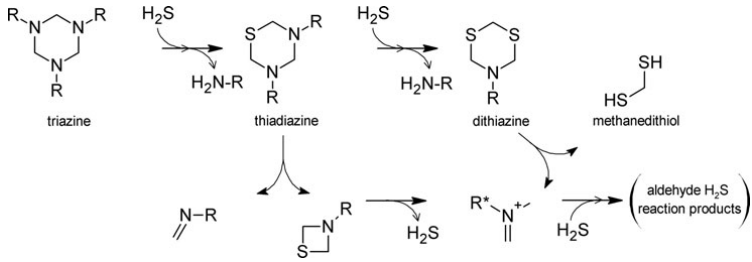

FIGURE 3 Generalized reaction system for the H_2S scavenging with triazines with hydroxy groups containing side groups. R* denotes that the hydroxyl group is rearranged into an oxo group.

the dithiazine involves a reconfiguration of the hydroxy group to an oxo group, the model may be further limited to primary and secondary hydroxy groups. An interesting experiment would be to investigate whether the use of a tertiary hydroxy group would prohibit the formation of the dithiazine by products. This could potentially limit the formation of fouling because methanedithiol is not produced, which is hypothesized to be responsible for the carbon sulfur chains linking the dithiazine polymer (Madsen and Søgaard, 2012; Taylor and Matherly, 2011). Another approach could be to replace the hydroxy groups with oxo groups in the triazine. This could have a similar effect as the use of a tertiary hydroxy group, and would remove the hydroxy functionality of the dithiazine, which has been found to be necessary to obtain the dithiazine polymer (Taylor and Matherly, 2011). However, by removing the hydroxy groups, the chemical properties of the triazines and its reaction products will also be affected. Most notably, the aqueous solubility would be decreased. A decrease in aqueous solubility could enhance precipitation of dithiazine from the aqueous phase and hereby increase the fouling problem. The use of an oxo group would from this perspective seem less attractive compared to using a tertiary hydroxy group.

CONCLUSIONS

The updated model describing the formation Of by products during the reaction between triazines with hydroxy group functionality and H_2S has been confirmed, by use of the triazine 1,3,5-(2-hydroxypropyl)-hexahydro-s-triazine. The model predicts that fouling with dithiazine polymers may be avoided by using triazines with tertiary hydroxy group or by removing the hydroxy group functionality from the triazine.

REFERENCES

Bakke, J. M., and Buhaug J. (2004). Hydrogen sulfide scavenging by 1,3,5-triazinanes. Comparison of the rates of reaction. *Ind. Eng. Chem. Res.* 43:1962–1965.

Bakke, J. M., Buhaug, J., and Riha J. (2001). Hydrolysis of 1,3,5-tris(2-hydroxyethyl)-hexahydro-s-triazine and its reaction with H_2S. *Ind. Eng. Chem. Res.* 40:6051–6054.

Kelland, M. A. (2009). *Production chemicals for the oil and gas industry*. Boca Raton, FL: CRC Press.

Madsen, H. T., and Søgaard, E. G. (2012). Use of ESI-MS to determine reaction pathway for hydrogen sulfide scavenging with 1,3,5-tri-(2-hydroxyethyl)-hexahydro-s-triazine. *Eur. J. Mass Spectrom.* 18:377–383.

Owens, T. R., and Clark, P. D. (2010). Triazine chemistry: Removing H2S and mercaptans. *ASRL Quart. Bull.* 67:1–21.

Taylor, G. N., and Matherly, R. (2011). Structural elucidation of the solid byproduct from the use of 1,3,5-tris(hydroxyalkyl)hexahydro-s-triazine based hydrogen sulfide scavengers. *Ind. Eng. Chem. Res.* 50:735–740.

Downloaded by [Aalborg University Library], [Henrik Madsen] at 02:16 19 June 2015

Paper V

Krzysztof P. Kowalski, Henrik Tækker Madsen and Erik G. Søgaard

Comparison of sand and membrane filtration as non-chemical pre-treatment strategies for pesticide removal with nanofiltration/low pressure reverse osmosis membranes

Water Science and Technology, **14** (2014), 532-539

Reprinted with permission from IWA Publishing

Comparison of sand and membrane filtration as non-chemical pre-treatment strategies for pesticide removal with nanofiltration/low pressure reverse osmosis membranes

Krzysztof P. Kowalski, Henrik T. Madsen and Erik G. Søgaard

ABSTRACT

Pilot plant investigations of sand and membrane filtration (microfiltration (MF)/ultrafiltration (UF)/nanofiltration (NF)/low pressure reverse osmosis (LPRO)) have been performed to treat groundwater polluted with pesticides. The results show that simple treatment, with use of aeration and sand filtration or MF/UF membranes, does not remove pesticides. However, by reducing the content of key foulants, the techniques can be used as a pre-treatment for nanofiltration and low pressure reverse osmosis that has proved to be capable of removing pesticides. It was found that a lower fouling potential could be obtained by using the membranes, but that sand filter was better at removing manganese and dissolved organic matter. The results indicate that combining aeration, sand filtration and membrane techniques might be a good option for pesticide removal without any addition of chemicals and minimized membrane maintenance.

Key words | aeration, fouling, iron, low pressure membranes, nanofiltration, pesticides

Krzysztof P. Kowalski* (corresponding author)
Henrik T. Madsen*
Erik G. Søgaard
Colloid and Interface Chemistry Group (CIChem),
Department of Biotechnology,
Chemistry and Environmental Engineering,
Aalborg University Esbjerg,
Niels Bohrs Vej 8,
6700 Esbjerg,
Denmark
E-mail: *kowalski@bio.aau.dk*

*Co-first authors

INTRODUCTION

Membrane technologies are becoming increasingly popular due to improvements in their robustness and energy efficiency. Continuation of this trend might result in near future replacement of the well-known sand filtration technique with membrane separation. Especially in cases where advanced treatment might be necessary to solve current issues such as groundwater pollution with pesticides compounds the method will be useful. However, any new approach for the water treatment has to comply with existing legislation (Danish Ministry of the Environment 2007), and Danish law limits the usage of the physico-chemical processes used in waterworks, prioritizing only simple water treatment with use of aeration and sand filtration. This strategy results in abandonment of the difficult water sources, like those polluted with pesticides, and to use those where simple treatment can be applied instead. However, there is an increasing awareness of pesticide pollution of groundwater resources used for drinking water, where the pollution has been found to be stable over a period of many years (Søgaard *et al.* 2001; Thorling *et al.* 2010). Because of the enduring pollution, it is necessary to employ a method to remove the pesticide compounds if the groundwater is to be used for drinking water. Today granular activated carbon followed by UV (GAC UV) is the preferred method for removal of pesticides in Denmark, but the use of GAC suffers from problems mainly related to saturation and foot print size (Plakas & Karabelas 2012; Søgaard & Madsen 2013).

A promising technique for removal of pesticides is nanofiltration (NF) and low pressure reverse osmosis (LPRO), which does not result in complete demineralization and operates at lower pressures compared to reverse osmosis (Plakas & Karabelas 2012). The use of NF/LPRO membranes for removal of pesticides is also favorable since it allows for a treatment that does not involve the addition of chemicals, and it can be used in a decentralized drinking water system.

doi: 10.2166/ws.2014.004

However, the concentrations of iron and manganese in groundwater are often high, and if they are not removed, they may precipitate and foul the NF/LPRO membrane. A pre-treatment method for iron removal could be to employ a tandem of aeration and sand filtration, which is used in the conventional treatment of groundwater. Here, ferrous iron is oxidized by help of oxygen from the air and filtrated as iron(III) oxides precipitates in the sand filter (Søgaard *et al.* 2001; Pacini *et al.* 2005).

Another possibility could be replacing sand filtration with low pressure membranes such as microfiltration and ultrafiltration (MF/UF). It has been shown in previous studies that a combination of aeration and microfiltration, where a polymeric polyethersulfone membrane with an absolute porosity 0.2 μm was used, might be adequate for iron removal; however, it required sufficient reaction time and pH adjusted to 8 with the help of sodium hydroxide (Ellis *et al.* 2000).

Another approach that has been studied is the usage of a chemical oxidant, like chlorine to enable fast and efficient iron oxidation prior to UF (Choo *et al.* 2005). The main issue with using MF/UF membranes for filtration of rich iron solutions is that it causes significant problems with fouling, because of the iron precipitation and formation of colloidal iron. This means that the MF/UF membranes require a regular and efficient cleaning process to avoid plugging of the membrane (Soffer *et al.* 2004; Korchef *et al.* 2009). For this reason, the use of ceramic membranes could be a good option. They have higher mechanical stability compared to polymeric membranes enabling the application of high backwash pressure for fouling removal (Hofs *et al.* 2011).

In this study we evaluate conventional and membrane processes for production of drinking water from groundwater, focusing on the pesticides removal. Following the Danish policy, especially its limitations, the treatment processes were performed without any chemical reagent enhancement.

The initial experiments investigated the fate of pesticides during sand filtration and ceramic MF/UF membranes. These experiments were performed to assess whether the current technologies were capable of affecting the pesticides. The main investigations then focused on the use of sand filtration and microfiltration/ultrafiltration as pre-treatment techniques for pesticide removal with NF/LPRO. The two techniques were compared with respect to removal efficiency of compounds responsible for inorganic, organic, particulate and biological fouling. Thus, permeates were examined not only for mineral and organic matter content, but also turbidity, particle size and bacteria removal were determined. Moreover, the unified membrane fouling index (UMFI) (Huang *et al.* 2008) was measured for each permeate since fouling indexes are a typical way of classifying the fouling potential of a given water source.

MATERIALS AND METHODS

Water characterization

The experiments were performed with use of natural groundwater that was acquired from an abandoned drinking water well in Vognsbølparken, Esbjerg, Denmark. Composition of the groundwater can be seen in Table 1. For investigation of manganese and pesticides, the raw groundwater was spiked with manganese(II) ions in form of $MnSO_4 \cdot H_2O$, Sigma Aldrich and a mixture of pesticides that contained atrazine (Pestanal, Fluka), atrazine-d_5 (Pestanal, Fluka), bentazon (Pestanal, Fluka), 2,6-dichlorobenzamide (BAM) (Pestanal, Fluka) and desethyl-desisopropyl-atrazin (DEIA) (Pestanal, Fluka). All pesticides were purchased at Sigma-Aldrich. Methanol and acetonitrile (HPLC grade) and acetone were purchased from VWR. Demineralized water was produced in house with a Silex II ion exchanger from SILHORKO.

Table 1 | Composition of raw groundwater taken from pilot plant for membrane filtration

Parameter	Raw
pH	6.6–6.8
Turbidity [NTU]	3.0–4.0
O_2 [mg/L]	<0.5
Fe total [mg/L]	3.5–4.2
Fe(II) [% of total Fe]	90–100
Ca [mg/L]	35
Mg [mg/L]	3.6
Cl^- [mg/L]	35
SO_4^{2-} [mg/L]	2
UV [Abs at 254 nm]	0.35 ± 0.05

Aeration and sand filtration method

For the investigation of the aeration and sand filtration process, a pilot plant installed at the well site was used. The plant is shown in Figure 1. Aeration was performed with MicroDrop Aqua aeration unit containing open walled cylindrical plastic tubes that like a drizzling filter increases water–air contact surface. For sand filtration a pressurized filter (1 m^3 of quartz sand 0.2–1 mm) was used.

Two procedures were used: continuous flow of groundwater through the system and recirculation of a groundwater batch. The first procedure was used to evaluate the iron and spiked manganese (reaching a concentration of 1.2 mg/L in feed water) removal and turbidity lowering, while the second procedure was used to evaluate the effect on pesticides. In the recirculation procedure 120 L of groundwater was collected in a holding tank where it was spiked with pesticides to obtain a concentration of 2 μg/L. This concentration value was chosen to avoid the pesticides having an effect on the microorganisms in the sand filter, and to avoid saturation. If the pesticides adsorb to the sand filter, saturation may be reached quickly by use of higher concentrations and hereby hide the adsorption effect. Also concentrations in this range are close to what is found in real polluted groundwater. The spiked solution was then allowed to recirculate for 15 minutes for homogenization. Before each experiment, water was allowed to run through the system for 30 minutes to obtain fresh groundwater. Triplicate samples of 1 L were taken at three places: before aeration, after aeration and after sand filter. For each sample pH and dissolved oxygen (DO) was measured.

Aeration and MF/UF method

MF/UF membrane filtration was carried out with four silicon carbide ceramic MF/UF membranes with reported pore sizes: 3, 1, 0.1 and 0.04 μm from CoMeTas (now LiqTech) – system shown in Figure 1. The membranes differs in surface area and geometry; i.e. membranes with pores sizes of 3 and 1 μm membrane had area of 0.09 m^2

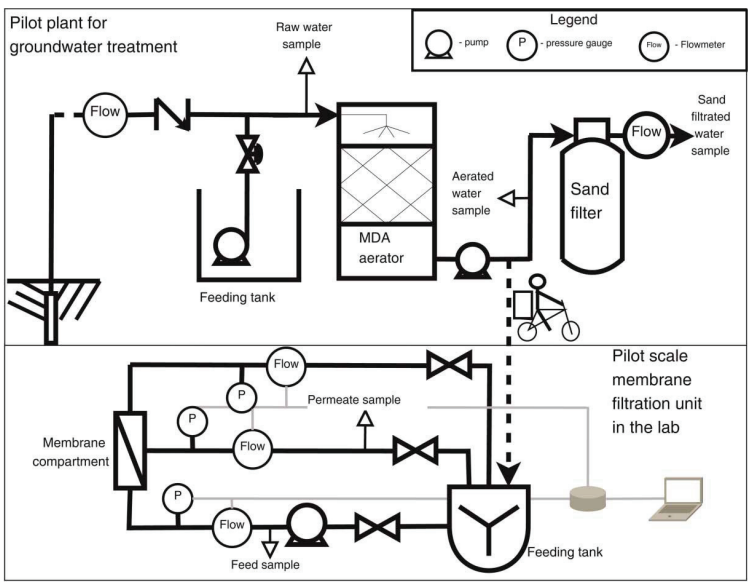

Figure 1 | Pilot plant scheme for groundwater treatment.

and 31 channels and those with pores sizes of 0.1 and 0.04 μm had an area of 0.05 m^2 and 19 channels.

For experimental purposes 100 L of aerated groundwater was collected at the pilot plant and transported to the membrane filtration unit. Pesticide removal was investigated by spiking pesticide mixture to the feed water to obtain a concentration of 2 μg/L, and the filtration was performed for each membrane separately with a transmembrane pressure between 200 and 300 mbar in a recirculated cross-flow mode. Two samples of 400 mL were taken from the feed, retentate and the permeate. Flow and pressure were measured for each stream, and was used to monitor the degree of fouling on the membranes. To clean the membranes, a 3 bar back flush was used. To evaluate the efficiency of the filtration, particle size distribution was determined before and after filtration.

Nanofiltration method

Nanofiltration and low pressure osmoses were investigated with a DDS Lab-Unit 20 equipped with two commercial membranes: NF 99 HF from Alfa Laval, Nakskov, Denmark and NF90 from Dow chemicals. The NF99HF is a classic NF membrane that shows selective removal of divalent ions, whereas the NF90 membrane is characterized as a tight NF membrane, which might also be classified as a LPRO membrane. The nanofiltration experiments were conducted by first recirculating distilled water through the system for 30 minutes at 10 bars to clean and compress the membranes. Then the distilled water was replaced by 4 L of pesticide solution with 1 mg/L concentration. Concentrations of 1 mg/L were chosen to avoid solid phase extraction as a preanalytical method and thereby increase the variance of the results. The use of pesticide concentrations of this value is standard in membrane filtration experiments and is not expected to influence the true rejection. Before samples were collected, the filtration system was allowed to run for 1 hour to ensure that adsorption to membranes and equipment would not influence the results. After 1 hour of recirculation triplicate samples were extracted over a 10 minute period and transferred directly to vials for analysis. The filtration was run at 25 °C, 10 bars, flow of 8 L/min and a total membrane area of 59 cm^2. Because only small samples were extracted, the recovery was low and the concentration of the solution would not affect rejection.

Analytical methods

From the primary sample were taken 40 mL for sample digestion together with nitric acid in an autoclave (30 minutes at 120 °C). The prepared samples were analyzed by use of inductively coupled plasma atomic emission spectroscopy (ICP-AES) (Perkin Elmer Optima 3000 DV) for content of Fe, Mn, Ca and Mg all with a detection limit of 0.1 mg/L.

Pesticides were analyzed with a solid phase extraction (SPE) high-performance liquid chromatography/electrospray ionization mass spectrometry (HPLC/ESI-MS) method. The procedure for the solid phase extraction was: activation of column with 6 mL methanol, equilibration with 6 mL of demineralized water, application of 500 mL of sample on column, elution of interferences with 6 mL demineralized water, vacuum drying of column for 30 minutes, elution of analytes with 10 mL acetone, evaporation of acetone at 70 °C and dissolution in 0.5 mL acetonitrile spiked with 0.1 mg/L internal standard (atrazine-d_5). For solid phase extraction, TELOS ENV 200 mg/6 mL was used. The HPLC method was specific for each pesticide. For atrazine, BAM and bentazon an eluent of methanol (A) and 5 mM ammonium acetate pH 3, adjusted with formic acid (B) was used, while for DEIA the pH was set to 6.5. For atrazine, BAM and DEIA an eluent mixture of 70/30 A/B was used, while for bentazon a 65/35 mixture was used. A ZORBAX Eclipse Plus C18, 3.5 μm, column was used. On the ESI-MS, the nebulizer pressure was set at 40 psi, the nebulizer flow at 9 L/min and the dry temperature at 350 °C.

pH was measured by Meter Lab PHM 250 pH meter (Radiometer Analytical) and oxygen with OxyMeter (Oxyguard Handy MK II) in the freshly collected samples. The Merck photometric methods were implemented to determine the following: iron speciation (Fe(II) and Fe total) with method no. 1.00796.0001, chloride ions with method no. 1.14730.0001 and sulphate with method no. 1.14548.0001. Turbidity was measured with the compact AQUALYTIC® infrared turbidity meter.

Particle size was determined by help of a PhotoCor dynamic light scattering (DLS) instrument that was used to gather light scattering data. Bacteria count was performed according to the Danish Standard 2251:1983, where collected sterile samples were cultivated for 7 days with agar (DS 2251:1983 1983-01-01).

Unified membrane fouling index

To obtain an overall indication of the effectiveness of sand filtration and MF/UF membranes for reducing the fouling potential, the UMFI, based on Hermia's model (Huang *et al.* 2008), was applied. In this model fouling is often assumed to be purely due to cake filtration, in which case the UMFI can be obtained from the slope of a linear relationship between experimentally obtained specific flux, J_s', and cumulative permeate volume, V_s:

$$\frac{1}{J_s'} = 1 + (\mathrm{UMFI})V_s$$

where J_s' is dimensionless normalized specific flux, equal to 1/TMP′ and TMP′ is normalized transmembrane pressure $\mathrm{TMP}_t/\mathrm{TMP}_0$; V_s is the permeate throughput defined as the cumulative volume of permeate per membrane surface area ($\mathrm{L/m^2}$).

The model was applied for constant pressure (2 bar) dead-end filtration test using a 0.04 my cellulose filter with area of 0.00096 $\mathrm{m^2}$.

RESULTS AND DISCUSSION

Removal of pesticides

Based on the pore size of sand filters and MF/UF membranes, it is not expected to be able to remove pesticides. However, several factors could influence the fate of pesticides through these processes and hereby affect the level of pesticides. It is possible that some of the pesticides are removed together with the iron oxides. This could happen through adsorption to the iron oxide colloids, which would lead to co-precipitation of the pesticides. Another possibility is that the enhanced aeration by help of the MicroDrop system could lead to stripping off some of the pesticides, especially the smaller ones such as DEIA and BAM, similar to that known to occur for smaller chlorinated solvents. Finally, it could be possible that the microorganisms in the sand filter would be able to metabolize some of the pesticides.

As seen in Figure 2, no change in pesticide concentration was observed during aeration, sand filtration or the MF/UF membranes. The observed differences are explained by the combined variance of the sampling, SPE and instrumental procedure. Neither sand filtration nor MF/UF processes can as such be expected to affect pesticide concentrations. Instead the two polymeric membranes were found to be capable of removing the pesticides. For the two larger pesticides, atrazine and bentazon, the NF membrane is sufficient, whereas to remove the two smaller pesticides, BAM and DEIA, a tight NF or LPRO membrane is necessary. The results show that in a removal procedure of pesticides in water, sand filtration and/or MF/UF membranes are better used as pre-treatment techniques for the NF/LPRO processes.

Pre-treatment of groundwater

To evaluate the suitability of the four ceramic membranes and the sand filtration process as pre-treatment techniques for subsequent NF/LPRO process, they were compared on

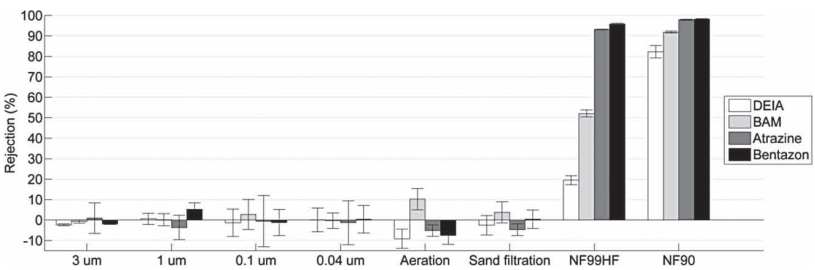

Figure 2 | Comparison of the removal of pesticides by ceramic MF/UF, aeration, sand filtration and NF/LPRO membranes. Data points represent the average of the collected samples plotted with error bars indicating the standard deviation of the measurements.

their ability to reduce inorganic, organic, particulate and biological fouling potentials. Properties of groundwater samples collected before and after the different processes are presented in Figure 3. For filtration purposes aerated groundwater was used, where DO content was higher (9.5 mg/L) resulting in differences between values of some factors from raw groundwater presented in Table 1.

With respect to the inorganic fouling potential, the sand filter and the ceramic membranes were evaluated on their ability to remove iron and manganese. Concerning the removal of iron, the sand filter is found to outperform the two MF membranes, while the UF membranes are able to remove slightly more iron than the sand filter. None of the membranes were found to remove manganese, but the sand filter was found to reduce it from 1.2 to 0.06 mg/L. This points at a difference in the removal mechanism for the two pre-treatment methods. Membrane filtration operates in the principle of size exclusion, and as such it was anticipated that iron removal efficiency would be correlated with membrane pore size. Unexpectedly, MF with 3 μm pore size was found to give higher iron removal than MF with 1 μm pore size. This finding was confirmed in several repeated experiments with two different membrane units of the same type. It is possible that the pore size reported by the producer was not correct, which would explain why the 3 μm membrane was found to be consistently better on all parameters compared to the 1 μm membrane. Other possible explanations could also be internal pore blocking of the 3 my membrane or difference in the pore size distribution of the two membranes. The specific underlying reason was not investigated in this study. Removal of iron and manganese in a sand filter is based on precipitations rather than size exclusion. Sand filtration enables autocatalytic processes involving precipitated iron hydroxides on the sand media surfaces, which results in much faster iron oxidation and precipitation compared to its rate of oxidation in an aerated water solution of iron(II) (Davison & Seed 1983; Geroni & Sapsford 2011). Furthermore, the effect of naturally occurring iron and manganese oxidizing bacteria cannot be neglected. For example by help of the iron oxidizing bacteria *Gallionella ferruginea* that was also found to grew uninhibited and perform biological iron oxidation in partly oxygen-saturated natural water in circumneutral pH range (Søgaard *et al.* 2001; Pacini *et al.* 2005; de Vet *et al.* 2011). The fact that a large part of the oxidation of iron and manganese occurs in the sand filter, gives the

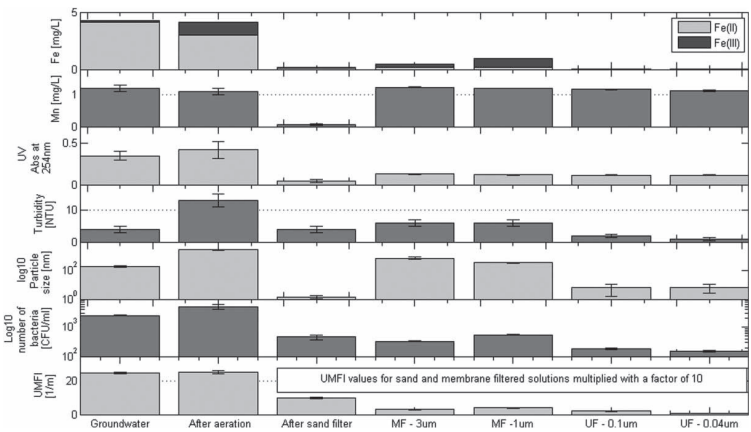

Figure 3 | Quality of effluents collected after different stage of groundwater treatment (presented results for solution after aeration correspond to feed water used in MF and UF); membrane filtration was performed with TMP of 200 mbar in cross-flow mode, values are averages of the collected samples and the error bars represent the variance of the measurements from duplicate samples collected from the same experimental set.

sand filter an advantage over membrane filtration, that require pre-oxidation and particulate matter formation to occur prior to filtration (Ellis *et al.* 2000).

The fouling potential of organic matter was evaluated by measuring the UV absorption at 254 nm. Here the sand filter was found to result in a higher removal level compared to all four membranes, which were found to give equal removals. The fact that the membranes give the same content of organic matter in their permeates indicates that the organic compounds that permeates are smaller than the pore size of the membranes. The removal of natural organic matter (NOM) in the sand filter could be because of biological activity, where microorganisms are capable of metabolizing part of the organic matter. Moreover, the diverse efficiency of iron removal could have impacted organic matter removal, as it was suggested in other studies indicating that the precipitated iron can play a part in removing NOM from water by sorption (Choo *et al.* 2005).

The two ceramic UF membranes were found to give the highest reduction in turbidity, while the sand filter gave a slightly higher reduction compared to the MF membranes. When comparing the average particle size, it is seen that the smallest particles are found in the sand filter permeate. The difference between turbidity and particle size performance, even though the fact that the both factors refer to particulate matter, might be caused by the fact that the DLS device measures average particle size and not their quantity. Moreover, iron removal efficiency corresponds to the particle size found in permeates, which suggest that the colloidal iron was an important part of particle size results.

To assess the biological fouling potential, the number of colony forming units (CFUs) was measured before and after filtration. The membranes gave higher reductions in the number of CFUs compared to the sand filter, but none of them were found to completely remove the microorganisms in the groundwater. This is a clear indication that the labelled pore sizes of these membranes may not be correct, or that the pore size distribution is relatively large since membranes with pore sizes below 0.2 μm should ensure a complete removal of CFUs (Bobbitt & Betts 1992; Hagen 1998; Hofs *et al.* 2011). In a previous study, the pore size of the used 0.04 μm membrane was determined with porometry to be 0.96 μm (Hofs *et al.* 2011). In general though, membranes will be better than sand filters at reducing biological fouling. The sand filter is in part a biological process, and microorganisms from the sand filter may detach from the sand filter, and end up in the permeate.

The UMFI ranged from 0.07 m^{-1} for the 0.04 μm permeate to 1.0 m^{-1} for the sand filter permeate. The UMFI was obtained for permeates from experiments with a Mn-spiked solution. The difference between UMFI values seems to be correlated to the CFU counts and the turbidity, which indicates that biological and particulate fouling are the main causes of the measured UMFI values.

The UMFI values may be considered as the overall indicator of the fouling potential, and based on these values, the 0.04 μm should be considered as the best pre-treatment method. However, this view may be too simplified. The analyses show that the sand filter and the membranes both have strengths and weaknesses. The sand filter is good at removing iron, manganese and organic matter, but ineffective in removal of particulate and biological matter. The membranes can obtain high removals of iron, particles and microorganisms, but dissolved matter and particles below the pore size of the membranes will not be removed. This should be considered when choosing a pre-treatment strategy. If the groundwater is low in organic matter and manganese, aeration and a UF membrane system will be sufficient, but if the content of dissolved organic matter and manganese is high, a combination of aeration, sand filtration and UF membranes may be the best choice for a pre-treatment strategy.

CONCLUSIONS

Aeration and sand filtration/MF/UF membranes were found to be unable of removing pesticides from polluted groundwater, and these techniques should instead be used as pre-treatment methods for subsequent NF/LPRO treatments. Sand filtration was found to be effective at removing iron, manganese and dissolved organic matter, whereas its effect on particulate and biological matter was found to be limited. Ceramic UF membranes were found to be effective at removing iron, particulate and biological matter, but unable to remove manganese and dissolved organic matter.

The results indicate that the main cause of fouling in groundwater might be iron, biological and particulate matter that was found to be correlated with the UMFI of sand filtrated permeate.

The lowest UMFI was obtained by the use of the UF membrane with the smallest pore size (0.04 μm) used in this study, and is the most promising pre-treatment technique. However, in cases with high concentrations of dissolved organic matter and manganese, a serial combination of aeration, sand filtration and ultrafiltration may be the best choice.

REFERENCES

Bobbitt, J. A. & Betts, R. P. 1992 The removal of bacteria from solutions by membrane filtration. *J. Microbiol. Methods* **16** (3), 215–220.

Choo, K., Lee, H. & Choi, S. 2005 Iron and manganese removal and membrane fouling during UF in conjunction with prechlorination for drinking water treatment. *J. Membr. Sci.* **267** (1–2), 18–26.

Danish Ministry of the Environment 2007 Executive order no. 1451, Executive order for water extraction and waterworks.

Davison, W. & Seed, G. 1983 The kinetics of the oxidation of ferrous iron in synthetic and natural waters. *Geochim. Cosmochim. Acta* **47** (1), 67–79.

de Vet, W. W. J. M., Dinkla, I. J. T., Rietveld, L. C. & van Loosdrecht, M. C. M. 2011 Biological iron oxidation by *Gallionella* spp. in drinking water production under fully aerated conditions. *Water Res.* **45** (17), 5389–5398.

DS 2251 1983 (1983-01-01). Water quality – Determination of aerobic total viable count at 21 centigrade. Danish Standard 2251:1983.

Ellis, D., Bouchard, C. & Lantagne, G. 2000 Removal of iron and manganese from groundwater by oxidation and microfiltration. *Desalination* **130** (3), 255–264.

Geroni, J. N. & Sapsford, D. J. 2011 Kinetics of iron (II) oxidation determined in the field. *Appl. Geochem.* **26** (8), 1452–1457.

Hagen, K. 1998 Removal of particles, bacteria and parasites with ultrafiltration for drinking water treatment. *Desalination* **119** (1–3), 85–91.

Hofs, B., Ogier, J., Vries, D., Beerendonk, E. F. & Cornelissen, E. R. 2011 Comparison of ceramic and polymeric membrane permeability and fouling using surface water. *Separat. Purif. Technol.* **79** (3), 365–374.

Huang, H., Young, T. A. & Jacangelo, J. G. 2008 Unified membrane fouling index for low pressure membrane filtration of natural waters: Principles and methodology. *Environ. Sci. Technol.* **42** (3), 714–720.

Korchef, A., Kerkeni, I., Amor, M. B., Galland, S. & Persin, F. 2009 Iron removal from aqueous solution by oxidation, precipitation and ultrafiltration. *Desalination Water Treat.* **9** (1–3), 1–8.

Pacini, V. A., Ingallinella, A. M. & Sanguinetti, G. 2005 Removal of iron and manganese using biological roughing up flow filtration technology. *Water Res.* **39** (18), 4463–4475.

Plakas, K. V. & Karabelas, A. J. 2012 Removal of pesticides from water by NF and RO membranes – A review. *Desalination* **287**, 255–265.

Soffer, Y., Adin, A. & Gilron, J. 2004 Threshold flux in fouling of UF membranes by colloidal iron. *Desalination* **161** (3), 207–221.

Søgaard, E. G. & Madsen, H. T. 2013 Groundwater chemistry and treatment: application to Danish waterworks. In: *Water Treatment*, Dr Walid Elshorbagy (ed.). InTech, DOI: 10.5772/54166. Available from: http://www.intechopen.com/books/water-treatment/groundwater-chemistry-and-treatment-application-to-danish-waterworks.

Søgaard, E. G., Aruna, R., Abraham-Peskir, J. & Bender Koch, C. 2001 Conditions for biological precipitation of iron by *Gallionella ferruginea* in a slightly polluted ground water. *Appl. Geochem.* **16** (9–10), 1129–1137.

Thorling, L., Hansen, B., Langtofte, C., Brüsch, W., Møller, W. W. & Mielby, S. 2010 Grundvand Status og udvikling 1989–2009. Technical Report. Geological Survey of Denmark and Greenland, Copenhagen, Denmark.

First received 23 September 2013; accepted in revised form 20 January 2014. Available online 31 January 2014

Paper VI

Henrik Tækker Madsen and Erik G. Søgaard

Applicability and modelling of nanofiltration and reverse osmosis for remediation of groundwater polluted with pesticides and pesticide transformation products

Separation and Purification Technology, **125** (2014), 111-119

Reprinted with permission from Elsevier

Separation and Purification Technology 125 (2014) 111–119

Contents lists available at ScienceDirect

Separation and Purification Technology

journal homepage: www.elsevier.com/locate/seppur

Applicability and modelling of nanofiltration and reverse osmosis for remediation of groundwater polluted with pesticides and pesticide transformation products

Henrik T. Madsen *, Erik G. Søgaard

Department of Biotechnology, Chemistry and Environmental Technology, Aalborg University, Esbjerg, Denmark

ARTICLE INFO

Article history:
Received 3 November 2013
Received in revised form 17 January 2014
Accepted 23 January 2014
Available online 3 February 2014

Keywords:
Pesticide
Pesticide transformation product
Groundwater
Nanofiltration
Steric modelling

ABSTRACT

The main body of research on pesticide removal with membranes has looked at pesticides used for pest control, but during transport from surface to groundwater aquifers, pesticides are transformed. Therefore the real polluting compounds are often transformation products, and this vastly increases the total number of pollutants in need of treatment, which also creates a need for a simple way of predicting expected rejections to avoid the daunting task of investigating all these experimentally. In this study, the applicability of NF/LPRO/RO membranes for treatment of groundwater polluted with some of these key transformation products is assessed experimentally and compared to that of regular pesticides. Also, it was investigated whether the rejection could be modelled with a simple steric model. It was found that NF membranes capable of rejecting the regular pesticides did not give satisfactory rejections of the transformation products, mainly because of the reduced size of these. Further, the rejection could be described with a pore flow model, but different definitions of the molecular width were needed to describe rejection for NF and LPRO/RO membranes. With the model it was predicted that rejections over 90% can be obtained with an LPRO membrane for most pesticides and transformation products found in Danish groundwater.

© 2014 Elsevier B.V. All rights reserved.

1. Introduction

Pesticide pollution of surface and groundwater resources is an increasing problem in many parts of the world [1]. In Denmark almost the entire drinking water production is based on groundwater of which 44% has been found to be contaminated with pesticides [2], and it is estimated that between the years 1999 and 2009, pesticides have resulted in the abandonment of around 130 drinking water wells per year [3]. The research on pesticide removal is extensive, and traditionally the focus has been on the pesticides actually used for pest control, but for groundwater pollution this choice may be misguided. During percolation from surface to aquifer, pesticides are often transformed, and the compounds found in real groundwater are therefore different from the pesticides that dominate literature. These new compounds are called pesticide transformation products (PTPs), and for Danish groundwater they represent the largest part of the pesticide pollution [4].

Traditional Danish drinking water treatment consists of aeration and rapid sand filtration, which has been found to have no effect on pesticides and PTPs [5]. Therefore, activated carbon filtration is applied in cases where it has not been possible to find new unpolluted aquifers [6]. Activated carbon is generally an efficient method for removal of organic micropollutants, but it also suffers from a number of problems mainly related to saturation, foot print size and difficulties in removing small polar compounds [1]. An alternative to activated carbon is the use of nanofiltration (NF) and low pressure reverse osmosis (LPRO) membranes.

NF and LPRO membranes have been found to be an effective method for removal of pesticides, although the specific rejection of the pesticides is highly dependent on both membrane and pesticide characteristics [1,7,8]. In general size exclusion has been found to be the most important parameter determining rejection of pesticides, which has been seen from correlations between measured rejection values and molecular weight of the pesticides [1,9–11]. However, it has also been found that the rejection of pesticides is higher in real waters compared to distilled water [11], and that the presence of divalent ions (Ca^{2+}) [10,12] and specific types of organic matter [13] may impact the rejection. Other factors such as the dipole moment of the pesticides [14], relative hydrophilicity/

* Corresponding author. Address: Department of Biotechnology, Chemistry and Environmental Engineering, Aalborg University, Niels Bohrs Vej 8, Esbjerg 6700, Denmark. Tel.: +45 20960733.

E-mail address: htm@bio.aau.dk (H.T. Madsen).

http://dx.doi.org/10.1016/j.seppur.2014.01.038
1383-5866/© 2014 Elsevier B.V. All rights reserved.

hydrophobicity [15,16] and charge [17] have also been found to affect rejection, adding to the complexity. From an engineering point of view, it would very advantageous if rejections could be approximated reasonably well by assuming only steric effects because this would then only require knowledge of the size of the pesticides/PTPs and the pore size of the membrane; both of which are readily available. Studies have shown that under ideal conditions (laboratory grade water, low solute/membrane interaction, low solute dipole moment), steric models can be used to achieve acceptable results for rejection of organic molecules by NF membranes, even with simple models assuming cylindrical pores with the same pore size such as the steric hindrance pore model [18]. Recently Kiso et al. proposed a steric pore flow model based on geometrical parameters of the solutes to predict rejections, and found this model to be very successful compared to the use of molecular weight [19,20]. The model was however applied to hydrophilic alcohol compounds of relatively simple geometry that should not interact significantly with the membrane surface. Whether the same model can be used for pesticides/PTPs have not been investigated.

In this study we attempted to evaluate the applicability of membrane filtration for treatment of groundwater polluted with not only pesticides, but also PTPs. This was done by selecting two pesticides: atrazine and bentazon and two PTPs: BAM and DEIA. DEIA is a transformation product of atrazine and the pesticide/PTP pair could as such be used to directly investigate the effect of the transformation process on the applicability of the membranes. BAM and bentazon represented pollutants for which the expected rejection was important to determine. The possibility of using a purely steric model to calculate the rejections was investigated by applying the model of Kiso et al. [19]. To verify the use of the model, the fitted pore sizes were subsequently used to calculate rejection values of two other pesticides, prometryn and isoproturon, that has been investigated in a separate study. Furthermore, to give an evaluation of the overall applicability of the investigated membranes to treat any polluted groundwater, predictions were made on the rejection of the remaining pesticides and PTPs included in the Danish groundwater monitoring program. Finally, the effect of groundwater on the rejection was investigated by comparing the results from the model with measurements of streaming potential and pesticide/ion-pair formation.

2. Experimental work

2.1. Materials and methods

2.1.1. Pesticides

Two pesticides and two PTPs were used in the experiments: atrazine, bentazon, 2,6-dichlorobenzamide (BAM) and desethyl-desisopropyl-atrazine (DEIA): BAM and DEIA are PTPs of the pesticides dichlobenil and atrazine. All were purchased at Sigma–Aldrich (Pestanal, Fluka).

The pesticides and PTPs were chosen based on their occurrence in Danish groundwater samples. BAM and DEIA are the two main polluting compounds, with BAM being found in 18.8–20.2% and DEIA in 11.0–16.1% of the groundwater analyses [4]. Of the pesticides still in use, bentazon is the one found in the largest amount of groundwater samples, 3.4–4.9% [4]. Atrazine was banned for use in 1994, but it is still found in 5.2% of the groundwater samples [2]. It is also one of the most studied pesticides in literature. In an overview of membrane/pesticide studies presented by Karabelas and Plakas [21], atrazine accounted for 23.9% of the total sum of pesticides used in the experiments. Given its widespread use in scientific work, atrazine is used to link this study to former studies.

Data for the four compounds are presented in Table 1. The amount of data on these compounds is scarce, and the values often originate from isolated studies that have not been confirmed, which lead to some contradictory values. Based on the log $K_{o/w}$ values for bentazon and BAM, bentazon would be expected to have the highest aqueous solubility, but the reported solubilities give BAM the highest aqueous solubility. The p*K*a values are also often reported for protonated species, without that being properly indicated. The applicability of these data may as such be questioned. The geometric parameters have been determined with the method described in Section 2.4. Width and height are defined here as the side lengths of the rectangle enclosing the molecule perpendicular to its length axis with height being taken as the longest side.

2.1.2. Groundwater samples

Groundwater was acquired from two waterworks: Astrup (south-west Jutland, Esbjerg, Denmark) and Hvidovre (East Zealand, Copenhagen, Denmark). These two groundwaters represent minimum and maximum values of hardness and total ionic concentration that can be encountered in Denmark, as seen from the compositions listed in Table 2. Both waters are also characterised by a low content of organics, which may be considered a best case scenario since it lowers the effect that NOM might have on the measured rejections.

Demineralised water was produced in house with a Silex II ion exchanger from SILHORKO, and used as a reference water type.

2.1.3. Membranes

Five different membranes were used in the experiments: NF90, XLE, BW30 (Dow Chemicals), NF99 and NF99HF (Alfa Laval). NF90 has been used in previous studies [12,13,27], and is classified as a tight NF membrane. XLE is characterised as an extra low energy reverse osmosis membrane, and BW30 as a loose reverse osmosis membrane. The two Alfa Laval membranes are NF membranes

Table 1
Properties of the pesticides used in this study.

	Atrazine	Bentazon	BAM	DEIA
Chemical structure	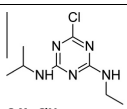	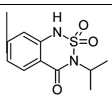		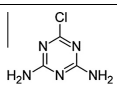
Formula	$C_8H_{14}ClN_5$	$C_{10}H_{12}N_2O_3S$	$C_7H_5Cl_2NO$	$C_3H_4ClN_5$
Molecular weight (Da)	215.69	240.28	190.028	145.55
Length (Å)	13.76	11.98	9.200	8.595
Width (Å)	6.267	7.493	5.784	3.950
Height (Å)	8.752	8.378	9.042	8.060
Log K_{ow}	2.68 [13]	−0.46 [22]	0.77 [23]	−0.1 [24]
Aqueous solubility (mg/L) 20 °C	33 [22]	570 [22]	2730 [25]	66 [24]
p*K*a	1.7 [12]	3.3 [22]	13–14 [26]	–

Table 2
Compositions of groundwaters used in experiments.

Parameter	Astrup	Hvidovre
Ca^{2+} (mg/L)	37.1	180
Mg^{2+} (mg/L)	5.53	29
Na^{+} (mg/L)	16.2	63
K^{+} (mg/L)	1.66	6.3
Cl^{-} (mg/L)	38.0	150
SO_4^{2-} (mg/L)	58.6	140
HCO_3^{-} (mg/L)	82.7	409
pH	7.6	7.2
C_{total} (mM)	4.9	21
TOC (mg/L)	<1	<1
UV_{254} (cm^{-1})	0.005	0.030

where NF99HF is claimed to be more permeable to divalent ions compared to NF99. In this way the membranes span the spectrum from NF to RO, which may be necessary to obtain sufficient rejection.

The membranes were found to have rejection values (%) of minerals as shown in Table 3. All membranes show a higher rejection of divalent ions relative to monovalent ions, with the difference being most pronounced for the two NF membranes. It can also be seen that the NF99 membrane is more selective towards divalent ions compared to the NF99HF membrane. The NF90 and XLE membranes are classified as being between NF and RO membranes, but the difference in rejection of divalent and monovalent ions is small, and close to the rejection values obtained with the RO membrane, BW30. From their mineral rejection it could seem as if NF90 and XLE should be considered RO membranes.

A clearer distinction between the NF90/XLE and BW30 can be seen by comparing the flux data. The NF90/XLE membranes have significantly higher fluxes compared to BW30, and may as such be classified as LPRO membranes. The membranes also differ in hydrophilicity/hydrophobicity with the polyamide membranes having the highest contact angles.

2.2. Filtration protocol

Filtration was performed with a DDS Lab-Unit M20 (Alfa Laval, Nakskov, Denmark) of which a schematic illustration can be seen in Fig. 1. The filtration unit uses flat sheet membranes stacked as membrane plates in between two stainless steel AISI 316 flanges that via a hydraulic system compress the membrane plate stack. Each membrane plate consists of two 29.5 cm^2 membrane sheets clamped around a permeate collection plate. Additional membrane plates can be used to increase the total membrane area, but in this study only one membrane plate was used, giving a total membrane area of 59 cm^2. In experiments 4 L 1 mg/L pesticide solution was prepared and recirculated through the system for one hour at operating conditions before samples were extracted. This was done to allow the system to reach a steady state in which adsorption of the pesticides to membranes and the filtration equipment would not influence the result. In an initial investigation the concentrations in the feed mixture and permeate were found to be stable after 10 min of filtration, but one hour was chosen to also accommodate for compression of the membrane and complete homogenization of the solution. During this first hour both permeate and concentrate streams were returned to the feed tank. The pump delivered a flow rate of 8 L/min, which could not be controlled. This high flow rate is designed to reduce concentration polarization as much as possible. In all experiments the temperature was kept constant at 25 °C, and the applied pressure set to 10 bar. Over a period of ten minutes three samples were extracted for feed and permeate. Feed samples were extracted directly to HPLC vials, while 20 mL was extracted for the permeate samples. The size of the samples resulted in a very small recovery of only 1.5%, which removed effects of concentrating the solution on the measured rejection values.

Table 3
Mineral rejection (%) data for the five membranes used in the study. Pure water flux is measured at a TMP of 10 bar.

	NF99HF	NF99	NF90	XLE	BW30
Ca^{2+}	69.0	74.0	98.5	97.2	98.5
Mg^{2+}	71.2	84.0	96.5	95.8	96.1
Na^{+}	53.0	45.9	91.1	91.8	93.7
K^{+}	52.1	44.1	90.2	90.2	90.9
SO_4^{2-}	88.8	94.3	97.7	97.0	97.5
Cl^{-}	41.3	40.5	94.4	94.2	95.2
HCO_3^{-}	63.5	69.4	95.1	93.3	95.9
Pure water flux ($L\ h^{-1}\ m^{-2}$)	60.4	44.3	36.9	38.3	19.9
Contact angle	<20	23.9 ± 1.6	96 ± 3.0	112 ± 1.7	66 ± 3.8
Material*	PIP	PIP	PA	PA	PA

* PIP = polypiperazine, PA = polyamide

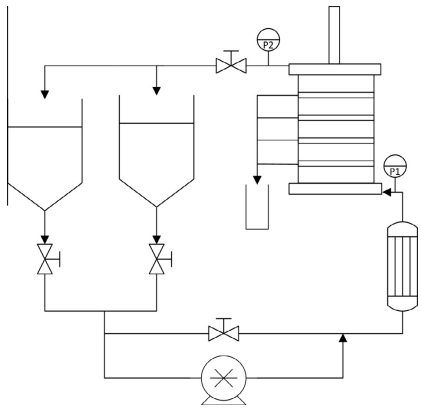

Fig. 1. Schematic drawing of the filtration system used in the experiments. The pump is a Rannie piston pump and the heat exchanger before the membrane stack is operated in counter flow. Permeate pressure is equal to the room pressure and TMP is therefore controlled with the back pressure valve on the concentrate stream. The system is equipped with holding tanks allowing for operation with different amounts of solution or collection of a side stream is desired. This can be controlled with the two valves placed beneath the two holding tanks. The valve placed above the pump in the schematic drawing allows for a by-pass of the pump, which is used during start-up to facilitate a slow increase in pressure. Pressure is measured at the inlet (P1) and outlet (P2) of the membrane stack.

2.3. Methods of analysis

Pesticide samples were analysed with a HPLC/ESI-MS (1260 Infinity and 1100 series LC/MSD Trap, Agilent Technology) method, equipped with a ZORBAX Eclipse Plus C18, 3.5 μm, column and using eluent mixtures of methanol (A) and 5 mM ammonium acetate (B). For atrazine, BAM and bentazon the pH in B was adjusted to 3 with formic acid, while for DEIA the pH was set to 6.5 [28]. For atrazine, BAM and DEIA an eluent mixture of 70/30 A/B was used, while for bentazon a 65/35 mixture was used. On the ESI-MS, the nebuliser pressure was set to 40 psi, the nebuliser flow to 9 L/min and the dry gas temperature to 350 °C.

For the permeate samples with concentrations below 0.1 mg/L a solid phase extraction procedure, with TELOS ENV 200 mg/6 mL

columns, was employed to concentrate the samples. The procedure for the solid phase extraction was: activation of column with 6 mL methanol, equilibration with 6 mL of demineralised water, application of 20 mL of sample on column, elution of interferences with 6 mL demineralised water, vacuum drying of column for 30 min, elution of analytes with 10 mL acetone, evaporation of acetone at 70 °C and dissolution in 1 mL acetonitrile. Methanol and acetonitrile (HPLC grade), formic acid (98–100%) and acetone were purchased from VWR.

For direct analysis on the electrospray ionization mass spectrometer (ESI-MS), 0.5 mL sample was injected with a syringe pump with the ESI-MS set to the same configuration as for HPLC/ESI–MS.

Macro ions were analysed with ICP (Optima 3000 DV, Perkin Elmer), IC (820 IC Separation Center, Metrohm) and autotitration. ICP was used to analysis for Ca, Mg, K and Na, IC was used to analysis for Cl^- and SO_4^{2-}, and HCO_3^- was determined by autotitration.

Zeta potential (ZetaCAD, CAD Instruments) was determined by measuring streaming potential between a membrane and a specific water type. A ZC10500 cell, where the flow is perpendicular to the membrane surface, was used for measurement of streaming potential in the pores. Contact angle (DSA 100, KRÜSS) was used to estimate hydrophobicity of the membranes.

2.4. Modelling with steric pore flow model

To investigate whether the rejection can be modelled as steric hindrance, the method described by Kiso et al. [19] was used. Since the model is described in detail in the before mentioned papers, we will not present the complete mathematical background here, but instead refer to the papers. In this model, a pore flow approach is used to describe the rejection, under the assumption that only steric effects contribute to rejection. The general principle behind the calculation method of the model is to use measured rejections to find the pore radius that gives the smallest variation between the measured and calculated rejections. By plotting the calculated rejections (R_c) against the measured rejections (R_m), the goodness of the fit can be evaluated, and if a high correlation is obtained, it is an indication that the rejection can be calculated from the molecular geometry of the pesticides. Rejection values are calculated with Eq. (1).

$$R_{cal} = 1 - \frac{C_p}{C_f} = 1 - \frac{\Phi K_c}{1 - (1 - \Phi K_c)\exp(-\mathrm{Pe})} \quad (1)$$

where C_p and C_f are permeat and feed concentration, respectively; K_c is the solute hindrance factor for convective flow through the pore; Pe is the membrane Peclet number; and Φ is the steric partition factor.

In the model by Kiso et al. [19], Φ is evaluated by modelling the molecules as freely rotating parallelepipeds, where length and molecular width (MWd) are used to calculate the rejection. MWd is calculated as the average side length of the rectangle enclosing the molecule perpendicular to the length axis of the molecule. However, for a molecule in which there is a difference in the side lengths of this rectangle, the longer of the two sides will be the most important in determining the fit through a cylindrical pore. This may be especially important for some of the pesticides that are relatively flat, and therefore get a large height/width ratio. From this perspective it may be a better approach to consider the molecules as cylinders, with the longer of the two sides in the rectangle as the cylinder diameter as suggest by Van der Bruggen et al. [18]. For comparison we investigated both approaches.

Part of the model is to estimate the drag and lag coefficients in the pores. To do this the Stokes radius of the solutes is used. In this work, the Stokes radius of a given solute was calculated from the average side length (S) of the parallelepiped enclosing the molecule by using the following correlation.

$$r_s = 1.051 \cdot S - 0.061 \cdot 10^{-9}, (nm) R^2 = 0.925 \quad (2)$$

The correlation was obtained by modelling the compounds for which the Stokes radius was given by Kiso et al. [29], calculating S and then fitting them against the values for Stokes radius. This correlation was used instead of the correlation given by Kiso et al. [19] to have a correlation where the molecular geometric parameters were obtained via the same procedure as was used to model the pesticides/PTPs.

For determination of the molecular geometric parameters, the program Gaussian was used. All molecules were modelled by using the density functional theorem, B3LYP, with a split valence basis set, 6-31++G(d). The addition of (d) to the basis set allows for polarization of heavy atoms, and ++ indicates that diffuse functions are added to both heavy atoms and hydrogen atoms. The allowance for polarization and use of diffuse functions increases the accuracy of the molecular model. To determine the spatial volume of the molecules, the electrostatic potential at the isovalue density surface of 0.002 $e^-/Å^3$, was used. An electrostatic potential at this isovalue has been found to estimate the Van der Waals surface [30], which is taken to be the actual spatial reach of the molecules.

3. Results and discussion

3.1. Rejection of pesticides and PTPs

Rejection values measured for demineralized water are shown in Fig. 2. All five membranes were found to reject the two larger pesticides, atrazine and bentazon, at levels over 88%, indicating their usefulness to treat groundwater contaminated with these pesticides. However, for the two PTPs: BAM and DEIA, the two investigated NF membranes obtained markedly lower rejections. For DEIA rejection values between 10% and 20% were measured, which shows the effect of the transformation of atrazine to DEIA on the rejection. It is possible that higher rejections can be obtained with other NF membranes, but based on the membranes used in this study, it will be necessary to use a LPRO/RO membrane for removal of PTPs like BAM and DEIA.

Of the LPRO/RO membranes XLE was found to achieve the highest rejection. The difference was especially prominent for DEIA and BAM, whereas for atrazine and bentazon, the rejection values for NF90, XLE and BW30 were very close. The difference between the XLE and the NF90 membrane is interesting. The two membranes have similar characteristics, but for the smaller PTPs XLE

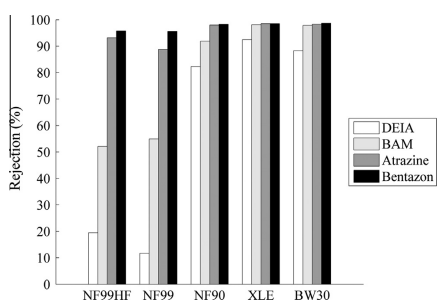

Fig. 2. Rejection values for DEIA, BAM, atrazine and bentazon obtained with each of the five membranes.

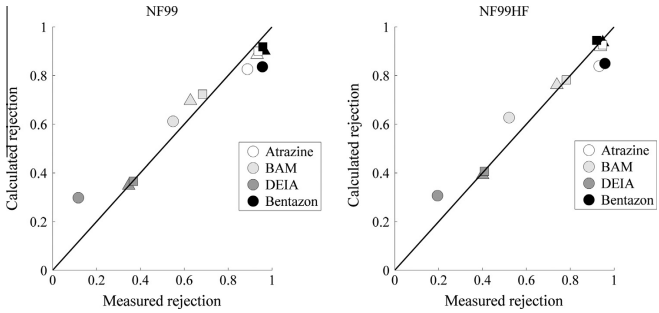

Fig. 3. Fit for measured rejection values of NF99 and NF99HF modelled by the approach specified by Kiso et al. [19]. Circles = demineralised water, triangles = Astrup water, squares = Hvidovre water.

achieves the highest rejection. The same trend was observed in a study by Plakas and Karabelas [12], where also the smallest pesticide in their study was better rejected by XLE compared to NF90. Thus, based on the results of both studies, it seems that for pesticides and PTPs smaller than atrazine, XLE is capable of achieving higher rejection compared to NF90. Whether this is purely due to steric effects is unknown. It is also possible that the NF90 membrane interacts more strongly with the dipole moment of the pesticides, which has been shown to reduce rejection if the pesticides align along their dipole moment in such a way that their steric hindrance is lowered [14].

3.2. Modelling of rejection as steric hindrance

In Fig. 3 the steric hindrance model with MWd calculated as specified by Kiso et al. [19], has been applied to the rejection data for the two NF membranes. Both fits show a clear correlation between the size of the pesticides and the values of rejection, which underlines the observation that the relative size between pesticides and pores is the most important parameter determining pesticide rejection. It also shows that for these particular membranes and compounds, it is the reduction in size that is the main cause of the lower rejection values of the PTPs. When the model is applied to the rejection data for the NF90, XLE and BW30 membranes, a poor fit is obtained (results not shown). Here the best pore size fit results in complete or very high (>0.999) rejection of atrazine, BAM and bentazon, showing that the performance of the LPRO/RO membranes is not very well described by this approach.

If instead the MWd suggested by Van der Bruggen et al. is used [18], a better fit for the rejection of the pesticides with the LPRO/RO membranes is obtained, see Fig. 4. For XLE and BW30, the rejections of BAM, bentazon and atrazine are slightly overestimated, but are still considerably closer to the observed value than when using the MWd specified by Kiso et al. [19]. On the other hand, the rejection of the pesticides by the two NF membranes cannot be modelled with this approach. When using the cylindrical pesticide model, the rejection of small molecules such as DEIA by the NF membranes is overestimated, while the rejection of larger molecules such as atrazine and bentazon is underestimated.

This difference in how to model the observed rejections points to different methods of rejection for the two types of membranes. For the NF membranes both height and width seem to be important for the rejection, while for the LPRO/RO membranes only the longer of the two sides determines the rejection. The two NF membranes are hydrophilic, and because the pesticides/PTPs are relatively non-polar and uncharged, only little interaction between them and the membranes is expected, and rejection may be expected to be mostly due to steric effects. In such a case the goodness of a model would depend on its ability to describe the fit of a molecule within a pore. In the investigated model, the pores are assumed to be cylindrical and in such a case length, height and width of the molecules should all affect the fit of the molecules in the pores to some degree. In such a situation the MWd by Kiso et al. [19] could represent a good approximation of the actual size of the molecules, which may explain why this MWd gives the best fit for the NF membranes. Compared to the NF membranes, the LPRO/RO membranes are hydrophobic, and this may lead to interaction between the membrane and the pesticides/PTPs. It has been shown that purely steric models may overestimate the rejection in cases of strong affinity between the membranes and organic molecules, because they fail to take this affinity into consideration [31]. This would explain the poor results obtained with the approach of Kiso et al. [19], but not why the steric approach with the use of the MWd suggested by Van der Bruggen et al. [18] gives good results. It is possible though that the cylindrical MWd is correlated to the affinity between membranes and pesticides/PTPs. Attractive forces between pesticides/PTPs and membranes would be strongest when the contact surface is maximized, which would be correlated with the longest side lengths. Whether the pesticides/PTPs truly behave as cylinders with the longest side length as the cylinder diameter, or whether the way of viewing them as such cylinders approximates their true behaviour, is not known.

3.3. Verification of model for LPRO/RO membranes

To investigate if the predictive ability of the model for the LPRO/RO membranes could be verified, two additional pesticides, prometryn and isoproturon, were modelled in Gaussian. These two pesticides have been used alongside atrazine in a study by Plakas and Karabelas [12], where both NF90 and XLE were used. They found similar rejections for atrazine, and the results for prometryn and isoproturon may therefore be assumed to be transferable to this study for comparison. Rejections were calculated with the model for demineralised water, and are shown in Table 4 together with the geometrical parameters.

In general the modelled rejections are found to be in good agreement with the observed values, with only relatively small differences. The differences may be due to both variations in filtration protocols, the accumulated experimental uncertainties from both studies, and effects unaccounted for in the model. Still, with these

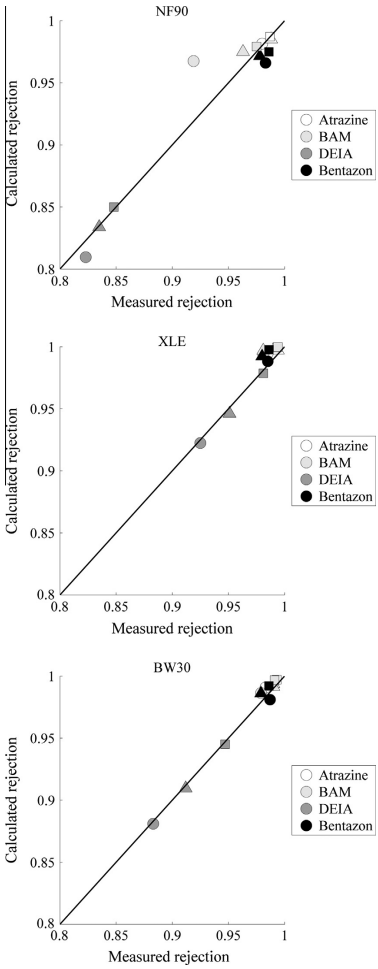

Fig. 4. Fit for measured rejection values of NF90, XLE and BW30 modelled by the new cylindrical approach. Circles = demineralised water, triangles = Astrup water, squares = Hvidovre water.

uncertainties in mind, it seems that the proposed model is capable of predicting rejection values for pesticides with acceptable precision, and it offers a simple way of evaluating the applicability of a given membrane towards the remediation of water polluted with pesticides and PTPs.

Although the calculated rejections of prometryn and isoproturon seems to support the modelling approach it still has to be noted that these two pesticides are similar in their molecular structure and chemical properties to the four compounds investigated in this study. This means that they may be expected to behave similarly, but pesticides/PTPs with very different properties such as very hydrophobic pesticides/PTPs may interact more strongly with the membranes making the purely steric approach less useful.

Table 4
Geometric parameters for prometryn and isoproturon.

Pesticides	Length (Å)	Height (Å)	Width (Å)	Membrane	R_{obs}	R_{cal}
Prometryn	13.65	9.713	6.502	NF90	0.998	0.997
				XLE	0.981	0.999
Isoproturon	14.32	7.385	7.051	NF90	0.951	0.931
				XLE	0.966	0.965

3.4. Predicted rejections of remaining pesticides and PTPs

Of the LPRO/RO membranes, XLE was found to give the highest rejection values, while NF99HF was the better of the two NF membranes, and it was decided to assess the applicability of these particular membranes to remediate a given polluted groundwater. To do this, the other pesticides and PTPs included in the Danish groundwater monitoring program were modelled to predict rejection values. These compounds are similar in their structure and properties to the four pesticides investigated experimentally and may be expected to behave similarly. Very hydrophobic pesticides such as the organochlorines are not found in Danish groundwater, and most often the PTPs becomes increasingly hydrophilic compared to their mother compounds when they undergo transformation. From these considerations it seems acceptable to apply the steric model. Rejection values were evaluated for the two groundwaters to get the span of rejection values that can be expected to be encountered in Danish groundwater. The modeled results and the geometrical parameters are shown in Table 5.

From the predicted rejection values it can be seen that nanofiltration with NF99HF can be used to treat a polluted aquifer, but as seen in the experiments with DEIA and BAM, the efficiency is highly dependent on the type of pesticide or PTP. Rejection above 90% in both types of groundwater is only predicted for 7 of the compounds, but for 17 of the compounds rejection above 80% is predicted. By using two NF99HF membranes in series a final rejection of over 96% is possible, which could make the system sufficiently efficient.

For many of the pesticides and PTPs in the Danish monitoring program high rejections (>95%) can be expected with the XLE membrane, and this membrane could be suitable to treat most pesticide polluted groundwaters. The rejection is in general lower for the PTPs, although it is not always the case. The rejection of metribuzin is actually lower compared to its two PTPs because the transformation increases the height and width of the PTPs compared to metribuzin. Even small changes in the molecular structure can have a measureable effect on the expected rejection. This is seen for the rejection of the three compounds: Dichlorprop, mechlorprop and 4-CPP. Dichlorprop and mechlorprop have a chloro and a methyl group at the second carbon atom of the phenoxy ring, respectively, whereas 4-CPP has no side group here. Because groups at this locus are placed perpendicular to the length axis of the molecules, they determine the height, and dichlorprop and mechlorprop get larger heights compared to 4-CPP. As such, the expected rejection for 4-CPP is lower compared to dichlorprop and mechlorprop although the change to the molecular structure is relatively small. These examples highlight the importance of investigating PTPs and not only pesticides. Again it should be highlighted that these are effects predicted to occur on the basis of steric effects. The changes in the molecular structure towards more hydrophilic compounds may also affect the final rejection, but

Table 5
Predicted values of rejection (R_{pred}, %) for the remaining pesticides and PTPs in the Danish groundwater monitoring program.

Compound	Type	Length (Å)	Height (Å)	Width (Å)	NF99HF		XLE	
					$R_{pred.}$ astrup	$R_{pred.}$ hvidovre	$R_{pred.}$ astrup	$R_{pred.}$ hvidovre
Dichlorprop	Pesticide	12.50	8.214	5.856	85	87	99	100
Mechlorprop	Pesticide	12.51	8.386	5.436	83	84	99	100
4-CPP	PTP	12.50	7.292	6.302	83	85	96	98
2,6-DCPP	PTP	11.26	9.010	6.337	89	91	100	100
Glyphosate	Pesticide	10.53	6.939	6.233	71	73	91	94
AMPA	PTP	7.666	6.390	6.002	45	47	65	74
Hexazinone	Pesticide	13.65	7.937	6.859	92	93	99	99
Metribuzin	Pesticide	12.12	7.111	6.587	83	84	95	97
Desamino-diketo-metribuzin	PTP	10.26	7.727	6.912	82	84	97	98
Diketo-metribuzin	PTP	10.13	7.586	6.774	80	82	97	98
Simazine	Pesticide	13.83	8.714	4.905	83	85	100	100
Desethyl atrazine	PTP	11.13	8.504	6.314	86	88	100	100
Desisopropyl atrazine	PTP	11.15	8.333	4.339	62	65	98	100
Desethyl-hydroxy-atrazine	PTP	11.11	7.852	6.256	81	83	97	99
Desisopropyl-hydroxy-atrazine	PTP	11.11	7.817	4.266	57	59	96	98
Desethyl-desisopropyl-hydroxy-atrazine	PTP	8.514	7.649	3.783	33	35	89	95
2-Hydroxyterbutylazine	PTP	13.00	9.318	6.710	95	95	100	100
2-Hydroxy-desetyl-terbutylazine	PTP	10.59	8.781	6.702	89	90	100	100
Trichloro acetic acid (TCA)	Pesticide	7.392	7.206	6.265	55	57	081	89
CyPM	PTP	16.55	11.51	10.11	100	100	100	100
Picolinafen	Pesticide	18.91	9.943	7.133	98	99	100	100
CL153815	PTP	15.00	8.954	7.175	96	96	100	100
PPU	PTP	13.40	11.10	10.20	100	100	100	100
Desamino-PPU	PTP	13.32	12.53	7.496	100	100	100	100

Table 6
Calculated average pore radius (nm) in different waters.

	NF90	XLE	BW30	NF99HF	NF99
Dem. water	0.841	0.769	0.797	0.876	0.886
Astrup	0.827	0.748	0.777	0.792	0.833
Hvidovre	0.815	0.708	0.748	0.780	0.814

Table 7
Zeta potentials (mV) for the five membranes. Measurements were carried out at the pH values listed in Table 2. The pH value for the demineralised water was 5.0.

	NF99HF	NF99	NF90	XLE	BW30
Dem. water	−0.04 ± 0.02	0.02 ± 0.01	−0.05 ± 0.00	−0.06 ± 0.01	−0.04 ± 0.01
Astrup	−10.6 ± 0.7	1.9 ± 0.4	−7.5 ± 1.2	−20.7 ± 1.9	−12.7 ± 1.2
Hvidovre	−18.0 ± 0.7	7.6 ± 1.1	−5.6 ± 0.5	−25.9 ± 1.6	−19.2 ± 1.5

based on the results from the comparison of atrazine and DEIA, the change in the steric hindrance seems to be the most important.

3.5. Effect of different groundwaters

As can be seen from Figs. 3 and 4, the rejection of the pesticides was found to increase for all membranes in the following order demineralised water < Astrup water < Hvidovre water. The steric models do therefore indicate that the effect of the groundwaters is to decrease the average pore size of the membranes.

To calculate the pore size for NF90, XLE and BW30 the cylindrical model has been used, while the MWd specified by Kiso et al. [19] has been used for NF99HF and NF99. Since the calculation of the pore size is dependent on the estimate of the solute size, the two sets of pore sizes are not directly comparable. The calculated pore sizes can be found in Table 6.

Since the ionic concentrations increase with the different waters, it is possible that the increased rejection is not because the pore size decrease, but because the apparent size of the pesticides and PTPs is increased through interactions with the water matrix. Increase in apparent molecular size would lead to increased rejection, which could be interpreted as decreasing pore size. To investigate for such interactions electrospray ionization mass spectrometry (ESI–MS) was employed. ESI–MS works by creating charged species that can subsequently be analysed in the mass spectrometer. Although ESI–MS does not show the true ionic composition of the solution [32], it does represent an extreme case for ion pair formation. During the electrospray process, the solvent is evaporated, which drives the formation of ion pairs by concentrating the non-volatile ions along with the pesticides/PTPs. The ions are forced into contact with the molecules, and if any interactions were to take place at a significant level, it should be observed in this analysis. Also, the presence of pesticide/PTP complexes with organic matter may be investigated.

No complexes with other organic compounds and no calciated species were found for any of the four compounds. Sodium was found to interact with atrazine, BAM and bentazon, but only weak peaks were seen, and for DEIA no sodiated peak was seen. DEIA was the pesticide for which the largest change in rejection was found. This indicates that little or no interaction can be expected between the ionic environments and the pesticides. In general the ESI–MS analysis shows that the increased rejection cannot be explained by increased interactions between the pesticides/PTPs and the water matrixes, and that the change in rejection must be explained by interactions between the waters and the membranes.

It has been suggested that increased rejection of micropollutants in real waters compared to distilled and demineralised water is due to a reduction of the electrical double layer inside the membrane pores, which leads to a contraction of the pores [1,33]. The size of the double layer may traditionally be evaluated by measuring the zeta potential, which is equal to the potential at the shear plane of the double layer. A reduction of the double layer should as such result in a decreased zeta potential. However, for RO membranes the zeta potential has been found to increase with ionic strength [34], and this was also found to occur for four of the five membranes in this investigation, see Table 7. Only for NF90 did the zeta potential decrease in Hvidovre water compared to Astrup water, and only slightly. The increasing zeta potential has been explained by ion adsorption onto the membranes [34], and the adsorption of ions in the pores has also been suggested as an

explanation to observed increases in rejection [11,35,36]. This explanation is in accordance with the adsorption–amphoteric model by Bandini et al. [37,38], which describes the resulting charge of the membrane in an ionic environment to be the combined result of acid/base dissociation of hydrophilic sites, counter-ion site binding on dissociated hydrophilic sites, and competitive adsorption of ions on hydrophobic sites. Anions adsorption will have a tendency to prevail over cation adsorption due to their lower hydrated radii [38], which may explain why for four of the membranes the zeta potential is found to be increasingly negative. Based on these considerations, it seems that the increased rejection values are not due to pore contraction, but rather a result of pore blocking by ions.

4. Conclusion

Because many pesticide transformation products are both smaller and more hydrophilic than the original pesticides their filtration behaviour is very different, and it may be necessary to use different membranes to remove each type of pollutant. Rejections above 90% of large pesticides such as atrazine and bentazon could be obtained with nanofiltration membranes such as NF99HF, but these could not remove small pesticide transformation products like BAM and DEIA. To obtain sufficient removal of these compounds, it was necessary to employ LPRO membranes, and of the membranes investigated in this study, XLE gave the highest rejection.

It was found that rejection of the four investigated compounds could be reasonably described with a purely steric model assuming a uniform pore size of the membranes, showing that the main effect of the transformation of pesticides is to change their steric hindrance. Different descriptors for the molecular width were found to give the best fit for the NF and the LPRO/RO membranes. For the NF membranes a molecular width based on a rectangular view of the pesticides/PTPs as specified by Kiso et al. [19] gave the best fit, while for LPRO/RO membranes it was better to consider the pesticides/PTPs as being cylindrical as suggested by Van der Bruggen et al. [18]. This modelling approach was then used to predict rejection values for the remaining pesticides/PTPs included in the Danish groundwater monitoring program, indicating that most of these could be expected to be efficiently removed from groundwater by use of the XLE membrane.

Rejection values were found to increase when using groundwaters with higher ionic content, and this increase could be modelled as decreasing pore size. For the four investigated pesticide compounds, no interactions were found with the ions in the waters, and could not explain the increased rejections. Instead, the observed increase in zeta potential indicates that the increased rejections are due to ion adsorption on the membrane leading to a narrowing of the pores.

Acknowledgements

Financial support from the Danish Ministry of Science, Technology, and Innovation in the form of a Ph.D. study grant is acknowledged. Gratitude also goes to Professor Bart Van der Bruggen, KU Leuven, Belgium for advice and discussion on the content of the paper.

Appendix A. Supplementary material

Supplementary data associated with this article can be found, in the online version, at http://dx.doi.org/10.1016/j.seppur.2014.01.038.

References

[1] K.V. Plakas, A.J. Karabelas, Removal of pesticides from water by NF and RO membranes – a review, Desalination 287 (2012) 255–265.
[2] L. Thorling, B. Hansen, C.L. Larsen, W. Brüsch, R.R. Møller, S. Mielby, et al., Grundvand – status og udvikling 1989–2010 (2011).
[3] L. Thorling, B. Hansen, C.L. Larsen, W. Brüsch, R.R. Møller, S. Mielby, et al., Grundvand – status og udvikling 1989–2009 (2010).
[4] L. Thorling, B. Hansen, C.L. Larsen, W. Brüsch, R.R. Møller, S. Mielby, Grundvand – status og udvikling, 2012. 1989–2011.
[5] E.G. Søgaard, R. Aruna, J. Abraham-Peskir, C.B. Koch, Conditions for biological precipitation of iron by Gallionella ferruginea in a slightly polluted groundwater, Appl. Geochem. 16 (2001) 1129–1137.
[6] E.G. Søgaard, H.T. Madsen, Groundwater chemistry and treatment: application to danish waterworks, in: W. Elshorbagy, R.K. Chowdhury (Eds.), Water Treat., first ed., InTech, 2013, pp. 223–246.
[7] C. Bellona, J.E. Drewes, P. Xu, G. Amy, Factors affecting the rejection of organic solutes during NF/RO treatment – a literature review, Water Res. 38 (2004) 2795–2809.
[8] B. Van der Bruggen, C. Vandecasteele, Removal of pollutants from surface water and groundwater by nanofiltration: overview of possible applications in the drinking water industry, Environ. Pollut. 122 (2003) 435–445.
[9] R. Boussahel, S. Bouland, K.M. Moussaoui, A. Montiel, Removal of pesticide residues in water using the nanofiltration process, Desalination 132 (2000) 205–209.
[10] R. Boussahel, A. Montiel, M. Baudu, Effects of organic and inorganic matter on pesticide rejection by nanofiltration, Desalination 145 (2002) 109–114.
[11] Y. Zhang, B. Van der Bruggen, G. Chen, L. Braeken, C. Vandecasteele, Removal of pesticides by nanofiltration: effect of the water matrix, Sep. Purif. Technol. 38 (2004) 163–172.
[12] K.V. Plakas, A.J. Karabelas, Membrane retention of herbicides from single and multi-solute media: the effect of ionic environment, J. Memb. Sci. 320 (2008) 325–334.
[13] K.V. Plakas, A.J. Karabelas, Triazine retention by nanofiltration in the presence of organic matter: the role of humic substance characteristics, J. Memb. Sci. 336 (2009) 86–100.
[14] B. Van der Bruggen, J. Schaep, W. Maes, D. Wilms, C. Vandercasteele, Nanofiltration as a treatment method for the removal of pesticides from groundwater, Desalination 117 (1998) 139–147.
[15] Y. Kiso, Y. Sugiura, T. Kitao, K. Nishimura, Effects of hydrophobicity and molecular size on rejection of aromatic pesticides with nanofiltration membranes, J. Memb. Sci. 192 (2001) 1–10.
[16] Y. Kiso, Y. Nishimura, T. Kitao, K. Nishimura, Rejection properties of non-phenylic pesticides with nanofiltration membranes, J. Memb. Sci. 171 (2000) 229–237.
[17] P. Berg, G. Hagmeyer, R. Gimbel, Removal of pesticides and other micropollutants by nanofiltration, Desalination 113 (1997) 205–208.
[18] B. Van Der Bruggen, J. Schaep, D. Wilms, C. Vandecasteele, A comparison of models to describe the maximal retention of organic molecules in nanofiltration, Sep. Sci. Technol. 35 (2000) 169–182.
[19] Y. Kiso, K. Muroshige, T. Oguchi, M. Hirose, T. Ohara, T. Shintani, Pore radius estimation based on organic solute molecular shape and effects of pressure on pore radius for a reverse osmosis membrane, J. Memb. Sci. 369 (2011) 290–298.
[20] Y. Kiso, K. Muroshige, T. Oguchi, T. Yamada, M. Hhirose, T. Ohara, et al., Effect of molecular shape on rejection of uncharged organic compounds by nanofiltration membranes and on calculated pore radii, J. Memb. Sci. 358 (2010) 101–113.
[21] A. Karabelas, K. Plakas, Membrane treatment of potable water for pesticides removal, in: P.M. Larramendy (Ed.), Herbic. Theory Appl., InTech, 2011, pp. 369–408.
[22] C.D.S. Tomlin, The pesticide manual: a world compendium, 15th ed., British Crop Production Council, 2011.
[23] Y. Nakagawa, K. Izumi, N. Oikawa, T. Sotomatsu, M. Shigemura, T. Fujita, Analysis and prediction of hydrophobicity parameters of substituted acetanilides, benzamides and related aromatic compounds, Environ. Toxicol. Chem. 11 (1992) 901–916.
[24] A. Sotto, M.J. López-Muñoz, J.M. Arsuaga, J. Aguado, A. Revilla, Membrane treatment applied to aqueous solutions containing atrazine photocatalytic oxidation products, Desalin, Water Treat. 21 (2010) 175–180.
[25] H. Geyer, R. Viswanathan, D. Freitag, F. Korte, Relationship between water solubility of the organic chemicals and their bioaccumulation by the alga chlorella, Chemosphere 10 (1981) 1307–1313.
[26] G.G. Jensen, E. Björklund, A. Simonsen, B. Halling-Sørensen, Determination of 2,6-dichlorobenzamide and its degradation products in water samples using solid-phase extraction followed by liquid chromatography-tandem mass spectrometry, J. Chromatogr. A. 1216 (2009) 5199–5206.
[27] M.J. López-Muñoz, A. Sotto, J.M. Arsuaga, B. Van der Bruggen, Influence of membrane, solute and solution properties on the retention of phenolic compounds in aqueous solution by nanofiltration membranes, Sep. Purif. Technol. 66 (2009) 194–201.
[28] G.A. Smith, B.V. Pepich, D.J. Munch, Determination of triazine pesticides and their degradates in drinking water by liquid chromatography electrospray ionization tandem mass spectrometry (LC/ESI–MS/MS) (2007).

[29] Y. Kiso, T. Kitao, K. Jinno, M. Miyagi, The effects of molecular width on permeation of organic solute through cellulose acetate reverse osmosis membranes, J. Memb. Sci. 74 (1992) 95–103.
[30] G.D. Purvis, On the use of isovalued surfaces to determine molecule shape and reaction pathways, J. Comput. Aided. Mol. Des. 5 (1991) 55–80.
[31] A.R.D. Verliefde, E.R. Cornelissen, S.G.J. Heijman, E.M.V. Hoek, G.L. Amy, B. Van der Bruggen, et al., Influence of solute – membrane affinity on rejection of uncharged organic solutes by nanofiltration membranes, Environ. Sci. Technol. 43 (2009) 2400–2406.
[32] S. Banerjee, S. Mazumdar, Electrospray ionization mass spectrometry: a technique to access the information beyond the molecular weight of the analyte, Int. J. Anal. Chem. 2012 (2012).
[33] L.D. Nghiem, A.I. Shäfer, Trace contaminant removal with nanofiltration, in: A.I. Shäfer, A.G. Fane, T.D. Waite (Eds.), Nanofiltration, Princ. Appl., Elsevier Advanced Technology, Oxford, UK, 2005, pp. 479–520.
[34] M. Elimelech, W.H. Chen, J.J. Waypa, Measuring the zeta (electrokinetic) potential of reverse osmosis membranes by a streaming potential analyzer, Desalination 95 (1994) 269–286.
[35] J. Schaep, B. Van der Bruggen, C. Vandercasteele, Influence of ion size and charge in nanofiltration, Sep. Purif. Technol. 14 (1998) 155–162.
[36] M. Thanuttamavong, K. Yamammoto, J.I. Oh, K.H. Choo, Rejection characteristics of organic and inorganic pollutants by ultra low-pressure nanofiltration of surface water for drinking water treatment, Desalination 145 (2002) 257–264.
[37] L. Bruni, S. Bandini, Studies on the role of site-binding and competitive adsorption in determining the charge of nanofiltration membranes, Desalination 241 (2009) 315–330.
[38] A. Szymczyk, P. Fievet, S. Bandini, On the amphoteric behavior of Desal DK nanofiltration membranes at low salt concentrations, J. Memb. Sci. 355 (2010) 60–68.

Paper VII

Henrik Tækker Madsen, Niada Bajraktari, Claus Hélix-Nielsen,
Bart Van der Bruggen and Erik G. Søgaard

Use of biomimetic forward osmosis membrane for trace organics removal

Journal of Membrane Science, **476** (2015), 469-474

Reprinted with permission from Elsevier

Journal of Membrane Science 476 (2015) 469–474

Contents lists available at ScienceDirect

Journal of Membrane Science

journal homepage: www.elsevier.com/locate/memsci

Use of biomimetic forward osmosis membrane for trace organics removal

Henrik T. Madsen [a,*], Niada Bajraktari [b], Claus Hélix-Nielsen [b], Bart Van der Bruggen [c], Erik G. Søgaard [a]

[a] Department of Biotechnology, Chemistry and Environmental Engineering, Aalborg University, Esbjerg, Denmark
[b] Department of Environmental Engineering, Technical University of Denmark, Kgs. Lyngby, Denmark
[c] Department of Chemical Engineering, K.U. Leuven, Leuven, Belgium

ARTICLE INFO

Article history:
Received 16 June 2014
Received in revised form
24 November 2014
Accepted 30 November 2014
Available online 10 December 2014

Keywords:
Biomimetic
Aquaporin
Forward osmosis
Trace organic
Pesticide

ABSTRACT

The use of forward osmosis for the removal of trace organics from water has recently attracted considerable attention as an alternative to traditional pressure driven membrane filtration. However, the existing forward osmosis membranes have been found to be ineffective at rejecting small neutral organic pollutants, which limits the applicability of the forward osmosis process. In this study a newly developed biomimetic membrane was tested for the removal of three selected trace organics that can be considered as a bench marking test for a membrane's ability to reject small neutral organic pollutants in aqueous solution. The performance of this membrane was compared with a standard cellulose acetate forward osmosis membrane. The aquaporin membrane was found to have rejection values above 97% for all three trace organics, which was significantly higher than the cellulose acetate membrane. This difference is caused by differences in the transport mechanisms. For the cellulose acetate membrane rejection is controlled by steric hindrance, which results in a size dependent rejection of the trace organics, whereas rejection by the aquaporin membrane is controlled by diffusion of the trace organics. Furthermore, the aquaporin membrane was found to have a higher pure water flux.

© 2014 Elsevier B.V. All rights reserved.

1. Introduction

Pollution of water resources with trace organics such as pesticides, endocrine disruptors and pharmaceuticals is becoming a growing problem as both the awareness and the analytical detection capabilities of these compounds increase.

One way of remediating polluted water is to use membrane filtration. The most intensely studied membrane technique has been the use of pressure driven NF membranes, which have been found to be effective in most cases [1,2]. However, when the pollutants are small (< 200 g/mol), it is often necessary to use tighter membranes such as low pressure RO (LPRO) or RO membranes to obtain sufficient removal [3]. The high pressure used in these operations increases the cost of the remediation and, due to concentration polarisation, also increases the risk of fouling and scaling. To overcome these problems the use of forward osmosis (FO) has recently attracted attention [4]. In FO the general principle is to use a draw solution to create an osmotic gradient across a semipermeable membrane, which should be highly permeable to water and reject the trace organics. To make the FO process continuous, the draw solution must be reclaimed in a second separation step. The two step process makes FO more complicated compared to pressure driven processes, but because the composition of the draw can be engineered, the overall process may still be advantageous. However, because of the reclamation of the draw, an insufficient rejection by the FO membrane may lead to accumulation of the trace organics in the draw solution [5], which may be problematic for long term permeate quality. In continuous FO, the specific rejection of a given trace organic by the FO membrane is therefore very important for the overall applicability of the process.

The rejection by FO membranes has been studied for a wide range of trace organics, and has shown great potential [5–12]. For the same membrane, the use of an osmotic gradient (FO mode) has been shown to give higher rejections compared to the use of a pressure gradient (RO mode) [6], illustrating a possible advantage of using FO setups instead of pressure driven setups for removal of trace organics. However, rejections obtained with FO membranes have been comparable to rejections obtained with NF membranes [5], which means that the rejection of small neutral organics has been low in FO studies. It is possible to obtain higher rejections if NF/LPRO membranes are used as the FO membrane, but these

* Corresponding author. Tel.: +45 20960733.
E-mail address: htm@bio.aau.dk (H.T. Madsen).

http://dx.doi.org/10.1016/j.memsci.2014.11.055
0376-7388/© 2014 Elsevier B.V. All rights reserved.

membranes have significantly lower fluxes than real FO membranes [11]. For the FO technique to become universally applicable for the removal of trace organics, a membrane is needed with higher rejection without compromising the water flux.

In this study we have investigated the possibility of using a newly developed biomimetic FO membrane to remove trace organics. The membrane is based on aquaporin technology, where aquaporin proteins have been integrated into the active layer of the membrane. Aquaporins are pore-forming proteins that when integrated into a membrane structure facilitate gradient driven water diffusion. Because the facilitated transport mechanism is passive, the proteins can operate with a stable geometrical structure that allows for single channel turnover rates up to 10^9 water molecules per second [13]. The rapid transport of water means that membranes based on aquaporin technology potentially can have very high permeabilities compared to traditional membranes [14]. Although some of the aquaporins are permeable to molecules other than water, such as the aquaglyceroporin GlpF that transports both water and glycerol and is permeable to arsenite, urea and glycine, aquaporins, such as AqpZ, that exclusively transports water also exist [15]. From the perspective of trace organic removal, the combination of the high permeability and the specific transport of water is very interesting, since it offers the possibility of having a dense active layer to obtain high rejections of even small neutral trace organics without compromising flux [16,17]. The purpose of this study is not to investigate the specific role of aquaporins in trace organic removal. Instead the potential of the biomimetic membrane is evaluated by comparing it to the most widely studied commercial FO membrane, the cellulose acetate FO membrane by Hydration Technology Innovations. The two membranes are compared on their ability to remove three selected pesticides: atrazine (215.7 g/mol), 2,6-dichlorobenzamide (BAM, 190.0 g/mol) and desethyl-desisopropyl-atrazine (DEIA, 145.6 g/mol). These are important groundwater pollutants, with especially BAM and DEIA often being found in groundwater samples [3,18]. Atrazine is found to a lesser degree, but in membrane/pesticide studies, it is the single most used pesticide [2], and it can as such be considered a reference compound that can be used to link membrane/trace organic studies.

Besides their environmental relevance, these three compounds also span the range of sizes that can be expected for small neutral trace organics [3]. They can as such be said to be bench marker compounds for a membrane's ability to treat water polluted with trace organics.

2. Experimental

2.1. Forward osmosis membranes

Two forward osmosis membranes were used in this study: an asymmetric cellulose triacetate FO membrane acquired from Hydration Technology Innovations (HTI, Albany, OR) and a biomimetic aquaporin (AqP) membrane provided by Aquaporin A/S (Aquaporin A/S, Copenhagen, Denmark). The HTI membrane has been used in numerous FO studies on removal of trace organics [5–11], and is therefore well suited to be used as a comparative membrane when investigating new membranes. This also allows for the direct comparison with the results presented in other papers where this membrane has been used. The AqP membrane is a newly developed biomimetic membrane with aquaporin protein channels incorporated into the active layer of the membrane. Briefly, the AqP membrane is made as a thin film composite membrane where vesicles (~200 nm in diameter) with embedded aquaporin proteins are stabilized by a polyamide layer supported by a porous support [17].

2.2. Forward osmosis system

A small FO system developed by Aquaporin A/S was used in the experiments. The scale of the system allows for easy and quick experiments where only small amounts of chemicals are necessary and where adsorption to the equipment is limited to a minimum.

Briefly, the system consists of a 1.5 mL compartment and a circulatory system with an effective volume of 100 mL and the system can be operated in two modes: concentrator or dilutor mode, as illustrated in Fig. 2b. In the concentrator mode the solution with the trace organics is placed in the compartment, while a draw solution is kept in the circulatory system. In this way the trace organic solution becomes concentrated and feed and concentrate concentration can be determined. However, because of the large difference in volume between the compartment and the circulatory system, permeate concentration cannot be determined when working with dilute trace organic solutions. In the dilutor mode, the draw solution is kept in the compartment, while the trace organic solution is recirculated. Because of the modest dilution of the permeate, permeate concentration can be determined, and due to the insignificant loss of trace organic solution in the circulatory system, the feed concentration can be assumed to be constant throughout the experiment. Rejection can thus be calculated as

$$R = \left(1 - \frac{C_P}{C_F}\right)100\% \quad (1)$$

where C_P is the permeate concentration and C_F the feed concentration. Rejection was therefore determined using the dilutor mode. Since it is the permeate concentration at the membrane interface that is used in the model, the permeate concentration was corrected for the dilution in the draw by measuring the volume of the liquid in the 1.5 mL compartment at the beginning and the end of the experiment.

In the experiments a specific volume of solution was transferred to the chamber, and the recirculation was started. The filtration was then allowed to run until either a recovery of 50% or a dilution of a factor 2, after which the solution was transferred from the chamber to a vial and weighed to determine the exact volume. Permeate volume was then calculated as the difference in volume.

A 1 M NaCl solution was used as draw. Since the draw is diluted when used in the dilutor mode, the starting draw concentration in these experiments was 1.33 M. By running the filtration until a dilution of a factor 2, the average concentration was 1 M.

Prior to each experiment with trace organics, the membrane was used to filter a solution with the trace organic for 1 h to avoid effects from adsorption to the fresh membrane allowing stable rejection values to be obtained.

The membrane was in all experiments used in the FO mode, with the active layer facing the feed with the pesticides. Water fluxes were determined using solutions free of trace organics.

2.3. Selected trace organics

Three pesticides were used as representative for small neutral trace organics: atrazine, 2,6-dichlorobenzamide (BAM) and desethyl-desisopropyl-atrazine (DEIA). All were purchased at Sigma-Aldrich (Pestanal, Fluka). Information about the chemical structure and geometrical properties of the three pesticides are shown in Table 1. 1 mg/L solutions were used in the experiments with the pesticides being dissolved in MilliQ water.

2.4. Analytical methods

Pesticides were analysed with HPLC/UV (1200 Infinity, Agilent Technology), equipped with a ZORBAX Eclipse XDB-C18 5 μm column and using eluent mixtures of acetonitrile (A) and MilliQ (B). For atrazine a 70/30 (A/B) mixture was used, for BAM a 50/50 mixture and for DEIA a 30/70 mixture. The injection volume was 100 μL and the flow rate 400 μL/min. The chosen absorption wavelength was 220 nm for atrazine and 210 nm for BAM and DEIA.

Table 1
Overview of chemical structure and size parameters. The geometrical parameters were determined by modelling the molecular structure with the software Gaussian, and then adding an electrostatic potential to estimate the van der Waal surface, which can be considered the effective size of the molecule. Length is defined as the longest axis through the molecule, and width and height are defined as the side lengths of the rectangle enclosing the molecule perpendicular to the length axis. Volume was taken as the volume of the enclosing parallelepiped. A more thorough description of the method for determination of the geometrical parameters can be found elsewhere [3].

	Atrazine	BAM	DEIA
Chemical structure	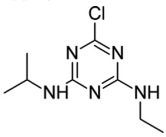	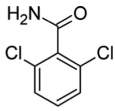	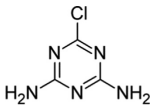
Formula	$C_8H_{14}ClN_5$	$C_7H_5Cl_2NO$	$C_3H_4ClN_5$
Molecular weight (g/mol)	215.69	190.03	145.55
Length (nm)	1.38	0.920	0.860
Width (nm)	0.627	0.578	0.395
Height (nm)	0.875	0.904	0.806
Volume (nm^3)	0.755	0.481	0.274

2.5. Models for rejection mechanism

Two models were used to investigate the mechanism of rejection, i.e., a steric pore flow model [3,19] and a Fickian solution diffusion model [20].

In the steric model the molecules are modelled as rotating parallelepiped and the membrane as having a uniform pore size. These are rough generalisations as the molecules orientation may be affected by the membrane [21] and because the porous structure of membranes consists of a distribution of pore sizes [22]. However, it has been found that the model does describe filtration based on steric hindrance sufficiently well [3,19]. The model is based on

$$R = 1 - \frac{C_P}{C_F} = 1 - \frac{\Phi K_C}{1-(1-\Phi K_C)\exp(-Pe)} \quad (2)$$

where Pe is the Peclet number, K_C the solute hindrance factor for convective flow through the pores and Φ is the steric partition factor. Since the molecules are not considered spherical a more elaborate procedure is required to determine the steric partition factor, an excellent description has been given by Kiso et al. [19].

The general approach is to use the measured rejections to find the pore size of the membrane that best describes the rejection, and then use this pore size to calculate the theoretical rejections. By plotting modelled rejections against the measured rejections, it is possible to examine whether the rejection is due to steric hindrance.

A simple solution diffusion model based on Fickian diffusion was used to investigate for diffusive transport mechanisms and can be described with

$$J = \frac{P}{l}\Delta C \quad (3)$$

where J is the flux, l the membrane thickness, ΔC the average concentration difference across the membrane and P the permeability. The permeability is the product of the diffusion coefficient of the specific trace organic through the membrane and the sorption coefficient of the trace organic to the membrane material. In the experiments, the permeability can be determined by measuring the flux of the trace organics across the membrane over a range of concentration values. In practice, this was done by keeping the pesticides in the circulatory system, and using MilliQ water without NaCl on both sides of the membrane to remove the flux of water. The pesticide flux could then be determined by measuring the pesticide concentration in the compartment after a given amount of time. To ensure a constant feed concentration, 100 mL pesticide solution was used in the circulatory system with concentrations of 1, 5 and 10 mg/L. The system was left for 3 h to ensure the membrane had been saturated with pesticides after which a fresh aliquot of 1 mL MilliQ water was placed in the compartment. The system was then left for 5 h after which the pesticide concentration was determined.

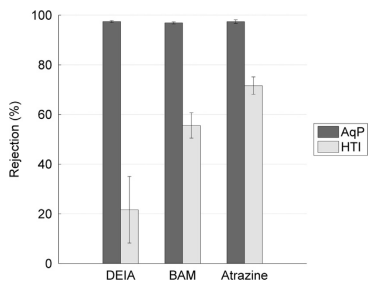

Fig. 1. Comparison of the rejection obtained with the AqP and the HTI membrane. The error bars represent the standard deviation from triplicate determinations with three different membrane pieces.

3. Results and discussion

3.1. Potential of the AqP membrane

From Fig. 1 it is seen that the AqP membrane is capable of obtaining high rejections (> 97%) for all three of the pesticides. The exact rejection could not be determined accurately because the permeate concentrations were below the limit of quantification. Because of the small volume, solid phase extraction could not be performed, and the permeate concentration had to be determined from direct analysis of the samples. Still, the overall finding is that high rejections for even small neutral compounds like DEIA are possible.

The rejection results for the HTI membrane increase with the size of the pesticides, but never reach the high levels obtained with the AqP membrane. These rejection values are in line with what has been previously reported in other studies [5,7–9], and highlight the HTI membrane's inability to reject small neutral trace organics.

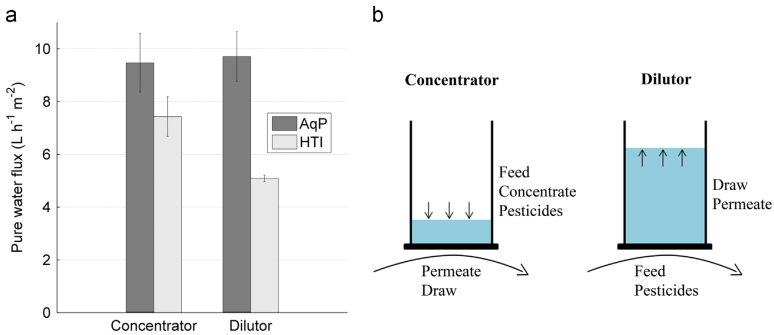

Fig. 2. Flux comparison (a) and sketch of setup run in the concentrator and the dilutor mode (b). The fluxes obtained for the AqP and HTI membrane in both the concentrator and the dilutor setup are compared. The error bars represent the standard deviation calculated from triplicate determinations for three different membrane pieces.

In Fig. 2a, the two membranes are compared with respect to pure water flux, and it can be seen that the AqP membrane has a statistically significant higher flux than the HTI membrane. It is also interesting to note that the pure water flux of the HTI membrane is dependent on whether the membrane is used in the concentrator or the dilutor mode, while the pure water flux of the AqP membrane is not statistically different.

The reason for the decreased flux of the HTI membrane when it is used in the dilutor mode may be due to aggravated concentration polarisation. In the dilutor mode there is no mixing on the draw side, and the draw solution in the pores and the immediate vicinity of the membrane surface may therefore become diluted creating a smaller concentration gradient between draw and feed. In the concentrator mode, the recirculation of the draw gives some mixing through forced convective flow, which can reduce the concentration polarisation and increase flux. However, when FO membranes are operated in FO mode (active layer facing the feed), the water flux has been found to be independent of the cross-flow rate of the draw [23], as is also seen for the AqP membrane. The exact reason for the observed differences between the two membranes is therefore unknown, but may potentially be related to the different structures with the HTI membrane being an asymmetric membrane and the AqP membrane a TFC membrane.

It should be noted that aquaporin free TFC FO membranes with high water flux have also been manufactured [24]. However, although use of TFC FO membranes has been found to increase rejection of trace organics, rejection values $>91\%$ for neutral hydrophilic trace organics with molar masses <266 g/mol have not been found [8,12]. The rejection values reported in this study are the highest reported TCF FO rejection values for neutral trace organics, and especially the high rejection of DEIA is notable due to its small size (145.6 g/mol).

3.2. Mechanism of rejection

Since the rejection of the three pesticides by the HTI membrane increased along with the molecular weight, the mechanism of rejection was investigated with the steric model; see Fig. 3. As can be seen, the model is capable of describing the rejection very well and predicts an average pore radius of 1.04 nm. This is somewhat different from the results by Xie et al. [6] who reported an average pore radius of 0.37 nm. Their result was however obtained by considering the solutes to be spherical and with the solute radius taken as the Stoke radius. Using the model specified in Section 2.5 where the molecules are considered to have both length and width, it has been found that more accurate results can be obtained and that the predicted pore radii values are higher compared to when the molecules are considered to be spherical [19]. Also in these calculations, the molecular geometries have been determined at the isovalue density surface for the electrostatic potential at a value of 2 e^-/nm^3. This is an estimate of the van der Waals surface of the molecules [25], and may give geometrical parameters different from those that are arrived at when the Stoke radius is estimated with molecular weight based approaches such as the combined use of the Wilke–Chang and the Stokes–Einstein equation as used by Xie et al. [6,26]. Also, in the study by Xie et al. [6] the pore size for the FO membrane was reported to have been determined in RO mode by applying pressure, whereas in this study the pore size was determined in FO mode. What may be more important in explaining the difference is that two different sets of equations have been used to calculate the hydrodynamic hindrance coefficients. However, our main conclusion is that the rejection with the HTI membrane is mainly caused by steric hindrance.

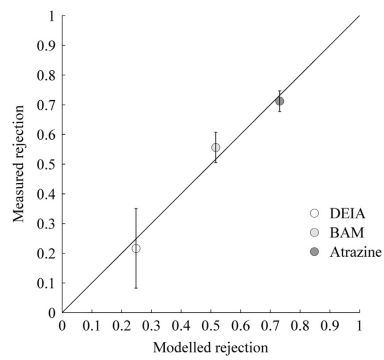

Fig. 3. Fit of HTI rejection results to a steric pore flow model. The average rejection results are used to calculate a pore size of the HTI membrane, which is then used to calculate theoretical rejection values. The closer the data points to the line, the better the fit of the model. $R^2=0.975$. The plotted data points are the average values of triplicate experiments, with the standard deviations added as error bars.

Because similar rejections were seen for all three pesticides with the AqP membrane, the rejection mechanism could not be

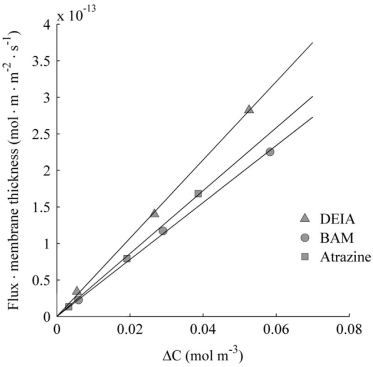

Pesticide	Permeability (m^2/s)	Modelled rejection (%)
DEIA	$5.36 \cdot 10^{-12}$	98.0
BAM	$3.90 \cdot 10^{-12}$	98.6
Atrazine	$4.31 \cdot 10^{-12}$	98.4

Fig. 4. Permeation of the three pesticides through the AqP membrane. The flux has been normalised with respect to the membrane thickness (112 μm), to allow for a direct determination of the permeability from the slope of the fit. For all three pesticides the *R* squared value of the fit is 0.999.

modelled as steric hindrance. Instead it was attempted to determine the permeability for each of the three pesticides to see if the rejection could be described with a solution diffusion model.

As can be seen from the three fits in Fig. 4, there is a linear correlation between the flux of the pesticides through the AqP membrane and the concentration gradient across the membrane. That the highest permeability is found for DEIA may be ascribed to its smaller size compared to the two other compounds, which may make it easier for it to diffuse through the membrane matrix. The most significant finding is however, that when these permeabilities are used to model the rejection, it gives values that are very close to the measured values. With the uncertainty in the determination of the permeate concentration in mind, the match between the measured and the modelled values is very good, and the rejection mechanism of the AqP membrane may therefore be said to be diffusion controlled. A result of this is that higher rejection values can be obtained by applying a draw solution with a higher osmotic pressure.

4. Conclusions

The rejection of three selected trace organics with two forward osmosis membranes, the CTA membrane from HTI and a new aquaporin membrane from Aquaporin A/S, was investigated. The HTI membrane was found to give only partial rejections for the three compounds, which was in accordance with what others have found for the same membrane. The rejection was found to be controlled by steric hindrance based on excellent steric model fitting. The aquaporin membrane was found to give rejections $>97\%$ for all three compounds, and based on the fitting results of the solution diffusion model, the rejection was controlled by diffusion of the trace organics through the membrane. Furthermore, the aquaporin membrane was found to have a statistically higher flux compared to the HTI CTA membrane. As a result, the aquaporin membrane seems to represent an exciting new type of forward osmosis membrane capable of removing even small neutral organic pollutants efficiently without compromising flux.

Acknowledgements

Financial support from the Otto Mønsted Foundation and the Danish Ministry of Science, Technology and Innovation was received and made a research stay at KU Leuven, Belgium, possible. The project also was supported by *IBISS: Industrial Biomimetics for Sensing and Separation*, a platform funded by the Danish National Advanced Technology Foundation, grant number 97-2012-4.

References

[1] K.V. Plakas, A.J. Karabelas, Removal of pesticides from water by NF and RO membranes—a review, Desalination 287 (2012) 255–265. http://dx.doi.org/10.1016/j.desal.2011.08.003.
[2] A. Karabelas, K. Plakas, Membrane treatment of potable water for pesticides removal, in: P.M. Larramendy (Ed.), Herbicides, Theory and Applications, InTech, 2011, pp. 369–408. http://dx.doi.org/10.5772/13240.
[3] H.T. Madsen, E.G. Søgaard, Applicability and modelling of nanofiltration and reverse osmosis for remediation of groundwater polluted with pesticides and pesticide transformation products, Sep. Purif. Technol. 125 (2014) 111–119. http://dx.doi.org/10.1016/j.seppur.2014.01.038.
[4] T. Cath, A. Childress, M. Elimelech, Forward osmosis: principles, applications, and recent developments, J. Membr. Sci. 281 (2006) 70–87. http://dx.doi.org/10.1016/j.memsci.2006.05.048.
[5] A. D'Haese, P. Le-Clech, S. Van Nevel, K. Verbeken, E.R. Cornelissen, S.J. Khan, et al., Trace organic solutes in closed-loop forward osmosis applications: influence of membrane fouling and modeling of solute build-up, Water Res. 47 (2013) 5232–5244. http://dx.doi.org/10.1016/j.watres.2013.06.006.
[6] M. Xie, L.D. Nghiem, W.E. Price, M. Elimelech, Comparison of the removal of hydrophobic trace organic contaminants by forward osmosis and reverse osmosis, Water Res. 46 (2012) 2683–2692. http://dx.doi.org/10.1016/j.watres.2012.02.023.
[7] N.T. Hancock, P. Xu, D.M. Heil, C. Bellona, T.Y. Cath, Comprehensive bench- and pilot-scale investigation of trace organic compounds rejection by forward osmosis, Environ. Sci. Technol. 45 (2011) 8483–8490. http://dx.doi.org/10.1021/es201654k.
[8] M. Xie, W.E. Price, L.D. Nghiem, M. Elimelech, Effects of feed and draw solution temperature and transmembrane temperature difference on the rejection of trace organic contaminants by forward osmosis, J. Membr. Sci. 438 (2013) 57–64. http://dx.doi.org/10.1016/j.memsci.2013.03.031.
[9] R. Valladares Linares, V. Yangali-Quintanilla, Z. Li, G. Amy, Rejection of micropollutants by clean and fouled forward osmosis membrane, Water Res. 45 (2011) 6737–6744. http://dx.doi.org/10.1016/j.watres.2011.10.037.
[10] M. Xie, W.E. Price, L.D. Nghiem, Rejection of pharmaceutically active compounds by forward osmosis: role of solution pH and membrane orientation, Sep. Purif. Technol. 93 (2012) 107–114. http://dx.doi.org/10.1016/j.seppur.2012.03.030.
[11] A.A. Alturki, J.A. McDonald, S.J. Khan, W.E. Price, L.D. Nghiem, M. Elimelech, Removal of trace organic contaminants by the forward osmosis process, Sep. Purif. Technol. 103 (2013) 258–266. http://dx.doi.org/10.1016/j.seppur.2012.10.036.
[12] B.D. Coday, B.G.M. Yaffe, P. Xu, T.Y. Cath, Rejection of trace organic compounds by forward osmosis membranes: a literature review, Environ. Sci. Technol. 48 (2014) 3612–3624. http://dx.doi.org/10.1021/es4038676.
[13] M.Ø. Jensen, O.G. Mouritsen, Single-channel water permeabilities of *Escherichia coli* aquaporins AqpZ and GlpF, Biophys. J. 90 (2006) 2270–2284. http://dx.doi.org/10.1529/biophysj.105.073965.
[14] M. Kumar, M. Grzelakowski, J. Zilles, M. Clark, W. Meier, Highly permeable polymeric membranes based on the incorporation of the functional water

channel protein Aquaporin Z, Proc. Natl. Acad. Sci. USA 104 (2007) 20719–20724. http://dx.doi.org/10.1073/pnas.0708762104.

[15] C.H. Nielsen, Biomimetic membranes for sensor and separation applications, Anal. Bioanal. Chem. 395 (2009) 697–718. http://dx.doi.org/10.1007/s00216-009-2960-0.

[16] C.Y. Tang, Y. Zhao, R. Wang, C. Hélix-Nielsen, A.G. Fane, Desalination by biomimetic aquaporin membranes: review of status and prospects, Desalination 308 (2013) 34–40.

[17] Y. Zhao, C. Qiu, X. Li, A. Vararattanavech, W. Shen, J. Torres, et al., Synthesis of robust and high-performance aquaporin-based biomimetic membranes by interfacial polymerization-membrane preparation and RO performance characterization, J. Membr. Sci. 423–424 (2012) 422–428. http://dx.doi.org/10.1016/j.memsci.2012.08.039.

[18] L. Thorling, B. Hansen, C. Langtofte, W. Brüsch, R.R. Møller, S. Mielby (Technical report), Grundvand: Status og udvikling 1989–2011 (Groundwater: Status and Development 1989–2011), Geological Survey of Denmark and Greenland, 2012.

[19] Y. Kiso, K. Muroshige, T. Oguchi, M. Hirose, T. Ohara, T. Shintani, Pore radius estimation based on organic solute molecular shape and effects of pressure on pore radius for a reverse osmosis membrane, J. Membr. Sci. 369 (2011) 290–298.

[20] J.G. Wijmans, R.W. Baker, The solution-diffusion model: a review, J. Membr. Sci. 107 (1995) 1–21. http://dx.doi.org/10.1016/0376-7388(95)00102-I.

[21] B. Van der Bruggen, J. Schaep, W. Maes, D. Wilms, C. Vandercasteele, Nanofiltration as a treatment method for the removal of pesticides from ground water, Desalination 117 (1998) 139–147.

[22] B. Van Der Bruggen, J. Schaep, D. Wilms, C. Vandecasteele, A comparison of models to describe the maximal retention of organic molecules in nanofiltration, Sep. Sci. Technol. 35 (2000) 169–182. http://dx.doi.org/10.1081/SS-100100150.

[23] C.H. Tan, H.Y. Ng, Modified models to predict flux behavior in forward osmosis in consideration of external and internal concentration polarizations, J. Membr. Sci. 324 (2008) 209–219. http://dx.doi.org/10.1016/j.memsci.2008.07.020.

[24] J. Wei, X. Liu, C. Qiu, R. Wang, C.Y. Tang, Influence of monomer concentrations on the performance of polyamide-based thin film composite forward osmosis membranes, J. Membr. Sci. 381 (2011) 110–117. http://dx.doi.org/10.1016/j.memsci.2011.07.034.

[25] G.D. Purvis, On the use of isovalued surfaces to determine molecule shape and reaction pathways, J. Comput. Aided. Mol. Des. 5 (1991) 55–80.

[26] L.D. Nghiem, A.I. Schäfer, M. Elimelech, Removal of natural hormones by nanofiltration membranes: measurement, modeling, and mechanisms, Environ. Sci. Technol. 38 (2004) 1888–1896.

Paper VIII

Henrik Tækker Madsen, Abdallah Ammi-said,
Bart Van der Bruggen and Erik G. Søgaard

Addition of adsorbents to NF membrane to obtain complete pesticide removal

Water, Air & Soil Pollution, **226** (2015)

Reprinted with permission from Springer

Water Air Soil Pollut (2015) 226:160
DOI 10.1007/s11270-015-2419-1

Addition of Adsorbents to Nanofiltration Membrane to Obtain Complete Pesticide Removal

Henrik T. Madsen · Abdallah Ammi-said · Bart Van der Bruggen · Erik G. Søgaard

Received: 16 January 2015 / Accepted: 6 April 2015
© Springer International Publishing Switzerland 2015

Abstract Removal of micropollutants from water with NF/RO membranes has received much attention in recent years. However, because of especially diffusion through the polyamide layer, NF/RO membranes never achieve complete removal, which may be a problem given the possibility of micropollutants causing adverse effects in even very low concentrations. In this paper, we have investigated a strategy of implementing adsorbents into the support layer of a NF membrane to increase the overall removal of three selected pesticides by combining membrane rejection and adsorption into one unit operation. The objective of the study was to act as proof of concept for the scheme, as well as to gain insights into how adsorbents may be inserted into the membrane support, and how they affect the membrane performance. The results showed that the addition of the adsorbents to the membrane increased the adsorption capacity of the membrane, and that the adsorbents could be embedded in the membrane without affecting the flux and rejection behaviour. This however depended very much on the specific manufacturing method. Furthermore, the adsorption capacity was found to vary significantly for the three pesticides, indicating a need for adsorbents designed to specifically target a given micropollutant. Overall, the concept of a complete removal membrane is realisable, but several challenges remain to be solved.

Keywords Membrane filtration · Nanofiltration · Adsorption · Pesticides

H. T. Madsen (✉) · E. G. Søgaard
Department of Biotechnology, Chemistry and Environmental Engineering, Aalborg University, Niels Bohrs Vej 8, 6700 Esbjerg, Denmark
e-mail: htm@bio.aau.dk

A. Ammi-said
Laboratory of Hydrometallurgy and Molecular Inorganic Chemistry, Faculty of Chemistry, USTHB, Algiers, Algeria

B. Van der Bruggen
Department of Chemical Engineering, K.U. Leuven, Leuven, Belgium

A. Ammi-said
Department of Chemistry, Faculty of Sciences, UMBB, Boumerdès, Algeria

1 Introduction

Pollution of water resources with organic micropollutants such as pesticides, endocrine disruptors and pharmaceuticals is becoming an increasing global problem (Plakas and Karabelas 2012). Today, the pollution is widespread and micropollutants are found in both natural waters, waste waters and drinking water. An example of this can be found in the fifth global environment outlook report by the UNEP, where it is stated that more than 90 % of water and fish samples today are found to be contaminated with pesticides (*Global Environment Outlook 5, United Nations Environment Programme* 2012). Especially the pollution of drinking water resources may be problematic, and in many places, there is a zero tolerance policy against the presence of micropollutants in drinking water.

Published online: 25 April 2015

One way of removing the micropollutants from the water is by the use of membrane technology such as nanofiltration and reverse osmosis. These have been reported to be effective in removing the micropollutants (Bellona et al. 2004; Hancock et al. 2011; Kimura et al. 2003; Plakas and Karabelas 2012; Xie et al. 2012; Yangali-Quintanilla et al. 2010), but often one important aspect is overlooked; namely, that the NF/RO membranes are incapable of giving a complete removal of the micropollutants. Even in the best cases, rejections are around 98–99 % with the remaining 1–2 % of the micropollutants permeating the membrane (Karabelas and Plakas 2011). This is due to diffusion of the micropollutants through the polyamide layer and cannot be completely avoided for existing NF/RO membranes. If the goal is drinking water completely free of micropollutants, then permeation of even such a small fraction of the micropollutants may be a problem. Furthermore, as micropollutants enter the environment, they often undergo transformation processes, which make them smaller and increasingly polar (Kookana et al. 1998; Sánchez-González et al. 2013; Schipper et al. 2008; Thorling et al. 2013), and therefore increasingly difficult to remove with NF/RO membranes (Madsen and Søgaard 2014). As such, there is a need for a new generation of NF/RO membranes for micropollutant removal that can ensure low costs of filtration and zero permeation of micropollutants.

One way of increasing the total removal of the micropollutants is to view the NF/RO membrane as part of a system, where the filtration step is combined with a second treatment technique, most often adsorption. In such a system, adsorption can be applied either prior to the membrane filtration (Kazner et al. 2008; Sarkar et al. 2007) or after as a polishing step on the permeate stream (Verliefde et al. 2007). Using adsorption prior to filtration can lead to fouling on the membrane if the adsorbents are suspended as with powdered activated carbon (PAC), and it may not be the most efficient way of using the adsorption capacity of the adsorbents. The latter being due to the fact that the adsorbents would come in contact with all of the micropollutants, and not only the fraction permeating the membrane, but also the other constituents in the water, e.g. NOM. If the adsorption step is applied post membrane filtration, an additional separation step would be required if a suspended adsorbent is used, and if a stationary adsorption process, e.g. GAC, is used it will be necessary to also apply UV treatment to the GAC effluent to overcome the issue with microbial growth on the adsorption media. Furthermore, in both scenarios, the treatment is made increasingly complicated by the use of multiple unit operations. A third solution could therefore be to merge the membrane filtration and the adsorption process into one unit operation. This would simplify the treatment and could enhance the adsorption process since it would allow for the use of more advanced adsorption materials, such as specifically optimised nanoparticles (Kim and Van der Bruggen 2010; Ng et al. 2013). The use of these kinds of adsorption materials is not part of the current study, but remains an interesting prospect.

In this study, we have investigated the addition of different adsorbents to a nanofiltration membrane, with special focus on PAC. The PAC was chosen both because activated carbon is the most used adsorbing material and because of its low cost. Carbon nanotubes (CNTs) and acid activated clay were also tested as adsorbents. CNTs due to their documented use as pesticide adsorbents (Pyrzynska 2011; Zhou et al. 2006), and activated clay as a possible low cost alternative. One of the challenges in using adsorbents in membranes is the relative low amount of adsorbent that can be added to the membrane compared to a traditional adsorption column, which makes it necessary to use the available adsorption capacity intelligently and/or consider regeneration strategies. In this study, focus was on how to incorporate the adsorbents in the membrane and on establishing proof of concept, while regeneration is saved for future work. The adsorbents were added to the supporting PES layer of the membrane and were hereby separated from the bulk solution micropollutants. This was done to avoid adsorption of all micropollutants that come into contact with the membrane, and instead to focus the adsorption capacity on the permeating micropollutants. The introduction of adsorbents into a supporting layer with a thin film on top represents a new approach in membrane synthesis. The effect of the particles on the membrane morphology, flux and rejection capability has been studied by comparison with a nanofiltration membrane without adsorbents. Also, the effect of the adsorbents on the membrane's adsorption capability and the long-term adsorption performance has been evaluated. Rejection and adsorption were evaluated for three selected micropollutants: desethyl-desisopropyl-atrazine (DEIA), 2,6-dichlorobenzamide (BAM) and atrazine. These are pesticides and important groundwater pollutants. Furthermore, DEIA and BAM represent cases of

small polar transformation products for which removal with traditional membranes is difficult, and by comparing results for atrazine, the mother compound of DEIA, and DEIA the effect of the transformation process on the removal efficiency could be studied. Atrazine is in itself an important pollutant and despite being banned from use in 2004 in the EU under directive 91/414/EEC, it is still one of the most used pesticides in the USA (Grube et al. 2011) and is used in Australia (Australian Pesticides and Veterinary Medicines Authority 2008). From a scientific point of view, it is especially interesting to include atrazine in pesticide/membrane studies since it is the most heavily studied pesticide in such studies. In an overview of pesticide/membrane studies, atrazine was found to account for 23.9 % of the total sum of pesticides used in the experiments (Karabelas and Plakas 2011). The use of atrazine therefore allows for comparison of membrane performance across different studies.

The addition of adsorbing particles to the membrane introduces complications related to stability and rejection capability when manufacturing a thin film membrane, and the variability of the physicochemical properties of the micropollutants creates challenges in finding the optimal adsorbent. In this paper, we present results on how a composite adsorbent NF membrane may be constructed and discuss how effective it may be in treating water polluted with pesticides. Due to the challenges in this field, the paper can in many ways be considered a "lessons to be learned" paper, and it introduces the concept of the complete rejection membrane for micropollutants.

2 Experimental Work

2.1 Materials

Atrazine, BAM and DEIA were purchased at Sigma-Aldrich (Pestanal, Fluka). Details and the physicochemical properties of these can be found elsewhere (Madsen and Søgaard 2014). PES beads (Radel-100, Solvay, Speciality Polymers Germany GmbH, Düsseldorf, Germany), *N*-methyl-2-pyrrolidone (NMP; 99.5 %, Sigma Aldrich, St. Louis, MO, USA), distilled water and a non-woven fabric layer (FO2471, Viledon, Weinheim,Germany) were used to manufacture the PES support layer. Polyamide thin films were formed from the diamine monomer piperazine (PIP; 99 %) and the acid chloride monomer trimesoylchloride (TMC; 98 %). These were provided by Across Organics (Geel, Belgium). The solvents used for PIP and TMC were MilliQ water and hexane (technical, Nyssens Graphics, Belgium), respectively. PAC was acquired from Merck. Multi walled CNTs (OD×ID×L; 10 nm×4.5 nm×3–6 μm) was purchased from Sigma Aldrich.

Activated clay was produced for this specific study through an acid treatment procedure. Raw green clay was provided from El-Golea region in Ghardaïa city (Southeast Algeria), and fine fraction was obtained by dispersion, sedimentation and siphoning of particles ≤2 μm in size. After rendering each sample homoionic and sodic, the clay was activated with sulphuric acid at 80 °C in the order to improve physicochemical characteristics. Twenty grams of sample were mixed with 100 mL of 1.5 M sulfuric acid solution was refluxed in a 250 mL glass flask for 4 h. After acid treatment, the solids were separated, washed with distilled water and dried at 105 °C overnight. Illite was identified as the clay structure by XRD, and the specific surface area was determined to be 113.6 m^2/g.

2.2 Pesticide Analysis

Pesticides were analysed with a HPLC/UV system (1200 Infinity, Agilent Technology), equipped with a ZORBAX Eclipse XDB-C18 5 μm column and using eluent mixtures of acetonitrile (A) and MilliQ (B). For atrazine, a 70/30 (A/B) mixture was used; for BAM, 50/50 mixture and for DEIA, a 30/70 mixture. The injection volume was 100 μL and the flow rate 400 μL/min. The chosen absorption wavelength was 220 nm for atrazine and 210 nm for BAM and DEIA.

2.3 Membrane Preparation

Thin film composite (TFC) membranes were prepared according to the procedure described by Zhang et al. (2012), where the conditions for the preparation of a NF membrane were optimised. In general, the membrane was prepared by first casting a PES layer on a non-woven support and then adding the thin polypiperazine layer on top of the PES. When particles were added to the membrane, they were added to the PES layer.

The PES support layer was prepared via phase inversion of the PES solution by immersion precipitation in a non-solvent (distilled water) bath. First, 12.5 g of PES beads were dissolved in 40.5 mL NMP to create a

homogenous 23 % *wt/wt* polymer solution. The PES solution was left stirring for 1 day, and air bubbles were removed prior to casting. For membranes with adsorbent particles, these were added to the NMP solution prior to the PES beads in concentrations of 0.1, 0.5, 1.0 and 2.0 wt/wt% ($m_{adsorbent}/m_{NMP}$) (0.33, 1.67, 3.33 and 6.66 wt/wt% ($m_{adsorbent}/m_{PES}$)). Before casting, the non-woven support was taped to a glass plate to ensure a completely flat surface. Then the non-woven support was wetted with NMP to prevent the casting solution from penetrating into the non-woven support. A 250 μm PES film was spread over the non-woven fabric with a casting knife pushed by a filmograph (K4340 Automatic Film Applicator, Elcometer), and the film was then immediately immersed into a non-solvent bath at room temperature. After 15 min, the PES membrane was removed from the non-solvent bath, and washed thoroughly with distilled water before being stored in a distilled water bath.

The PIP top layer was made via interfacial polymerization. A piece of the PES membrane was clamped together between two frames, and excess water was removed from the surface with pressurized air. Then 10 mL of a 4 wt/vol% aqueous PIP solution was spread over the surface and allowed to stay there for 30 s, after which the excess PIP was drained off and the membrane surface dried with pressurized air. Ten millilitres of a 0.5 wt/vol% TMC solution was spread over the surface and left to react for 30 s to form the polypiperazine layer, after which the excess hexane was poured off. The membrane was then washed with 10 mL pure hexane to remove unreacted monomers and transferred to a vacuum oven set at 60 °C to promote crosslinking. Finally, the membrane was rinsed successively with distilled water.

In the study, the use of a sandwich structure for the support layer is also discussed. In a sandwich structure, the support structure is split in two layers, a bottom layer of 150 μm containing the adsorbents, and a top layer of 100 μm with no adsorbents. Two approaches were attempted to make this structure. First in which successive phase inversions were used and second in which both layers were cast on the top of each other before phase inversion. In the first approach, a 150 μm layer of the PES solution containing adsorbents was spread over the non-woven fabric and then immersed in the non-solvent bath. After precipitation and drying, a 100 μm layer of pure PES solution was spread on the top of the solidified layer and then immersed into a fresh non-solvent bath. Using this method led to poor adhesion between the two support layers, and it was therefore abandoned. In the second approach, 150 μm adsorbent containing PES solution was spread on the non-woven fabric. Immediately after this, a 100 μm layer of pure PES solution was spread on the top of the first layer. This was done by using a casting knife with a casting height of 250 μm. Finally, the two-layered film was immersed in the non-solvent bath for precipitation. By casting both support layers before phase inversion, a stable support structure was obtained, and this second approach was therefore the chosen method for this study.

2.4 Filtration Protocol

The membranes were tested in a dead-end filtration setup (Sterlitech HP4750 Stirred Cell) at room temperature and 10 bar transmembrane pressure. The active membrane area was 14.6 cm^2, and the maximum feed volume was 250 mL. Before adsorption experiments, the membranes were compacted until a steady flux was measured. This was taken as the pure water flux. To measure adsorption, the procedure described by Plakas and Karabelas (Plakas and Karabelas 2008) was used as inspiration. In our experiments, a solution (100 or 200 mL) of 1 mg/L pesticide was transferred to the filtration cell and filtered until a recovery of 50 %. Then permeate, concentrate and feed concentrations and volumes were determined and a mass balance was used to determine the mass of adsorbed pesticide.

$$m_{ads} = c_F \cdot V_F - (c_P \cdot V_P + c_C \cdot V_C) \quad (1)$$

Since the filtration cell is of the dead-end type, it may be subjected to concentration polarisation, which could affect rejection. However, due to the use of a magnetic stirrer in the filtration cell and similar rejection performances of the membranes with and without adsorbents, it is not estimated to affect the conclusions on the adsorption performance.

2.5 Membrane Characterisation

Membranes were characterised with contact angle measurements (DSA 10 Mk2, Krüss, Germany) with MilliQ as the liquid. Each membrane was characterised by measurements on at least three separate membrane samples with each sample being analysed with three drops.

To visualise the surface and cross section of the membranes, SEM images were taken (Philips XL30 FEG).

3 Results and Discussion

3.1 Effect of Adsorbent on Membrane

A direct implementation of the adsorbents into the PES support layer was found to have detrimental effects on the performance of the TFC membrane. In Fig. 1, it can be seen that all three types of adsorbents led to equal feed and concentrate concentrations, hereby showing that no real rejection was taking place. Flux was also affected negatively as shown in Fig. 2, where, for all the investigated adsorbent concentrations, the flux was significantly lower than the flux of the pure membrane. The flux of the 0.1, 0.5 and 1.0 % active carbon membranes was all equal, but increasing the concentration from 1.0 to 2.0 % resulted in much lower fluxes. This was observed for all three types of adsorbents and seemed to be a feature determined primarily by concentration and not type of adsorbent. However, from the inset plot, it can be seen that the effect apparently was largest for activated carbon and clay, indicating some effect of the type of adsorbent. The results in the inset plot in Fig. 2 also indicate that the effect of the concentration is discrete and not continuous. The recorded fluxes for the 2 % membranes were either equal to the flux found for the lower concentrations or much lower. In the experiments, the flux of all membranes was high at the start of the compaction, but continued to decrease for the 2 %

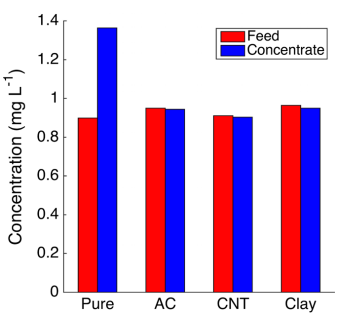

Fig. 1 Feed and concentrate concentration of atrazine NF membranes with no adsorbents (Pure), activated carbon (AC), carbon nanotubes (CNTs) and clay. The results were independent of adsorbent concentration

membranes. It may seem surprising that changes in the support layer of a TFC membrane can lead to changes in performance since this is thought to be governed mainly by the top layer, but similar results have been found elsewhere (Sotto et al. 2012), where desalination performance of a membrane was enhanced by alterations of the support layer.

Because rejection is a property of the top layer, the results indicate that the top layer was affected by the addition of the adsorbents. This is supported by the contact angle measurements of the membranes shown in Fig. 3. If the top layer was unaffected by the adsorbents and covered the adsorbent filled support membrane completely, no significant difference in contact angle would be expected between the pure and the adsorbent membranes. However, the contact angle was found to increase when adding the adsorbents to the membrane. For PAC, the contact angle increased with the concentration of the adsorbents from 0.1 to 1.0 % indicating that the influence is related to the amount of adsorbents. Further increase in PAC concentration did on the other hand not lead to further increases in contact angle, but rather a small decrease. This could be an indication that the addition of adsorbents can affect the contact angle of the membrane through more than one mechanism. An interesting observation is that the contact angle also increases with the same amount when using the hydrophilic clay particles. This indicates that the increased hydrophobicity is not due to adsorbents penetrating the top layer and affecting the polarity, but rather due to increased access to the support membrane, which is more hydrophobic. Access to the support layer could also explain why the membranes loose rejection capability, since it would indicate the existence of imperfections in the top layer through which pesticides could permeate the membrane unhindered. However, imperfections in the top layer would not be expected to result in lower water fluxes as was observed, but rather higher or similar fluxes. A possible explanation for why this was observed is that the effective pore volume of the support membrane could be reduced by the introduction of the adsorbents, or that an increasing amount of unconnected pores are formed in the phase inversion process.

To investigate the effect of the adsorbents on the membrane morphology in greater detail, SEM images were taken, see Fig. 4. The addition of the carbon particles still results in the formation of a finger-pore structure in the UF membrane, but also seems to affect

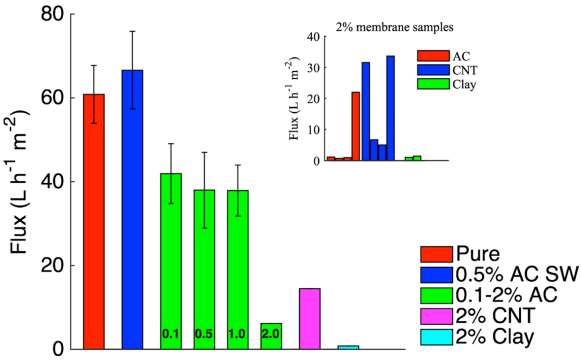

Fig. 2 Effect of adsorbent concentration on membrane flux. *Error bars* represent standard deviation from quadruple measurements of different membrane pieces. No error bars are added to the 2 % membranes, and instead the variation is represented by the inset plot of the flux of each of the measured samples. This is because variation here was very high and was better represented by the inset plot

the structure of the UF membrane near the surface. Compared to the pure membrane (Fig. 4a), the structure of the adsorbent loaded membranes (Fig. 4b–e) seems to contain a higher number of smaller enclosed pores close to the surface of the membrane. This is especially visible from the ×5000 SEM images to the right in Fig. 4. The same observation has also been reported elsewhere to occur for PES membranes with clay nanoparticles (Mierzwa et al. 2013) and may explain the decreased flux. A higher number of horizontally blocked pores or less vertically connected pores would lead to lower fluxes. Further, the presence of smaller pores close to the membrane may also result in direct blockage of the pores by the adsorbents. The reason for the increased number of smaller pores may be that the adsorbent particles near the surface are large enough to act as terminating surfaces for the finger pore formation. Once finger pore formation has begun, growth is propagated by the shrinkage of the solidified polymer, which drains the freshly precipitated polymer at the bottom of the pore to the sides of the pore. Pore growth is terminated when the polymer solution at the bottom of the pore is solidified before it can be drained to the side (Strathmann and Kock 1977). If the casting solution adheres to the surface of the adsorbents, the polymer fluid may be prevented from moving to the sides of the finger pore, and thus solidify at the particle surface and sealing of the pore at an early stage. The addition of the adsorbents to the polymer solution was also found to increase viscosity. Higher viscosity could also lower mobility of the polymer solution leading to early termination of the finger pores.

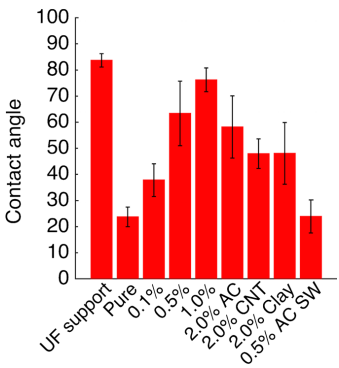

Fig. 3 Contact angle measurements of membranes with different amounts of adsorbents added to the support layer. *Error bars* represent the standard deviation of the measurements on three membrane pieces

From the recorded SEM images, it was not possible to identify a collapse of the membrane structure for the 2 % membrane to explain the drastically lower flux. However, it is possible that an increased number of smaller pores near the membrane surface may result in a less stable structure, which during compaction may collapse to give a denser layer.

Since the detrimental effects seemed to be related to adsorbents near the membrane surface, a new membrane construction method was investigated.

3.2 Construction of Sandwich Membrane

To separate the adsorbents from the thin layer, a sandwich construction (SW) was made. In this method, a 150 μm PES layer with adsorbents was spread over the

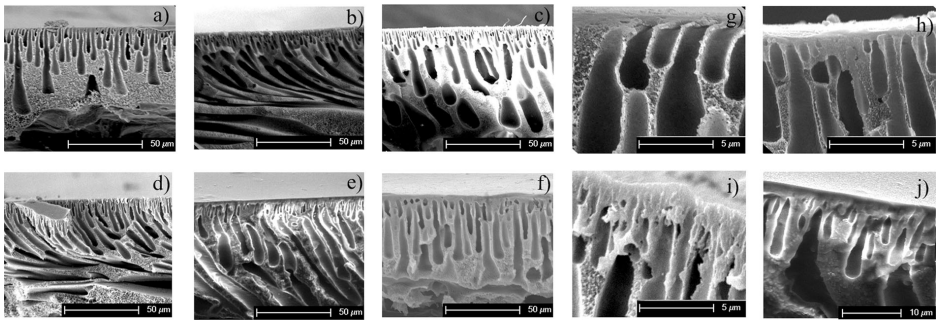

Fig. 4 SEM images of cross-sectional views of membranes at ×500 (**a**–**f**) and ×5000 (**g**–**j**) resolution. **a** Pure membrane, **b** 0.1 % PAC, **c** 0.5 % PAC, **d** 1.0 % PAC, **e** 2.0 % PAC, **f** 0.5 % PAC SW, **g** pure membrane, **h** 0.5 % AC, **i** 1.0 % AC and **j** 2.0 % AC (×2000)

non-woven support, after which a 100 μm layer of pure PES was spread on the top of this layer. This produced a PES membrane of the same thickness, but without direct contact between the adsorbents and the thin film. To have a high concentration of adsorbent without compromising the stability of the membrane, a concentration of 0.5 % activated carbon was chosen. Activated carbon was chosen based on initial adsorption experiments in which it was found to outperform the clay and due to its lower cost compared to CNTs.

As can be seen from Figs. 2 and 3, the use of a sandwich structure resulted in a pure water flux and a contact angle that was identical to that of the membrane without adsorbents (pure), indicating that the particles were effectively separated from the top layer. From the SEM images in Fig. 4, it can be seen that the morphology was also similar with long connected finger pores. The membrane was also capable of rejecting the pesticides as shown in Fig. 4, where the measured rejection for the pure and the 0.5 % AC SW membrane are compared. The apparent rejection is higher for the 0.5 % AC SW membrane, but as can be seen this is mainly due to difference in adsorption. When the rejections are corrected for adsorption, it is not possible to statistically distinguish the performance of the two membranes. Together with the flux and contact angle results, this shows that the performance of the membranes is not affected by the addition of the activated carbon when the sandwich structure is used.

Further, it can also be seen from Fig. 5 that there is a large difference in the rejection of each of the three pesticides, and that the rejection for especially DEIA and BAM is so low that this kind of membrane would usually not be classified as applicable for remediation. However, for a study of changed adsorption behaviour, the membrane is useful because it allows for measureable quantities of permeating pesticides, which can be used to determine the degree of adsorption. If a membrane with high rejection (>95 %) had been used, the permeate concentration would be too low to accurately determine the amount of pesticide that had been adsorbed.

3.3 Effect of Adsorbent on Membrane Adsorption Capability

To evaluate the effect of the activated carbon on the adsorption capability of the membrane, the two

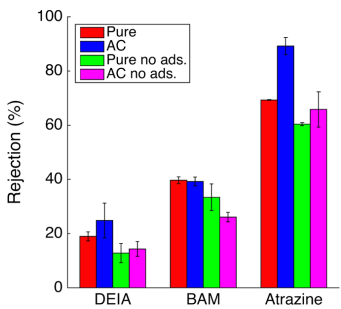

Fig. 5 Comparison of rejection for a pure membrane and a sandwich membrane observed in the initial 100 mL of collected permeate. The bars "Pure no ads." and "AC no ads." illustrate the rejection values for the two membranes when adsorption is removed. These values are calculated by adding the adsorbed mass of pesticide to the permeate concentration to obtain the theoretical permeate concentration when no adsorption takes place. *Error bars* represent the standard deviation of triplicate measurements

membranes were compared on the degree of adsorbed pesticide per square metre of membrane area after collection of 100 mL permeate, see Fig. 6. Here, it can be seen that the adsorption increased significantly for all of the pesticides, but with a large difference between DEIA/BAM and atrazine. By adding PAC to the membrane, the adsorption of DEIA increased with a factor of 1.6 and BAM adsorption doubled, but adsorption of atrazine quadrupled, showing a higher affinity of atrazine to the PAC. However, because of the differences in rejection for the three pesticides, fewer atrazine molecules will have permeated the membrane and hereby been in contact with the PAC relative to DEIA molecules after collection of 100 mL permeate, and the bar plot in Fig. 5 cannot be used to directly compare the difference in affinity. If the degree of adsorption is compared at equal amount of permeating pesticides, where permeating pesticides are taken as the sum of the moles of pesticide in the permeate and the moles of adsorbed pesticide, a better comparison of the different affinities for the pesticides to the activated carbon can be achieved. By using this approach, it can be seen that 3.4 and 5.5 times more atrazine can be adsorbed compared to BAM and DEIA, respectively (Table 1).

The differences in affinity illustrate the effect of the transformation process of atrazine on the adsorption efficiency. By losing its ethyl and isopropyl side groups, atrazine becomes smaller and increasingly polar, both of which affects the adsorption negatively. The decreased size will allow DEIA to permeate pores of the PAC particles more easily reducing steric adsorption, and the increasing polarity will decrease the hydrophobic intermolecular attraction between PAC and DEIA.

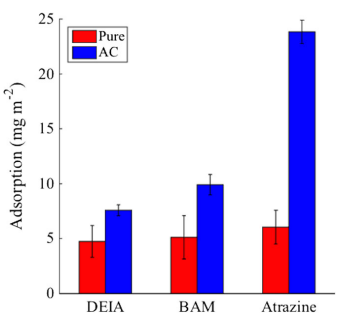

Fig. 6 The adsorption capability of the pure and the active carbon sandwich membrane. The *bars* show the mass of adsorbed pesticide after collection of the initial 100 mL permeate of a 1 mg/L feed solution. *Error bars* represent the standard deviation of triplicate measurements

3.4 Long Run Adsorption

To evaluate the long run adsorption capability of the membrane, the accumulated amount of adsorbed pesticide, Fig. 7, and the adsorption efficiency (α), Fig. 8, was determined as a function of the amount of permeating pesticides. Based on the same reasoning as before, the amount of permeating pesticides was used as the independent variable instead of the volume of collected permeate. The adsorption efficiency was calculated as the percentage of the permeating pesticides that was adsorbed in the membrane as described with Eq. 2.

$$\alpha = \frac{m_{\text{ads}}}{m_{\text{ads}} + m_{\text{P}}} \tag{2}$$

Where m_{ads} is the mass of the specific pesticide adsorbed in the membrane as determined with Eq. 1, and m_P is the mass of the pesticide in the permeate. The sum of these represents the mass of the pesticide that would be present in the permeate if no adsorption took place.

As in Fig. 6, the difference in affinity of the three pesticides can be seen from the two plots in Figs. 7 and 8. From the plot in Fig. 7, it can also be seen that due to the difference in affinity, the absolute difference in accumulated amount of adsorbed pesticide continues to increase as more pesticide molecules permeate the membrane. However, especially for atrazine the incremental increase between measurements decreases. This is shown more clearly in Fig. 8, where it can be seen that for atrazine, the adsorption efficiency decreases from initially 68.7 to 12–13 % after 500 μmol m^{-2}. A decrease is also seen for BAM and DEIA, although not as significant as for atrazine. The reason that an adsorption efficiency of 100 % is never achieved for any of the three pesticides is most likely due to the very short contact time in an adsorbing membrane compared to a traditional adsorption column. An interesting observation for all three pesticides is that after the initial decrease, the adsorption efficiency seems to reach a steady level. The result is that the plot of the accumulated amount of adsorbed pesticide in Fig. 7 becomes linear when this steady state adsorption is reached, and the membrane was therefore never found to become saturated.

Table 1 Comparison of standard measures for adsorption

Pesticide	Adsorption after 100 mL permeate (mg/m^2)		Adsorption after 500 μmol/m^2 of pesticide (mg/m^2)	
		Ratio to atrazine		Ratio to atrazine
Atrazine	23.6	1	42.4	1
BAM	10.0	0.42	12.4	0.29
DEIA	7.56	0.32	7.66	0.18

The table compares the relative adsorption performance of the membrane based on either a specific volume of pesticide solution or specific number of moles of pesticides. These will be different due to different rejection values of the three pesticides. Five hundred micromoles per metre squared is equal to 110 mL DEIA, 148 mL BAM and 305 mL atrazine permeate

3.5 Evaluation of Membrane Performance

Two key performance indicators for a membrane with incorporated adsorbents will be the operation capacity, V_{cap}, defined as the volume of feed water that can be treated before the adsorption efficiency of the membrane falls beneath a fixed level, and the volume of permeate that can be produced in the process, $V_{P,ads}$. In the current study, the pesticide with the highest affinity for the adsorbents was atrazine, and it will therefore be used to evaluate the potential V_{cap} and $V_{P,ads}$ of a pesticide adsorbing membrane. In this evaluation, the membrane is assumed to be optimised for pesticide removal and will operate with a rejection of 98 % and a recovery of 70 %. The polluted water is assumed to have a concentration of 0.1 μg/L, which is typical for polluted groundwater (Thorling et al. 2013). Finally, the limiting adsorption efficiency is set to 65 %, a level which for atrazine was reached when 100 μmol/m^2 ($n_{p,lim}$) had permeated the membrane. V_{cap} can then be determined by calculating the volume of permeate produced at $n_{e,lim}$ ($V_{P,ads}$), and dividing this with the recovery. $V_{P,ads}$ can be determined from the permeate concentration, which will give the number of moles of pesticide that are transported through the membrane per volume permeate (C_P, μmol/m^3). Since we know that the adsorption capacity is used up when 100 μmol/m^2 pesticide have permeated the membrane, this number can be divided with the permeate concentration to yield $V_{P,ads}$.

$$V_{\mathrm{cap}} = \frac{V_{\mathrm{P,ads}}}{Rec} \tag{3}$$

$$V_{\mathrm{P,ads}} = \frac{n_{\mathrm{e,lim}}}{C_P} = n_{\mathrm{e,lim}} \frac{1 + \frac{1}{2}(1-r)\frac{Rec}{1-Rec}}{\frac{1}{2}C_{\mathrm{F}}(1-r)\left(1 + \frac{1}{1-Rec}\right)} \tag{4}$$

Where r is rejection and Rec is recovery both as decimals numbers between 0 and 1. In such a scenario,

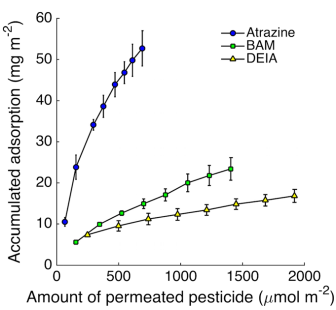

Fig. 7 Accumulation of pesticides in the membrane. The figure shows the accumulated amount of pesticide adsorbed in the membrane as a function of the moles of pesticides that have permeated/been in contact with the interior of the membrane. *Error bars* represent the standard deviation of triplicate measurements

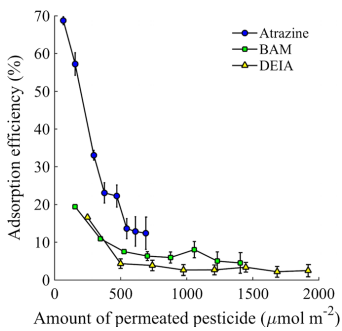

Fig. 8 Change in adsorption performance. The figure shows how adsorption efficiency changes as a function of the total amount of pesticides that has permeated the membrane. *Error bars* represent the standard deviation of triplicate measurements

V_{cap} is 7253 m^3/m^2 and $V_{P,ads}$ 5077 m^3/m^2. These are reasonably high numbers. If an average flux of 30 $L/m^2/h$ is assumed, then it would take 19.3 years to reach the 5077 m^3/m^2.

3.6 Micropollutant Free Water

As stated in the introduction, the motivation for adding adsorbents to membranes was to achieve a zero permeation of pesticides and other micropollutants through the membrane. It is clear that the membrane used in these experiments is not well suited for this task due to its low rejection of especially BAM and DEIA, but as argued in Section 3.2, the low rejection made the membrane suitable to study the changed adsorption behavior. An optimized membrane, like the one assumed in Section 3.5, would be able to achieve a much higher removal. However, since an adsorption efficiency of 100 % was never observed, even an optimized membrane would not be able to ensure zero permeation. To reach the goal of a micropollutant free permeate, the adsorption efficiency therefore needs to be improved. This could be done by developing adsorbents with higher affinities and increasing the contact between the micropollutants and the adsorbents. The latter could be done by increasing the adsorbent concentration and increasing the thickness of the adsorbing layer. Also, by lowering the flux, a longer contact time could be achieved. Design and operation of adsorbing membranes may therefore be very different from traditional membranes, where focus is on making the membrane as thin and the flux as high as possible, but by changing focus to micropollutant removal, it may be possible to come close to a membrane that can produce micropollutant free water.

3.7 Future Work

As shown in the calculation of the operational capacity, the membrane can potentially operate at sufficiently high adsorption efficiency during its entire lifetime. However, if the membrane is less ideal and the pesticide concentration is higher compared to the scenario described in Section 3.5, the membrane may reach its operational capacity within the expect lifetime. In such a case, the membrane must either be replaced or regenerated. A possible way of regenerating the membrane could be to clean it with suitable organic solvents, but this would not be without challenges. First of all, the solvent would need to be able to dissolve the adsorbed pesticides without damaging the membrane, which would need to be made of a solvent resistant material. Secondly, because the adsorption takes place inside the membrane, regeneration with solvents may be difficult since these will tend to be larger than water molecules and therefore more difficult to force through the membrane, especially if a RO membrane is used, and thirdly, the usefulness of solvents may also be limited if the membrane is used in drinking water production where such solvents are undesired.

A second issue that must be handled is the low affinity for small polar pesticides such as BAM and DEIA to the traditional adsorbents that was used in this study. Here is a need for other types of adsorbents. One possibility could be nanoparticles with physicochemical properties designed to adsorb compounds with specific polarity. This could be inorganic nanoparticles such as silica, where the surface properties can be modified through the use of silane coupling agents or organic nanoparticles produced from different starting materials.

Leaching of adsorbents from the membrane should also be investigated. No substantial leaching was observed in this study, but especially if nanoparticles are used as adsorbents, leaching of adsorbents in even low concentrations could pollute the permeate.

Finally, further research into the membrane production will also be needed. As was shown in this study, a sandwich structure can be effectively used to ensure a stable membrane. However, the method used in this study for the making of the double PES layer can be optimised. We applied the two layers of PES directly on top of each other before the phase inversion process, and even though the viscosity of the two solutions reduced mixing of the layers, mixing could not be completely avoided. This leads to less homogenous layers and increases the risk of contact between the adsorbents and the top layer.

4 Conclusion

In this work, we have investigated the implementation of adsorbents in a NF membrane matrix to lay the foundation for the production of a membrane that can obtain complete removal of micropollutants such as pesticides. It was found that in order to maintain flux and rejection, the membrane should be prepared as a sandwich construction in which a layer of PES without adsorbents were placed in between the PES layer with

adsorbents and the thin film top layer. When this was not done, flux decreased and rejection capability of the membrane was ruined. It was found that the presence of adsorbents near the surface of the support membrane lead to the formation of an increased amount of small enclosed pores, which may explain the decreased flux, and that increasing adsorbent concentration leads to increased contact angles, which could be an indication of contact with the hydrophobic support membrane.

By using a sandwich construction with 0.5 % PAC in the adsorbent layer, it was possible to significantly increase the adsorption capability of the membrane. The adsorption efficiency was found to decrease as pesticides permeated the membrane until reaching a steady state level of adsorption. Adsorption was highest for atrazine, whereas adsorption of the two pesticide transformation products BAM and DEIA was significantly lower. Comparison with atrazine and DEIA shows that transformation processes that lead to smaller and more polar compounds may make it increasingly difficult to remove the pollutant efficiently.

Acknowledgments Thanks go to Giuseppe Genduso and Jiuyang Lin for help with SEM and membrane manufacturing. Economic support was received from the Otto Mønsted foundation. Financial support from the Danish Ministry of Science, Technology, and Innovation in the form of a Ph.D. study grant is acknowledged

References

Australian Pesticides and Veterinary Medicines Authority. (2008). *Atrazine final review report and regulatory decision*. Australian Pesticides and Veterinary Medicines Authority.

Bellona, C., Drewes, J. E., Xu, P., & Amy, G. (2004). Factors affecting the rejection of organic solutes during NF/RO treatment—a literature review. *Water Research, 38*, 2795–2809. doi:10.1016/j.watres.2004.03.034.

Global Environment Outlook 5, United Nations Environment Programme. (2012).

Grube, A., Donaldson, D., Kiely, T., & Wu, L. (2011). *Pesticides industry sales and usage 2006 and 2007 market estimates*. United States Environmental Protection Agency.

Hancock, N. T., Xu, P., Heil, D. M., Bellona, C., & Cath, T. Y. (2011). Comprehensive bench- and pilot-scale investigation of trace organic compounds rejection by forward osmosis. *Environmental Science & Technology, 45*(19), 8483–8490. doi:10.1021/es201654k.

Karabelas, A., & Plakas, K. (2011). Membrane treatment of potable water for pesticides removal. In P. M. Larramendy (Ed.), *Herbicides, theory and applications* (pp. 369–408). InTech. doi:10.5772/13240.

Kazner, C., Lehnberg, K., Kovalova, L., Wintgens, T., Melin, T., Hollender, J., & Dott, W. (2008). Removal of endocrine disruptors and cytostatics from effluent by nanofiltration in combination with adsorption on powdered activated carbon. *Water Science & Technology, 58*(8), 1699–1706. doi:10.2166/wst.2008.542.

Kim, J., & Van der Bruggen, B. (2010). The use of nanoparticles in polymeric and ceramic membrane structures: Review of manufacturing procedures and performance improvement for water treatment. *Environmental Pollution, 158*(7), 2335–2349. doi:10.1016/j.envpol.2010.03.024.

Kimura, K., Amy, G., Drewes, J. E., Heberer, T., Kim, T.-U., & Watanabe, Y. (2003). Rejection of organic micropollutants (disinfection by-products, endocrine disrupting compounds, and pharmaceutically active compounds) by NF/RO membranes. *Journal of Membrane Science, 227*(1–2), 113–121. doi:10.1016/j.memsci.2003.09.005.

Kookana, R. S., Baskaran, S., & Naidu, R. (1998). Pesticide fate and behaviour in Australian soils in relation to contamination and management of soil and water: a review. *Australian Journal of Soil Research*, *36*. doi:10.1071/SR97109.

Madsen, H. T., & Søgaard, E. G. (2014). Applicability and modelling of nanofiltration and reverse osmosis for remediation of groundwater polluted with pesticides and pesticide transformation products. *Separation and Purification Technology, 125*, 111–119. doi:10.1016/j.seppur.2014.01.038.

Mierzwa, J. C., Arieta, V., Verlage, M., Carvalho, J., & Vecitis, C. D. (2013). Effect of clay nanoparticles on the structure and performance of polyethersulfone ultrafitltration membranes. *Desalination, 314*, 147–158.

Ng, L. Y., Mohammad, A. W., Leo, C. P., & Hilal, N. (2013). Polymeric membranes incorporated with metal/metal oxide nanoparticles: a comprehensive review. *Desalination, 308*, 15–33. doi:10.1016/j.desal.2010.11.033.

Plakas, K. V., & Karabelas, A. J. (2008). Membrane retention of herbicides from single and multi-solute media: the effect of ionic environment. *Journal of Membrane Science, 320*, 325–334. doi:10.1016/j.memsci.2008.04.016.

Plakas, K. V., & Karabelas, A. J. (2012). Removal of pesticides from water by NF and RO membranes—a review. *Desalination, 287*, 255–265. doi:10.1016/j.desal.2011.08.003.

Pyrzynska, K. (2011). Carbon nanotubes as sorbents in the analysis of pesticides. *Chemosphere, 83*(11), 1407–1413. doi:10.1016/j.chemosphere.2011.01.057.

Sánchez-González, S., Pose-Juan, E., Herrero-Hernández, E., Álvarez-Martín, A., Sánchez-Martín, M. J., & Rodríguez-Cruz, S. (2013). Pesticide residues in groundwaters and soils of agricultural areas in the Águeda River Basin from Spain and Portugal. *International Journal of Environmental Analytical Chemistry, 93*(15), 1585–1601. doi:10.1080/03067319.2013.814122.

Sarkar, B., Venkateswralu, N., Rao, R. N., Bhattacharjee, C., & Kale, V. (2007). Treatment of pesticide contaminated surface water for production of potable water by a coagulation-adsorption-nanofiltration approach. *Desalination, 212*(1–3), 129–140. doi:10.1016/j.desal.2006.09.021.

Schipper, P. N. M., Vissers, M. J. M., & van der Linden, A. M. A. (2008). Pesticides in groundwater and drinking water wells: Overview of the situation in the Netherlands. *Water Science*

& *Technology, 57*(8), 1277–1286. doi:10.2166/wst.2008.255.

Sotto, A., Rashed, A., Zhang, R.-X., Martínez, A., Braken, L., Luis, P., & Van der Bruggen, B. (2012). Improved membrane structures for seawater desalination by studying the influence of sublayers. *Desalination, 287*, 317–325. doi:10.1016/j.desal.2011.09.024.

Strathmann, H., & Kock, K. (1977). The formation mechanism of phase inversion membranes. *Desalination, 21*, 241–255.

Thorling, L., Brüsch, W., Hansen, B., Larsen, C. L., Mielby, S., Troldnorg, L., & Sørensen, B. L. (2013). *Grundvand - Status og udvikling 1989–2012 (Groundwater: Status and development 1989–2012). Technical report, Geological Survey of Denmark and Greenland, 2013.*

Verliefde, A. R. D., Heijman, S. G. J., Cornelissen, E. R., Amy, G., Van der Bruggen, B., & van Dijk, J. C. (2007). Influence of electrostatic interactions on the rejection with NF and assessment of the removal efficiency during NF/GAC treatment of pharmaceutically active compounds in surface water. *Water Research, 41*(15), 3227–3240. doi:10.1016/j.watres.2007.05.022.

Xie, M., Nghiem, L. D., Price, W. E., & Elimelech, M. (2012). Comparison of the removal of hydrophobic trace organic contaminants by forward osmosis and reverse osmosis. *Water Research, 46*(8), 2683–2692. doi:10.1016/j.watres.2012.02.023.

Yangali-Quintanilla, V., Maeng, S. K., Fujioka, T., Kennedy, M., & Amy, G. (2010). Proposing nanofiltration as acceptable barrier for organic contaminants in water reuse. *Journal of Membrane Science, 362*(1–2), 334–345. doi:10.1016/j.memsci.2010.06.058.

Zhang, R.-X., Vanneste, J., Poelmans, L., Sotto, A., Wang, X.-L., & Van der Bruggen, B. (2012). Effect of the manufacturing conditions on the structure and performance of thin-film composite membranes. *Journal of Applied Polymer Science, 135*, 3755–3769. doi:10.1002/app.36542.

Zhou, Q., Xiao, J., Wang, W., Liu, G., Shi, Q., & Wang, J. (2006). Determination of atrazine and simazine in environmental water samples using multiwalled carbon nanotubes as the adsorbents for preconcentration prior to high performance liquid chromatography with diode array detector. *Talanta, 68*(4), 1309–1315. doi:10.1016/j.talanta.2005.07.050.

Paper IX

Henrik Tækker Madsen, Erik G. Søgaard and Jens Muff

Study of degradation intermediates formed during electrochemical oxidation of pesticide residue 2,6-dichlorobenzamide (BAM) at boron doped diamond (BDD) and platinum-iridium anodes

Chemosphere, **109** (2014), 84-91

Reprinted with permission from Elsevier

Author's personal copy

Chemosphere 109 (2014) 84–91

Contents lists available at ScienceDirect

Chemosphere

journal homepage: www.elsevier.com/locate/chemosphere

Study of degradation intermediates formed during electrochemical oxidation of pesticide residue 2,6-dichlorobenzamide (BAM) at boron doped diamond (BDD) and platinum–iridium anodes

Henrik Tækker Madsen *, Erik Gydesen Søgaard, Jens Muff *

Department of Biotechnology, Chemistry and Environmental Engineering, Aalborg University, Niels Bohrs Vej 8, 6700 Esbjerg, Denmark

HIGHLIGHTS

- 2,6-Dichlorobenzamide is efficiently degraded by direct electrochemical oxidation.
- Degradation occur via hydroxylation and dechlorination until ring opening.
- BDD leads to lower amounts of stable intermediates compared to Pt–Ir.
- Combining HPLC/ESI–MS, HPLC–UV and TOC is powerful for intermediate studies.

ARTICLE INFO

Article history:
Received 19 November 2013
Received in revised form 4 March 2014
Accepted 6 March 2014
Available online 22 April 2014

Handling Editor: E. Brillas

Keywords:
Pesticide pollution
Electrochemical oxidation
Degradation intermediates
Groundwater
2,6-Dichlorobenzamide

ABSTRACT

Electrochemical oxidation is a promising technique for degradation of otherwise recalcitrant organic micropollutants in waters. In this study, the applicability of electrochemical oxidation was investigated concerning the degradation of the groundwater pollutant 2,6-dichlorobenzamide (BAM) through the electrochemical oxygen transfer process with two anode materials: Ti/Pt_{90}–Ir_{10} and boron doped diamond (Si/BDD). Besides the efficiency of the degradation of the main pollutant, it is also of outmost importance to control the formation and fate of stable degradation intermediates. These were investigated quantitatively with HPLC–MS and TOC measurements and qualitatively with a combined HPLC–UV and HPLC–MS protocol. 2,6-Dichlorobenzamide was found to be degraded most efficiently by the BDD cell, which also resulted in significantly lower amounts of intermediates formed during the process. The anodic degradation pathway was found to occur via substitution of hydroxyl groups until ring cleavage leading to carboxylic acids. For the BDD cell, there was a parallel cathodic degradation pathway that occurred via dechlorination. The combination of TOC with the combined HPLC–UV/MS was found to be a powerful method for determining the amount and nature of degradation intermediates.

© 2014 Elsevier Ltd. All rights reserved.

1. Introduction

Electrochemical oxidation (EO) is a technology within the family of Advanced Oxidation Processes (AOPs) used for treatment of aqueous non-biodegradable recalcitrant organic pollutants of high toxicity through oxidation by primarily, but not exclusively, highly reactive hydroxyl radicals (Comninellis et al., 2008). In recent years, the electrochemical oxidation water treatment technology has developed from fundamental research on synthesis of new electrode materials aimed at high oxidation power, resistance and durability and laboratory studies of treatment efficiencies of various industrial wastewaters and other polluted aqueous matrices into commercial available products utilizing boron-doped diamond (BDD) and the more traditional platinum based and dimensionally stable (DSA) mixed oxides anodes (Comninellis et al., 2008; Anglada et al., 2009; Panizza and Cerisola, 2009). Concurrent to the incipient market dissemination of the technology, much more research is still needed in order to fully understand the effect of the technology on the water matrices and the produced effluents. One challenge is elucidating degradation pathways of parent organic pollutants and identifying oxidation intermediates with the aim of ensuring final discharge of an environmentally safe effluent. Generalization of the degradation pathways for different organic contaminants has despite of similarities proved to be challenging, and laboratory studies targeting the individual contaminants are typically needed (Boye et al., 2006; Comninellis et al., 2008; Cavalcanti et al., 2013).

* Corresponding authors. Tel.: +45 20960733 (H.T. Madsen). Tel.: +45 99403564 (J. Muff).
E-mail addresses: htm@bio.aau.dk (H.T. Madsen), jm@bio.aau.dk (J. Muff).

http://dx.doi.org/10.1016/j.chemosphere.2014.03.020
0045-6535/© 2014 Elsevier Ltd. All rights reserved.

Author's personal copy

One contaminant in need of AOPs for effective and fast removal is the pesticide transformation product (PTP) 2,6-diclorobenzamide (BAM). BAM is a daughter product of the commonly used pesticide dichlorobenil, formed during the percolation of dichlorobenil to groundwater aquifers, and is the main contaminant found in Danish groundwater resources. Of the total number of groundwater aquifers that are included in the Danish groundwater monitoring program, 50% have been found to be contaminated with pesticides and PTPs, and in 18.8–20.2% of these cases, the primary contaminant is BAM (Thorling et al., 2012). BAM has been found to be a persisting pollutant. Although its use was banned in 1996, concentrations in the groundwater have not decreased significantly, and it is expected to be present in the aquifers for many years (Thorling et al., 2012). Removal of BAM is therefore necessary before the water can be consumed, but traditional Danish drinking water treatment has been shown to be ineffective against BAM and most other pesticides and PTPs (Søgaard et al., 2001). This makes BAM an obvious candidate for an AOP treatment, but so far no such study has been undertaken.

1.1. Electrochemical oxidation mechanisms

In the EO process, the organics are oxidized by a combination of two different processes, the electrochemical oxygen transfer process (EOTR) and indirect bulk oxidation. In the EOTR process, the organics are oxidized by intermediates of oxygen evolution with the first step being the discharge of water to form adsorbed active oxygen species; physisorbed hydroxyl radicals in the case of non-active anodes (1) or chemisorbed active oxygen in the case of active anodes (2), where a stronger adsorption of the hydroxyl radicals promotes a further removal of an electron (Comninellis, 1994; Kapałka et al., 2009).

$$MO_x + H_2O \rightarrow MO_x(^{\cdot}OH) + H^+ + e^- \quad (1)$$

$$MO_x(^{\cdot}OH) \rightarrow MO_{x+1} + H^+ + e^- \quad (2)$$

The sorbed reactive oxygen species are then capable of partial organic oxidation (in the case of MO_{x+1}) (3) and or full combustion (in the case of $MO_x(^{\cdot}OH)$) (4). The decomposition of the active oxygen species into molecular oxygen is the main competitive side reaction (5) that lowers the efficiencies (Comninellis, 1994).

$$MO_{x+1} + R \rightarrow MO_x + RO + H_2O + H^+ + e^- \quad (3)$$

$$MO_x(^{\cdot}OH) + R \rightarrow MO_x + CO_2 + H_2O + H^+ + e^- \quad (4)$$

$$MO_{x+1}/MO_x(^{\cdot}OH) \rightarrow MO_x + 1/2O_2(+H^+ + e^-) \quad (5)$$

In the indirect mediated organic oxidation process, electroactive ions or other solution constituents are oxidized at the anode surface in order to produce strong oxidants capable of bulk chemical oxidation (Panizza and Cerisola, 2009). In particular, chloride has proved to be an efficient mediator in the indirect oxygen transfer process in chloride rich media through the oxidation of chloride to hypochlorous acid/hypochlorite active chlorine species ((6) and (7), with an initiation potential of 1.64 V versus SHE or higher) or through adsorbed oxychloro-species (8) and (9) (Bonfatti et al., 2000).

$$2Cl^- \rightarrow Cl_2 + 2e^-$$

$$Cl_2 + H_2O \rightarrow HOCl + H^+ + Cl^- \rightleftharpoons OCl^- + 2H^+ + Cl^- \quad (7)$$

$$MO_x(^{\cdot}OH) + Cl^- \rightarrow MO_x(HOCl)_{ads} + e^- \quad (8)$$

$$MO_x(HOCl)_{ads} + R \rightarrow CO_2 + H_2O + Cl^- \quad (9)$$

The classification of different electrode materials into the classes of active and non-active anodes is based on their overpotentials for oxygen evolution, where a high overpotential results in a high hydroxyl radical production and higher mineralization efficiency. Classification of common electrode materials have been performed by the group of Comninellis (Comninellis et al., 2008; Kapałka et al., 2009), who presents boron doped diamond (BDD) as the limit of the non-active anodes and DSA anodes as the limit of the active anodes. Non-active anodes generally present the highest efficiencies considering the EOTR and have usually been found to be superior concerning rate of reaction and mineralization efficiency (Sirés et al., 2008; Samet et al., 2010; Malpass et al., 2013).

1.2. Aim of study

The aim of this study was to elucidate the degradation pathway of BAM treated by EO through the EOTR oxidation mechanism, and from this work develop a generalized evaluation procedure for studies of degradation pathways. Identification of intermediate species formed and their fate during the oxidation process is essential in order to evaluate the risk of formation of harmful byproducts that potentially can results in an increase in effluent toxicity. Identifying the degradation intermediates (DIs) of one pollutant can also be used in transferring the gained knowledge to similar contaminants. For reasons of comparison between active and non-active anodes two different electrochemical cells are used utilizing Si/BDD and Ti/Pt–Ir anodes. The latter platinum–iridium anode material is considered to belong primarily to the active anode class of electrode materials even though some hydroxyl radical formation can be expected.

2. Materials and methods

2.1. Chemicals

2,6-Dichlorobenzamide, 3,5-dichlorophenol, 2,4-dichlorobenzoic acid, 4-chlorobenzoic acid, benzoic acid, maleic acid and oxalic acid were all purchased at Sigma Aldrich with purity >98%. Methanol and acetonitrile (HPLC grade) were purchased from VWR. Demineralized water was produced in house with a Silex II ion exchanger from SILHORKO. Stock solutions of 100 mg L^{-1} were prepared in acetonitrile.

2.2. Electrochemical oxidation setup and procedure

The electrochemical oxidation was performed galvanostatically in a batch recirculation setup. An illustration of the setup can be found in a previous work (Muff et al., 2012). For each experiment, 3 L of model solution was pumped from a water cooled reservoir through the electrochemical cells. Two different commercial one-compartment electrochemical cells with different anode materials were applied. One of tubular design from Watersafe S.A. (Greece) with an internal cylindrical anode of titanium coated with platinum alloyed with iridium ($Ti/Pt_{90}–Ir_{10}$), with a total anode surface area of 60.3 cm^2 and the cathode comprising the outer walls of the cell made of stainless steel AISI 316 with an internal diameter of 42 mm. The electrode gap in the cell was 6 mm. The BDD cell was obtained from Adamant Technologies S.A. (Switzerland), a DiaCell type 100 cell with 70.0 cm^2 silicon coated boron doped diamond (Si/BDD) anode and corresponding cathode mounted as plates with a 3 mm electrode gap in between. The flow rate in the system was kept constant at 430 L h^{-1} and the applied current density were 50 mA cm^{-2} obtained by applied currents of 3.0 and 3.5 A for the two cells, respectively. The different geometry of the two cells induced different hydrodynamics that might

Author's personal copy

influence the efficiency. However, the hydrodynamics of both cells were evaluated at the applied flow rate of 430 L h^{-1}. Reynolds number calculations showed that the flow in both cells were in the laminar flow regime (Watersafe: 1052 and DiaCell: 1322) and mass transfer estimations by the diffusion limiting current technique showed that the mass transfer coefficients of both cells were similar (Watersafe: $k_m = 1.54 \times 10^{-5}$ m s^{-1} and DiaCell: $k_m = 1.47 \times 10^{-5}$ m s^{-1}, determined in previous work (Muff et al., 2012). The similar mass transfer coefficients were important, since they directly influence anode surface reactions. Based on this evaluation, the two cells were considered comparable with respect to this study.

As model solutions, 300 mg BAM was dissolved in 3 L demineralized water (100 mg L^{-1}) with 42.6 g (100 mM) of sodium sulfate added as supporting electrolyte. The solution was left stirring for at least 24 h prior to each experimental run for complete BAM dissolution. The experiments were operated at a constant temperature of 25 °C and with cell potentials of 4.7 V for the Pt–Ir cell and 8.1 V for the BDD cell. Sampling occurred from the reservoir for the aqueous analysis at specific time intervals.

2.3. Analytical procedures

The degradation of BAM and the formation of intermediate products were analyzed with a HPLC/UV/ESI–MS system (1260 Infinity and 1100 series LC/MSD Trap, Agilent Technology), equipped with a ZORBAX Eclipse Plus C18 column. A 40:60 (v/v) mixture of methanol and ammonium acetate buffer (pH 3) was used as eluent, and pumped with a flow rate of 400 μL min^{-1} at 25 °C. The UV detector was set at 225 nm. On the ESI–MS, the nebulizer pressure was set at 2.76 bar, the nebulizer flow at 9 L min^{-1}, and the dry gas temperature to 350 °C. Nitrogen was used for nebulization and dry gas. The spectra were recorded in positive mode. For quantitative determination of compounds, tandem mass spectroscopy was applied.

The extent of mineralization of organic matter in the samples was investigated by determining total organic carbon (TOC) in the aqueous samples with a multi N/C 2100 analyzer from Analytik Jena, and the total UV absorbance was determined with a Cary 50, Varian.

2.4. Procedure for determination of intermediates

To elucidate the chemical structure of DIs, the UV and MS detector on the HPLC were used in combination. Separately, each technique suffers from a number of drawbacks. The UV detector cannot be used for qualitative investigation of a peak unless a reference standard is used. The MS, with the electrospray interface, is influenced by the ionic content of the sample matrix, which eluates in the beginning of the analysis, where also smaller molecules such as organic acids and small amides will eluate. Together the two techniques can overcome these drawbacks to some degree. It is often easier to detect a peak with the UV detector due to the much more stable background signal/base line, and by knowing the retention time of a peak, the peak can be qualitatively analyzed using the MS. Also, because the sample matrix has no UV absorbance, the UV detector may be used to investigate the formation of smaller and fast eluating compounds. In our study, the general procedure was to observe peaks with the UV detector to determine retention times, after which the mass of the molecule responsible for the peak was determined with MS.

To support the analysis, reference compounds were used. This made it possible to study how specific changes to the molecular structure of the molecules influenced the retention times with our specific column and eluent composition. The main aims of these analyses were to study the effect of replacing the amide group with a carboxylic acid group, and the effect of the dechlorination process on the retention times.

3. Results and discussion

3.1. Degradation of BAM

As seen in Fig. 1, the degradation of BAM was found to follow first order kinetics for both cells with apparent rate constants of $k_{BDD} = 8.5 \times 10^{-3}$ min^{-1} ($R^2 = 0.997$) and $k_{Pt-Ir} = 4.6 \times 10^{-3}$ min^{-1} ($R^2 = 0.991$) obtained with an applied current density of 50 mA cm^{-2}. The difference in the rate constants was enlarged by the larger anode area of the BDD cell resulting in an increased current intensity, and the two kinetic parameters were more appropriately compared with respect to the specific amount of charge in ampere hours per liter passed through the solution instead of minutes. After this normalization the constants became: $k_{BDD} = 4.4 \times 10^{-1}$ $(Ah\ L^{-1})^{-1}$ and $k_{Pt-Ir} = 2.8 \times 10^{-1}$ $(Ah\ L^{-1})^{-1}$. Overall this shows that the BDD cell was more efficient at degrading BAM compared to the Pt–Ir cell.

A more markedly difference in the two processes was found when the total UV absorbance of the solutions during the EO process was compared, Fig. 2. Initially, both spectra were characterized by a small peak from 270 to 280 nm, minimum absorbance at 250 nm and a sharp increase in absorbance around 225 nm, just before absorption by the water solvent. To get a better impression of the variations in the UV absorbance spectra the specific absorbance at 225, 254 and 270 nm were plotted in the inset plots in Fig. 2. 225 and 254 nm were chosen since they represent wavelengths at which UV absorbance of organics are often evaluated, and 270 nm was chosen in order to follow the development of the initial minor peak in the original BAM spectrum.

For the Pt–Ir cell no immediate drop in UV intensity was seen. The absorbance around 225 nm was relatively constant up until 240 min (4 Ah L^{-1}), and at the same time the absorbance at higher wavelengths was found to increase, as seen from the inset in Fig. 2a. Only after 240 min did the absorbance begin to decrease.

The BDD cell was much more efficient at reducing the total absorbance. The peaks at 225 and 270 nm did immediately decrease, and the increase in the absorbance around 254 nm was much smaller compared to the increase seen for the Pt–Ir anode and it began to decrease already after 120 min (2.3 Ah L^{-1}).

Together with the degradation of BAM, these UV absorbance data indicated that the electrochemical processes of the BDD cell

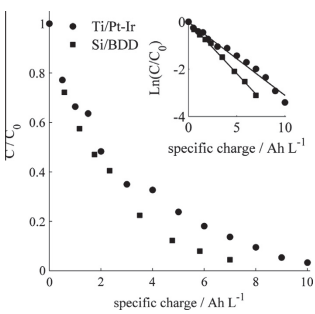

Fig. 1. Degradation kinetics for BAM during electrochemical oxidation by two different cells with Si/BDD and Ti/Pt–Ir as anode materials at 50 mA cm^{-2}. (a) Concentration of BAM versus time and (b) concentration of BAM versus specific charge.

Author's personal copy

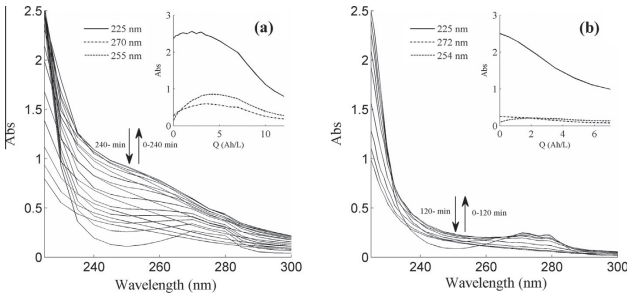

Fig. 2. Evolution in the UV spectrum of the solution during the EO process. (a) The Pt–Ir cell and (b) the BDD cell.

was much more efficient in complete BAM mineralization, whereas the processes at the Pt–Ir anode initially converted BAM to other UV absorbing compounds through partial oxidation. This difference of the two cells was expected and fits with the general understanding of the oxidation power and processes occurring during electrochemical oxidation of other organic contaminants, and has now been documented for BAM.

3.2. Quantification of degradation intermediates

To quantify the DIs formed during the process, the TOC concentration of the solutions was measured during the runs. A fast TOC removal from the solution would indicate efficient mineralization of BAM in the process, and in light of the UV absorption results, differences in the performance of the cells were expected. As seen in Fig. 3, the BDD cell did show a faster removal of TOC compared to the Pt–Ir cell with first order rate constants $k_{BDD} = 5.2 \times 10^{-3}\ min^{-1} = 2.7 \times 10^{-1}\ (Ah\ L^{-1})^{-1}$ ($R^2 = 0.992$) and $k_{Pt-Ir} = 1.2 \times 10^{-3}\ min^{-1} = 7.1 \times 10^{-2}\ (Ah\ L^{-1})^{-1}$ ($R^2 = 0.963$).

When the TOC data were combined with the BAM degradation data, it allowed for a determination of the total amount of organic carbon bound in DIs. The amount of DI carbon was calculated by determination of the area between the TOC curve and the curve representing the concentration of BAM related carbon calculated from the BAM degradation data. The evolution in the DI carbon (the grey area) was then plotted with respect to the specific charge passed through the solution as the insets in Fig. 4. As the subplots clearly show, much more BAM was completely mineralized near the surface of the BDD anode compared to the Pt–Ir anode. With the Pt–Ir cell, the level of stable DIs in the solution reached a level of 54% after 5.7 Ah L^{-1}, as represented by the amount of original carbon in the solution bound in intermediates (Fig. 4b), whereas the same number for the BDD cell only reached 20% after 3.0 Ah L^{-1} (Fig. 4a).

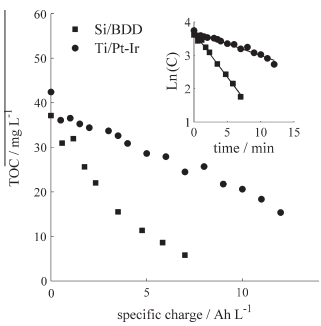

Fig. 3. TOC removal for the two cells with first order kinetic inset plot.

This difference observed in the amount of stable DI formed between the two cells was directly related to the oxidation power of the two anode materials. The BDD acted as a non-active anode where the hydroxyl radicals produced on the anode surface will have a sufficient high standard reduction potential for oxidation of both BAM and DIs. The Pt–Ir material is in the transition between active and non-active, but with predominant behavior as an active anode, where the chemisorbed oxygen will oxidize BAM more selectively due to the lower reduction potential. The unselective nature of the hydroxyl radicals from the BDD anode ensured that, when BAM was oxidized to a DI, the main part of the DI (80%) was subsequently further oxidized until complete mineralization.

The flow regime in the cells could also have an influence on the amount of DI produced during the treatment. For an effective mass transport of organics to the electrode surface, hydrodynamics providing turbulent conditions are often demanded for high faradaic yield (Mascia et al., 2010; Cordeiro et al., 2013). On the contrary, laminar flow in the cell could potentially minimize the DI formation. Results indicating this hypothesis were found by Mascia et al. (2010), although not highlighted because focus was on the overall rate of removal, which typically is the standard evaluation parameter. The reason for the lower amounts of DIs at laminar flow may be that under these conditions the transport of DIs from surface to bulk will primarily be diffusive. Therefore DIs will tend to stay in close proximity of the surface, where they are more likely to undergo further oxidation. A conceptual model of the BAM oxidation under laminar conditions is that BAM was degraded to its first DI at the entrance of the cell, after which this DI moves further along the surface until it reaches the outlet of the cell or undergoes complete mineralization. This potential influence of flow on the intermediate compound formation will be studied in detail in coming research.

Finally, the more selective nature of the chemisorbed active oxygen in the Pt–Ir cell ensured that BAM was preferentially degraded relative to its DIs, providing the observed accumulation of DIs seen in Fig. 4b.

3.3. Efficiency of the degradation process

Another way of comparing the efficiency of the two cells in mineralizing BAM was through the mineralization current efficiency

Author's personal copy

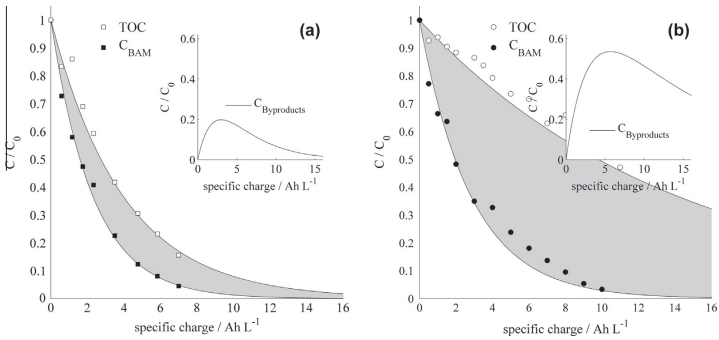

Fig. 4. Combined plots of TOC and BAM related carbon for determination of the total amount of DI bound carbon. (a) The results obtained with the BDD cell, and (b) the results obtained with the Pt–Ir cell. $C_{0,BAM}$ = 100 mg L^{-1}.

(MCE). The overall mineralization reaction of BAM could be written as follows:

$$C_7H_5ONCl_2 + 16H_2O \rightarrow 7CO_2 + NO_3^- + 2Cl^- + 37H^+ + 34e^- \quad (10)$$

This reaction showed that 34 electrons were involved in incinerating a BAM molecule completely into carbon dioxide. Due to the cost of electricity, current efficiency is an important parameter in electrochemical oxidation, and the MCE at a given time can be comparatively calculated using the experimental TOC data and the relationship (Brillas et al., 2004; Yoshihara and Murugananthan, 2009):

$$\mathrm{MCE} = \frac{\Delta(\mathrm{TOC})_{\mathrm{exp}}}{\Delta(\mathrm{TOC})_{\mathrm{theo}}} \cdot 100 \quad (11)$$

$\Delta(\mathrm{TOC})_{\mathrm{exp}}$ denotes the experimentally determined TOC removal in the time interval Δt $(t + \Delta t - t)$ in g L^{-1}. $\Delta(\mathrm{TOC})_{\mathrm{theo}}$ is the theoretically TOC removal considering that all electrical charge is consumed to yield reaction (11) calculated as follows:

$$\Delta(\mathrm{TOC})_{\mathrm{theo}} = \frac{I_{\mathrm{app}} \cdot M_{\mathrm{C}} \cdot \Delta t}{F \cdot V \cdot \mathrm{ne}} \quad (12)$$

I_{app} is the applied current intensity in C s^{-1}, M_{C} is the molar mass of carbon of 12 g mol^{-1}, Δt is the time interval in seconds, F is the Faraday constant of 96 490 C mol^{-1}, V is the volume in L and ne is the average number of electrons needed per carbon atom in BAM for its incineration (34/7 mol electrons per mole carbon).

The same procedure can be used to calculate the MCE with respect to the removal of BAM itself as parent product applying 189 g mol^{-1} as the molar mass of BAM and 34 electrons for its incineration in the calculation of the theoretical BAM removal.

In Fig. 5 the experimentally determined MCE for both anode materials is plotted for both BAM and TOC as a function of the specific charge. To investigate the fit of the MCE model, the theoretically MCEs is also plotted. These values are calculated from the derivatives to the exponential 1. Order BAM and TOC removal curves seen in Figs. 1 and 3.

In general, the MCEs were highest in the start of the process (up to 17%) where the total concentrations of organics were at its maximum providing the best probability for an efficient transport to the anode surface. The importance of the concentration on the MCE is shown in the insets in Fig. 5, where the MCEs were plotted as a function of the respective BAM and TOC concentration. At very low concentrations, the MCE became accordingly low. For the initial concentrations applied in this study, still more than 80% of the current in the circuit originated from oxygen liberation or other unwanted waste side reactions, but this can be improved by increasing the concentration of a given pollutant prior to degradation, and by decreasing the applied current density. Highest MCEs were seen by the BDD cell, and due to smaller quantity of DIs formed using this cell, the efficiency of the BAM and TOC removal was more alike compared to the Pt–Ir cell, where the slow TOC removal resulted in a low average efficiency in the range of 2–3% and a poor fit to the model due to higher analytical uncertainties.

3.4. Identification of degradation intermediates

In the evaluation of the potential risk of the DIs formed during the electrochemical oxidation process, it is not sufficient to look at the total quantity of DIs formed. The specific chemical nature of the DIs also has to be studied. In Table 1, retention times of peaks detected in the samples during the EO process are shown. The general procedure was to search for peaks with the UV detector and then determine the mass and intensity of the compound responsible for the peak with the mass spectrometer. For the very fast eluating peaks, it was not possible to obtain identification with the mass spectrometer.

It is interesting to note that there was a distinct difference in the DIs formed with the two cells, see Fig. 6. Quantification of the specific DIs through calibration of the intensities with concentrations was not possible due to the lack of calibration standards, so the height of the peaks for the different DIs cannot be compared. What could be compared was the sequence of appearance. For the Pt–Ir cell, the mother compound, BAM (190 m/z), was first converted to a daughter product with an m/z value of 206, which then was further converted into a compound with a m/z value of 188. The intensities of the DIs reached a maximum after 6 Ah L^{-1} and then decreased rapidly until they were beyond detection in the last sample. For the BDD cell, the 206 m/z peak was also seen. However, with this cell, it was not possible to find the 188 m/z peak. Instead, peaks at 156 m/z and 122 m/z were detected. These two peaks increased rapidly and reached a maximum intensity after 1 Ah L^{-1}. It may also be noted that the increase and decrease of these peaks coincided with development of the UV intensity as seen in Fig. 2.

As a tool for assisting with elucidating the chemical structure of the DIs, the retention times of known reference compounds with active groups similar to what was likely for the daughter products

Author's personal copy

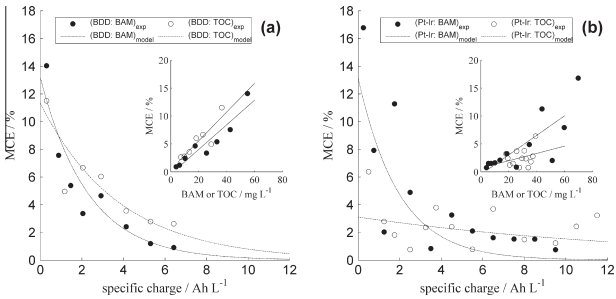

Fig. 5. The mineralization current efficiency (MCE) as a function of the specific charge deposited with respect to BAM and TOC respectively. (a) The BDD cell and (b) the Pt–Ir cell. Data points represent experimentally collected data, and the curves represent theoretical values determined from previously determined removal kinetics. The inset plots show the correlation between concentration and the MCE.

Table 1
Comparison of peaks detected during oxidation with the two electrochemical cells and standard compounds representing specific changes in the molecular structure. (+) For the UV detector in the BDD experiment, refers to the fact that this compound was poorly separated from the dominating BAM peak with the analytical separation method applied in this study. The peak was however easily observed in tandem mass spectrometry.

EO solution					Standard compounds		
Retention time (min)	BDD		Pt–Ir		Standard	MS m/z (+/−)	Retention time (min)
	MS (m/z)	UV (225 nm)	MS (m/z)	UV (225 nm)			
0.91	–	+	–	+	Oxalic acid	91/89	0.88
1.15	–	–	188	+	Maleic acid	117/115	0.99
1.40	206	+	206	+	Benzoic acid	223/221	5.11
1.79	122	+	–	–	2,4-Dichlorobenzoic acid	191/189	14.3
1.90	156	(+)	–	–	4-Chlorobenzoic acid	157/155	16.3
2.02	190	+	190	+	3,5-Dichlorophenol	163/161	48.0

were measured, see Table 1. From the comparison of the retention time of BAM with the retention time of 2,4-dichlorobenzoic acid and 3,5-dichlorophenol, it was clear that a loss or conversion of the amide group should result in markedly prolonged retention times for the DIs. As this was not seen in our spectra, it indicated that the amide group was not affected by the oxidation in either of the two cells. Table 1 also shows that loss of two chloro groups will lower the retention time, while the loss of only one of the chloro groups will have a less significant influence on the retention time. This is most probably due to the change in polarity induced by the changes in molecular structure, and it seemed reasonable to assume that as the polarity increased the retention time decreased. Lastly, Table 1 shows that small carboxylic acids were poorly retained by the applied column and eluated almost immediately.

Together with the masses of the peaks, these considerations indicated that the peaks at 206 and 188 m/z were BAM molecules, where the EO process has resulted in the first step a substitution of one hydroxyl group with a hydrogen atom (16 Da mass difference) and in the second step substitution of a chlorine atom with another hydroxyl group (18 Da mass difference). Substitution with hydroxyl groups has also been observed by others working with the degradation of aromatic compounds (Boye et al., 2006; Borràs et al., 2010; Wei et al., 2011; Rabaaoui et al., 2013), and seem to constitute the initial steps of the degradation. Based on steric considerations, the first substitution will probably occur on C4. The presence of a hydroxyl group will increase the polarity, and as predicted from the experiments with the reference compounds, the retention time of the 206 m/z peak was markedly shorter than the retention time of BAM. The 188 m/z peak was found to appear after the 206 m/z peak, which indicated that it was formed from the 206 m/z compound. Again the increased polarity of the 188 m/z compound was in accordance with the observed decrease in retention time.

The two additional peaks detected in the BDD experiment had masses lower than BAM, but with only weakly decreased retention times. The difference in mass was equal to the reductive loss of first one and then two chloro groups. It therefore seemed that for the BDD cell, there existed two parallel degradation pathways: an anodic and a cathodic, whereas only the anodic pathway was active for the Pt–Ir cell.

Based on the experimental findings, a pathway for the initial electrochemical degradation steps of BAM was proposed and is depicted in Fig. 6.

There are some unknowns. Firstly, the 188 m/z compound was not detected in the BDD experiment. However, as was shown in Fig. 4, the total amount of DIs was much lower when using the BDD cell compared to the Pt–Ir cell and furthermore, the amount of DIs for the BDD cell was the composite of the anodic and cathodic pathways. For the Pt–Ir cell the intensity of the 188 m/z peak was considerably lower than the signal of the 206 m/z peak, and the absence of the 188 m/z peak in the BDD experiment could therefore very well be due to a concentration below the detection limit. Secondly, a compound with a protonated mass of 170 Da has been proposed in the reaction scheme although this compound has not been observed. However, based on the experiments with the reference compounds, the amide group has not been found to be affected, and the next logical step of the anodic process would therefore be to continue the chloro/hydroxy substitution before any ring cleavage occurs. Due to its polarity, the 170 m/z compound would eluate even faster than the 188 m/z compound, which would bring it to eluate with the supporting electrolyte,

Author's personal copy

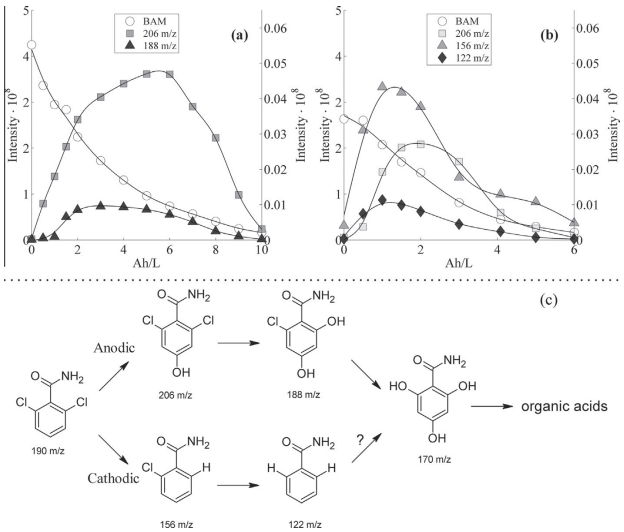

Fig. 6. Development in intensity of degradation intermediates detected with mass spectrometer and proposed pathway for the initial electrochemical degradation of BAM. The subplots (a and b) represent the experiments with the Pt–Ir cell (a) and the BDD cell (b). Intensities for the DIs are plotted on the right *y*-axis and the intensity of BAM on the left. Subplot (c) is the proposed degradation pathway. The cathodic pathway was only found to be active for the BDD cell, and although it was not found in the experiments, we suggest that this reaction pathway leads to the same hydroxylated ring structure (170 *m*/*z*) as for the anodic pathway.

and thereby make detection with the mass spectrometer impossible because of the dominating influence of the electrolyte ions. Different eluent mixtures were tried to investigate if a better separation could be obtained, but on the column used in these experiments that was not possible.

For the same reasons the peak at 0.91 min could not be identified either. It does however seem likely that the 0.91 min peak represented carboxylic acids formed in the process due to aromatic ring cleavage. This has been shown in other reported studies with electrochemical oxidation of similar aromatic compounds (Boye et al., 2006). Although of scientific interest, the specific nature of the carboxylic acids is of less interest from a practical point of view, since these compounds carry little toxicity and are readily biodegradable. With that said however, it is important to note that we did not find any transformation of the amide group, and the toxicity of small amides could pose a potential problem (Friedman, 2003). However, if present the concentrations were low and below the detection limit of the TOC.

3.5. Generalized protocol for determine of DIs

As shown in this manuscript, a protocol for determination of DIs should consist of two parts, an estimation of the total quantity of DIs and the specific chemical nature of these. For the first part, a degradation plot of the original pollutant and TOC can be used to effectively estimate the total amount of organic carbon in DIs. A simpler way is to measure the total UV absorbance, but this approach cannot to be used to quantify the amount of DIs, and is more appropriately used to compare different degradation processes. For the qualitative investigation, the combined technique of UV and mass spectrometry is very useful. Peaks are more easily found with the UV detector due to a stable base line, and it does not suffer from the interference of the supporting electrolyte. As seen in this study, a mass spectrometer with an electrospray interface will not be able to detect compounds that eluate at the same time as the supporting electrolyte. With the retention time determined, the mass spectrometer can be employed to investigate the nature of the compound further. Since the general effect of the EO process was to increase the polarity of the DIs, the choice of column on the HPLC is very important. It may be necessary to apply a second column to handle small polar compounds.

4. Conclusions

2,6-Dichlorobenzamide was found to be degraded by both electrochemical cells in the study utilizing respectively Si/BDD and Ti/Pt–Ir as anode materials representing a non-active anode type and a predominal active anode material. The BDD cell was found to be the most efficient, and it also resulted in the lowest amount of degradation intermediates formed during the process, which was ascribed to the unselective nature of the hydroxyl radicals formed at this high oxidation power anode. The total quantity of DIs in the solution during the treatment was estimated by subtracting the degraded amount of BAM related carbon from the TOC.

The initial degradation pathway was found to be different for the two cells. The BDD gave rise to both a cathodic and an anodic pathway, whereas the Pt–Ir cell only followed the anodic pathway. In the anodic pathway, first a hydrogen atom was substituted with a hydroxyl group, after which the chloro groups were substituted with hydroxyl groups. In the cathodic pathway, the chloro groups were substituted with hydrogen atoms. The final step was cleavage of the aromatic ring structure leading to unidentified carboxylic acids.

The combination of UV and mass spectrometer was found to be an effective combination for detecting and identifying the DIs.

Author's personal copy

Acknowledgements

Financial support from the Danish Ministry of Science, Technology, and Innovation in the form of a Ph.D. study grant is acknowledged.

References

Anglada, Á., Urtiaga, A., Ortiz, I., 2009. Contributions of electrochemical oxidation to waste-water treatment: fundamentals and review of applications. J. Chem. Technol. Biotechnol. 84, 1747–1755.
Bonfatti, F., Ferro, S., Lavezzo, F., Malacarne, M., Lodi, G., De Battisti, A., 2000. Electrochemical incineration of glucose as a model organic substrate II. Role of active chlorine mediation. J. Electrochem. Soc. 147, 592–596.
Borràs, N., Oliver, R., Arias, C., Brillas, E., 2010. Degradation of atrazine by electrochemical advanced oxidation processes using a boron-doped diamond anode. J. Phys. Chem. A 114, 6613–6621.
Boye, B., Brillas, E., Marselli, B., Michaud, P., Comninellis, C., Farnia, G., Sandona, G., 2006. Electrochemical incineration of chloromethylphenoxy herbicides in acid medium by anodic oxidation with boron-doped diamond electrode. Electrochim. Acta 51, 2872–2880.
Brillas, E., Boye, B., Sirés, I., Garrido, J.A., Rodríguez, R.M., Arias, C., Cabot, P.-L., Comninellis, C., 2004. Electrochemical destruction of chlorophenoxy herbicides by anodic oxidation and electro-Fenton using a boron-doped diamond electrode. Electrochim. Acta 49, 4487–4496.
Cavalcanti, E.B., Garcia-Segura, S., Centellas, F., Brillas, E., 2013. Electrochemical incineration of omeprazole in neutral aqueous medium using a platinum or boron-doped diamond anode: Degradation kinetics and oxidation products. Water Res. 47, 1803–1815.
Comninellis, C., 1994. Electrocatalysis in the electrochemical conversion/combustion of organic pollutants for waste water treatment. Electrochim. Acta 39, 1857–1862.
Comninellis, C., Kapalka, A., Malato, S., Parsons, S.A., Poulios, I., Mantzavinos, D., 2008. Advanced oxidation processes for water treatment: advances and trends for R & D. J. Chem. Technol. Biotechnol. 83, 769–776.
Cordeiro, G.S., Rocha, R.S., Valim, R.B., Migliorini, F.L., Baldan, M.R., Lanza, M.R.V., Ferreira, N.G., 2013. Degradation of profenofos in an electrochemical flow reactor using boron-doped diamond anodes. Diamond Relat. Mater. 32, 54–60.
Friedman, M., 2003. Chemistry, biochemistry, and safety of acrylamide. A review. J. Agric. Food Chem. 51, 4504–4526.
Kapałka, A., Fóti, G., Comninellis, C., 2009. The importance of electrode material in environmental electrochemistry: formation and reactivity of free hydroxyl radicals on boron-doped diamond electrodes. Electrochim. Acta 54, 2018–2023.
Malpass, G.R.P., Salazar-Banda, G.R., Miwa, D.W., Machado, S.A.S., Motheo, A.J., 2013. Comparing atrazine and cyanuric acid electro-oxidation on mixed oxide and boron-doped diamond electrodes. Environ. Technol. 34, 1043–1051.
Mascia, M., Vacca, A., Polcaro, A.M., Palmas, S., Ruiz, J.R., Da Pozzo, A., 2010. Electrochemical treatment of phenolic waters in presence of chloride with boron-doped diamond (BDD) anodes: experimental study and mathematical model. J. Hazard. Mater. 174, 314–322.
Muff, J., Jepsen, H., Søgaard, E., 2012. Bench-scale study of electrochemical oxidation for on-site treatment of polluted groundwater. J. Environ. Eng. 138, 915–922.
Panizza, M., Cerisola, G., 2009. Direct and mediated anodic oxidation of organic pollutants. Chem. Rev. 109, 6541–6569.
Rabaaoui, N., Saad, M.E.K., Moussaoui, Y., Allagui, M.S., Bedoui, A., Elaloui, E., 2013. Anodic oxidation of o-nitrophenol on BDD electrode: variable effects and mechanisms of degradation. J. Hazard. Mater. 250–251, 447–453.
Samet, Y., Agengui, L., Abdelhédi, R., 2010. Electrochemical degradation of chlorpyrifos pesticide in aqueous solutions by anodic oxidation at boron-doped diamond electrodes. Chem. Eng. J. 161, 167–172.
Sirés, I., Brillas, E., Cerisola, G., Panizza, M., 2008. Comparative depollution of mecoprop aqueous solutions by electrochemical incineration using BDD and PbO_2 as high oxidation power anodes. J. Electroanal. Chem. 613, 151–159.
Søgaard, E.G., Aruna, R., Abraham-Peskir, J., Koch, C.B., 2001. Conditions for biological precipitation of iron by gallionella ferruginea in a slightly polluted ground water. Appl. Geochem. 16, 1129–1137.
Thorling, L., Hansen, B., Langtofte, C., Brüsch, W., Møller, R.R., Mielby, S., 2012. Grundvand: Status og Udvikling 1989–2011 (groundwater: Status and Development 1989–2011). Technical report, Geological Survey of Denmark and Greenland, 2012.
Wei, J., Feng, Y., Sun, X., Liu, J., Zhu, L., 2011. Effectiveness and pathways of electrochemical degradation of pretilachlor herbicides. J. Hazard. Mater. 189, 84–91.
Yoshihara, S., Murugananthan, M., 2009. Decomposition of various endocrine-disrupting chemicals at boron-doped diamond electrode. Electrochim. Acta 54, 2031–2038.

Paper X

Henrik Tækker Madsen, Erik G. Søgaard and Jens Muff

Study of degradation intermediates formed during electrochemical oxidation of pesticide residue 2,6-dichlorobenzamide (BAM) in chloride medium at boron doped diamond (BDD) and platinum anodes

Chemosphere, **120** (2015), 756-763

Reprinted with permission from Elsevier

Chemosphere 120 (2015) 756–763

Contents lists available at ScienceDirect

Chemosphere

journal homepage: www.elsevier.com/locate/chemosphere

Study of degradation intermediates formed during electrochemical oxidation of pesticide residue 2,6-dichlorobenzamide (BAM) in chloride medium at boron doped diamond (BDD) and platinum anodes

Henrik Tækker Madsen *, Erik Gydesen Søgaard, Jens Muff

Department of Biotechnology, Chemistry and Environmental Engineering, Aalborg University, Niels Bohrs Vej 8, 6700 Esbjerg, Denmark

HIGHLIGHTS

- Chloride leads to a more diverse mixture of degradation intermediates.
- Active chlorine oxidation leads to fewer intermediates for Pt anodes.
- BDD leads to lower amounts of intermediates compared to Pt.
- Intermediates from BAM are formed via an amine or a carboxylic acid route.
- Mineralization is possible with both BDD and Pt.

ARTICLE INFO

Article history:
Received 12 June 2014
Received in revised form 22 September 2014
Accepted 26 October 2014
Available online 17 November 2014

Handling Editor: Shane Snyder

Keywords:
Pesticide pollution
Electrochemical oxidation
Degradation intermediates
Chloride medium
2,6-Dichlorobenzamide

ABSTRACT

For electrochemical oxidation to become applicable in water treatment outside of laboratories, a number of challenges must be elucidated. One is the formation and fate of degradation intermediates of targeted organics. In this study the degradation of the pesticide residue 2,6-dichlorobenzamide, an important groundwater pollutant, was investigated in a chloride rich solution with the purpose of studying the effect of active chlorine on the degradation pathway. To study the relative importance of the anodic oxidation and active chlorine oxidation in the bulk solution, a non-active BDD and an active Pt anode were compared. Also, the effect of the active chlorine oxidation on the total amount of degradation intermediates was investigated. We found that for 2,6-dichlorobenzamide, active chlorine oxidation was determining for the initial step of the degradation, and therefore yielded a completely different set of degradation intermediates compared to an inert electrolyte. For the Pt anode, the further degradation of the intermediates was also largely dependent on active chlorine oxidation, while for the BDD anode anodic oxidation was most important. It was also found that the presence of active chlorine led to fewer degradation intermediates compared to treatment in an inert electrolyte.

© 2014 Elsevier Ltd. All rights reserved.

1. Introduction

In numerous studies electrochemical treatment has proven to be an effective method for degradation of pesticides in water through oxidation by anodic generated oxidants as active oxygen species in the so-called electrochemical oxygen transfer process (EOTR) and bulk oxidants as active chlorine (Quiroz et al., 2011). However, most studies have mainly focused on the removal of the pesticide, and have not in detail investigated the formation of degradation intermediates (DIs), which may potentially be more persistent and toxic compared to the original pesticide (Sirtori et al., 2010). For electrochemical oxidation to become an accepted treatment method it is thus necessary to map the entire degradation pathway for a given pesticide, and control of DIs remains a challenge to be solved.

With respect to degradation pathways for pesticides, most knowledge has been gathered for phenoxy acid, triazines and organophosphates, with complete or partial pathways having been mapped for the following compounds: atrazine (Polcaro et al., 2005; Borràs et al., 2010), cyanuric acid, desethyl-desisopropyl-atrazine (DEIA) (Polcaro et al., 2005), 2,6-dichlorobenzamide (BAM) (Madsen et al., 2014), diuron, dichloroaniline (Polcaro et al., 2004), 4-chloro-2-methylphenoxy acetic acid (MCPA), 2-(4-chloro-2-methylphenoxy)-2-methyl-propionic acid (CPMP) (Boye et al., 2006), 2-(4-chloro-2-methylphenoxy) propionic acid (MCPP)

* Corresponding author. Tel.: +45 20960733.
E-mail address: htm@bio.aau.dk (H.T. Madsen).

http://dx.doi.org/10.1016/j.chemosphere.2014.10.058
0045-6535/© 2014 Elsevier Ltd. All rights reserved.

(Boye et al., 2006; Flox et al., 2006), malathion, parathion (Muff et al., 2009), methyl-parathion (Vlyssides et al., 2004; Muff et al., 2009), methamidophos (Martínez-Huitle et al., 2008), o-nitrophenol (Rabaaoui et al., 2013), pretilachlor (Wei et al., 2011) and propham (Ozcan et al., 2008). However, in all of the before mentioned studies except one (Vlyssides et al., 2004), an inert supporting electrolyte, predominantly sulfate or perchlorate, has been used. The advantage of applying this type of electrolyte in model solutions is that primarily the EOTR process is occurring, which simplifies the interpretation of overall degradation process, but in relation to real scenarios the presence of only inert ions may be considered unrealistic. In real waters, electroactive ions will most likely be present and these can lead to the formation of strong oxidizing agents (Panizza and Cerisola, 2009). The most typical of these is the formation of $HClO/ClO^-$ (active chlorine), due to the ubiquitous nature of the Cl^- ion. For further information on the mechanisms involved in electrochemical oxidation of organics in water please refer to this reference (Panizza and Cerisola, 2009). The presence of active chlorine leads to a degradation pathway parallel to that mediated by the EOTR process, and may therefore potentially result in the formation of a larger number of and different DIs. The active oxygen species in the EOTR process predominantly result in hydrogen abstraction or hydroxylation, whereas active chlorine can oxidize through different mechanisms and result in chlorination of the chemical structure of the pesticide (Muff and Søgaard, 2011).

In a previous study we have investigated the electrochemical degradation pathways of pesticide residue 2,6-dichlorobenzamide (BAM), an important and persistent groundwater pollutant, at boron-doped diamond (Si/BDD) and platinum-iridium anodes (Ti/Pt-Ir) anodes in a sodium sulfate electrolyte. We found in particular hydroxylation and for BDD dechlorination of the aromatic ring as the main routes towards ring opening and complete mineralization in the EOTR driven process (Madsen et al., 2014). In the present study the aim was to determine the degradation of BAM in a chloride rich medium, with the specific purpose of investigating the influence of the electrochemically formed active chlorine on the formation of DIs both with respect to structure and quantity. This allowed us to make a direct comparison between the two scenarios with and without chloride as a step towards the final aim of predicting the DIs formed in a real groundwater matrix. To investigate the importance of active oxygen species towards active chlorine mediated oxidation in more detail, the performance of an active platinum anode favoring active chlorine formation and a non-active BDD anode favoring EOTR were compared. More specifically, the two anodes were compared with respect to the rates of BAM and TOC removal, the structure and total amount of DIs formed during the degradation process and the evolution in intensity for each detected DI.

2. Materials and methods

2.1. Chemicals

BAM was purchased at Sigma Aldrich with purity >98%. Methanol, (HPLC grade) and ethyl acetate (technical grade) were purchased from VWR. Demineralized water was produced in house with a Silex II ion exchanger from SILHORKO.

2.2. Electrochemical oxidation setup and procedure

The electrochemical oxidation was performed galvanostatically in a batch recirculation setup. The electrolyte solution was pumped from the reservoir in upflow mode through the electrochemical cell (Electrocell, Denmark) and the cooling unit. The electrochemical cell was of plate like design with exchangeable electrodes, an electrode gap of 3 mm operated in one compartment mode. The active electrode area was 10 cm^2 on both electrodes, the cathode was in all experiments stainless steel (AISI 316) and the anodes were platinum coated titanium (Ti/Pt) and boron doped diamond coated niobium substrate (Nb/BDD).

Total electrolyte volume used was 1.0 L and 0.5 L depending on the experiment. Stock solutions of 100 mg L^{-1} BAM were prepared in 0.10 M NaCl solution.

10 mL samples were extracted for analysis, and immediately mixed with 1 mL 1 M Na_2SO_3 for quenching of excess oxidants.

2.3. Analytical procedures

The degradation of BAM and the formation of DIs were analyzed with a HPLC/UV/ESI-MS system (1260 Infinity and 1100 series LC/MSD Trap, ZORBAX Eclipse Plus C18 column, Agilent Technology), and a GC/MS system (Clarius 500, Perkin Elmer).

For the HPLC method, a 20:80 (v/v) mixture of acetonitrile and distilled water was used as eluent, and pumped with a flow rate of 400 μL min^{-1} at 25 °C. When using the UV detector the absorption wavelength was set at 210 nm, and the injection volume at 5 μL. On the ESI-MS, the nebulizer pressure was set at 2.76 bar, the nebulizer flow at 9 L min^{-1}, and the dry gas temperature to 350 °C. Nitrogen was used for nebulization and dry gas. The spectra were recorded in negative mode. For quantitative determination of compounds, tandem mass spectroscopy with multiple reaction monitoring (MRM) was applied, and the injection volume was 50 μL.

For the GC/MS method, the temperature was increased from 75 °C to 275 °C in the first 12 min and kept at this level until 15 min. Prior to analysis on the GC/MS, the samples were subjected to solid phase extraction using TELOS ENV 200 mg/6 mL columns. The solid phase extraction procedure was: activation of column with 6 mL methanol, equilibration with 6 mL demineralized water, application of 10 mL sample, elution of interferences with 6 mL demineralized water, vacuum drying of column for 60 min, elution of analytes with 10 mL ethyl acetate, evaporation of ethyl acetate of 80 °C and dissolution in 1 mL ethyl acetate with 1.0 g/L bromobenzene as internal standard.

The HPLC/UV system was used for the quantification of BAM, while the HPLC/ESI-MS system was used for DI identification and quantification. By running the ESI-MS in negative mode, the interferences of BAM and cations, in particular sodium, were avoided. Due to its amide group, BAM is only detectable in positive mode, and ionic interferences are usually always worse for cations relative to anions. The GC/MS was used to aid the identification of the DIs and also to investigate for DIs not detected by the ESI-MS.

The extent of mineralization of organic matter in the samples was investigated by determining total organic carbon (TOC) in the aqueous samples with a multi N/C 2000 analyzer from Analytik Jena, and the total UV absorbance was determined with a Cary 50, Varian.

3. Results and discussion

3.1. Degradation pathway for BAM in chloride medium

Using the analytical tools, the molecular composition of the samples were evaluated and interpreted into an overall scheme showing the proposed degradation pathways in the chloride medium (Fig. 1). In the following, the summarizing proposed degradation pathway is presented with the many arguments underlying the interpretations explained in subsequent paragraphs.

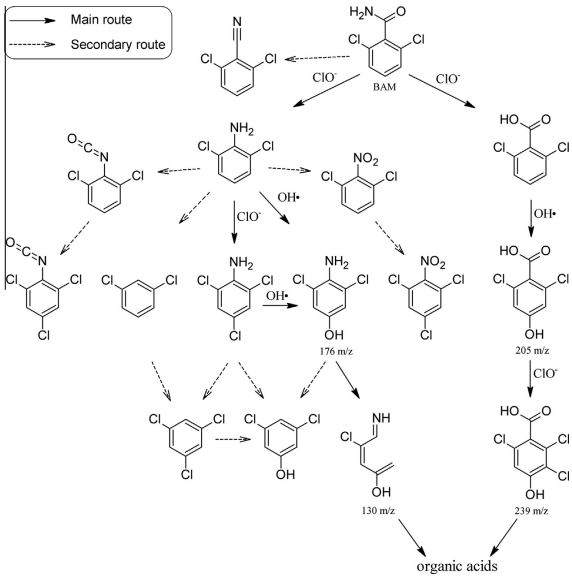

Fig. 1. Proposed degradation pathway for BAM in chloride medium. The scheme distinguishes between main and secondary routes. The compounds formed in the secondary routes were only detected with GC/MS after increasing the concentration 100× with SPE and in intensities much lower than the compounds of the main routes. The possible formation of condensate products is not shown.

When compared to our previous studies, the electrochemical degradation of BAM in a chloride medium was found to lead to a more complex mixture of degradation intermediates compared to when an inert sulfate electrolyte was used (Madsen et al., 2014). The initial step in the chloride electrolyte was an oxidation of the amide group, either to an amine or a carboxylic acid. In the amine route, BAM was first oxidized to 2,6-dichloroaniline (DCA), which was then further chlorinated to 2,4,6-trichloroaniline (TCA). In both of these reactions, the oxidizing agent was active chlorine (likely hypochlorite), which was verified in a standard hypochlorination experiment where sodium hypochlorite was used to oxidize BAM. At the anode, these compounds were hydroxylated to 2,6-dichloro-4-hydroxy-aniline (DCHA), which was further degraded to a small amine compound with a nominal mass of 131 Da. In the carboxylic acid route, BAM was oxidized to 2,6-dichlorobenzoic acid, which was hydroxylated (205 m/z) and then chlorinated (239 m/z). 2,6-Dichlorobenzoic acid itself was not detected, but this was due to very low sensitivity for this compound with both the HPLC and the GC method.

Next to these main routes of degradation, a number of secondary routes were observed. In the initial step, BAM may be converted to 2,6-dichlorobenzonitrile, and in the amine reaction path, the amine group may be oxidized to a nitro or an isocyanato-group, or may be completely removed. The compounds in the secondary routes were however formed in significantly smaller amounts with intensities around 1–5% of that of the compounds in the main route.

Oxidation of chloroanilines or pesticides such as dichlofenac and diuron that readily convert to chloroanilines have been investigated in a number of studies (Arias and Brillas, 1986; Brillas et al., 2010, 2004; Hadasch and Meunier, 1999; Mihály et al., 2001; Polcaro et al., 2004; Carrier et al., 2009; Homlok et al., 2012; Hussain et al., 2012), and it was interesting to compare degradation pathways across studies. In these studies, some of the same DIs as in this study have been found, showing similar reaction trends. There were however also notable differences. In some of the studies, where the oxidation was mediated by hydroxyl radicals, the amine group was found to be substituted for a hydroxy group (Arias and Brillas, 1986; Brillas et al., 2010), which was not the case in this study. Here the amine group was found to be intact through the entire main degradation path from DCA to the 131 Da compound, while the loss of the amine group represented a secondary route. In another study where the hydroxyl radicals were formed via ionizing radiation (Homlok et al., 2012), the amine group was found to intact through ring opening, which is more in line with the observations made in this study. The exact reason for the difference is unknown, but it is possible that the combination of EOTR and hypochlorite mediated oxidation in this study allows for ring opening prior to oxidation of the amine group. Another interesting finding from the other studies on chloroaniline oxidation is the formation of polyaniline condensate products (Hadasch and Meunier, 1999; Mihály et al., 2001; Carrier et al., 2009; Hussain et al., 2012). In this study an unidentified peak with a mass charge ratio of 288 m/z was observed in negative ESI-MS mode, and given its high molecular weight, it might be such a condensate product although its m/z value did not match with any of the previously reported compounds.

3.2. Identification of degradation intermediates

For the compounds detected with GC/MS, identification was primarily made from comparison with fragmentation spectra in a

Table 1
Identification of main degradation intermediates. The table displays the different parameters used in the identification process. nd Indicates for ESI-MS and GC/MS that the compound was not detected in this particular mode.

ESI-MS positive $m/z = M + 1$	ESI-MS negative $m/z = M - 1$	HPLC t_{ret} (min)	GC/MS $m/z = M$	Cl atoms	N atoms	Suggested structure
190 (BAM)	nd	3.2	189	2	1	
nd	205	1.7	nd	2	0	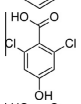
nd	239	2.3	nd	3	0	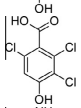
nd	130	10.1	nd	1	1	
nd (DCHA)	176	9.2	177	2	1	
nd (DCA)	nd	nd	161	2	1	
nd (TCA)	nd	nd	195	2	1	
nd	288	2.2	nd	2	1	? (Condensate)

NIST library. Not all compounds could however be detected on the GC/MS, and the structure of the peaks only observed with HPLC/ESI-MS therefore had be deduced from other parameters. These are listed in Table 1. To determine the number of nitrogen atoms the nitrogen rule was used, with an odd molecular mass charge ratio inferring the presence of an odd number of nitrogen atoms and an even number inferring the presence of zero or an even number of nitrogen atoms. In this study, this was taken as either one or zero nitrogen atoms since the occurrence of more than one nitrogen atom per molecule was deemed unlikely, except for condensate products. The number of chlorine atoms was determined from the relative intensity of the +2 isotope peak to the main peak. Also, since the ESI-MS was run in negative mode, detection here could be used to infer the presence of functional groups capable of deprotonating (–OH, –COOH). The retention time of the compounds on the HPLC was used to investigate their relative polarity, which could be used to distinguish amide from amine compounds.

For the 205 and 239 m/z peaks, their even molecular mass charge ratio showed that they had lost their nitrogen atom, and from the relative isotope peak intensity they were found to contain two and three chlorine atoms respectively. Also, from their HPLC retention times, they were found to have similar polarities as BAM. Together these observations suggested the two structures shown in Table 1.

The odd molecular mass charge ratio of the 130 m/z peak showed that it still contained a nitrogen atom and by comparing with the 176 m/z that showed similar HPLC retention, this was taken as strong indications for the presence of an amine rather than an amide group. The isotope ratio showed the compound to contain one chlorine atom, and since it was seen in negative ESI-MS it also contained a deprotonizable group. From these facts, two molecular formulas could be combined to give a molecular mass of 131 Da: $C_4H_2O_2NCl$ and C_5H_6ONCl. Due to the low hydrogen number of the first structure, the second was taken as the most likely. Finally, as seen in Fig. 6, the intensity of the 130 m/z peak was found to follow that of DCHA, which indicated that it was formed from DCHA. With these observations in mind, a proposed scheme for this conversion was made, see Fig. 2, where one of the chlorine atoms was substituted for a hydroxy group and the

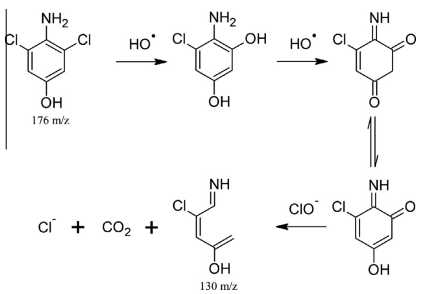

Fig. 2. Proposed scheme for formation of the 131 Da compound.

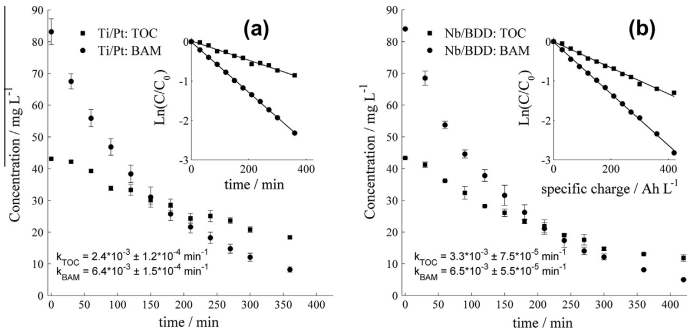

Fig. 3. Degradation plots and kinetics for removal of BAM and TOC with Ti/Pt (a) and Nb/BDD (b) anode. The main plots show the actual data with error bars, representing the standard deviation determined from a double determination. The inset plots show the pseudo first order fits from which the rate constants, lower left corner of plots, have been determined.

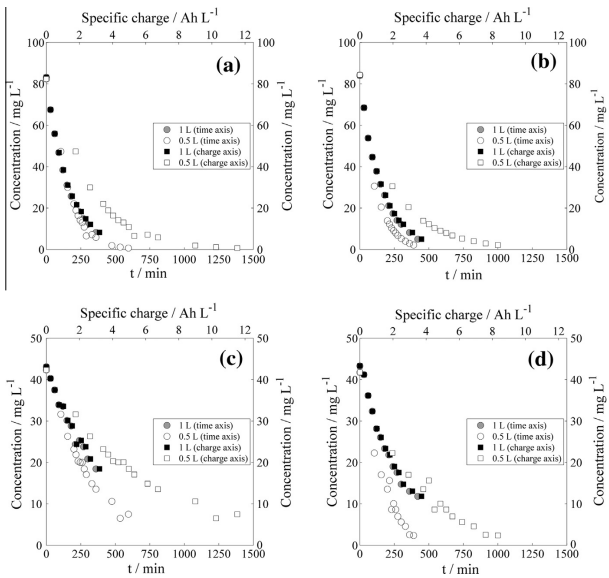

Fig. 4. Plot of BAM and TOC degradation in solutions with starting volumes of 0.5 L and 1.0 L. (a) Pt anode, BAM, (b) BDD anode, BAM, (c) Pt anode, TOC, and (d) BDD anode, TOC.

two hydroxy groups were then oxidized to carbonyl groups. Although neither of the two suggested compounds were detected, both of these processes are commonly suggested for EOTR oxidation of aromatics (Vlyssides et al., 2004; Boye et al., 2006; Ozcan et al., 2008), and the compounds may either have been too short lived or present in too low amounts to allow detection. Quinone can exist in equilibrium with an isomer, which can then react with active chlorine via the same reaction mechanism as seen for the conversion of BAM to DCA.

3.3. Influence of the nature of active oxygen species

As is typical in AOP studies, the kinetics for both TOC and BAM removal were found to be pseudo first order as seen in Fig. 3. More interestingly was that only TOC removal was found to be dependent on the applied anode. Similar rate constants were found for BAM for both Ti/Pt and Nb/BDD indicating that active chlorine oxidation was determining the initial oxidation of BAM. This was in accordance with the identified DIs, which were different from the

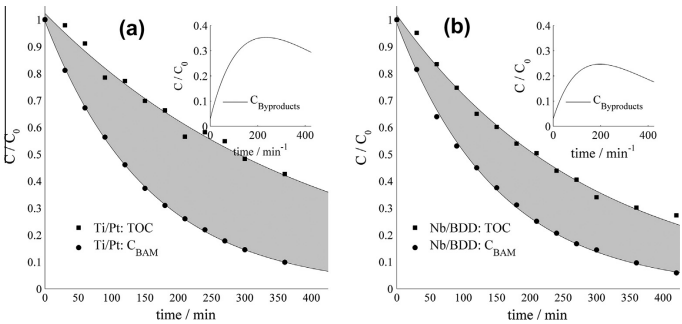

Fig. 5. Total amount of carbon originating from DIs formed during oxidation at Ti/Pt (a) and Nb/BDD (b) anodes. The grey area between the TOC and BAM curves represents the carbon bound in DIs. The subplots show the change in amount of DIs as a function of time.

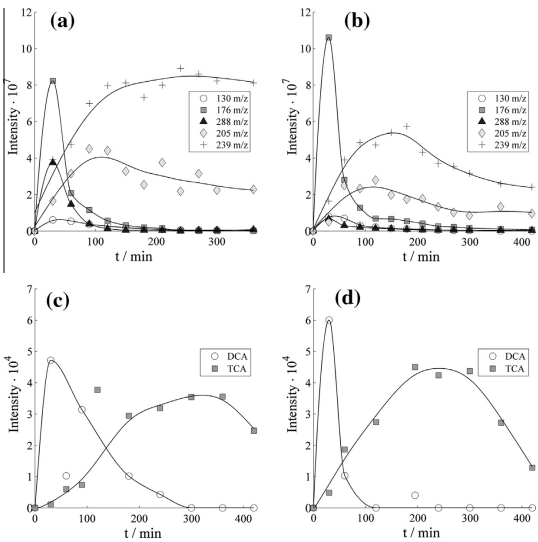

Fig. 6. Evolution in intensities of DIs. (a) Ti/Pt anode, HPLC/ESI-MS, (b) Nb/BDD anode, HPLC/ESI-MS, (c) Ti/Pt anode GC/MS and (d) Nb/BDD anode GC/MS. 2,6-dichloro-4-hydroxy-aniline (176 *m/z*) was detected with both HPLC-ESI/MS and GC/MS. It has not been plotted in the GC/MS plots (c and d), but was found to give similar intensities as DCA and TCA. From this it could be inferred that the two main degradation routes were of comparable importance. The chemical structure of the compounds can be found in Table 1.

ones seen for the EOTR oxidation of BAM in inert electrolyte (Madsen et al., 2014), as would be expected with a different initial step in the degradation scheme.

To elucidate the respective importance of the amount of active chlorine and the EOTR in the process the initial electrolyte volume was changed to 0.5 L, based on the hypothesis that due to the high flow rate (34.4 L h^{-1}) relative to the total volume, the bulk active chlorine concentration could be maintained at a constant high level independent of the solution volume. This would apply since the net production of active chlorine in the cell would be far larger than the consumption due to bulk reactions. Degradation mediated by active chlorine oxidation should therefore occur at the same rate for both an initial volume of 1.0 L and 0.5 L. Removal rate through EOTR was on the other hand inverse dependent on the electrolyte volume due to the dependency on recirculation frequency. On average from a macroscopic viewpoint, the BAM molecules were brought in anodic surface contact twice as frequently in the same time span when the solution volume was 0.5 L compared to 1.0 L.

The effect was investigated by plotting the degradation for both 0.5 L and 1.0 L in the same plot as a function of time (min) and specific charge passed through the electrolyte (A h L^{-1}), respectively

(Fig. 4). If active chlorine oxidation was dominant, the degradation curves would be overlapping in the time plot while the 0.5 L experiment would be less efficient in the specific charge plot. If EOTR oxidation was dominant, the specific charge plot would be overlapping while the rate of reaction was faster in the time plot of the 0.5 L experiment due to the doubled recirculation frequency.

For the Ti/Pt anode, the degradation curves for BAM in both 0.5 L and 1.0 L were almost completely overlapping when plotted as a function of time (Fig. 4a), while for the Nb/BDD anode the degradation was faster in the 0.5 L setup compared to the 1.0 L (Fig. 4b). These results showed that for the Ti/Pt anode, the initial step of the degradation of BAM was almost completely due to active chlorine oxidation, while both active chlorine and EOTR oxidation contributed to the degradation at the Nb/BDD anode. However, active chlorine oxidation was still dominating compared to EOTR at the Nb/BDD as seen from both the rate constants and the close resemblance of the 0.5 L and 1.0 L time plot.

As with BAM, the comparison between the two setups showed that TOC removal was largely determined by active chlorine oxidation for the Ti/Pt anode (Fig. 4c), while it was dominated by EOTR at the Nb/BDD anode. The dominance of the EOTR could even be seen for specific degradation intermediates, like the recalcitrant 239 m/z peak (supporting Fig. S1). Here, the peak intensities of the two experiments completely overlapped when plotted as a function of the applied specific charge.

Since TOC was less efficiently removed by active chlorine oxidation, the use of the active Ti/Pt anode led to a larger amount of total DIs as shown in Fig. 5a. In Fig. 5, the evolution with time of relative carbon originating from DIs is shown in subplots. However, it should be noted that since the active chlorine oxidation was more efficient compared to the EOTR at Ti/Pt with respect to TOC removal, the presence of chloride ions resulted in relatively fewer DIs compared to the degradation operated in inert electrolytes (Madsen et al., 2014). Electroactive ions may therefore both improve the rate of removal and result in fewer DIs for a primarily active anode as Ti/Pt. Since the TOC removal was predominantly determined by EOTR at the Nb/BDD anode, the amount of DIs (Fig. 5b) were similar to that determined previously for the single EOTR process (Madsen et al., 2014).

In Fig. 6, the evolutions in intensity of the individual DIs are shown for a representative experiment. It was mainly the chlorinated species (239 m/z and TCA) and the acid species that resulted in the difference in TOC removal by the two anodes. These compounds were more resistant to active chlorine oxidation which resulted in stable levels of these when using the Ti/Pt anode. When using the Nb/BDD anode all DIs were found to be oxidized, observations in accordance with the general comprehension of the preference of partial oxidation by active anodes and total mineralization by the increased amount of hydroxyl radicals at non-active anodes.

4. Conclusions

In the present study it was found that the presence of chloride ions in the electrochemical oxidation of BAM leads to a more diverse mixture of degradation intermediates (DIs) different from the ones formed in a single electrochemical oxygen transfer reaction (EOTR) process. This was primarily due to the initial oxidation being largely due to active chlorine (hypochlorous acid/hypochlorite) independent of the anode material. The degradation mainly occurred through two pathways. One in which the amide group at BAM was oxidized to an amine group and another in which it was oxidized to a carboxylic acid. The DIs then underwent both chlorination and hydroxylation until ring cleavage occurred.

When using the non-active Nb/BDD anode, the total amount of DIs was lower compared to the more active Ti/Pt anode, and the chlorinated DIs were removed more effectively. The reason for the difference was that for the Nb/BDD anode, TOC and DI removal were dominated by EOTR, whereas for the Ti/Pt anode TOC and DI removal were dominated by the less effective active chlorine oxidation.

Acknowledgements

Financial support from the Danish Ministry of Science, Technology, and Innovation in the form of a Ph.D. study Grant is acknowledged. Excellent laboratory support with the GC/MS analysis was provided by Dorte Spangsmark, Section of Chemical Engineering, Aalborg University, Denmark.

Appendix A. Supplementary material

Supplementary data associated with this article can be found, in the online version, at http://dx.doi.org/10.1016/j.chemosphere.2014.10.058.

References

Arias, A., Brillas, E., 1986. Electrochemical oxidation of 2,4-dichloroaniline in aqueous sulphuric acid medium at a platinum electrode. J. Electroanal. Chem. Interfacial Electrochem. 198, 303–318.
Borràs, N., Oliver, R., Arias, C., Brillas, E., 2010. Degradation of atrazine by electrochemical advanced oxidation processes using a boron-doped diamond anode. J. Phys. Chem. A 114, 6613–6621.
Boye, B., Brillas, E., Marselli, B., Michaud, P., Comninellis, C., Farnia, G., Sandonà, G., 2006. Electrochemical incineration of chloromethylphenoxy herbicides in acid medium by anodic oxidation with boron-doped diamond electrode. Electrochim. Acta 51, 2872–2880.
Brillas, E., Boye, B., Sirés, I., Garrido, J.A., Rodríguez, R.M., Arias, C., Cabot, P.-L., Comninellis, C., 2004. Electrochemical destruction of chlorophenoxy herbicides by anodic oxidation and electro-Fenton using a boron-doped diamond electrode. Electrochim. Acta 49, 4487–4496.
Brillas, E., Garcia-Segura, S., Skoumal, M., Arias, C., 2010. Electrochemical incineration of diclofenac in neutral aqueous medium by anodic oxidation using Pt and boron-doped diamond anodes. Chemosphere 79, 605–612.
Carrier, M., Besson, M., Guillard, C., Gonze, E., 2009. Removal of herbicide diuron and thermal degradation products under Catalytic Wet Air Oxidation conditions. Appl. Catal., B 91, 275–283.
Flox, C., Cabot, P.L., Centellas, F., Garrido, J.A., Rodríguez, R.M., Arias, C., Brillas, E., 2006. Electrochemical combustion of herbicide mecoprop in aqueous medium using a flow reactor with a boron-doped diamond anode. Chemosphere 64, 892–902.
Hadasch, A., Meunier, B., 1999. Oxidation of dichloroanilines and related anilides catalyzed by iron(III) tetrasulfonatophthalocyanine. Eur. J. Inorg. Chem. 1999, 2319–2325.
Homlok, R., Takács, E., Wojnárovits, L., 2012. Ionizing radiation induced reactions of 2,6-dichloroaniline in dilute aqueous solution. Radiat. Phys. Chem. 81, 1499–1502.
Hussain, I., Zhang, Y., Huang, S., Du, X., 2012. Degradation of p-chloroaniline by persulfate activated with zero-valent iron. Chem. Eng. J. 203, 269–276.
Madsen, H.T., Søgaard, E.G., Muff, J., 2014. Study of degradation intermediates formed during electrochemical oxidation of pesticide residue 2,6-dichlorobenzamide (BAM) at boron doped diamond (BDD) and platinum–iridium anodes. Chemosphere 109, 84–91.
Martínez-Huitle, C.A., De Battisti, A., Ferro, S., Reyna, S., Cerro-Lopez, M., Quiro, M.A., 2008. Removal of the pesticide methamidophos from aqueous solutions by electrooxidation using Pb/PbO_2, $TiSnO_2$ and Si/BDD electrodes. Environ. Sci. Technol. 42, 6929–6935.
Mihály, K., Zoltán, N., Tamás, K., Farsang, G., 2001. The electrochemical oxidation of 4-chloroaniline, 2,4-dichloroaniline and 2,4,6-trichloroaniline in acetonitrile solution. Electrochim. Acta 46, 1297–1306.
Muff, J., Søgaard, E.G., 2011. Identification and fate of halogenated PAHs formed during electrochemical treatment of saline aqueous solutions. J. Hazard. Mater. 186, 1993–2000.
Muff, J., Andersen, C.D., Erichsen, R., Soegaard, E.G., 2009. Electrochemical treatment of drainage water from toxic dump of pesticides and degradation products. Electrochim. Acta 54, 2062–2068.
Ozcan, A., Sahin, Y., Koparal, A.S., Oturan, M.A., 2008. Propham mineralization in aqueous medium by anodic oxidation using boron-doped diamond anode: influence of experimental parameters on degradation kinetics and mineralization efficiency. Water Res. 42, 2889–2898.
Panizza, M., Cerisola, G., 2009. Direct and mediated anodic oxidation of organic pollutants. Chem. Rev. 109, 6541–6569.
Polcaro, A.M., Mascia, M., Palmas, S., Vacca, A., 2004. Electrochemical degradation of diuron and dichloroaniline at BDD electrode. Electrochim. Acta 49, 649–656.

Polcaro, A.M., Vacca, A., Mascia, M., Palmas, S., 2005. Oxidation at boron doped diamond electrodes: an effective method to mineralise triazines. Electrochim. Acta 50, 1841–1847.
Quiroz, M.A., Bandala, E.R., Martínez-huitle, C.A., 2011. Advanced oxidation processes (AOPs) for removal of pesticides from aqueous media. In: Stoytcheva, M. (Ed.), Pesticides – Formulations, Effects, Fate, one ed. InTech, pp. 685–730.
Rabaaoui, N., Saad, M.E.K., Moussaoui, Y., Allagui, M.S., Bedoui, A., Elaloui, E., 2013. Anodic oxidation of o-nitrophenol on BDD electrode: variable effects and mechanisms of degradation. J. Hazard. Mater. 250–251, 447–453.
Sirtori, C., Agüera, A., Gernjak, W., Malato, S., 2010. Effect of water–matrix composition on trimethoprim solar photodegradation kinetics and pathways. Water Res. 44, 2735–2744.
Vlyssides, A., Barampouti, E.M., Mai, S., Arapoglou, D., Kotronarou, A., 2004. Degradation of methylparathion in aqueous solution by electrochemical oxidation. Environ. Sci. Technol. 38, 6125–6131.
Wei, J., Feng, Y., Sun, X., Liu, J., Zhu, L., 2011. Effectiveness and pathways of electrochemical degradation of pretilachlor herbicides. J. Hazard. Mater. 189, 84–91.

Paper XI

Henrik Tækker Madsen, Erik G. Søgaard and Jens Muff

Reduction in energy consumption of electrochemical pesticide degradation through combination with membrane filtration

Chemical Engineering Journal, **276** (2015), 358-364

Reprinted with permission from Elsevier

Chemical Engineering Journal 276 (2015) 358–364

Contents lists available at ScienceDirect

Chemical Engineering Journal

journal homepage: www.elsevier.com/locate/cej

Reduction in energy consumption of electrochemical pesticide degradation through combination with membrane filtration

Henrik Tækker Madsen *, Erik Gydesen Søgaard, Jens Muff

Section of Chemical Engineering, Department of Biotechnology, Chemistry and Environmental Engineering, Aalborg University, Niels Bohrs Vej 8, 6700 Esbjerg, Denmark

HIGHLIGHTS

- Use of NF/RO membranes and electrochemical oxidation were combined.
- Synergies could be obtained with use of a RO membrane.
- Synergies cannot be obtained when NF membranes are used.
- The total energy was reduced with 95% when using a RO membrane.

ARTICLE INFO

Article history:
Received 16 February 2015
Received in revised form 20 April 2015
Accepted 21 April 2015
Available online 28 April 2015

Keywords:
Reverse osmosis (RO)
Nanofiltration (NF)
Electrochemical oxidation
Combined treatment
2,6-Dichlorobenzamide (BAM)

ABSTRACT

A significant challenge for large-scale use of electrochemical oxidation (EO) is high energy consumption, and for EO to become accepted as a standard technique, the amount of energy consumed in the process must be reduced.

In this study, it was investigated how the energy consumption of EO could be lowered by combining the process with membrane filtration, in a setup where EO was applied to the membrane retentate stream. Use of two types of membranes, a nanofiltration (NF) and a reverse osmosis (RO) membrane, was investigated, and to provide realistic estimates on the energy consumption of the treatment, natural groundwater spiked with the pesticide residue 2,6-dichlorobenzamide (BAM) was used as matrix in the experiments. To understand the effect of the membranes on the energy consumption, their effect on the EO degradation efficiency was also determined.

The results showed that membranes significantly reduced the energy consumption of the EO processes. Using the RO membrane with a recovery of 90%, the energy consumption of the combined EO and membrane setup used 95% less energy (0.96 kW h/m^3) compared to the stand-alone EO treatment (18.5 kW h/m^3). The reduction in energy consumption was found to be a result of primarily two factors; (1) a smaller volume of water was in need in the energy intensive EO treatment, and (2) the high rejection of chloride by the RO membrane increased the rate of degradation through mediated active chlorine oxidation in the membrane retentate. It was not possible to obtain the same positive benefits using the NF membrane, which was mainly due to a lower chloride rejection and a too low rejection of BAM. The investigation showed that combining RO filtration with EO of the contaminants in the concentrate provides a promising strategy for the dissemination of advanced oxidative treatment techniques in larger scale and actual use for protection of the environment.

© 2015 Elsevier B.V. All rights reserved.

1. Introduction

Over the years, removal of micropollutants from water resources has attracted much attention in the scientific literature, and a number of approaches and techniques have been identified as effective means of remediation. Among these are degradation processes such as advanced oxidation processes (AOPs) [1–3]. However, AOPs suffer from drawbacks that so far have limited the transfer and breakthrough of the techniques from research studies to large scale micropollutant removal applications. The drawbacks are mainly high energy consumption and the formation and control of degradation intermediates (DIs), organic and inorganic byproducts [3,4]. One way of overcoming some of these challenges, hereby maturing the technologies for market applications, could be through combination with membrane filtration.

* Corresponding author. Tel.: +45 20960733.
E-mail address: htm@bio.aau.dk (H.T. Madsen).

http://dx.doi.org/10.1016/j.cej.2015.04.098
1385-8947/© 2015 Elsevier B.V. All rights reserved.

Generally, there are two strategies for combination of AOPs and membranes. One is to use an ultrafiltration (UF) or loose nanofiltration (NF) membrane to reduce turbidity and then apply an AOP method to treat the membrane permeate [5]. This strategy may be especially useful for AOPs dependent on UV and/or chemicals, since it lowers background absorption and side reactions, and since the energy consumption of the membrane filtration can be kept low due to the relative low pressure needed to drive UF/loose NF membranes [5,6]. There is on the other hand no control of organic DIs and byproducts, and around 70–90% of the water must be treated with the AOP depending on the specific water recovery of the membrane process [6,7].

The second strategy is to use NF/RO (reverse osmosis) membranes with almost complete rejection of the micropollutants and then apply the AOP to the retentate stream [6,7]. This strategy provides some degree of control over DIs and byproducts, since these are separated from the treated membrane permeate, and also the AOP only needs to be applied to around 10–30% of the water in the retentate stream. Furthermore, due to the reduction in volume, the micropollutant concentration will increase, and this has been found to lead to more energy efficient degradations due to the fact that AOP mediated degradation follows pseudo first order kinetics in most typical modes of operation [7–10] as described with Eq. (1):

$$-r = k' \cdot C, \quad k' = k \cdot [\mathrm{OH}^{\cdot}][\text{oxidants}] \tag{1}$$

where oxidants denote oxidizing species generated during the process.

The drawback of this strategy is that turbidity and natural organic matter (NOM) is not separated from the micropollutants, and this may in certain cases inhibit the effectiveness of UV and chemically driven AOPs. One AOP that can benefit from the high concentrations of species in the retentate is electrochemical oxidation (EO). EO has in the last 15 years been demonstrated as an powerful technique for degradation of aqueous contaminants such as pesticides in water through oxidation by anodic generated oxidants as active oxygen species in the so-called electrochemical oxygen transfer process (EOTR) and bulk oxidants as active chlorine species generated by chloride electrolysis. For further information on the mechanisms involved in electrochemical oxidation of organics in water please refer to this Ref. [11]. Since NF/RO membranes not only reject organic micropollutants, but also ionic species, conductivity will increase in the retentate, decreasing the ohmic resistance in the electrolyte thus lowering the energy required for the oxidation [2].

In literature, much knowledge on how membranes may affect the electrochemical oxidation is already present. Increasing electrolyte concentration has been found to decrease energy consumption in studies of electrochemical oxidation of pesticides [12–14], but there may also exist concentrations above which the energy consumption increases again due to a potentiostatic buffering of the chlorine redox system, which decreases the anode potential [15,16]. Furthermore, the specific ionic rejection by the membrane may also affect the efficiency gain in the subsequent electrochemical oxidation. If the membrane operates with a high rejection of electroactive species, in particular chloride, indirect active chlorine mediated oxidation pathways will be of increasing importance. If the membrane operates with a high rejection of more inert ions such as sulfate and a low rejection of chloride, surface mediated oxidation by hydroxyl radicals and other reactive oxygen species produced in the electrochemical oxygen transfer reaction (EOTR) may be more important. Besides differences in energy efficiency of the two processes, they lead to different degradation pathways and thus different types of DIs as well as total amount of DIs formed in the process [17,18]. Membrane concentrates, especially from RO, have already been identified as applicable water sources for electrochemical oxidation, but the studies have almost exclusively looked at the applicability of the electrochemical oxidation to treat the RO concentrate for specific contaminants, and in these papers, little attention has so far been devoted to investigating specific benefits of the combination [19–25].

In this study, the aim was to investigate the potential benefits of combining electrochemical oxidation with NF/RO membranes. This was done by studying how upstream use of the membranes affected the degradation efficiency of the electrochemical oxidation and the energy consumption required to obtain a total 1-log removal in one cubic meter of water. To provide realistic estimates, natural groundwater pretreated with aeration and sand filtration (tap water) spiked with a micropollutant was used rather than synthetic solutions. The micropollutant used in the study was the persistent pesticide residue 2,6-dichlorobenzamide (BAM), for which both the applicability of NF/RO membranes [26], electrochemical oxidation [17,18] and aeration/sand filtration [27,28] as stand-alone treatment methods have previously been studied by us. In the work on electrochemical oxidation of BAM, the degradation pathways were mapped and BAM was found to be completely mineralized [17,18]. The main challenge for a widespread use of electrochemical oxidation for treatment of this compound is therefore the amount of energy used in the process.

2. Materials and methods

2.1. Chemicals and materials

BAM was purchased at Sigma Aldrich with purity >98%. Water was taken from the tap (Esbjerg, Denmark). The composition of Esbjerg tap water and the 80% and 90% recovery retentates obtained by the NF and RO membrane are seen in Table 1. The water used in the study was Esbjerg (Denmark) tap water produced from groundwater and treated with aeration and sand filtration. To remove potential iron colloids added the water from the water distribution network, the tap water was filtered through a 0.45 μm filter. The spiral NF99HF NF membrane (element type NF-2517/48, length 432 mm, outer diameter 64 mm) was purchased from Alfa Laval (Nakskov, Denmark). The spiral XLE low pressure RO membrane (XLE-2521, length 533 mm, outer diameter 64 mm) was donated by Dow Chemicals. Filtration was performed with a DDS Lab-Unit M20 (Alfa Laval, Nakskov, Denmark), modified in house for use with spiral membranes. For the electrochemical oxidation experiments, an Electrocell Micro Flow Cell (Tarm, Denmark) with an AISI 316 cathode and Nb/BDD anode with active electrode areas of 10 cm^2 was used. The cell was of plate-like

Table 1
Composition of tap water and membrane retentates. The XLE 90% recovery retentate became supersaturated in $CaCO_3$, which precipitated out prior to analysis. The numbers in parenthesis are the theoretical numbers calculated based on the rejections reported in [26]. The supersaturation was not found to affect the degradation, but is a practical challenge for the membrane filtration step.

Recovery (%)	Tap	NF99HF		XLE	
	0	80	90	80	90
Na^+ (mg/L)	18	27	38	85	145
K^+ (mg/L)	2	4	8	12	28
Mg^{2+} (mg/L)	5	15	30	23	43
Ca^{2+} (mg/L)	48	114	191	175	152 (417)
Cl^- (mg/L)	33	42	53	167	288
SO_4^{2-} (mg/L)	25	88	202	116	218
HCO_3^- (mg/L)	142	344	546	531	435 (1060)
pH	8.1	8.7	8.5	7.9	8.4
Conductivity (μS)	348	708	1077	1398	2049

design with an electrode gap of 3 mm with internal turbulence promoters.

2.2. Experimental setups

The two experimental setups used for membrane filtration (NF and RO) and electrochemical oxidation (EO) are sketched in Fig. 1.

The electrochemical oxidation was performed galvanostatically in a batch recirculation setup with an anodic current density of 10 mA cm^{-2}. The electrolyte volume was 1 L in all experiments and the solution was pumped at a flow rate of 34.4 L h^{-1} from the reservoir through the electrochemical cell in upflow mode to maximize the turbulence and thus mass transfer in the cell. To ensure a constant water temperature of 25 °C, a cooler was installed after the cell. All experiments were run in duplicate. Applied voltage was provided to the cell from an analog power supply (Mersan Elektrik Cihazlari), and cell voltage and current was measured with separate multimeters (Agilent 34401A 6½ Digit Multimeter) for increased accuracy.

Concentrated NF and RO membrane retentates were prepared with recoveries of 80% and 90%, by filtration of 60 L of tap water to either 12 L (80% recovery) or 6 L (90% recovery). Prior to membrane filtration, the tap water was filtered with a 0.45 μm membrane to remove iron (hydr)oxide colloids from the water distribution network. The membranes were prepared according to the procedures of the manufactures, and allowed to compact by filtration with distilled water for 1 h at 5 bar before filtration of the tap water was commenced. Filtration with the NF99HF and XLE membrane was performed at 25 °C and 5 bar transmembrane pressure (TMP).

Spiked solutions of 10 mg L^{-1} BAM was used as the initial concentration in the experiments. This was far higher than what is found in most contaminated groundwater samples, but was used to avoid the need for solid phase extraction, which would decrease the precision of the results. The use of higher concentrations is standard in studies of electrochemical oxidation of pesticides [15,16,29–32], and is based on the assumption that the kinetics is not influenced by the initial concentration. To be able to distinguish the effects of the increase in the ionic concentration and the increase in BAM concentration, BAM was spiked into the retentates after desired recovery was obtained. The rejection of BAM for both membranes has previously been determined to be 73.8% (NF99HF) and 98.1% (XLE) [26], and based on these numbers, initial BAM concentrations in the four retentates were calculated to be 29.7 mg L^{-1} (80% recovery) and 40.5 mg L^{-1} (90% recovery) for the NF99HF membrane and 47.8 mg L^{-1} (80% recovery) and 91.3 mg L^{-1} (90% recovery) for the XLE membrane. Experiments with the retentate solution were conducted at both 10 mg L^{-1} BAM and the calculated retentate concentration.

2.3. Analytical procedures

The degradation of BAM was analyzed with a HPLC/UV system (1260 Infinity, ZORBAX Eclipse Plus C18 column, Agilent Technology). A 20:80 (v/v) mixture of acetonitrile and distilled water was used as eluent, and pumped with a flow rate of 400 μL min^{-1} at 25 °C. The absorption wavelength on the UV detector was set to 210 nm, and the injection volume at 5 μL.

2.4. Comparison parameters

To evaluate the benefits of combining electrochemical oxidation with NF/RO membranes the EO-membrane systems were compared on two parameters: Degradation efficiency of the electrochemical oxidation and total energy of the treatment.

Degradation efficiency was evaluated from the rate of BAM removal and the energy used by the electrochemical oxidation to obtain a 1-log reduction in concentration and mass. The 1-log reduction in concentration is a IUPAC recommended measure for comparison of AOP degradations, and is defined by Eq. (2) [33]:

$$EE_V = \frac{P \cdot t_{90}}{V \cdot \log\left(\frac{C_0}{C}\right)} \tag{2}$$

where P is the power in kW, t_{90} is the time in hours required to obtain a 1-log removal, V is the volume in m^3, C is the concentration of the organic after a 1-log removal and C_0 is the initial concentration.

Due to the kinetics of the rate law shown in Eq. (1), the energy required to obtain a 1-log removal based on concentration is theoretically independent on the initial concentration of the pesticide, and this removes some of the incentive to perform a membrane filtration pretreatment with the purpose of increasing initial concentration. However, since the independence of initial concentration does not apply when the 1-log removal is based on mass, a more efficient removal of organic mass per kW h may theoretically be obtained. Therefore we also determined the energy per kilogram of BAM required for a 1-log mass removal (3) [33]:

$$EE_m = \frac{P \cdot t_{90}}{V \cdot C_0 \cdot 0.9} \tag{3}$$

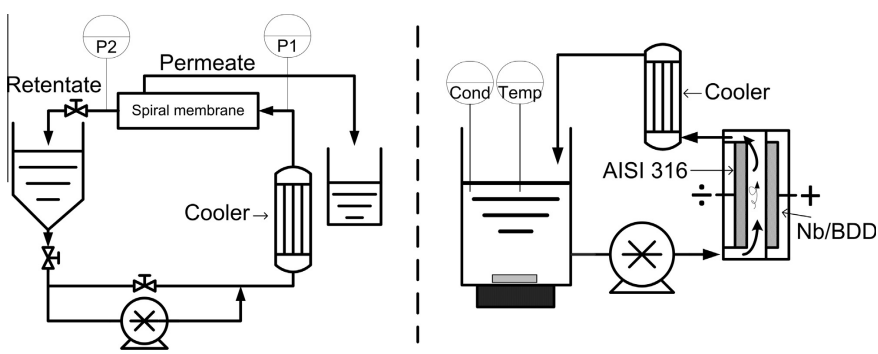

Fig. 1. Sketch of the two experimental setups used; the membrane filtration setup to the left and the electrochemical oxidation setup to the right.

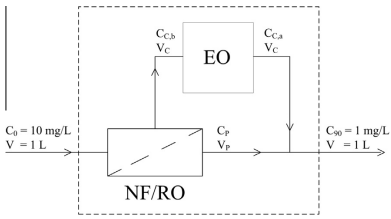

Fig. 2. Scheme for evaluating the total energy consumption of the treatment process.

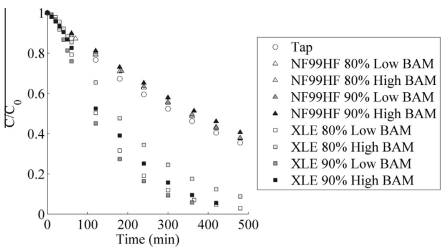

Fig. 3. Degradation curves for BAM in tap water and 80% and 90% recovery retentates from the NFF9HF and XLE membranes. The terms "High" and "Low" BAM are used to distinguish between experiments in which the increase in BAM was and was not taken into account. This was done to separate the effect of the changing ionic environment and the increase in BAM concentration. Tap water represents the case with no membrane filtration. The percentages refer to the recovery.

C_0 is the initial concentration in kg/m^3. The two energy estimates presented in Eqs. (2) and (3) illustrate the energy used to treat one cubic meter of a given water type, and can as such be used to evaluate the effect of the water, and hereby the membrane filtration, on the energy efficiency of the EO degradation in the given environment.

The total energy of the treatment was evaluated as the combined energy usage of the membranes and the electrochemical oxidation to treat obtain a 1-log reduction in concentration in one cubic meter of incoming feed. The reason for including this parameter is that from an operator and engineering point of view it is also of interest to evaluate the total energy input needed to treat a given water source, and since membrane filtration both adds to the energy consumption and influence the volume in need of electrochemical treatment, the numbers from Eqs. (2) and (3) cannot be used. Instead Eq. (4), based on the scheme presented in Fig. 2 must be used:

$$EE_{total} = E_{mem} + E_{EO} \tag{4}$$

where E_{mem} is the energy required by the membrane filtration, and E_{EO} is the energy needed in the electrochemical treatment. EE_{total} is as such the total energy of the entire treatment. The energy used in the membrane filtration depends on the type of membrane and the recovery. The energy consumed in the electrochemical treatment depends on the specific rejection of the membrane as well as the volume that needs to be treated, and Eq. (4) may therefore be expanded to Eq. (5):

$$EE_{total} = E_{mem} + \frac{P \cdot t \cdot V_C}{V} \tag{5}$$

where V is the inlet/outlet volume, V_C the volume of water sent for electrochemical treatment, and t the time necessary to obtain the final concentration $C_{C,a}$ required for a 1-log removal after the permeate and retentate streams are mixed. $C_{C,a}$ can be calculated with Eq. (6):

$$C_{C,a} = \frac{C_{90} \cdot V - C_P \cdot V_P}{V_C} \tag{6}$$

2.5. Estimation of membrane energy consumption

To estimate the energy consumption by the membrane filtration process, the software ROSA by Dow was used. In ROSA, the filtration process can be modeled by specifying the water composition, the flow conditions, the membrane configuration setup and the type of membrane.

Two membrane systems were set up in the model, one for 80% recovery and one for 90% recovery (Table 3).

Each setup was modeled for both types of membranes. Since only Dow Filmtec membranes can be used with ROSA, the NF99HF membrane could not be modeled directly. Its performance is however assumed to be similar to the Dow NF membrane NF270, since both membranes show similar performance with respect to rejections of mono- and divalent ions. The NF270 was thus used as a substitute in the modeling. After the simulation, the specific energy (kW h/m^3) required for the membrane treatment could be extracted (Table 3). A curiosity from the simulations was that less energy was required to obtain a recovery of 90% compared to 80%, which may be due to different efficiencies for the chosen 80% and 90% recovery setups. It is possible that more ideal setups can be found, but the ones used in this work can still be used to get an estimate of the energy consumption of the membrane filtration.

3. Results and discussion

3.1. Effect of membrane filtration on rate of degradation

In Fig. 3, the degradation curves for BAM obtained in tap water and the membrane retentates are compared. It is seen that degradation in the retentates of the NF membrane NF99HF occurred at a slightly lower rate compared to tap water. This was likely due to an increase in the concentration in the NF retentate of bicarbonate/carbonate that can act as a hydroxyl radical scavenger forming less reactive carbonate radicals (reactions (7) and (8)) and thus decreasing the efficiency of the hydroxyl radical mediated oxidation in the close vicinity of the electrode surface [34]:

$$OH^{\cdot} + HCO_3^- \rightarrow OH^- + HCO_3^{\cdot} \tag{7}$$

$$OH^{\cdot} + CO_3^{2-} \rightarrow OH^- + CO_3^{-\cdot} \tag{8}$$

It can also be seen that the 90% recovery retentate inhibited the rate of removal slightly more than the 80% recovery retentate, which is in accordance with the bicarbonate hypothesis.

Use of the RO membrane XLE significantly increased the rate of removal, but the evolution of the degradation curve did not follow the expected first order kinetics. Instead, the degradation could be divided into two distinct regions; an initial period with a very slow rate of BAM removal, followed by a period in which the rate of removal accelerated significantly until reaching stable first order kinetics. The rate of removal in the initial period was lower than the rates observed in both tap water and the NF99HF retentates, which again may be explained by increasing bicarbonate concentration, which was higher in both XLE retentates due to the higher rejection. The speed up of the process and the increase in the rate of removal compared to NF retentates may be due to formation of

active chlorine in the XLE retentates. The XLE membrane had a higher rejection of chloride compared to the NF99HF membrane, see Table 2, and this may explain why the increased rate of removal was not observed in the NF99HF retentates. For the XLE membrane, the rate of removal was also higher in the 90% recovery retentate compared to the 80% recovery retentate, which was in accordance with the active chlorine hypothesis. The observed initial delay in removal rate could be explained by an initial low concentration of active chlorine that first needed to build up before it could influence the removal rate.

From the pseudo first order model, Eq. (1), increased initial concentration of BAM was not expected to influence the rate of removal. However, as can be seen from the curves in Fig. 3, increasing BAM concentrations provided decreased rates of removal. The same effect had also previously been noticed by others [35] and may be caused by competitive oxidation between BAM and degradation intermediates. On the other hand, this hypothesis would not explain why the BAM removal kinetics were stable even as the concentration of BAM decreased. This dependence of the rate of removal on the initial concentration was interesting, since most electrochemical oxidation studies reported in literature have been carried out at concentrations similar to the levels used in this study, under the assumption that kinetics may be extrapolated and apply to the much lower environmentally relevant concentrations [15,16,29–32]. Based on these findings, it could seem either that the rate of removal might be higher at lower concentrations, or that a level exist above which the rate of removal decreases.

3.2. Effect of membrane filtration on EO energy consumption

Using the NF99HF membrane did not significantly change the energy required to obtain a 1-log removal of BAM compared to tap water, see Fig. 4. The increased conductivity in the NF99HF retentates lowered the ohmic resistance, but because the rate of removal was slightly inhibited, the energy required for a 1-log removal was almost the same.

For the XLE membrane a significant reduction in energy was observed. The energy reduction was a combined result of the higher rate of removal in the XLE retentate and the increased conductivity, which was even higher than in the NF99HF retentate.

In both membrane retentates, the increase in concentration of BAM was found to have a negative effect on the energy consumption, which again was due to the lower rate of removal observed in the solutions with increased BAM concentration.

Based on the column plot in Fig. 4, there seemed to be only little benefit in energy consumption from using the NF99HF membrane. However, as shown in Fig. 5 when comparing the energy required to obtain a 1-log removal per kg BAM, a more significant energy efficient removal of BAM was found in the NF99HF retentates compared to tap water. Comparing the results for the retentates with low and high BAM concentration, it is seen that the improvement was due to the increased BAM concentration.

Table 2
Overview of the different experimental setups used in the current study. All experiments were duplicated.

Exp. No.	Technology	Membrane	Recovery (%)	c(BAM) (mg L^{-1})
1	EO	–	0	10.0
2	NF-EO	NF99HF	80	10.0
3	NF-EO	NF99HF	90	10.0
4	NF-EO	NF99HF	80	29.7
5	NF-EO	NF99HF	90	40.5
6	RO-EO	XLE	80	10.0
7	RO-EO	XLE	90	10.0
8	RO-EO	XLE	80	47.8
9	RO-EO	XLE	90	91.3

Table 3
Input parameters for ROSA simulation of membrane energy consumption and calculated energies. The flow factor takes factors such as membrane compaction, fouling and scaling which may reduce the membrane performance into consideration. 0.85 can be considered as a relatively conservative number.

	Recovery	
	80%	90%
Feed flow (m^3 h^{-1})	3	3
Temperature (°C)	25	25
Flow factor	0.85	0.85
Pump efficiency (%)	80	80
Number of passes	1	1
Number of stages in pass	2	3
Number of pressure vessels/membranes in each vessel		
Stage 1	4/8	4/8
Stage 2	3/4	3/4
Stage 3	–	3/4
Energy consumption (kW h/m^3)		
NF99HF	0.14	0.13
XLE	0.21	0.19

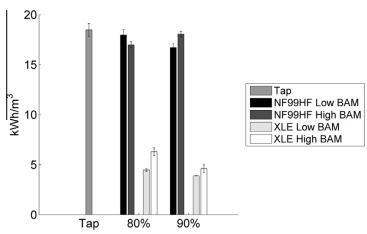

Fig. 4. Comparison of the energy required to obtain a 1-log removal of BAM. The terms "High" and "Low" BAM are used to distinguish between experiments in which the increase in BAM was and was not taken into account. This was done to separate the effect of the changing ionic environment and the increase in BAM concentration. Tap water represents the case with no membrane filtration. The percentages refer to the recovery.

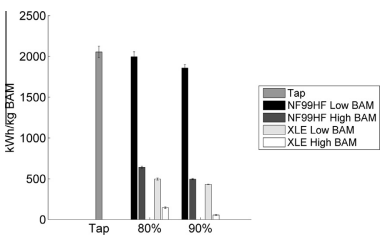

Fig. 5. Comparison of the energy required to per kg BAM to obtain a 1-log removal. The terms "High" and "Low" BAM are used to distinguish between experiments in which the increase in BAM was and was not taken into account. This was done to separate the effect of the changing ionic environment and the increase in BAM concentration. Tap water represents the case with no membrane filtration. The percentages refer to the recovery.

As before, the mass based energy reductions were even higher when the degradation was performed in the XLE retentates. Again this was due to the improved rate of removal and higher conductivity, but also because of the higher rejection of BAM, which led to higher initial concentrations of BAM in the XLE retentates. The effect of the two first parameters were significant

enough to ensure that already at a recovery of 80% and without accounting for the beneficial effect of increasing BAM concentration (80% XLE Low BAM, Fig. 4), the reduction in energy was larger than for the best result of the NF99HF membrane (90% NF99HF High BAM, Fig. 5).

The comparison of the two membranes illustrates the relative importance of the presence of electroactive and inert ions in the retentate. Since the NF99HF membrane predominantly rejected relatively inert divalent ions such as sulfate, the rate of degradation in the NF retentates was very close to that for the tap water. On the other hand, the XLE membrane rejected the electroactive chloride ion strongly, which benefited the removal. Since the difference in rejection of sulfate and chloride is fundamental for NF and RO membranes, the present results obtained for the NF99HF and XLE offers a generally valid comparison between the usefulness of NF and RO membranes for combination with electrochemical oxidation. Based on these findings, NF membranes can be expected to result in fewer improvements in the degradation efficiency for an electrochemical oxidation. The lower rejection of ionic species provides a smaller increase in conductivity compared to RO membranes, and especially the lower rejection of chloride seems to be important.

3.3. Effect of membrane filtration on total energy consumption

To truely evaluate the effect of combining membranes and electrochemical oxidation, we compared the total energy of the membrane-EO system used to obtain a 1-log removal per cubic meter of water as outlined by Eq. (5).

Based on the feed concentrations and specific rejections of the membranes, the final concentration in each of the membrane retentates required to obtain a 1-log removal, when the treated concentrate was mixed with the permeate ($C_{C,a}$), were calculated. For the XLE membrane, final BAM concentrations of 2.8 mg/L (80% recovery) and 1.3 mg/L (90% recovery) were calculated. Mixing retentates with these concentrations with the permeate streams would result in a final stream with a concentration 1-log lower than the feed concentration. The NF99HF membrane was found not to be applicable in this analysis. Because of its low rejection of BAM, it was not possible to use the NF99HF membrane to treat the water at the chosen recoveries, since the permeate concentration became to high to allow a final 1-log removal when mixing the permeate and treated retentate.

In Fig. 6, the total energy as calculated by Eq. (5) are compared for the three scenarios: No membrane, 80% recovery and 90% recovery with the XLE membrane. Used directly on tap water, EO alone required 18.5 kW h/m^3 to obtain a 1-log removal, while the combined RO–EO schemes at 80% and 90% RO recovery required a total of 1.47 and 0.96 kW h/m^3. This corresponded to a reduction in the energy consumption of 92.1% and 94.8% compared to single use of EO. The numbers are relatively robust. If for instance an uncertainty of 10% is ascribed to both the estimated energy consumption of the RO process and the time required for the EO process (e.g. as a result of less ideal flow conditions than in this experiment or other factors decreasing the efficiency), energy consumptions for the RO(80%)–EO and the RO(90%)–EO increased to 1.62 kW h/m^3 and 1.05 kW h/m^3, reducing the overall energy improvement marginally to 91.3% and 94.3%. Part of the reduction of the energy consumption was due to improved degradation kinetics and higher conductivity, but, as seen through comparison with Fig. 4, significantly larger energy reductions were found, when the total energy of the system was considered. Also, less energy in total was required to treat the 90% recovery retentate although the actual electrochemical oxidation was less energy efficient in this retentate as previously shown in Fig. 4. This showed that the reduction of the volume in need of electrochemical

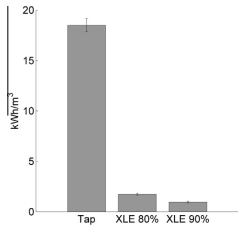

Fig. 6. Total energy of both membrane and electrochemical oxidation to obtain a 1-log removal of BAM in one cubic meter of groundwater. Tap water represents the scenario without the membrane, where all the water undergoes electrochemical treatment, whereas it is only 20% and 10% of the water in the XLE 80% and XLE 90% recovery scenarios.

treatment was the single most important factor. The reason for this was the large difference in the energy consumption per cubic meter of water between the electrochemical oxidation process and the membrane filtration process.

The NF99HF membrane was not applicable in this scenario concerning BAM as chemical of concern. However, for a larger pesticide for which a higher rejection could be obtained by NF membranes, large energy saving compared to the use of electrochemical oxidation directly to the tap water, could potentially still be obtained by using this type of membrane. These energy savings would however mainly be related to the reduction in the volume in need of electrochemical treatment, and due to the relative large difference in the energy consumption of the electrochemical treatment and the membrane processes and the relatively small difference in energy consumption by the NF99HF and the XLE membrane, it would generally be more energy efficient to use the XLE membrane instead of the NF99HF membrane. In general, use of NF membranes will not lead to larger reductions in the total energy consumption compared to RO membranes.

4. Conclusions

The total energy required for an electrochemical treatment of tap water polluted with the pesticide residue BAM could be reduced with 94.8% by combining the treatment with membrane filtration using the RO membrane XLE operating with a recovery of 90%. The main reason for this reduction in energy originated from a significant reduction of the volume of water in need of electrochemical treatment, but also the increased conductivity and the high rejection of chloride, which was oxidized to active chlorine capable of bulk BAM removal, increased the energy efficiency of the degradation.

Use of NF membranes such as NF99HF may also result in more energy efficient treatments. However, NF membranes often suffer from lower rejections, which as in this study, may deem them unsuitable for a combined treatment because the permeate concentration becomes too high. Also, where the XLE membrane increased the efficiency of the electrochemical oxidation, the degradation efficiency in the NF99HF concentrates was very close to tap water. The reason was the difference in the specific rejections of the ionic species by the two membranes. The NF99HF membrane rejected a smaller part of the ions, resulting in a smaller increase in conductivity compared to the XLE membrane, and due to the low rejection of chloride, the formation of active chlorine did not impact the degradation significantly.

Generally, RO membranes will be more suitable for combination with electrochemical oxidation compared to NF membranes.

Although NF membranes require less energy in the filtration, the higher energy consumption of the RO membrane is compensated by a higher increase in conductivity and improved degradation kinetics if chloride is present. As such, through combination with especially low pressure RO membranes, the use of electrochemical oxidation may become economically competitive with other techniques for micropollutant removal.

Acknowledgement

Financial support from the Danish Ministry of Science, Technology, and Innovation in the form of a Ph.D. study grant is acknowledged.

References

[1] K.V. Plakas, A.J. Karabelas, Removal of pesticides from water by NF and RO membranes – a review, Desalination 287 (2012) 255–265, http://dx.doi.org/10.1016/j.desal.2011.08.003.
[2] Å. Anglada, A. Urtiaga, I. Ortiz, Contributions of electrochemical oxidation to waste-water treatment: fundamentals and review of applications, J. Chem. Technol. Biotechnol. 84 (2009) 1747–1755, http://dx.doi.org/10.1002/jctb.2214.
[3] C. Comninellis, A. Kapalka, S. Malato, S.A. Parsons, I. Poulios, D. Mantzavinos, Advanced oxidation processes for water treatment: advances and trends for R&D, J. Chem. Technol. Biotechnol. 83 (2008) 769–776, http://dx.doi.org/10.1002/jctb.
[4] M.E.H. Bergmann, A.S. Koparal, T. Iourtchouk, Electrochemical advanced oxidation processes, formation of halogenate and perhalogenate species: a critical review, Crit. Rev. Environ. Sci. Technol. 44 (2014) 348–390, http://dx.doi.org/10.1080/10643389.2012.718948.
[5] V.J. Pereira, J. Galinha, M.T. Barreto Crespo, C.T. Matos, J.G. Crespo, Integration of nanofiltration, UV photolysis, and advanced oxidation processes for removal of hormones from surface water sources, Sep. Purif. Technol. 95 (2012) 89–96.
[6] A.M. Urtiaga, G. Pérez, R. Ibáñez, I. Ortiz, Removal of pharmaceuticals from a WWTP secondary effluent by ultrafiltration/reverse osmosis followed by electrochemical oxidation of the RO concentrate, Desalination 331 (2013) 26–34, http://dx.doi.org/10.1016/j.desal.2013.10.010.
[7] S. Miralles-Cuevas, A. Arques, M.I. Maldonado, J.A. Sánchez-Pérez, S.M. Rodriguez, Combined nanofiltration and photo-Fenton treatment of water containing micropollutants, Chem. Eng. J. 224 (2013) 89–95.
[8] I. Sirés, E. Brillas, G. Cerisola, M. Panizza, Comparative depollution of mecoprop aqueous solutions by electrochemical incineration using BDD and PbO_2 as high oxidation power anodes, J. Electroanal. Chem. 613 (2008) 151–159, http://dx.doi.org/10.1016/j.jelechem.2007.10.023.
[9] Y. Samet, L. Agengui, R. Abdelhédi, Electrochemical degradation of chlorpyrifos pesticide in aqueous solutions by anodic oxidation at boron-doped diamond electrodes, Chem. Eng. J. 161 (2010) 167–172, http://dx.doi.org/10.1016/j.cej.2010.04.060.
[10] N. Oturan, M. Hamza, S. Ammar, R. Abdelhédi, M.a. Oturan, Oxidation/mineralization of 2-Nitrophenol in aqueous medium by electrochemical advanced oxidation processes using Pt/carbon-felt and BDD/carbon-felt cells, J. Electroanal. Chem. 661 (2011) 66–71, http://dx.doi.org/10.1016/j.jelechem.2011.07.017.
[11] M. Panizza, G. Cerisola, Direct and mediated anodic oxidation of organic pollutants, Chem. Rev. 109 (2009) 6541–6569, http://dx.doi.org/10.1021/cr9001319.
[12] H.C. Yatmaz, Y. Uzman, Degradation of pesticide monochrotophos from aqueous solutions by electrochemical methods, Int. J. Electrochem. Sci. 4 (2009) 614–626.
[13] D. Arapoglou, A. Vlyssides, C. Israilides, A. Zorpas, P. Karlis, Detoxification of methyl-parathion pesticide in aqueous solutions by electrochemical oxidation, J. Hazard. Mater. 98 (2003) 191–199.
[14] G.R.P. Malpass, D.W. Miwa, S.A.S. Machado, P. Olivi, A.J. Motheo, Oxidation of the pesticide atrazine at DSA electrodes, J. Hazard. Mater. 137 (2006) 565–572, http://dx.doi.org/10.1016/j.jhazmat.2006.02.045.
[15] M. Errami, R. Salghi, A. Zarrouk, A. Chakir, B. Hammouti, L. Bazzi, et al., Electrochemical combustion of insecticides endosulfan and deltamethrin in aqueous medium using a boron-doped diamond anode, J. Electrochem. Sci. 7 (2012) 4272–4285.
[16] H. Bouya, M. Errami, R. Salghi, A. Zarrouk, B. Hammouti, L. Bazzi, et al., Electrochemical degradation of cypermethrin pesticide on a SnO_2 anode, Int. J. Electrochem. Sci. 7 (2012) 3453–3465.
[17] H.T. Madsen, E.G. Søgaard, J. Muff, Study of degradation intermediates formed during electrochemical oxidation of pesticide residue 2,6-dichlorobenzamide (BAM) at boron doped diamond (BDD) and platinum–iridium anodes, Chemosphere 109 (2014) 84–91, http://dx.doi.org/10.1016/j.chemosphere.2014.03.020.
[18] H.T. Madsen, E.G. Søgaard, J. Muff, Study of degradation intermediates formed during electrochemical oxidation of pesticide residue 2,6-dichlorobenzamide (BAM) in chloride medium at boron doped diamond (BDD) and platinum anodes, Chemosphere 120 (2015) 756–763, http://dx.doi.org/10.1016/j.chemosphere.2014.10.058.
[19] J. Radjenovic, A. Bagastyo, R.A. Rozendal, Y. Mu, J. Keller, K. Rabaey, Electrochemical oxidation of trace organic contaminants in reverse osmosis concentrate using RuO_2/IrO_2-coated titanium anodes, Water Res. 45 (2011) 1579–1586, http://dx.doi.org/10.1016/j.watres.2010.11.035.
[20] A.Y. Bagastyo, D.J. Batstone, I. Kristiana, W. Gernjak, C. Joll, J. Radjenovic, Electrochemical oxidation of reverse osmosis concentrate on boron-doped diamond anodes at circumneutral and acidic pH, Water Res. 46 (2012) 6104–6112, http://dx.doi.org/10.1016/j.watres.2012.08.038.
[21] A.Y. Bagastyo, D.J. Batstone, K. Rabaey, J. Radjenovic, Electrochemical oxidation of electrodialysed reverse osmosis concentrate on Ti/Pt–IrO_2, Ti/SnO_2–Sb and boron-doped diamond electrodes, Water Res. 47 (2013) 242–250, http://dx.doi.org/10.1016/j.watres.2012.10.001.
[22] K. Van Hege, M. Verhaege, W. Verstraete, Electro-oxidative abatement of low-salinity reverse osmosis membrane concentrates, Water Res. 38 (2004) 1550–1558, http://dx.doi.org/10.1016/j.watres.2003.12.023.
[23] K. Van Hege, M. Verhaege, W. Verstraete, Indirect electrochemical oxidation of reverse osmosis membrane concentrates at boron-doped diamond electrodes, Electrochem. Commun. 4 (2002) 296–300, http://dx.doi.org/10.1016/S1388-2481(02)00276-X.
[24] A. Pérez-González, A.M. Urtiaga, R. Ibáñez, I. Ortiz, State of the art and review on the treatment technologies of water reverse osmosis concentrates, Water Res. 46 (2012) 267–283, http://dx.doi.org/10.1016/j.watres.2011.10.046.
[25] E. Dialynas, D. Mantzavinos, E. Diamadopoulos, Advanced treatment of the reverse osmosis concentrate produced during reclamation of municipal wastewater, Water Res. 42 (2008) 4603–4608, http://dx.doi.org/10.1016/j.watres.2008.08.008.
[26] H.T. Madsen, E.G. Søgaard, Applicability and modelling of nanofiltration and reverse osmosis for remediation of groundwater polluted with pesticides and pesticide transformation products, Sep. Purif. Technol. 125 (2014) 111–119, http://dx.doi.org/10.1016/j.seppur.2014.01.038.
[27] E.G. Søgaard, R. Aruna, J. Abraham-Peskir, C.B. Koch, Conditions for biological precipitation of iron by *Gallionella ferruginea* in a slightly polluted ground water, Appl. Geochem. 16 (2001) 1129–1137.
[28] K.P. Kowalski, H.T. Madsen, E.G. Søgaard, Comparison of sand and membrane filtration as non-chemical pre-treatment strategies for pesticide removal with nanofiltration/low pressure reverse osmosis membranes, Water Sci. Technol. Water Supply 14 (2014) 532, http://dx.doi.org/10.2166/ws.2014.004.
[29] N. Borràs, R. Oliver, C. Arias, E. Brillas, Degradation of atrazine by electrochemical advanced oxidation processes using a boron-doped diamond anode, J. Phys. Chem. A 114 (2010) 6613–6621, http://dx.doi.org/10.1021/jp1035647.
[30] E. Brillas, S. Garcia-Segura, M. Skoumal, C. Arias, Electrochemical incineration of diclofenac in neutral aqueous medium by anodic oxidation using Pt and boron-doped diamond anodes, Chemosphere 79 (2010) 605–612, http://dx.doi.org/10.1016/j.chemosphere.2010.03.004.
[31] E.B. Cavalcanti, S. Garcia-Segura, F. Centellas, E. Brillas, Electrochemical incineration of omeprazole in neutral aqueous medium using a platinum or boron-doped diamond anode: degradation kinetics and oxidation products, Water Res. 47 (2013) 1803–1815, http://dx.doi.org/10.1016/j.watres.2013.01.002.
[32] C. Flox, P.L. Cabot, F. Centellas, J.A. Garrido, R.M. Rodríguez, C. Arias, et al., Electrochemical combustion of herbicide mecoprop in aqueous medium using a flow reactor with a boron-doped diamond anode, Chemosphere 64 (2006) 892–902, http://dx.doi.org/10.1016/j.chemosphere.2006.01.050.
[33] J.R. Bolton, K.G. Bircher, W. Tumas, C.A. Tolman, Figures-of-merit for the technical development and application of advanced oxidation technologies for both electric- and solar-driven systems, Pure Appl. Chem. 73 (2001) 627–637.
[34] L.R. Bennedsen, J. Muff, E.G. Søgaard, Influence of chloride and carbonates on the reactivity of activated persulfate, Chemosphere 86 (2012) 1092–1097, http://dx.doi.org/10.1016/j.chemosphere.2011.12.011.
[35] M. Errami, R. Salghi, M. Zougagh, A. Zarrouk, E.H. Bazzi, A. Chakir, et al., Electrochemical degradation of buprofezin insecticide in aqueous solutions by anodic oxidation at boron-doped diamond electrode, Res. Chem. Intermed. 39 (2012) 505–516, http://dx.doi.org/10.1007/s11164-012-0574-1.

ISBN: 978-87-93100-57-2

TRYK: UNIPRINT AAU